

SOME PARAMETERS TO CHARACTERIZE CHAMOMILE HARVESTING MACHINES

ADRIANA MUSCALU¹, PETRU CARDEI¹, RALUCA SFIRU¹,
AUGUSTINA PRUTEANU¹

¹ INMA Bucharest, Romania

amuscalis@yahoo.com, petru_cardei@yahoo.com

Abstract

Chamomile is one of the oldest and well known as medicinal plants being grown in numerous countries, especially for the essential oil that is extracted from the inflorescences, other important phytotherapeutic properties making chamomile a very valuable product on profile markets. Out of the agricultural works in the specific technology for cultivating chamomile, the quality of the plant material is considerably influenced by the harvesting process. Thus, for achieving profitable yields, mechanized harvesting of chamomile represents both an essential prerequisite and a guarantee. The paper presents an assessment of equipment from a certain category of agricultural machinery, namely of those destined for harvesting chamomile, in order to hierarchize their performances, in the view of an optimum selection and acquisition by farmers, as well as for orienting producers towards equipment specific for advanced agriculture.

Keywords: inflorescences, statistical surveys

INTRODUCTION

Chamomile, known since antiquity, is a particularly important medicinal plant and widely used in various industries.

Cultivation of medicinal plants may be an opportunity for some farmers to diversify their structure, reduce their risks and significantly increase the profits of their agricultural business. On the other hand, this activity requires specific knowledge in the field of production technology, the use, sometimes, of special machinery/equipment as well as a certain means of capitalizing, in conditions of quality and safety. [6, 8] These reasons have led to the drastic reduction of areas cultivated with medicinal plants in many countries across Europe, imports being preferred. [1,13].

Although two decades ago Romania was one of the leading countries producing medicinal and aromatic plants in Europe, in recent years there has been a continuous and accelerated decrease of the areas cultivated with these species, so that in 2014 and 2015, they were maintained at the same low level of approx. 3.2 thousand ha [14].

Worldwide, chamomile (*Matricaria Chamomilla L.*) is grown on approximately 20,000 ha. The main producing countries are: Argentina, Egypt, France, Germany, Italy, Hungary, the countries of the former Yugoslavia [4, 9].

For the use of chamomile as a medicinal plant, the raw material must meet high quality standards, the valuable blue oil, rich in azulenes, being mainly found in inflorescences. In order not to diminish its quality, it is important that when harvesting, the chamomile flowers have a stem as short as possible. [3, 4, 10, 11]

The chamomile is harvested when most of the inflorescences, the ligulate flowers opened and are disposed horizontally (after 9 am), while the tubular ones are flowering having a yellow colour (the bloomed ones) and greenish-yellow (the unbloomed ones) in the hot days with clear sky. The volatile oil content is the highest in the phase where the ratio of flower buds and opened flower

heads is **1:1**. [10, 11] Thus, the quality of the plant material is strongly influenced by the harvesting time and mode. Chamomile inflorescences are harvested manually or mechanically by pulling out.

Manual harvesting is carried out by qualified staff and results in high quality products; otherwise the quality of the products is not uniform. In some cases, this harvesting method is the only available, although in Europe, it can be expensive, with low productivity [7]. Sometimes, after the inflorescences have been harvested, by cutting at a certain height from the ground, the *herba* (consisting of stem, leaves and possibly flowers) is harvested mechanically to be used for making various tea recipes [10, 11].

Cultivation of chamomile on large areas in Europe can only be accomplished by mechanizing the harvesting works. [3, 7] The mechanized harvesting of chamomile inflorescences is done with specialized comb-type parts (with curved or straight teeth) or with working parts having the comb effect, arranged on a harvester with a circular motion. This can be performed in the sense of machine moving or in the opposite direction [2, 3, 5, 7, 17]. The machines used for harvesting chamomile inflorescences may be trailed or self-propelled. [2, 3, 5, 7, 12, 17]

MATERIALS AND METHODS

The sources of the considerations in this article are the technical-economic data obtained from the web pages and advertising leaflets of the companies producing machinery and equipment for chamomile harvesting. The sources are the companies: *Europrima* from Serbia, *Herbas* from Croatia, *Travizaporoja* from Ukraine, presented in references [15, 16, 18]. These companies produce chamomile trailed harvesters.

Europrima produces machines that harvest herbs by cutting with special devices (NB 2005 V and NB 2006E/P models) as well as machines that harvest chamomile with finger-effect special working parts (model VB2002). As they serve the same purpose, we found it useful to compare them. We also considered it important to present the high performance self-propelled machines produced as prototype in Italy (2010) and Germany (2013), which harvest chamomile flowers with comb-type active parts [3, 5, 17].

Generally, machine prospectuses show information about: machine mass, working width, working speed, engine power, productivity and other information. Not all companies give all this information. Using the information given above, statistical surveys can be made directly on data from sources or statistical estimators developed for various purposes. The use of this information is facilitated by organizing it in a database for which Microsoft Office Excel was used and named DBHC.xls. Now, in Europe, there are few companies that make machines for chamomile harvesting. For this reason, the database is not very large, containing information only about it.

Direct statistical estimators

The hierarchy of the masses highlights useful information for designers or potential users of such machines, warning them of the possible consequences when working with such machines: higher consumption of large mass machines, more pronounced effect on compaction of the soil, reduced manoeuvrability of these machines etc.

The hierarchy of working width correlated with productivity calculation allows potential users / buyers to choose the most suitable machines in terms of geographical and climatic profile, the size of culture plots, depending on the financial resources and the length of time when harvesting is efficient.

The same observations can be made in terms of hierarchy of working capacity¹ whether it is taken directly from sources or is estimated based on working width and working speed.

Elaborated statistical estimators

To estimate specialized technical/economic characteristics, useful to designers of such machines and equipment and less to potential buyers, we have developed calculation formulas that use data from sources. These estimators are:

- *Specific working width*: is a complex parameter of the machine defined as the ratio between the mass and the working width of the machine. The measurement unit of this parameter is kg/m. The calculation formula is the following:

$$m_l = \frac{M}{l} \quad (1)$$

Where M is the machine mass in kg , l is the working width in m , while m_l is the working width specific mass.

- *Working width specific power* is a complex parameter of the machine defined as the ratio between the engine drive power and the working width of the machine. The measurement unit of this parameter is kW/m. The calculation formula is the following:

$$P_l = \frac{P}{l} \quad (2)$$

Where P is the machine power in kW , l is the working width in m , while P_l is the working width specific power.

Maximum theoretical productivity: is a complex parameter of the machine defined as the product between the working speed and the machine working width of the machine. The measurement unit of this parameter is ha/h. The calculation formula is the following:

$$W_t = 0.1 \cdot v \cdot l \quad (3)$$

where v is the machine working speed in km/h , l is the working width in m , while W_t is the maximum theoretical productivity in ha/h.

Consumption of material per unit of theoretical maximum productivity: is a complex parameter of the machine defined as the ratio between the mass and theoretical maximum productivity. The measurement unit of this parameter is kg h/ha. The calculation formula is the following:

$$m_w = \frac{M}{W_t} \quad (4)$$

Where M is the machine mass in kg , W_t is the maximum productivity in ha/h , while m_w is the consumption of material per productivity unit.

There are many such technical and economic estimators that are used to make a hierarchy of agricultural machines and to optimize their working regime. These estimators require data that sources do not generally offer (e.g. fuel consumption).

For chamomile harvesters quality indices, referring to inflorescences harvesting degree, the purity of the harvested material, the high quality inflorescences (flowers stem < 20mm), the damage degree of the harvested flowers, the losses on the soil, are very important and they are expressed as a percentage. Because this type of data depend, to a large extent, on the characteristics of the crop, the geo-climatic data, the chamomile harvester-producing companies eventually provide only productivity-related information.

In the case of testing self-propelled prototypes in chamomile cultures where the cultivation technology had been respected, the working performance results and quality indices presented above were promising, constituting an important premise for optimizing these machines.

RESULTS AND DISCUSSION

Elementary statistical results

For the performance of the machines and equipment we have data about, it's interesting to have the graphic representation first. From the DBHC.xls database work form we consider the graphs that represent the mass of machines and equipment included in this database (Fig. 1), the minimum and maximum working widths (Fig. 2), respectively the minimum and maximum working speeds (Fig. 3). In these graphs we can see the variation of the above sizes for the machines and equipment included in the database.

Figure 1 shows the variation in mass for chamomile harvesters for which it has been specified; thus is why self-propelled machines don't appear in this hierarchy.

Figure 2 shows the variation of the minimum and maximum working widths, depending on the data that could be found and selected. For machines that harvest chamomile with specialized working parts, the working width cannot be varied (between a minimum value and a maximum value), so in the graph it is represented as the maximum value.

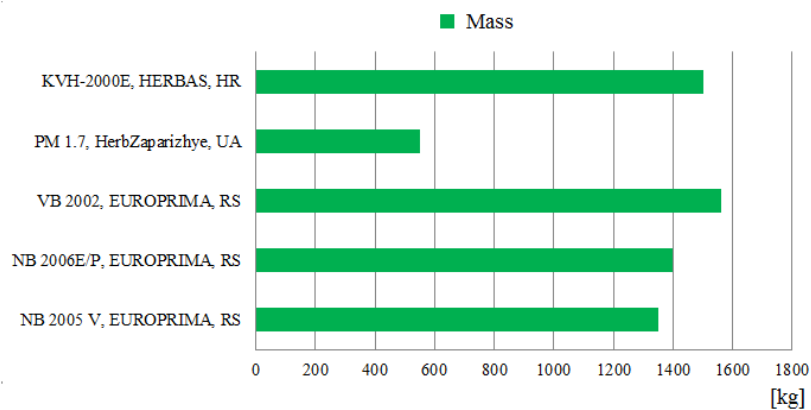


Fig.1 Mass variation for chamomile harvesting machines

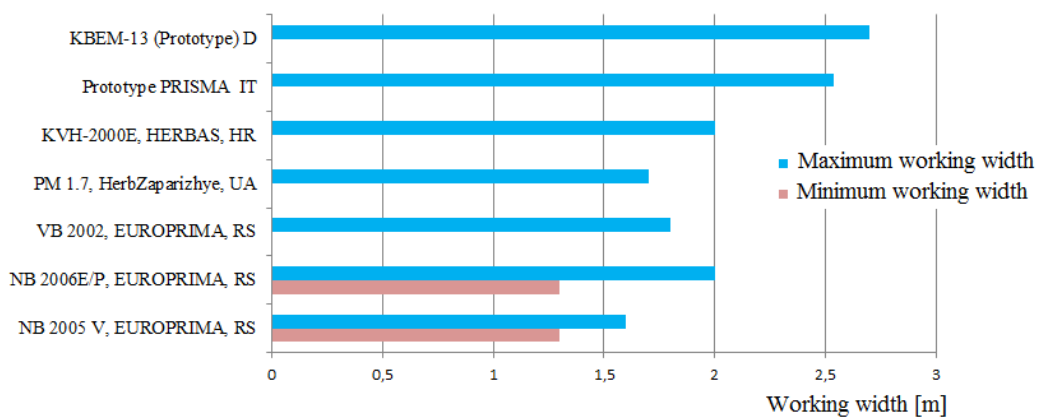


Fig.2. Working width variation for chamomile harvesting machines

Figure 3 shows the variation in the minimum and maximum working speeds, depending on the data that could be found and selected. For self-propelled machines, the minimum and maximum working speeds are those used in the experiments.

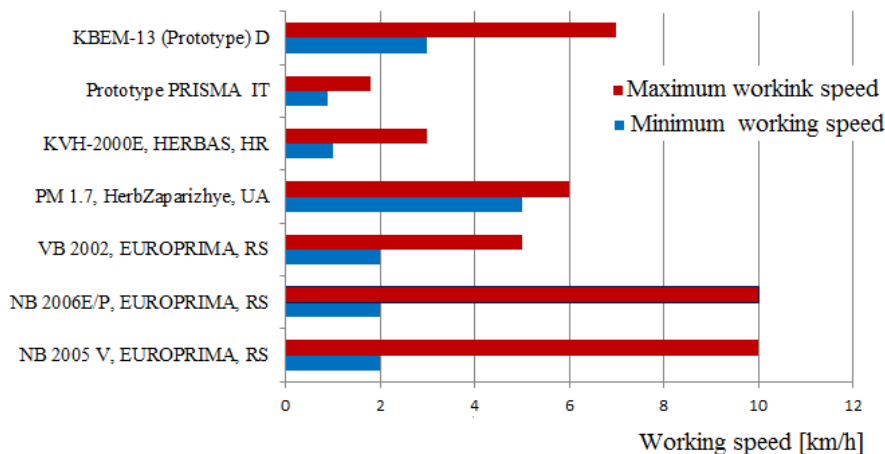


Fig.3 Working speed variation for chamomile harvesting machines

For the maximum working width, the arithmetic mean (in the case of the machines this feature is given for) is 2.05 m and the average square deviation is 0.419 m. It is highly probable that the machines with these working widths in the range centred on the average value and the length equal to double the average square deviation, are the ones with the highest on the market. For this reason, the information extracted can guide the manufacturer to an important working parameter of a chamomile harvester.

Complex statistical results

These results are based on calculation formulas elaborated on the basis of gross values in the database and are given for the machines that had all the data for their calculation. The calculation formulas of these estimators are given in relations (1, 2, 3, 4). The graphical representations of these estimators distribution for the machines in the database are shown in the figures below.

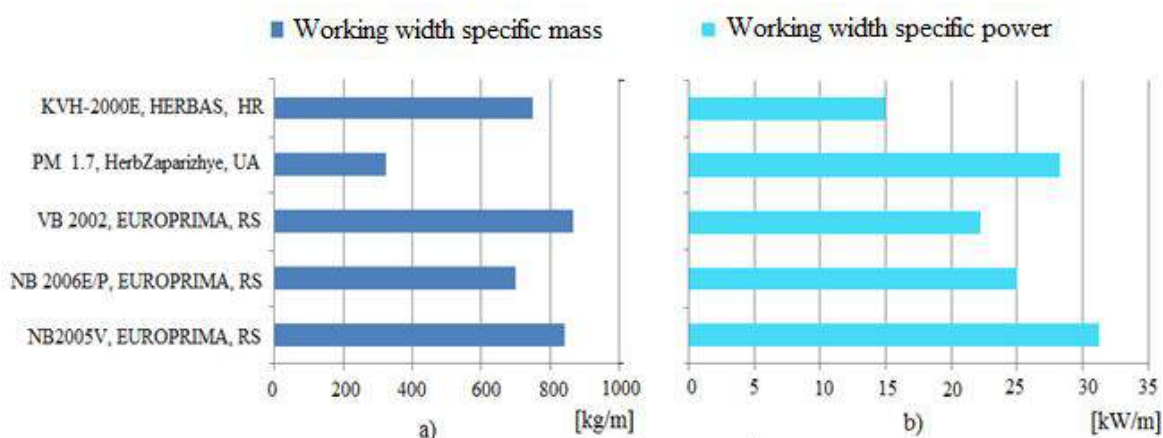


Fig. 4. Complex estimators variation:a) – Working width specific mass;
b) – Working width specific power;

It can be seen in Fig. 4.a that the highest material consumption per unit of working width is registered for the model VB 2002 (EUOPRIMA company, Serbia), which does not have the largest working width of the machines which also have the mass specified. Comparable values are registered for the NB 2005 V model, of the same company, as well as for the KVH-2000E model (Herbas company, Croatia), which has the largest working width among the machines with the mass specified. Also, it can be seen in fig. 4.b that the highest power consumption per unit of working width is registered for the model NB 2005V (EUOPRIMA company, Serbia), a value comparable with the PM 1.7 model (HerbZaparizhye company, Ukraine). For the latter, the power reserve is justified because, if necessary, the machine can be completed with a transport device.

Fig. 5 shows the variation in theoretical maximum productivity.

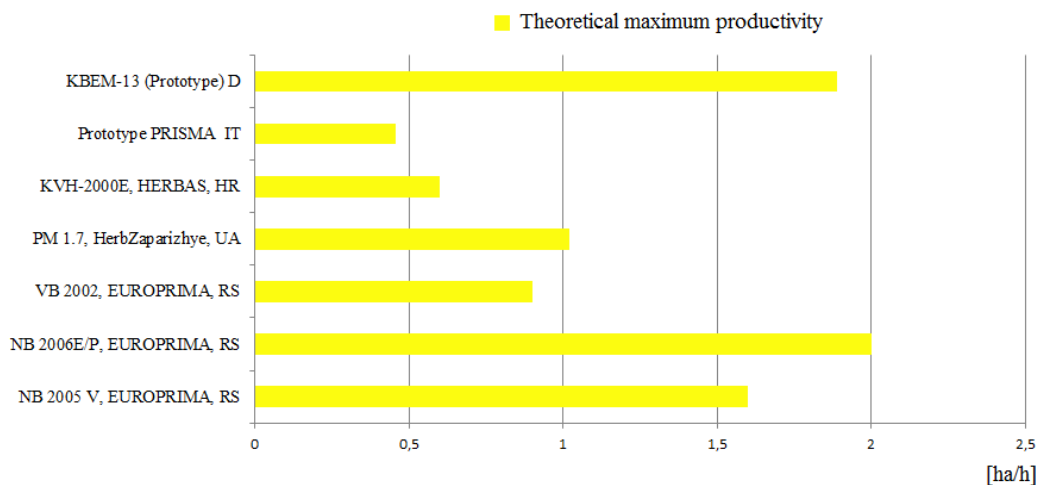


Fig. 5. Variation of theoretical maximum productivity

In fig. 5 we can notice that the highest theoretical productivity is registered in the case of NB 2006E/P model, which harvests chamomile by cutting. A comparable value was registered for the KBEM-13 prototype, which harvests chamomile flowers with comb-type working parts. In the case of the P.R.I.S.M.A. prototype, the lowest productivity was registered, but the quality of the harvested material was high, according to the experimental results. The experimental results registered for the prototypes should be viewed with some caution, until their serial production. In general, working speed is an extremely important parameter of any agricultural machine, but it depends to a large extent on the concrete working conditions in the field, as well as the user's skill, the values given being indicative.

The graphical presentation of the complex estimator distribution ends with the presentation in Fig. 6. of the material consumption variation per unit of theoretical productivity.

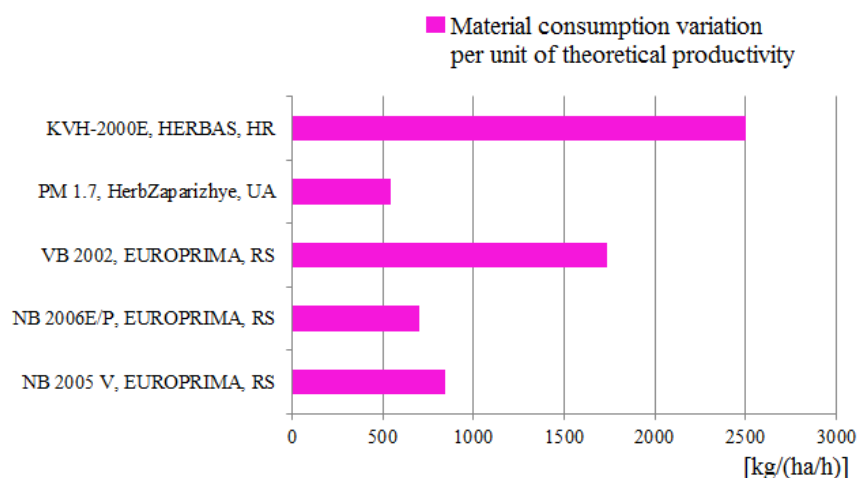


Fig.6 Material consumption variation per unit of theoretical productivity

Figure 6 shows that the highest material consumption per unit of theoretical productivity is registered in the case of KVH-2000E model, (Herbas, Croatia), and the smallest in the case of PM1.7 model (HerbZaparizhye, Ukraine).

CONCLUSION

The databases containing the technical-economic characteristics of the agricultural machines offer the possibility of using them in order to rank their performances in the working processes. Thus, for example, if we have offers from multiple dealers, we can develop synthetic hierarchical estimators that take into account price and performance. The potential buyer can choose the machine optimally. Also, the choice of the farmer can be further oriented with the limits of the financial resources, the relief conditions, etc.

The database of information from the mentioned sources about the chamomile harvesting machines provides the designers with estimates of the performance parameters of the most modern machines produced and indicates what materials, dimensions, etc. must be used in order to enter the top machine range.

Also, the database made available to manufacturers provides them with the range of information they need to complete to form complex performance estimators, with high resolution power.

In addition, the database is a source of information for the companies producing machines in order to improve the performance characteristics of their own products, in order to orientate towards equipment specific to the advanced agriculture.

Perspectives refer to the completion of this database with equipment destined for harvesting other medicinal and aromatic plant species too. It should not be forgotten that, as a general rule, farmers prefer equipment with a degree of universality. Thus, we can refer to the possibility of creating algorithms of automatic choice in the database, for a minimum of input data, which can be used in the consulting firms/ activity.

ACKNOWLEDGEMENT

The work has been funded by Ministry of Research and Innovation, within the project entitled „Innovative technology and equipment for increasing the quality of plant raw material obtained from medicinal and aromatic plants, in the view of elaborating competitive organic products”, PN 16 24 03 03.

REFERENCES

1. Barbieri C., 2013. Medicinal and aromatic plants legislation in the European Union, Italy and several of its regions, *Journal Natural Product Research*, 27, (17);
2. Brabandt H. and Ehlert D., 2011. Chamomile harvester: a review. *Industrial Crops and Products*, 34, (1), 818-824;
3. Ehlert D and Beier K. 2014. Development of picking devices for chamomile harvesters, *Journal of Applied Research on Medicinal and Aromatic Plants* (1), 73-80;
4. Ehlert D., Adamek R., Giebel A. and Horn H. 2011. Influence of comb parameters on picking properties for chamomile flowers (*Matricaria Recutita*), *Industrial Crops and Products* (33): 241-247, Elsevier;
5. Ehlert E. 2014. Development of a chamomile harvester, *Landtechnik* 69 (2);
6. herbas.hr/kombajn-za-kamilicu/?lang=en;
7. Ivanovic S, Pajic M. and Markovic T. 2014. Economic effectiveness of mechanized harvesting of Chamomile, *Economics of Agriculture*, (2), Belgrad, pg.319-330;
8. Martinov M, Konstantinovic M. 2007. Harvesting. In: *Medicinal and aromatic crops. Harvesting, drying, and processing* (Öztekın S, Martinov M, eds.). The Haworth Press Inc., NY (USA), 56-84.
9. Máthé, Á. and Máthé, I. 2008. Quality assurance of cultivated and gathered medicinal plants. *Acta Hort. (ISHS)* 765, : 67-76;
10. Moumita Das, 2015 *Chamomile: Medicinal, Biochemical, and Agricultural Aspects*, CRC Pres, by Taylor and francis Group, :2-3
11. Muntean L.S. 2010. *The use and cultivation of medicinal and aromatical plants in Romania, Hop and Medicinal Plant No.1-2*, , Academicpres Printing House Cluj Napoca, : 34-43;ISSN 2360 – 0179
12. Pajic M., Pajic V. Ivanovic S., Oljaca M. and Gligorevic K. 2016. Influence of harvester type and harvesting time on quality of harvested chamomile, *Journal of Agricultural Sciences* . 61, No. 201-213;
13. Păun E., Mihalea A., Dumitrescu A., Verzea M. and Cosocariu O. 1988. *Treaty of cultivated medicinal and aromatic plants*,.I-II, Academy Publishing House, Bucharest,;
14. *Romanian Statistical Yearbook 2015*;
15. Schippmann U., Leaman D. and Cunningham A.B. 2002. *Impact of Cultivation and Gathering of Medicinal Plants on Biodiversity: Global Trends and Issues*, FAO. *Biodiversity and the Ecosystem Approach in Agriculture, Forestry and Fisheries.*, Satellite event on the occasion of the Ninth Regular Session of the Commission on Genetic, Resources for Food and Agriculture. Rome;
16. www.euoprima.rs/;
17. www.ongsnc.com/prototipi-2/;
18. www.travizaporoja.com.ua/;

INFLUENCE OF ORGANIC FERTILIZERS AND MULCHING ON SUSTAINABLE PRODUCTION OF BROCCOLI AND CELERY

ABUL-SOUD, M., A.A.FARAG and Z. Y. MAHARIK

Central Laboratory for Agricultural Climate, ARC, Dokki 12411, Giza- Egypt

Abstract

Needing to increase the sustainable production of vegetables under semi-arid Egyptian conditions to match food security demands created the driving forces to investigate different resources of organic fertilizers and improve the agricultural practice of vegetable production. The experiment was carried out during the two winter successive seasons of 2015/2016 and 2016/2017 under net multi span house in protected cultivation site, Central Laboratory for Agricultural Climate (CLAC), Agricultural Research Centre, Giza, Egypt. The study aimed to investigate the application of different organic fertilizers (cattle manure, rabbit manure and vermicompost) combined with two soil treatments (bare soil and mulching) on the growth and yield of celery and broccoli. The experimental design performed in split plot design. The application of vermicompost in soil as an organic fertilizer recorded the highest values of the growth and yield characteristics of celery and broccoli compared to the other treatments. Mulching soil also gave the higher results of vegetative and yield characteristics of celery and broccoli compared to bare soil. the highest yields of celery and broccoli were gave by the application of vermicompost combined with mulching treatment while the application of rabbit manure combined with bare soil had the lowest yield. The vermicomposting of urban organic wastes and applied it to the soil as an organic fertilizer instead of burial or inceneration led to increase the yield of celery and broccoli beside sequestrate CO₂ in the soil and decrease its emission.

Keywords: *Organic fertilizer, vermicompost, cattle manure, rabbit manure, mulching, broccoli, celery, yield and quality.*

INTRODUCTION

Green revolution can be attained through adopting the technologies such as countless use of synthetic chemicals like fertilizers and pesticides; adoption of nutrient responsive, high-yielding varieties of crops, greater exploitation of irrigation potentials etc. has boosted the production output in most cases. There is no doubt that in Egypt, where on one side pollution is increasing day by day due to accumulation of organic waste and on the other side there is a great shortage of organic manure. The organic manure could increase the fertility and productivity of the land and produce nutritive and safe food Ramesh *et al.*, 2005. Recycling organic waste of different resources in the form of compost can be an alternative to meet the increasing demands for organic manures; this will also help to reduce environmental pollution arising out of accumulated bio wastes Kumar, 2005.

The use of organic matter such as animal manures and composts has long been recognized in agriculture as beneficial for plant growth and yield and the maintenance of soil fertility. The new approaches to the use of organic amendments in farming have proven to be effective means of improving soil structure, enhancing soil fertility and increasing crop yields (Bwamiki *et al* 1998,. Hoitink, 1993 and Johnston *et al.* 1995).

Organic manures such as cattle manure and poultry manure improve the soil structure, aeration, slow release nutrient which support root development leading to higher yield and better

quality of broccoli and Cauliflower plants (Abou El- Magd *et al.*, 2005; Farag and Shaimaa, 2016). Organic manure play direct role in plant growth as a source of all necessary macro and micronutrients in available forms during mineralization and improving physical and chemical properties of soils (Chaterjee *et al.*, 2005).

A process related to composting which can improve the beneficial utilization of organic wastes is vermicomposting. It is a non-thermophilic process by which organic materials are converted by earthworms and microorganisms into rich soil amendments with greatly increased microbial activity and nutrient availability. Vermicomposts are products derived from the accelerated biological degradation of organic wastes by earthworms and microorganisms. Albanell *et al.*, 1988; Orozco *et al.*, 1996, Edwards and Neuhauser 1998 and Abul-Soud *et al.*, 2009.

Different organic wastes can be used in vermicompost production by different species of earthworms which include horse waste (Garg and Kaushik, 2005); cattle dung (Kaushik and Garg, 2003) cow slurry (Hand *et al.*, 1988); urban solid waste (Abul-Soud *et al.*, 2009); city leaf litter and food wastes (Singh and Sharma, 2002 and Abul-Soud *et al.*, 2009); paper waste and residues of plant decomposition.

Mulches are used for various reasons but water conservation and erosion control are the most important objective for its use in agriculture in dry regions. Other reason for high mulching use includes soil temperature modification, soil conservation, nutrient addition, improvement in soil structure, weed control and crop quality control. Mulching reduces the deterioration of soil by way of preventing the runoff and soil loss, minimizes the weed infestation and checks the water evaporation. Kumar *et al.* 2005, Abul-Soud *et al.* 2010. The plastic mulch increased minimum temperature of soil, accelerated plant height, early growth, early yield, and bring satisfactory weed control without any application of herbicides (Najafabadi *et al.*, 2012; Farag *et al.*, 2010).

Sustainable agriculture needs sustained support of organic fertilizers and good agricultural practices. The study target is to investigate the interaction between soil plastic mulch and different organic fertilizers effective on growth and yield of celery and broccoli for sustainable production.

MATERIALS AND METHODS

The experiment was carried out during the two growing winter season of 2015/2016 and 2016/2017 under multi span net house (9 x 30 x 4.5 m) at Central Laboratory for Agricultural Climate (CLAC), Agricultural Research Center, Ministry of Agriculture and land reclamation, Egypt. For investigate the effect of mulching and bare soil with their interactions with different source of organic fertilizer (cattle manure, rabbit manure and vermicompost) on celery and broccoli plants.

The plant

Celery (*Apium graveolens var. dulace cv. Royal crown*) and Broccoli (*Brassica oleracea L. ssp. italica*). The seedlings transplanted in soil at 13th and 15 November of 2015 and 2016 respectively. One seedling of each celery and broccoli was planted at 50 cm in the row where the distance between the rows was 60 cm (2 rows/bed) and between the beds was 70 cm.

The study treatments

This experiment included two factors. The first factor was soil mulching (bare soil (B.S) and mulching soil (M.S) with black polyethylene sheet 60 micron) and the second factors were included three sources of organic fertilizer (cattle manure as a control (C.M), rabbit manure R.M) and vermicompost (V.C).

The experimental design was a split-plot design with 3 replicates. The mulching soil were assigned as main plots and organic fertilizer as subplots.

The field experiment material

The experimental trial was conducted in clay soil using drip irrigation system under multi span net (white 20 % shading) house. Emitter discharge rate was 4 l/hr, The chemical fertilizers were injected within irrigation water system.

The recommended dose of mineral fertilizers were applied according to Ministry of Agriculture and Land Reclamation (2009). The fertigation was programmed to work 3 times / week and the duration of irrigation time depended upon the season.

All the other agriculture practices of peas cultivation were in accordance with the standard recommendations for commercial growers by Agriculture Research center (ARC). Ministry of Agriculture, Egypt.

The physical properties (saturation point % (SP), field capacity % (FC), wilting point % (WP) and bulk density g/cm³ (BD) of the soil were determined according to (Wilson 1983 and Raul 1996) and chemical properties (regarding to Chapman and Pratt 1961 and FAO (1980)) of the clay experimental soil were determined before cultivation and organic fertilizers applications (Table 1).

Table (1): Chemical and physical analyses of the experiment soil at Dokki site.

Soil depth	Chemical properties							
	ECe mmohs	pH	Ca ⁺⁺ meg/L	Mg ⁺⁺ meg/L	Na ⁺ meg/L	K ⁺ meg/L	Hco ₃ . meg/L	CL- meg/L
0 – 30 Cm	1.33	7.8	2.68	1.09	1.94	1.86	1.93	2.39
	Physical properties							
	Sand %	Clay %	Silt %	Texture	SP %	FC %	WP %	BD g/cm ³
	13.9	67.5	18.6	Clay	20.2	30.4	14.3	1.31

The different organic fertilizers were added during soil preparation at the standard rate (20 m³/feddan). Physical and chemical properties of different Organic fertilizers were analyzed in Table (2).

The source of cattle manure and rabbit manure used in the study were obtained from the Agriculture Fac. Farm, Cairo univerisity while the vermicompost was offered by the activities of " Integrated environmental management of urban organic wastes using vermicomposting and green roof (VCGR) project", CLAC. The vermicomposting process and vermicompost production were done according to Abul-Soud *et al.*, 2009, 2014, 2015 (a and b). Cattle manure + rabbit manure + urban organic wastes (vegetables and fruit scraps + news paper) proportions (1: 1 : 1) were vermicomposting different organic materials input.

Table (2): Chemical properties of different Organic fertilizers

Organic fertilizer	EC (dS / m)	pH (1:2.5)	O.M (%)	N (%)	C/N ratio	P (%)	K (%)
Cattle manure	4.15	7.90	39.6	1.35	1:21	0.5	0.56
Rabbit manure	5.11	8.95	77.29	1.79	1:15	0.59	0.67
Vermicompost	6.67	7.41	59.22	1.56	1:12.5	1.27	1.19

The measurments

Samples of three plants for Broccoli plants of each experimental plot were taken to determine growth parameters (plant high, leaves number per plant as well as fresh and dry weight of shoots) after 60 days. The yield parameters was masger at mature stage (Head weight (g/plant), and head diameter).

Celery plants : After 75 days from transplanting, samples of three plants of each experimental plot were taken to determine growth parameters as follows: plant height (cm), leaves number per plant, fresh weight, dry weight.

Broccoli and Celery Leaves contents of N, P and K (%) were estimated. Three plant samples at the harvest stage of each plot were dried at 70 °C in an air forced oven for constant weight. Dried plant samples were digested in mixture of HClO₄ and H₂SO₄ acids according to the method described by Allen (1974). The contents of N, P and K were estimated in the acid digested solution. Total nitrogen was determined by Kjeldahl method and Phosphorus content was determined by colorimetric method according to the procedure described by Page *et al.*, (1982). Potassium content was determined photo-metrically using Flame photometer as described by Chapman and Pratt (1961).

The chemical properties of different organic fertilizers illustrated in Table (2) were estimated according to FAO 1980 and Inbar *et al.*, 1993.

The statistical analysis:

Data were statistically analyzed using the analysis of variance method one way ANOVA with SAS package software version 6 (SAS Institute, 1990). Tukey test was used to compare the significant differences among means of the treatments at 0.05 level of probability, the procedure described by Snedecor and Cochran (1981).

RESULTS

The effect of soil mulching and different organic fertilizers on soil temperature

The application of different organic fertilizers had no significant effect on soil temperature. The results of organic fertilizers sources on soil temperature for both broccoli and celery were neglected regarding to the high similarity results. The main factor on soil temperature due to soil mulching under the current study for both broccoli and celery during the two studied seasons.

Average soil temperature at 15 cm depth during the experimental two seasons illustrated in (Fig. 1). The results indicated that applying the mulch by black polyethylene sheet 60 micron increased soil temperature between 1.22 and 1.55 C° compared to bare soil. These findings are in agreement with many other field studies El-Nerm, 2006; Singh and Kamal, 2012; Moursy *et al.*, 2015 which have confirmed the increment of soil temperature due to the greater absorb solar radiation. However, the warmer soil temperatures can quicken seedling emergence and growth to achieve the desired population structure at an earlier growth stage Zhou *et al.*, 2009 in which maximize the absorption of solar radiation and enhance the yield Li *et al.*, 2013. Furthermore, elevated soil temperature can be lethal for nematode and soil borne pathogens as well as many weed seeds before its germination through solarization. Khan *et al.*, 2003; Singh *et al.*, 2007.

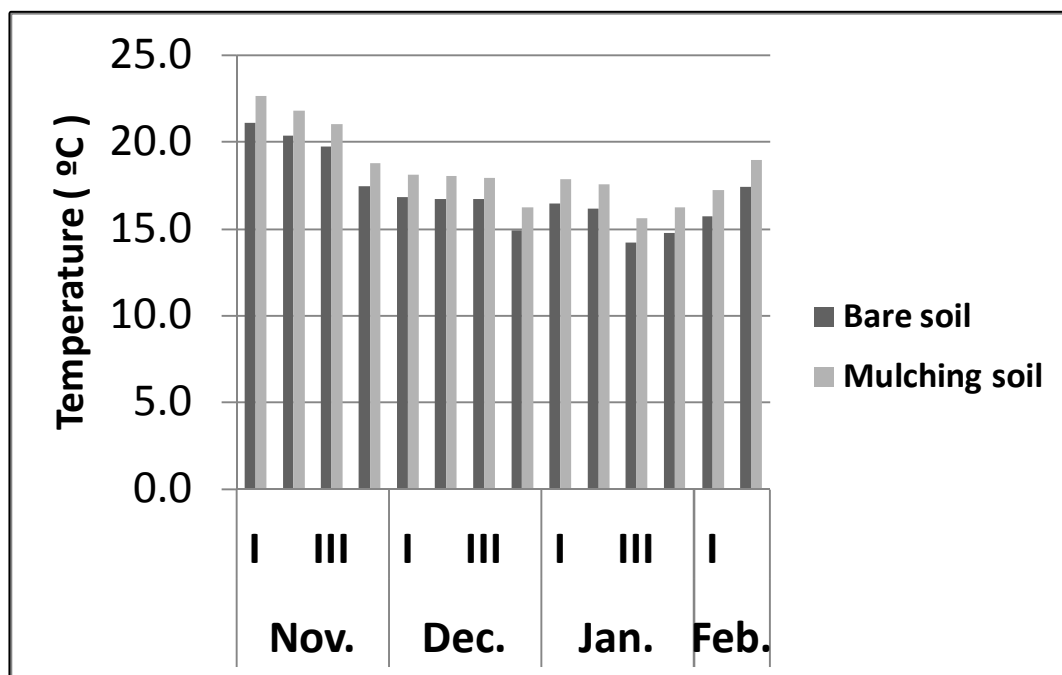


Fig. 1: The average mean temperature under polyethylene compared to the control (bare soil) in the studied 2015/2016 and 2016/2017 seasons.

I: 1st week; II 2nd week; III: 3rd week; IV: 4th week.

The effect of soil mulching and different organic fertilizers on broccoli vegetative growth and yield

The effect of different soil treatments combined sources of organic fertilizer on vegetative and yield parameters of broccoli are presented in table (4). Regarding to the effect of soil treatments, plant high, leaves number per plant and fresh weight of shoots and yield parameters (Head weight (g/plant), and head diameter) recorded the higher values with mulching compared to bare soil. Whill, there was no significant different on the dey weight.

Concerning to the effect of different sources of organic fertilizer, added viernecompast during soil preparation recorded the highest vegetative growth and yield parameters, while, rabbit manure recorded the lowest value. Vermicompost presented significant positive effect on the vegetative growth and yield of broccoli.

As for the interaction between soil treatments and sources of organic fertilizer in table (4) data indicated that, mulching combined with viernecompast gave the heights values for all vegetative growth and yield parameters. On the other hand, the lowest value were recorded with rabbit manure combined with bare soil

Table (4): Effect of different organic fertilizers and soil treatments on vegetative and yield characteristics of broccoli.

Broccoli	Organic fertilizer source							
	First season (2015/2016)				Second season (2016/2017)			
	Plant high (cm)							
Soil treat.	R.M	C.M	V.C	Mean A	R.M	C.M	V.C	Mean A
Mulching soil	77.5 b	82.5 a	84.0 a	81.3A	74.2 ab	77.8 a	80.8 a	77.5A
Bare soil	67.5 c	75.0 b	76.5 b	73.0B	64.8 c	66.5 bc	74.0 ab	68.4B
Mean B	72.5C	78.8B	80.3A		69.5B	72.1B	77.4A	
Number of leaves								
Mulching soil	25.0 bc	25.7 ab	27.5 a	26.1A	23.3 bc	24.0 a	25.7 a	24.3A
Bare soil	22.8 c	23.5 bc	24.6 bc	23.6B	21.3 c	22.0 bc	23.0bc	22.1B
Mean B	23.9B	24.6B	26.1A		22.3B	23.0B	24.3A	
Fresh weight (g/ plant)								
Mulching soil	1045.7 bc	1241.7 b	1675.3 a	1320.9A	1048.7 cd	1261.3 b	1513.3 a	1274.4A
Bare soil	900.3 c	1228.0 b	1273.3 b	1133.9B	922.3 d	1160.3 bc	1236.0 bc	1106.2B
Mean B	973.0C	1234.8B	1474.3A		985.5C	1210.8B	1374.7A	
Dry weight (g)								
Mulching soil	104.7bc	94.3 bc	143.0 a	112.8A	98.83 b	96.17 b	129.50a	108.17A
Bare soil	92.3 c	104.7 bc	114.3 ab	103.8A	95.33 b	99.33 b	112.00 ab	102.22A
Mean B	96.7B	99.5B	128.7A		97.08B	97.75B	120.75A	
Head weight (g)								
Mulching soil	316.5 d	347.5 bc	396.5 a	353.5A	291.0 cd	332.5 b	367.7 a	330.4A
Bare soil	289.7 d	322.7 cd	369.3 ab	327.2B	286.0 d	294.7 c	339.5 ab	300.7B
Mean B	303.1C	335.1B	382.9A		279.5C	313.6B	353.6A	
Head diameter (cm)								
Mulching soil	12.7 de	14.4 bc	15.3 a	14.1A	12.5 c	13.7 b	11.8 c	13.5A
Bare soil	12.3 e	13.7 cd	14.5 ab	13.5B	11.1 d	12.7 c	13.7 b	12.5B
Mean B	12.5C	14.1B	14.9A		11.8C	13.2B	14.0A	

Rabbit manure (R.M), cattle manure (C.M), viermecompost (V.C)

Nitrogen, phosphorus and potassium content (%) of broccoli plants

The effect of different soil treatments combined and sources of organic fertilizer on nitrogen, phosphorus and potassium content (%) in shoot of broccoli plants is presented in table (5). Implement mulching gave the higher nitrogen, phosphorus and potassium content (%) in shoot of broccoli plants compared to bare soil. On the other hand, added viermecompost recorded the heights nitrogen, phosphorus and potassium content (%). On the contrary; the lowest values were recorded with added cattle manure followed by rabbit manure with significant different between them except in potassium content (%) there were no significant different between them. Concerning the interaction between soil treatments and sources of organic fertilizer, applied the

combined between viermecompast and mulching gave the heights nitrogen, phosphorus and potassium content (%). While, the combined between rabbit manure and bare soil gave the lowest values.

Table (5): Effect of different organic fertilizer and soil treatments on nitrogen, phosphorus and potassium content (%) in shoot of broccoli plants.

Broccoli	Organic fertilizer source							
	First season (2015/2016)				Second season (2016/2017)			
	Nitrogen (%)							
Soil treat.	R.M	C.M	V.C	Mean A	R.M	C.M	V.C	Mean A
Mulching soil	1.86 bc	1.91 b	2.01 a	1.93 A	1.79 bc	1.85 b	1.97 a	1.87 A
Bare soil	1.64 e	1.75 d	1.8 cd	1.73 B	1.56 e	1.68 d	1.75 c	1.66 B
Mean B	1.75 C	1.83 B	1.91 A		1.68 C	1.77 B	1.86 A	
Phosphorus (%)								
Mulching soil	0.26 cd	0.28 bc	0.32 a	0.29 A	0.25 cd	0.27 abc	0.3 a	0.28 A
Bare soil	0.25 d	0.27 bcd	0.3 ab	0.27 B	0.24 d	0.26 bcd	0.29 ab	0.26 B
Mean B	0.26 C	0.28 B	0.31 A		0.25 C	0.27 B	0.29 A	
Potassium (%)								
Mulching soil	2.52 bc	2.58 b	2.8 a	2.63 A	2.47 b	2.5 b	2.69 a	2.55 A
Bare soil	2.45 d	2.46 cd	2.79 a	2.57 B	2.38 c	2.36 c	2.65 a	2.46 B
Mean B	2.49 B	2.52 B	2.79 A		2.43 B	2.43 B	2.67 A	

Rabbit manure (R.M), cattle manure (C.M), viermecompost (V.C)

The effect of soil mulching and different organic fertilizers on celery

Vegetative growth and yield

The effect of different soil treatments and sources of organic fertilizer combination on vegetative and yield characteristics of celery are presented in table (6).

The effect of soil treatments, mulching gave the higher values for all vegetative growth and yield parameters compared to bare soil.

Referring to the effect of different sources of organic fertilizer, the highest vegetative growth and yield parameters were estimated with applied viermecompast during soil preparation followed by cattle manure. While, rabbit manure recorded the lowest value.

As for the interaction between soil treatments and sources of organic fertilizer in table (6) data indicated that, adding viermecompast with mulching combination gave the heights values for all vegetative growth and yield parameters. While, rabbit manure with bare soil recorded the lowest values.

Table (6): Effect of different organic fertilizer and soil treatments on vegetative and yield characteristics of celery.

Celery	Organic fertilizer source							
	First season (2015/2016)				Second season (2016/2017)			
	Soil treat.	Plant height (cm)						
		R.M	C.M	V.C	Mean A	R.M	C.M	V.C
Mulching soil	53.0 ab	52.7 ab	57.3 a	54.3 A	57.0 ab	56.7 ab	62.3 a	58.7 A
Bare soil	44.3 c	48.3 bc	52.3 ab	48.3 B	48.3 c	53.0 bc	56.0 7 b	52.7 B
Mean B	48.7 B	50.5 B	54.8 A		52.7 B	54.8 B	59.5 A	
	Number of leaves							
Mulching soil	24.5 ab	24.3 ab	26.7 a	25.2 A	26.7 ab	26.3 ab	28.7 a	27.2 A
Bare soil	20.7 c	22.7 bc	24.3 ab	22.7C	22.7 c	24.7 bc	26.3 ab	24.6 B
Mean B	22.58 B	23.5 B	25.5 A		24.7 B	25.5 B	27.5 A	
	Plant fresh weight (g)							
Mulching soil	1300.0 b	1522.0 a	1547.7 a	1456.6A	1347.7 b	1590.0 a	1621.0 a	1519.6 A
Bare soil	944.7 d	1028.3 c	1061.0 c	1011.3 B	990.0 d	1124.7 c	1108.7 cd	1074.6 B
Mean B	1122.3 B	1275.2A	1304.3A		1169.0B	1357.3A	1364.8A	
	Dry weight (g)							
Mulching soil	91.0 C	111.7 b	122.7 a	108.4 A	96.0 c	117.0 b	128.0 a	113.7 A
Bare soil	62.3 e	69.7 de	74.7 d	68.9 B	69.3 e	77.3D e	79.0 d	75.2 B
Mean B	76.7 C	90.7 B	98.7 A		82.7 C	97.2 B	103.5 A	

Rabbit manure (R.M), cattle manure (C.M), viermecompost (V.C)

Nitrogen, phosphorus and potassium content (%) of Celery plants

The effect of different soil treatments combined and sources of organic fertilizer on nitrogen, phosphorus and potassium content (%) in shoot of celery plants is presented in table (7). Concerning the effect of soil treatments on the content of nitrogen, phosphorus and potassium content (%) in shoot of celery plants data show that, mulching caused a significant increase in nitrogen, phosphorus and potassium content (%) in shoot of celery plants as compared with bare soil (control treatment). In addition, adding viermecompast recorded the heights values of nitrogen, phosphorus and potassium content (%) in shoot of celery plants while rabbit manure gave the lowest values. As for the interaction effect between soil treatments and sources of organic fertilizer on the content of nitrogen, phosphorus and potassium (%) data revealed that, the heights content of nitrogen, phosphorus and potassium content (%) in shoot of celery plant were recorded with mulching combined with viermecompost. On the other hand, the lowest values of N, P and K were recorded with rabbit manure combined with bare soil.

Table (7): Effect of different organic fertilizer and soil treatments on nitrogen, phosphorus and potassium content (%) in shoot of celery plants.

Broccoli	Organic fertilizer source							
	First season (2015/2016)				Second season (2016/2017)			
	Nitrogen (%)							
Soil treat.	R.M	C.M	V.C	Mean A	R.M	C.M	V.C	Mean A
Mulching soil	1.01 cd	1.70 b	1.85 a	1.52 A	0.99 cd	1.67 b	1.81 a	1.49 A
Bare soil	0.91 d	1.14c	1.50 b	1.18 B	0.89 d	1.11 c	1.47 b	1.16 B
Mean B	0.96 C	1.42 B	1.68 A		0.94 C	1.39 B	1.64 A	
Phosphorus (%)								
Mulching soil	1.06 d	1.18 c	1.42 a	1.22 A	1.26 ab	1.16 ab	1.39 a	1.27 A
Bare soil	0.93 e	1.14 c	1.29 b	1.12 B	0.91 b	1.12 ab	1.26 a	1.10 B
Mean B	0.99 C	1.16 B	1.36 A		1.08 B	1.14 B	1.33 A	
Potassium (%)								
Mulching soil	3.40 c	4.13 ab	4.37 a	3.97 A	3.33 c	4.05 ab	4.28 a	3.89A
Bare soil	3.20 c	3.88 b	4.24 b	3.77 B	3.14 c	3.80 b	4.16 a	3.70B
Mean B	3.30 C	4.01 B	4.30 A		3.23 C	3.93 B	4.22 A	

Rabbit manure (R.M), cattle manure (C.M), vierme compost (V.C)

DISCUSSION

From all the resultues. Data indicated that, used vierme compost lead to incresing all vegetative and yield characteristics as well as contents of N, P and K (%) of broccoli and celery. These results may be attributed to the suitable root environment and more nutrient availability. These results may be agreement with Azarmi *et al.* (2009), Pant *et al.* 2009, Reddy and Ohkura 2004, Gajalakshmi and Abbasi 2002, Moghadam *et al.* 2012 and Uma and Malathi 2009 they concluded that leaf dry weight, chlorophyll content and number of leaves of cucumber (*Cucumis sativus*) increased on vermicompost applications Furthermore, Alvarez and Grigera, (2005) stated there is evidence that humic acids extracted from vermicompost stimulated increase in the number of roots, giving the plant ability to scavenge nutrient from the growing environment for growth and development. A promotion effect of vermicompost on chlorophyll contents might be attributed to the fact that N is a constituent of chlorophyll molecule. Moreover, nitrogen is the main constituent of all amino acids in proteins and lipids that acting as a structural compounds of the chloroplast. Reddy *et al.* 1998 reported that addition of vermicompost into vegetables crop field with N, P,K nutrients could be very effective response on the growth of vegetables crops. The mineralization of organic matter, decrease of soil pH by organic acids produced in vermicompost and increases micronutrient complexes formation. Same results were obtained in several horticultural crops such as tomato (Hashemimajd, *et al.* 2004 and Gutiérrez-Miceli *et al.*, 2007), pepper (Arancon *et al.*, 2005), garlic (Argüello *et al.*, 2009), aubergine (Gajalakshmi and Abbasi, 2004), strawberry (Arancon *et al.*, 2004), and green gram (Karmegam *et al.*, 1999). As for the effect of mulching soil the previous results in these study indicated that using mulch enhanced all vegetative and yield characteristics as well as contents of N, P and K (%)of broccoli and celery. These results may be due to, mulching increased soil moisture, organic matter contents leading to suitable environment

for root penetration. Ghuman and sur. (2001) concluded that mulching decreases bulk density of the surface soil. The soil organic matter increased due decomposition of applied mulch. Applications of crop residue mulches increase soil organic carbon contents (Havlin *et al.*1990, Paustin *et al.* 1997, Duiker and Lal 1999, Saroa and Lal 2003). Lal *et al.* (1980) and Khurshid *et al.*(2006) concluded that organic matter was significantly higher when more mulch was applied. Acharya and Sharma (1994) and Muhammad *et al.* (2009) observed that mulched treatments show significantly greater total uptake of nitrogen, phosphorus and potassium than corresponding unmulched ones. Aliudin (1986) reported that mulches conserved more soil moistures, enhances vegetative growth and yield contributing characters of garlic.

CONCLUSION

The study offered multi option for using different organic fertilizer sources. The recommended under these study could be summerized as impplement soil mulching compined vermicompos as an organic fertilizer to obtained the highest yield of broccoli and celery under Egyptian condition.

The further objective of mitigate greenhouse gases (GHG) save environment, nutrient resource and essential nutrients would achieved by vermicomposting technique implementation on organic urban wastes. Vermicompost appears to be a promising substitute for organic fertilizers. It is also a sustainable solution for management of organic wastes which are major source of environmental pollution.

ACKNOWLEDGEMENTS

The authors acknowledge the support was provided by "Integrated environmental management of urban organic wastes using vermicomposting and green roof (VCGR) project" No. 1145, funded by Science and Technology Development Fund (STDF), Egypt.

REFERENCES

1. Abou El- Magd, M.M, Hoda, A. Mohamed and Z.F. Fawzy 2005. Relationship growth, yield of broccoli with increasing N, P or K ratio in a mixture of NPK fertilizers (Brassica oleracea var italica plenck). Annals of Agriculture Science, Moshtohor. 43(2): 791-805.
2. Abul-Soud M. A., Emam, M. S. A., Abdrabbo, M. A. A. , Hashem, F. A. and Shaimaa H. Abd-Elrahman. 2014. Sustainable Urban Horticulture of Sweet Pepper via Vermicomposting in Summer Season. Journal of advances in agriculture 3 (1): 110-111.
3. Abul-Soud M.A., Emam M.S.A. and Abd El-Rahman N., G. 2015(a). The potential use of vermicompost in soilless culture for producing strawberry. International Journal of Plant & Soil Scienc; 8 (5): 1 – 15.
4. Abul-Soud M.A., Emam M.S.A., Hawash A.H., Hassan M. and Maharik, Z. Y. 2015(b). The utilize of vermicomposting outputs in ecology soilless culture of lettuce. Journal of Agriculture and Ecology Research, 5(1): 1-15, Article no.JAERI.20008
5. Abul-Soud, M., El-Ansary, D.O. and Hussein, A.M. 2010. Effects of Different Cattle Manure Rates and Mulching on Weed Control and Growth and Yield of Squash Journal of Applied Sciences Research, 6(9): 1379-1386.
6. Abul-Soud, M., Hassanein, M. K. , Ablmaaty, S.M., Medany, M. and Abu- Hadid, A.F. 2009.Vermiculture and vermicomposting technologies use in sustainable agriculture in Egypt, Egypt. J. Agric. Res., 87 (1).389-403
7. Acharya C L and Sharma, P. D. (1994). Tillage and mulch effects on soil physical environment, root growth, nutrient uptake and yield of maize and wheat on an Alfisol in north-west India. Soil Tillage Research 4: 291–302

8. Albanell, E., Plaixats, J. and Cabrero, T. (1988) Chemical changes during vermicomposting (*Eisenia fetida*) of sheep manure mixed with cotton industrial wastes. *Biology and Fertility of Soils*, 6:266-269.
9. Aliudin T., (1986). Effect of Soil tillage and application of mulch on yield of field grown garlic. *Buletin-Penelitian-Hortikultura* 8: 12-15
10. Allen, S. E. (1974). *Chemical Analysis of Ecological Materials*. Black-Well, Oxford. : 565.
11. Alvarez R., and Grigera, S. 2005. Analysis of soil fertility and managements on yields of wheat and corn in the rolling pampa of Argentina. *J. Agron.Crop Sci.*, 191: 321-329.
12. Arancon, N.Q., Edwards, C.A., Bierman, P., Metzger, J.D. and Lucht, C. (2005). Effects of
13. Arancon, N.Q., Edwards, C.A., Bierman, P., Welch, C. and Metzger, J.D. (2004). Influences of vermicomposts on field strawberries: 1. effects on growth and yields. *Bioresource Technology* 93: 145-153.
14. Argüello, J.A., Ledesma, A., Núñez, S.B., Rodríguez, C.H. and Díaz Goldfarb, M.D.C.,
15. Azarmi R., M.T. Giglou and R.D. Taleshmikail (2009). Influence of vermicompost on soil chemical and physical properties in tomato (*Lycopersicum esculentum*) field. *Afr J Biotechnol* 7(14):2397–2401
16. Bwamiki, D.P., Zake, J.Y.K., Bekunda, M.A, Woome, P.L., Bergstrom LH. And Kirchman, 1998. Use of coffee husks as an organic amendment to improve soil fertility in Ugandan banana production. *Carbon and nitrogen dynamics in natural and agricultural tropical ecosystem*. 1998, 113-127.
17. Chapman, H.D. and Pratt, P. F. (1961). *Methods of Analysis for Soil, Plant and Water*. University of California, USA.
18. Chatterjee, B.M.,P. Ghanti, U. Thapa and P. Tripathy (2005). Effect of organic nutrition in sprouting broccoli (*Brassica alaraceae* var. *italica* plenck), *Vegetable Science*, 33 (1): 51-54.
19. Duiker S W and Lal , R. (1999) Crop residue and tillage effects on carbon sequestration in a Luvisol in central Ohio. *Soil Tillage Research* 52, 73–81 .
20. Edwards, C. A. and Neuhauser, E. F. (1998) *Earthworms in Waste and Environmental Management*, SPB Acad. Publ., The Hague, The Netherlands.
21. El-Nemr, M.A., 2006. Effect of Mulch Types on Soil Environmental Conditions and Their Effect on the Growth and Yield of Cucumber Plants. *Journal of Applied Sciences*, 2(2): 67-73.
22. FAO (Food and Agriculture Organization) (1980). *Soil and Plant Analysis*. *Soils Bulletin* 38/2,250.
23. Farag A. A. and Shaimaa H. Abd-Elrahman. (2016). Greenhouse Gas Emission from Cauliflower Grown under Different Nitrogen Rates and Mulches. *International Journal of Plant & Soil Science*. 9(1): 1-10.
24. Farag, A.A., Abdrabbo, M. A.A. and Hassanein, M. M. K. (2010). Response of Cucumber for Mulch Colors and Phosphorus Levels under Greenhouse. *Egyptian Journal of Horticulture* 37 (1)53-62.
25. Gajalakshmi S., Abbasi, S.A. (2002) Effect of the application of water hyacinth compost/vermicompost on the growth and flowering of *Crossandra undulaefolia*, and on several vegetables. *Bioresour Technol* 85(2):197–199
26. Gajalakshmi,S. and Abbasi, S.A. (2004). Neem leaves as a source of fertilizer-cum-pesticide vermicompost. *Bioresource Technology* 92: 291-296.

27. Garg, V.K. and Kaushik, P. 2005. Vermistabilization of textile mill sludge spiked with poultry droppings by an epigeic earthworm *Eisenia foetida*. *Biores. Technol.*, 96: 1063–1071.
28. Ghuman B. S. and Sur, H. S. (2001). Tillage and residue management effects on soil properties and yields of rainfed maize and wheat in a subhumid subtropical climate. *Soil Tillage Research* 58: 1–10
29. Gutiérrez-Miceli, F.A., Santiago-Borraz, J., Montes Molina, J.A., Nafate, C.C., Abdud-Archila, M., Oliva Llaven, M.A., Rincón-Rosales, R. and Deendoven L. (2007). Vermicompost as a soil supplement to improve growth, yield and fruit quality of tomato (*Lycopersicon esculentum*). *Bioresource Technology* 98: 2781-2786.
30. Hand, P., Hayes, W. A., Frankland, J.C. and Satchell, J.E. (1988). The vermicomposting of cow slurry. *Pedobiologia* 31, 199–209.
31. Hashemimajd, K., Kalbasi, M., Golchin, A. and Shariatmadari, H. (2004). Comparison of vermicompost and composts as potting media for growth of tomatoes. *Journal of Plant Nutrition*. 6:1107-1123.
32. Havlin J. L., Kissel, D. E. , Maddus, L. D. , Claassen, M. M. and Long, J. H. (1990). Crop rotation and tillage effects on soil organic carbon and nitrogen. *Soil Science Society of American Journal* 54: 448–452 .
33. Hoitink, H.A.J. 1993. Proceedings Review: International Symposium on composting research. *Compost Science and Utilization*. :37.
34. Inbar, Y., Chen, Y., Hadar, Y. 1993. *Journal of Environmental Quality*., 22: 875-863.
35. Johnston, A.M., Janzen, H.H., Smith, E.G., 1995. Long-term spring wheat response to summerfallow frequency and organic amendment in southern Alberta. *Canadian Journal of Plant Science* 75 (2): 347-354.
36. Karmegam, N., Alagumalai, K. and Daniel, T. (1999). Effect of vermicompost on the growth and yield of green gram (*Phaseolus aureus* Roxb.). *Tropical Agriculture* 76: 143-146.
37. Kaushik, P. and Garg, V.K. (2003). Vermicomposting of mixed solid textile mill sludge and cow dung with epigeic earthworm *Eisenia foetida*. *Biores. Technol.*, 90: 311–316.
38. Khan, A.R., Srivastava, R.C., Ghorai, A.K. and Singh, S.R. 2003. Efficient Soil Solarization for Weed Control in Rainfed Upland Rice Ecosystem. *International Agrophysics*. 17 (3): 99-103.
39. Khurshid K., Iqbal, M., Arif, M. S. and Nawaz, A. (2006). Effect of tillage and mulch on soil physical properties and growth of maize. *International Journal of Agriculture & Biology* 8: 593–596
40. Kumar, A., (2005). “Vermis and Vermitechnology”, A.P.H Publishing Corporation, New Delhi.5: 71.
41. Lal R., De Vleeschauwer, D. and Nganje, R. M. (1980). Changes in properties of a newly cleared tropical Alfisols as affected by mulching. *Soil Science Society of American Journal* 44: 827–833 .
42. Li, S.X., Wang, Z.H., Li, S.Q., Gao, Y.J. and Tian, X.H. 2013. Effect of Plastic Sheet Mulch, Wheat Straw Mulch, and Maize Growth on Water Loss by Evaporation in Dry Land Areas of China. *Agricultural Water Management*, 116: 39–49.
43. Ministry of Agriculture and Land Reclamation (2009). Symptoms of nutrient deficiency on some field and horticultural crops. *Soils, Water and Environ. Res. Inst., Agric. Res. Center*.

44. Moghadam A.R.L., Ardebill, Z.O. and Saidi, F. (2012) Vermicompost induced changes in growth and development of *Lilium Asiatic* hybrid var. Navona. *Afr J Agric Res* 7(17):2609–2621
45. Moursy, S.F., Mostafa, A.F. and Solieman, Y.N. 2015. Polyethylene and Rice Straw as Soil Mulching: Reflection of Soil Mulch Type on Soil Temperature, Soil Borne Diseases, Plant Growth and Yield of Tomato. *Global Journal of Advance Research*, 2 (10): 1497-1519.
46. Muhammad A. P., Muhammad, I. and Khuram, S. (2009). Effect of mulch on soil physical properties and NPK concentration in Maize (*Zea mays*) shoots under two tillage system. *International Journal of Agriculture & Biology* 11: 120-124
47. Najafabadi MBM, Peyvasta, G.H., Asila, M.H., Olfatia, J.A. and Rabieeb, M. (2012). Mulching effects on the yield and quality of garlic as second crop in rice fields. *Int. J. Plant Prod*, 6(3):279-290.
48. Orozco, S.H., Cegarra, J., Trujillo, L.M., and Roig, A. (1996) Vermicompostsing of coffee pulp using the earthworm *Eisenia fetida*: effects on C and N contents and the availability of nutrients. *Biology and Fertility of Soils*. 22: 162-166.
49. Page, A. L., Miller, R. H. and Keeny, D. R. (1982). *Methods of Soil Analysis. Part 2. Chemical and Microbiological Properties* (2nd ed.) Amer. Soc. Agron. Monograph No. 9, Madison, Wisconsin, USA.
50. Pant A.P., Radovich, T.J.K., Hue, N.V., Talcott, S.T. and Krenek, K.A. (2009) Vermicompost extracts influence growth, mineral nutrients, phytonutrients and antioxidant activity in pak choi (*Brassica rapa* cv. Bonsai, chinensis group) grown under vermicompost and chemical fertilizer. *J sci Food Agric* 89(14):2383–2392
51. Paustin K., Collins, H. P. and Paul, E. A. (1997). Management controls of soil carbon. In: Paul, E., *et al.* (eds.), *SOM in Temperate Agroecosystems: Long Term Experiments in North America*, : 15–49. CRC Press Inc
52. Ramesh, P., Singh, M., and Rao, S.A. (2005). “Organic Farming: Its Relevance to the Indian Context. *Curr. Sci.*, 88 (4):561-568.
53. Raul, I.C. (1996). *Measuring physical properties*. Rutgers Cooperative Extension. New Jersey Agriculture Experiment Station. New Jersey University.
54. Reddy M.V. and Ohkura, K. (2004). Vermicomposting of rice –straw and its effects on sorghum growth. *Trop Ecol* 45(2): 327- 331.
55. Reddy R., M.A.N. Reddy, Y.T.N.Reddy, N.S.Reddy, N. Anjanappa and R. Reddy (1998). Effect of organic and inorganic sources of NPK on growth and yield of pea [*Pisum sativum*(L)]. *Legume Research* 21(1):57–60.
56. Saroa G. S. and Lal, R. (2003) Soil restorative effects of mulching on aggregation and carbon sequestration in a Miamian soil in Central Ohio. *Land Degrade Development* 14: 481–493 .
57. SAS Institute (1990). *SAS Procedures Guide. Version 6, third edition*. SAS Institute, Cary.
58. Singh, A. and Sharma, S. (2002). Composting of a crop residue through treatment with microorganisms and subsequent vermicomposting. *Biores. Technol.* 85, 107–111.
59. Singh, K. and Kamal, S. 2012. Effect of Black Plastic Mulch on Soil Temperature and Tomato Yield in Mid Hills of Garhwal Himalayas. *Journal of Horticulture and Forestry* 4: 78-80.
60. Singh, S.S., Haidar, M.G., Khan, A.R., Sikka, A.K., Prasad, L.K., John, L.G. and Singh, J.P. 2007. Effect of Nematode Management on Rice Grain Yield in Nursery. *Afro Asian Journal of Nematology*, 17 (1): 13 -16

61. Snedecor, G.W. and Cochran, W.G. (1981). "Statistical Methods" 7th ed., Iowa State Univ., Press, Ames, Iowa, USA, 225-330. vermicomposts produced from cattle manure, food waste and paper waste on the growth and yield of peppers in the field. *Pedobiologia*, 49: 297-306.
62. Uma B. and Malathi, M. (2009) Vermicompost as a soil supplement to improve growth and yield of *Amaranthus* species. *Res J Agric Biol Sci* 5(6):1054–1060
63. Wilson, G. C. S. (1983). The physio-chemical and physical properties of horticultural substrates. *Acta Horticulture*.150: 19-32.
64. Zhou, L.M., Li, F.M., Jin, S.L. and Song, Y.J. 2009. How Two Ridges and the Furrow Mulched With Plastic Film Affect Soil Water, Soil Temperature and Yield of Maize on the Semiarid Loess Plateau of China. *Field Crops Research*, 113: 41–47. 18.

تأثير استخدام الاسمدة العضوية و تغطية التربة على الانتاج المستدام للبركلى و الكرفس

محمد ابو السعود ، احمد عونى احمد فرج ، زكريا يحيى محاريق

المعمل المركزى للمناخ الزراعى ، مركز البحوث الزراعية ، الجيزة ، مصر

نتيجة الحاجة الملحة الى الانتاج المستدام من الخضر تحت الظروف الشبة جافة فى مصر و لزيادة الانتاج كان من الضرورى الاتجاة الى استخدام مصادر مختلفة من الاسمدة العضوية وذلك لتحسين انتاجية محاصيل الخضر. ولتحقيق هدف البحث تم اجراء التجارب خلال موسمى شتاء ٢٠١٦/٢٠١٥ تحت صوبة متعددة الاقبية مغطاة بالشبك وذلك بالمعمل المركزى للمناخ الزراعى - مركز البحوث الزراعية - جيزة - مصر وذلك لدراسة تطبيق اضافات مختلفة من الاسمدة العضوية (سماد مواشى ، سماد ارانب ، مكمورة دودة الارض) بالارتباط مع دراسة معاملات لتغطية التربة (بدون تغطية ، تغطية التربة (ملش)) وتأثير ذلك على انتاجية كل من محصول البركلى و الكرفس .

قد اوضحت النتائج المنحصل عليها ما يلى:

- تطبيق استخدام مكمورة دودة الارض كمصدر للتسميد اثناء تجهيز الارض للزراعة اعطى اعلى النتائج لكل من النمو الخضرى و المحصول فى كل من الكرفس و البركلى
- تغطية التربة بالملش اعطى اعلى النتائج لكل من النمو الخضرى و المحصول لكل من الكرفس و البركلى
- تطبيق اضافة مكمورة دودة الارض مع تغطية التربة بالملش اعطى اعلى النتائج للنمو الخضرى و المحصول فى حين تطبيق اضافة سماد الارانب و بدون تغطية التربة اعطى اقل النتائج لكل من محصول الكرفس و البركلى
- مكمورة دودة الارض الناتجة من مخلفات المدن و التى تم تطبيقها كسماد عضوى فى التربة ادت الى زيادة محصول كل من الكرفس و البركلى مع تخزين غاز ثانى اكسيد الكربون فى التربة و تقليل الانبعاثات.
- لذلك يوصى اضافة سماد مكمورة دودة الارض اثناء تجهيز الارض للزراعة مع تغطية الارض بالملش .

PERFORMANCE OF A PHOTOVOLTAIC SYSTEM TO POWER A DEVELOPED ELECTRIC TRACTOR

EMARA, R. Z.¹, M. A. ELTAWIL², S. E. ABOUZAHER²,
G. H. ELSAYED¹ and I. A. ABDELMOTALEB²

¹ *Agricultural Engineering Research Institute, ARC, Dokki, Giza, Egypt.*

² *Faculty of Agriculture, Kafrelsheikh University, Kafrelsheikh, Egypt.*

Abstract

Solar photovoltaic (PV) systems have shown their potentiality in its usage rural projects around the world. With decreasing continual prices of PV systems, it becomes economically attractive and growing experience gained with the use of PV in the agriculture activities, in turn obtaining a significant impact on rural development. The current work aims to study the performance of PV system [power output, (P_{output}), and conversion efficiency, (η_{PV})] to operate a developed standalone an electric solar tractor under two tilt angles of PV panel (0 and 30°). Also, control circuits of brush DC motor based on pulse width modulation (PWM) were designed, manufactured and evaluated. The designed system allows controlling speed of the DC motor in both of forward and reversing direction. The obtained results indicated that, the daily average (P_{output}) of PV reaches about 1.95 and 2.15 kWh for 0 and 30° tilt angles, respectively. While the daily average of η_{PV} is about 13.2 and 13.3 % for 0 and 30° tilt angles, respectively. These results were corresponding to daily average insolation of 788.89 and 859.33 W/m² at daily average PV module temperature of 36.2 and 37.4°C for 0 and 30°, respectively. The experimental setup offers many advantages such as simple structure, low cost, accurate, quite efficient, and light mass. This work is considered as a primary step for the commercial use of a solar powered electric tractor for light service in the agricultural farm.

Keywords: tilt angle; electrical vehicle; solar modules; conversion efficiency, standalone automated tractor.

INTRODUCTION

Electric and hybrid engines are the ancestors of modern power sources, and will likely be the descendants of them as well. Advanced technology, along with the desire to improve efficiency and functionality of current vehicles will likely lead to near and long-term development of hybrid electric vehicles (HEV). The Energy Storage System (ESS) is the most important challenges for development of HEVs. In this relevant power density, energy density, and cost deem typically are the three most important considerations. So, the ESS design rely or depending on the electric motor selection, the vehicle's power electric range requirement, space and weight constraints, safety, recharging, and cost considerations.

Renewable energy sources (RES) are friendly with the environment. In turn, optimal use of these resources minimizes environmental stresses, produce minimum secondary wastes and are sustainable based on current and future economically social needs. Sun is the source of all energies and the primary forms of solar energies are heat and light. Sunlight and heat are transformed and absorbed by the environment in a multi ways.

Renewable energy technologies offer an excellent opportunity for mitigation of greenhouse gas emission and reducing global warming through substituting conventional energy sources (Panwar et al., 2011).

The renewable energy is the primary, domestic and clean or inexhaustible energy resources (Dincer, 2001 and Bilgen et al., 2004). RESs are also called alternative energy sources. As concern, RES represents 14% of the total world energy demand (UNDP, 2000). The share of RESs is expected to increase very significantly (30-80% in 2100) (Fridleifsson, 2001).

Renewable energy system development results in improving energy supply reliability and organic fuel economy; increasing the living standers population; ensuring sustainable development of the remote regions in the desert areas; implementing of the obligations of the countries about fulfilling the international agreements relating to environmental protection (Farhad et al., 2008; Sims, 2004 and Zakhidov, 2008).

Increasing consumption of fossil fuel to meet the current energy demands alarm over the energy crisis generating a resurgence of interests in promoting renewable alternatives to face the developing world's growing energy needs (Youm et al., 2000; and Horst and Hovorka, 2009). To monitor emission of the greenhouse gas emissions signed made to comply the overall pollution prevention targets, the Kyoto Protocol agreement (Holm-Nielsen, et al., 2009). Sustainable development requires methods and tools to measure and compare the environmental impact of human activities for various products (Dincer, 2001).

Electrical energy is the pivot of all developmental efforts in both the developed and the developing countries because conventional energy sources are finite and fast depleting (Okoro and Madueme, 2006). In the last decades, energy related problems are becoming more and more important and involve the ideal use of resources, the environmental impact owing to the emission of pollutants and the consumption of conventional energy resources (Stoppato, 2008).

The power output of the PV module depends on number of cells that make the module, type of cells, total surface area of the module, solar radiation, module temperature, wind velocity, etc. The electric drive systems used in industrial applications are increasingly required to meet higher performance and reliability requirements. The DC motor is an attractive piece of equipment in many industrial applications requiring variable speed and load characteristics due to its ease of controllability (Thakare and Kompelli, 2014).

With regard to the DC motors, there are attempts to control the motor speed either by a variable resistor or variable resistor connected to a transistor. While the latter approach works well but it generates heat and increase waste power. The use simple pulse width modulation (PWM) with DC motor eliminates these problems. It controls the motor speed by driving the motor with short pulses. These pulses vary in duration to change the speed of the motor. The longer the pulses, the faster the motor turns, and vice versa (Hughes, 2006).

The current study was intended to develop a stand-alone solar electrical tractor for light service in the agricultural field. The capability of a solar PV system as the main source of power to operate a developed automated tractor was investigated. Several control circuits were designed, manufactured and used to control the motion of the developed tractor. The developed solar powered automated tractor (SPAT) is a multipurpose, integrated energy system for a series of services, which include energy storage, power production on demand. The main advantage is to reduce the pollution derived from fossil fuels (traditional fuel) by using renewable energy and automated control. The power output, (P_{output}), and conversion efficiency (η_{PV}) for solar module as input to a stand-alone solar tractor at two tilt angles of PV panel and different time of the day

corresponding to weather conditions were studied as the main target of this investigation. The control circuits were simulated and evaluated.

MATERIALS AND METHODS

The experimental setup was designed, manufactured, assembled and evaluated in Rice Mechanization Center at Meet El-Deeba, Kafr El-Sheikh Governorate, AEnRI, ARC, Egypt, which locates at latitude 31.07°N and longitude 30.57°E.

To carry out this study, five stages of work and testes have been done as follows:

I) Constructing a suggested light vehicle representing a solar powered electrical tractor to suit light services; II) Investigating the performance of PV system at 0° and 30° tilt angles facing south stationary positions; III) Simulating all control circuits to determine all electronic component values such as resistors and capacitors included in PWM application; IV) Carrying out the preliminary experiments to check and to explore, and overcome the associated mechanical and electronic problems, and V) Investigating the performance of the developed solar powered automated tractor (SPAT) for light service viz spraying operation under local Egyptian conditions.

Constructing the targeted SPAT:

Main frame (chassis):

The main frame was made from steel beams have C (channel) section of 7.5 x 4 x 0.5 cm to carry the components of the SPAT. It has 80 cm vertical clearance above the ground surface to avoid plant damage. After finishing the main frame, the following components were attached Fig. 1.



Fig. 1: The main frame of the SPAT.

Traction Motor:

A DC brush motor was used as a power source for forward and reverse tractor motion. The specifications of that motor are follows:

Model	MO213
Power, W	900
Voltage, Vdc	24
Current, A	25
Output, rpm	220
Protection class	IP 54

Power transmission system:

Two sprockets were connected by a chain and used for speed reduction. First sprocket has 13 teeth and fixed at motor rotor, while the other has 38 teeth and fixed at differential unit as shown in Fig. (2a). Fig. (2b) shows A HALAWA tricycle differential device (corona) which used to transmit the power to tractor rear wheels. The speed reduction ratio between in and out is 2.5:1. The differential unit is connected to the transmission system by a universal joint. A special pair wheels were used as the rear wheels of the SPAT in order to provide the forward and reverse motion. The distance between tractor wheels is adjustable for both front and rear axes from 130 to 170 cm which is suitable for common row crops.



Fig. 2: The transmission devices (a) and differential system (b).

Steering System:

A pair of front wheels belong to a rice transplanter equipped with manufactured axes was used and connected to two vertical axes ended by two similar sprockets and both were equipped on a horizontal beam which has three holes. Both horizontal beams were inserted within a rectangular cross-sectional steel pipe having the same three holes on both sides. This steel pipe was pivoted on the tractor frame at the center point to have the capability to cope with the off-road situations. A DC motor was used as a source of power for the steering mechanism and controlled by a racer steering wheel model YAW 500 which send the signals to the steering motor through a microcontroller circuit. The motor was fixed on one link of PEUGEOT scatra to convert the circular motion to linear motion for the left wheel vertical axe. Then motion transfer to the right wheel was terminated by the two similar sprockets fixed on two wheels vertical axes and connected by a chain.

PV system:

A PV module having the electrical and technical data presented in Table 1. It was fixed on a rectangular steel metal 100 cm width and 200 cm length. The frame was made of angle steel of 2.54cm width and 0.3cm thickness. This frame has the capability to change the module tilt angle and was attached to the main frame as illustrated in Fig. (3). However, two tilt angles (0 and 30°) were selected to be under investigation in the present study.

Under field conditions, the output power is logically less than the rated peak power. Therefore, the new PV powered light service tractor will be evaluated under field conditions.

The main block diagram showing the energy flow of the developed SPAT is shown in Fig. (4). The block diagram of control circuits is shown in Fig. (4). The microcontroller PIC18f4550 was used as the dominate and linking component of the control circuits.

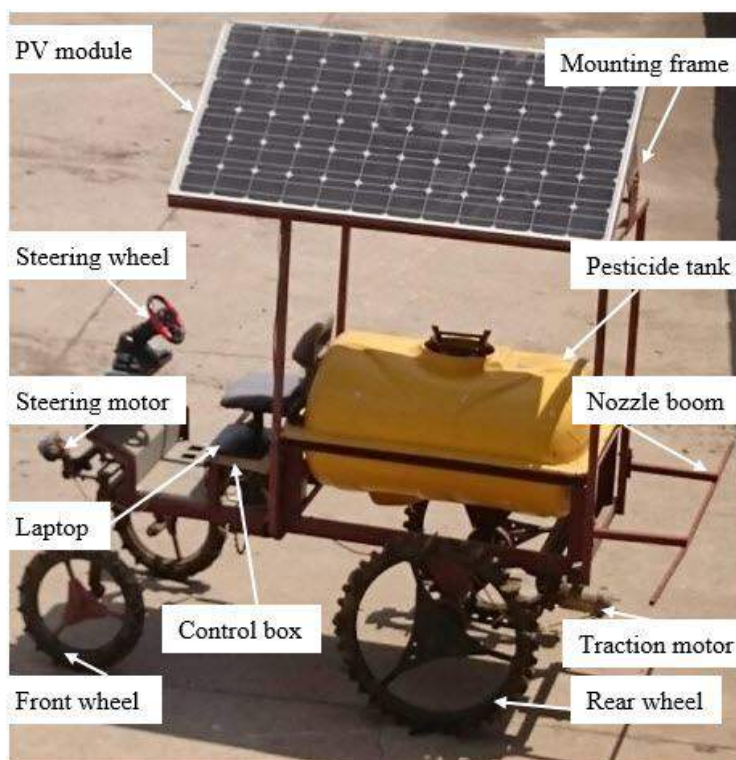


Fig. 3: Photograph of the developed SPAT

Table 1: Electrical and technical data for the PV module.

Model	IS4000P
P _{max} , W	300
I _{mp} , A	7.90
I _{sc} , A	8.58
V _{oc} , V	45.3
V _{mp} , V	37.9
Solar cells efficiency, %	17.2
Modules efficiency, %	15.54
NOCT, °C	45
Maximum system voltage, V	1000
Temperature range, °C	-40 to +85
Hail resistance, mm/km/h	up to 25 / 90
Relative humidity, %	up to 100
Dimensions, mm	1960 x 985 x 45 (±2)
Dimensions of laminate, mm	1952 x 977 x 5 (±2)
Weight, kg	27 framed – 24 laminates
Power tolerance, %	± 3
Surface load, kg/m ²	550

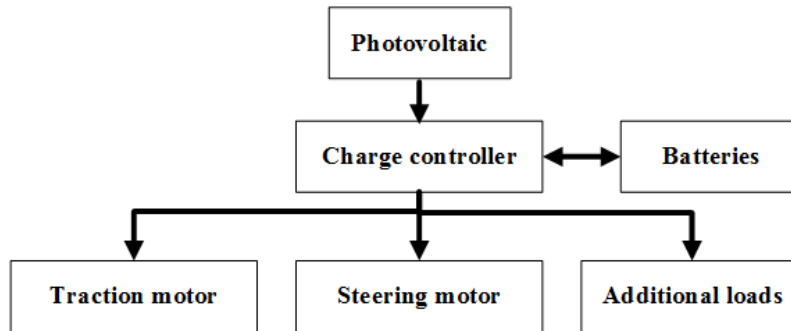


Fig. 4: Block diagram of the energy flow.

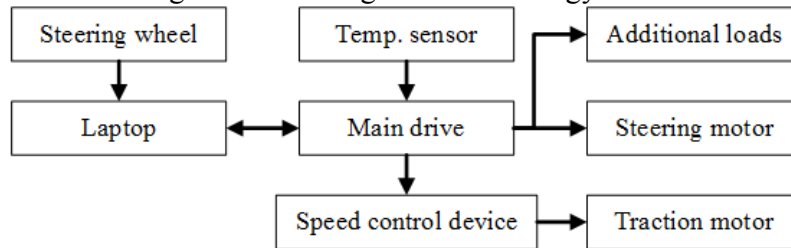


Fig. 4: Block diagram of control circuits.

Two solar batteries of 12 VDC/55Ah were connected in series to get 24 VDC output and used for storing of power generated by the PV module during daytime to meet the load requirements. The batteries were charged fully before starting the work. For electrical connections, a 50 mm² cross sectional area cable was used to keep the voltage loss from the PV module and battery less than 0.5%.

The conversion efficiency, η_{panel} (the efficiency with which the solar energy is converted into electrical energy by solar cells) can be computed as the ratio of maximum output power delivered by the PV panel to the total incoming solar power at a given cell temperature. The conversion efficiency is used to evaluate the PV performance as follow (Tiwari and Dubey, 2010):

$$\eta_{PV} = P_{max}/P_{in} = [(I_{max} \times V_{max})/(Ins \times A_c)] \times 100 \tag{1}$$

The PV input power (P_{in} , W) to the system is given by the following Eqn.:

$$P_{in} = Ins \times A_c \tag{2}$$

Where:

I_{max} and V_{max} = The current and voltage for maximum power, respectively measured at ambient temperature.

Ins = Incident solar radiation on the PV surface, W/ m² and A_c = Surface area of the PV module, m².

A Charge controller model (Solarix PRS 3030) was used to regulate the energy storage to the batteries or in other words to control the energy flow between the appliance load and batteries. Also, the charge controller protects the batteries from over charge or deep discharge.

SPAT assembly: The developed components of SPAT were assembled and equipped with a 600 liters fiberglass tank and a nozzle boom frame as shown in Fig. (3). In addition, a control system was developed and attached to the assembled unit as well. The control system details are illustrated in the following sections.

Speed control device for traction motor: Pulse width modulation (PWM) technique was employed to develop the speed control device. PWM is the technique of using switching devices to produce the effect of a continuously varying analogue signal accompanied with very high electrical efficiency.

For the current study and to develop the suggested speed control drive a one chip TL494CN, 3 MOSFETs RFP70N06 and 2 Diodes MUR1560 were used. Figs. (5 and 6) indicate a schematic diagram and a photograph of designed speed control device.

A simulation procedure was conducted using NI Multisim simulation program to determine the required characteristics of resistors and capacitors. The simulation proved that, this device offers the flexibility to tailor the power supply control circuit to a specific application, as well as.

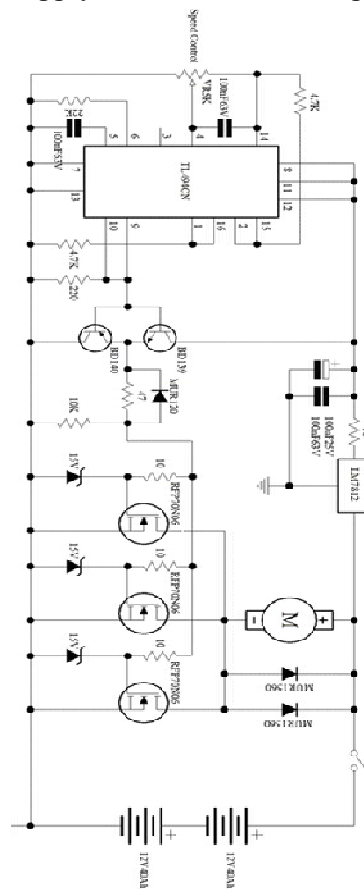


Fig. 5: A schematic diagram of the designed speed control drive.

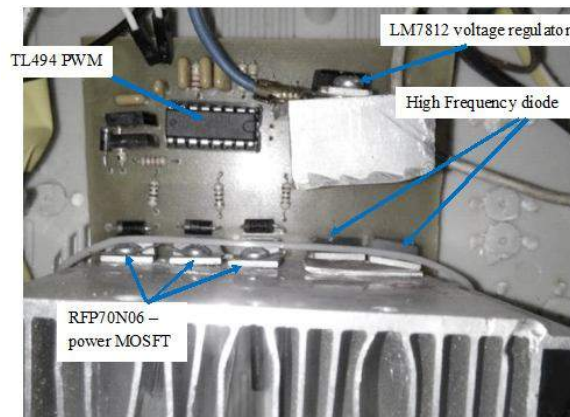


Fig. 6: A photograph of the designed speed control device.

PWM is controlled by TL494 which has the advantage that can be controlled by using the on-off frequency of 500Hz, with the rise and fall time of 10 μ s. Finally, the speed of the traction DC motor was controlled by a turn potentiometer VR1 which can be fixed as internal part of a pedal system to work as an accelerator.

Duty cycle and frequency

The device signal is switched on and off with a given period and is in the “on” state at voltage V_{on} for a fixed fraction of them period. This “on” time is referred to the “duty cycle” and is stated as a percentage. The duty cycle and PWM frequency are calculated as follows (*Rashid, 2014*):

$$Duty\ Cycle\ (\%) = \frac{On\ Time}{Period} \times 100$$

$$PWM\ Frequency = \frac{1}{Period}$$

Operating system:

Fig. (7) shows the flow chart of the application program for the SPAT. Two scenarios were suggested to operate the SPAT. First is the manual operation through laptop monitor or the steering wheel. The second is the automated one in which a restoring process is done according to a previously recorded process. The following paragraphs illustrate these scenarios.

Developing the application software program

Visual basic programming language (VB.net 2013) was used to develop the suggested application program as designed in Fig. (8). The developed software program was created for operating and monitoring the SPAT as well as storing and restoring data. The program has the feature that it can be used for manual operation through some buttons or automatically according to a previously stored process. Fig. (8) shows the application program interface as it appears on the laptop screen.

Manual operation through laptop:

At this point four commands which indicate the four general directions forward, backward, right and left could be executed with help of the application program interface (Fig. 8) and pressing the suitable button on the keyboard or by a mouse as illustrated in the following cases.

Forward and backward movement: by pressing the forward or backward buttons the laptop sends signal to the microcontroller through USB port then the SPAT moves forward or backward. To stop the forward or backward movement, the invers button, i.e. backward or forward, respectively should be pressed once.

Turning movement: to turn the SPAT to right or to left direction the right or left buttons should be pressed continuously then the laptop sends a signal to the microcontroller through USB port which leads the SPAT to turn right or left till stop pressing. Then the SPAT stops turning right or left and continue moving in the last position.

Manual operation through steering system:

As mentioned before there is a steering system which consists of a stick for forward and backward movement in addition to a steering wheel for turning right and left movement. However, the steering system sends commands to laptop through USB port and the last sends it to the microcontroller as mentioned in the previous section.

Automated operation by restoring a previously stored action:

Storing process: the time and direction of movement will be stored through any of the previously mentioned manual methods by pressing the record button before running. To stop storing the stop button should be pressed.

Restoring process: to restore and activate a recorded process, the restore button should be pressed when the SPAT located at the same starting point as it was in the storing process.

In case of attaching loads with the SPAT:

Different attaching loads with the SPAT require an appropriate constant forward speed corresponds to each load. This can be done by pressing one of the different load levels buttons A, B, C and D. However, load levels A, B, C and D could be rested before each specific light service.

Main measurements:

Solar radiation (MJm^{-2}) was measured at the same level of the PV panel using a thermoelectric pyranometer (identification No. 8-S-1-2, Make of TWC Tokyo, total accuracy of $\pm 5\%$). The DC open circuit voltage (V_{oc} , V), load voltage (V_L , V), short circuit current (I_{sc} , A) and load current (I_L , A) of the PV panel were measured with the help of Unit-T multimeter, Model DT830B.

The ambient air temperature (T_{amb} , °C) and PV panel temperature (T_p , °C) were measured using calibrated T type copper–constant thermocouples (range of -200°C to 1250°C , accuracy of $\pm 1^\circ\text{C}$) that were connected to a digital record. A van-type anemometer (0.4–30m/s, accuracy of $\pm 0.1\text{m/s}$) was used to measure wind velocity.

PV module temperature was measured at five locations on the back side of the module. Investigation of the performance of the PV system at 0° tilt angle was conducted throughout 5 days from 10th to 14th March 2014 and the average was determined. As well as performance at 30° tilt angle was conducted throughout 5 days from 20th to 24th March 2014 and the average temperature was determined. Also, PWM signals were analyzed by digital storage oscilloscope model TPS2014 (rang of 100 MHz and 200 MHz Bandwidths).

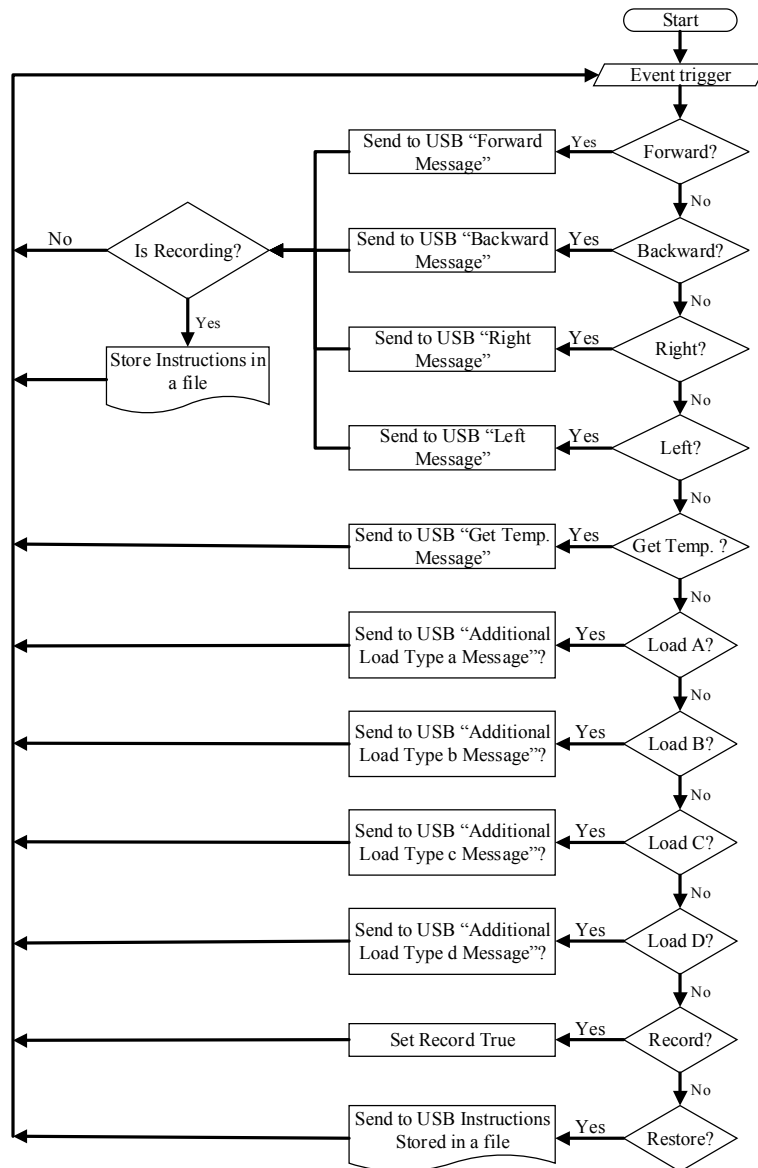


Fig. 7: The flow chart of the application program for the SPAT.

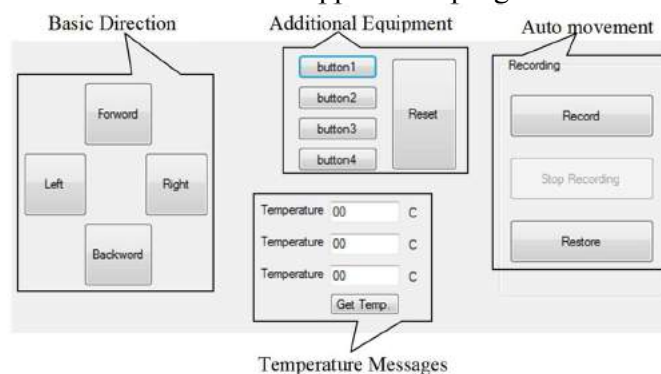


Fig. 8: Application program interface between embedded system and user.

RESULTS AND DISCUSSION

Weather conditions of the experimental site:

Weather data of the experimental site indicated that, the accumulated daily average solar radiation was ranged from 21.4 to 23.9 MJ/m² per day (from hour 9:00 to 17:00) for tilt angles 0° and 30°, respectively. While the daily average wind speed was ranged from 1.2 to 3.1 m/s throughout the experimental period of all treatments. The average of higher and lower recorded ambient temperatures were 30.1 and 19.1°C, respectively at 30° tilt angle and were 30 and 22°C, respectively at 0° tilt angle as shown in Figs. (9 and 10).

Performance of the PV system:

The performance of the PV system in terms of output power (P_{output}), efficiency (η_{PV}), open circuit voltage (V_{OC}), short circuit current (I_{SC}) and PV module temperature (T_{PV}) along with the impacted weather conditions namely solar radiation, wind speed and ambient temperature as illustrated in Figs. (9 and 10) for both of 0° and 30° tilt angles, respectively. To declare the performance of the PV system, the module was fixed at 0° and 30° tilt angles and each tilt angle was investigated under a stationary situation of the SPAT. The output power (P_{output}), conversion efficiency (η_{PV}), open circuit voltage (V_{OC}), short circuit current (I_{SC}) and PV module temperature (T_{PV}), were determined and evaluated.

Power output

Also, figs. (9 and 10) show the variation of output power (P_{output}) of the PV module along with solar radiation; module temperature, (T_{PV}), and wind speed at the recorded hour of the day for 0° and 30° tilt angles, respectively.

It is cleared that the (P_{output}) is proportional to solar intensity (S_{Ins}). The analysis of recorded data indicated that, the output power of solar module changed significantly with solar radiation.

The maximum P_{output} of 265.5 and 301 W were recorded at noon (13.00 h) for 0° and 30° tilt angles, respectively. The reason for that may be due to, the generated I_{sc} was increased more than the drop-in voltage.

The daily accumulated energy output was about 1.93 and 2.3 kWh/m²/day for 0° and 30° tilt angles respectively. It is clear that, the daily energy output for 30° was higher than 0°, and this may be due to the insolation falls mostly at low incident angle with respect to the PV module. While in case of 0°, there are some reflections because insolation falls with angle to the PV module. Therefore, angle of 30° is considered as the optimal tilt angle for PV module. As shown in Figures 10 and 11, the higher values of P_{output} was observed around noon and tend to have lower values at the morning and afternoon. However, as it was expected this behaves the general trend of the solar radiation.

Open circuit voltage and short circuit current

The variation of the detected open circuit voltage (V_{oc}) and short circuit current (I_{sc}) of solar module was illustrated in Figures 10 and 11 as well. The recorded data indicated that, the V_{oc} changed significantly with hour of the day along with the ambient temperature (T_{amb}) which directly affects the module/panel temperature, then indirectly affects the V_{oc} . The maximum open circuit voltages were observed at the morning and late afternoon when the module temperature was lower. This is in agreement with that observed by *Onyegebu (1989); Ettawil and Imara (2005) and Ettawil (2012)*.

The short circuit current (I_{sc}) is directly proportional to solar radiation. It increases with increasing solar radiation due to the increase in the number of photons generating the photo current,

in addition to the perceptible improvement in I_{sc} with the increase in module temperature (*Shaltout et al., 1995; and Eltawil, 2012*).

PV conversion efficiency

The hourly variation of conversion efficiency (η_{PV}) for PV module is illustrated in Figures 10 and 11. It was observed that the conversion efficiency is relatively high during the early and late hours of the day, while the low values were recorded at noon as a result of the adverse thermal effect of solar radiation. Accordingly, the conversion efficiency is inversely proportional to the module/panel temperature. The daily average PV conversion efficiency was 13.2 and 13.3 % for 0° and 30° tilt angles, respectively, which corresponding to daily average solar radiation about 7.1 and 7.55 kWh/m²/d and PV module temperature about 40.6 and 43.7 °C for 0° and 30° tilt angles, respectively.

Fig. (11) indicates the hourly variation percentage of T_{PV} , V_{oc} , I_{sc} , P_{output} and η_{PV} due to increasing PV tilt angle from 0° to 30° . Referring to the trendlines of the change percentage and as it was expected that both I_{sc} and P_{output} of PV module increases by increasing solar radiation with positive change. At the same time, one can conceive an almost stable trend for the change percentage of T_{PV} and V_{oc} . Regarding to the PV efficiency (η_{PV}), it has a decreasing behavior of the change percentage with increasing the solar radiation due to change tilt angle from 0° to 30° . It can be concluded that the tilt angle of 30° revealed an advantage in the performance compared to 0° . It should be mentioned here that; the obtained results were recorded at stationary conditions of the SPAT. However, the tilt angle of 0° was selected to evaluate the performance of the SPAT under a light duty operation to overcome the expected turning and change the direction of motion. While, the tilt angle of 30° can be used at rest or off time to enhance the batteries charging process to meet the load requirements.

Speed control device output:

The circuit of the speed controller which mainly consists of a TL494 pulse width modulator (PWM) and three MOSFETs was designed, constructed and used to control the DC motor drive. The prototype for this circuit is simulated using NI Multisim simulation program as mentioned above. Resulting in the motor being powered for a greater portion of each cycle. Fig. (12) shows the no load voltage waveform on the output terminals with 0%, 10%, 20%, 35%, 50%, 65%, 80% and 100% PWM on the operation, respectively.

Analyzing waveform indicates that, frequency value was fixed at 500 Hz that means no change at voltage requirement so change duty cycle means change current requirement. i.e. motor speed refers to voltage while torque refers to current. The base frequency of the generated PWM signal is 500 Hz, which means the time period is 2 ms (2000 μ s) (*Thakare and Kompelli, 2014*). The frequency is kept constant to generate exactly the same inverted PWM as is generated by the TL494.

The width of the pulses increases but the frequency is constant at 500 Hz. Increasing the frequency led to decrease the impedance. Therefore, the high frequency is used in order to decrease the impedance of the motor and keep the current of the motor almost constant without change.

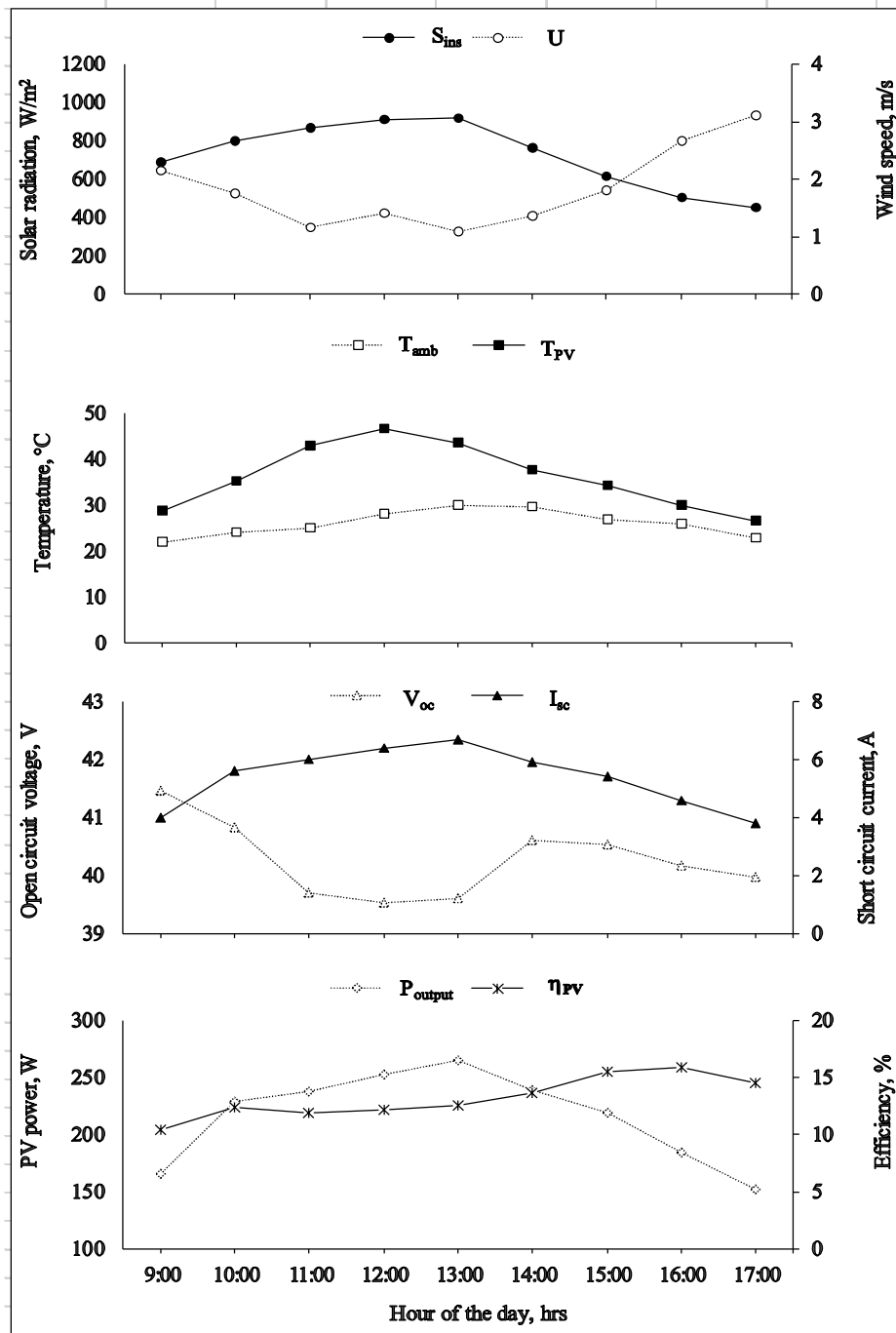


Fig. 9: The PV module output power (P_{output}), conversion efficiency (η_{PV}), open circuit voltage (V_{OC}), short circuit current (I_{SC}) and module temperature (T_{PV}) along with the impacted weather conditions at 0° tilt angle.

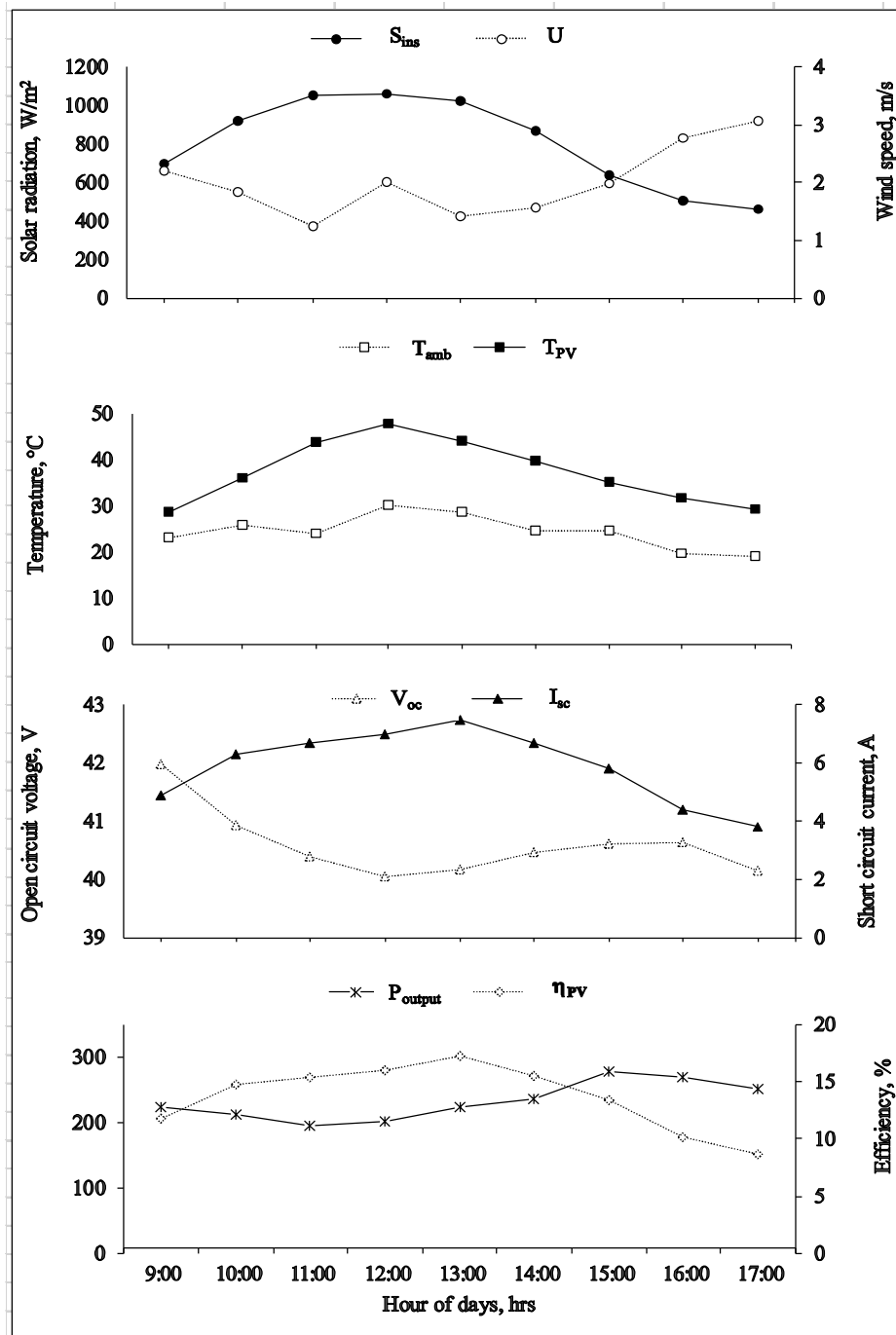


Fig. 10: The PV module output power (P_{output}), conversion efficiency (η_{PV}), open circuit voltage (V_{OC}), short circuit current (I_{SC}) and PV module temperature (T_{PV}) along with the impacted weather conditions at 30° tilt angle.

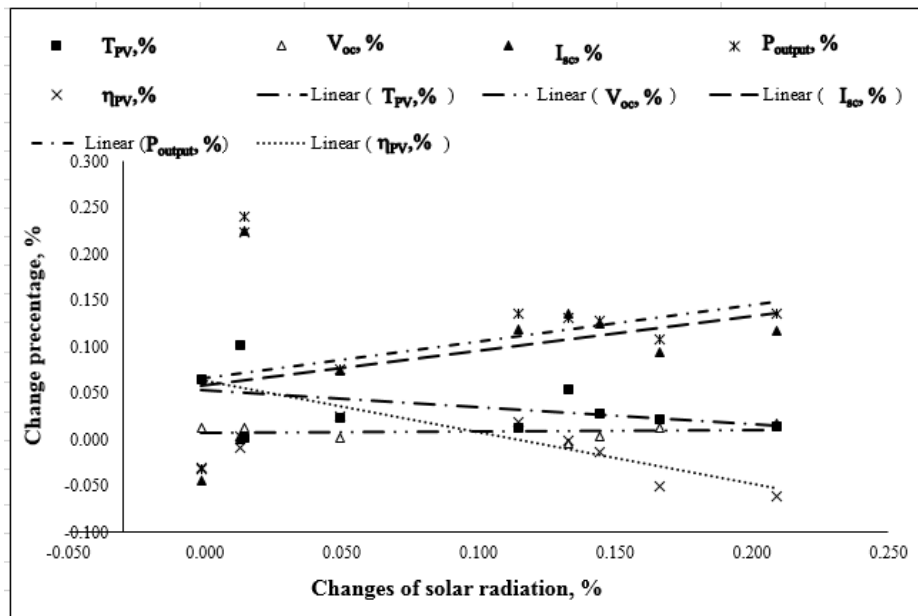


Fig. 11: Hourly variation percentage in T_{amb} , T_{PV} , V_{oc} , I_{sc} , P_{output} and η_{PV} due to increasing PV tilt angle from 0° to 30° .

The desired speed can be obtained by changing the duty cycle. The PWM is used to control duty cycle of DC motor drive. Power is supplied to the motor in square wave of constant voltage but varying pulse-width or duty cycle. Duty cycle refers to the percentage of one cycle during which duty cycle of a continuous train of pulses. Since the frequency is held constant while the on-off time is varied, the duty cycle of PWM is determined by the pulse width. Thus, the power increases duty cycle in PWM (Shrivastava, et. al., 2012). This contributes to higher motor speed at 100 % duty cycle compared to lower duty cycle.

As mentioned above there is a variable resistance was fixed on speed pedal to be used as SPAT accelerator. This variable resistance (variable speed) was calibrated at different duty cycle. The obtained results indicated that, there is a liner relationship between resistance and duty cycle as shown in Fig. (13). These results can be used when the operator of SPAT need to operate his system with specific field capacity.

It should be noted that the testing the solar tractor without load and under load will be discussed in another paper. This is a beging step for the design of the solar tractor.

CONCLUSION

An experimental investigation was carried out to evaluate the solar PV system as main source of power to operate a developed light service automated electric tractor. In addition, a control circuits were designed and used to control the DC motor drive. The performance of this system depends on various conditions such as: weather condition, PV module, charge controller, batteries, DC motor, power transmission system, driving system, etc. The PV system performance was evaluated at two tilt angles namely 0° to 30° .

The zero-tilt angle was selected because the tractor moves in different direction in the field. The 30° tilt angle may be adapted for charging the battery when the tractor is in standing position (Rest) or moving in straightway long period. Experimental data were obtained continuously during daytime at various conditions to examine the electrical performance of this system.

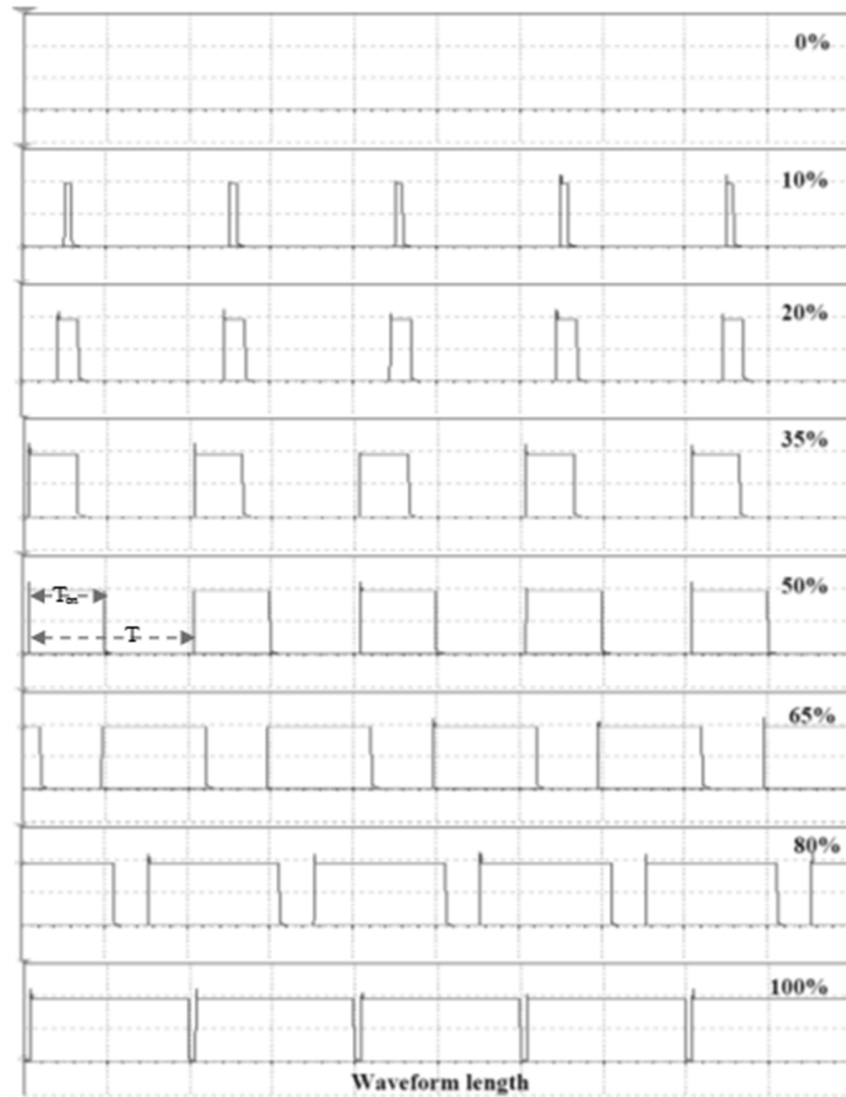


Fig. 12: The simulation of no load voltage waveform on the output terminals with 0, 10, 20, 35, 50, 65, 80 and 100% PWM.

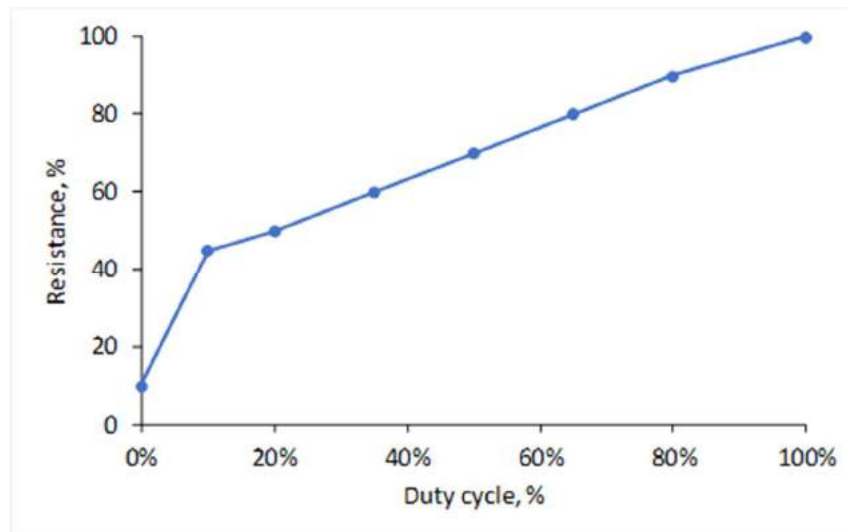


Fig. 13: The relationship between variable resistance, %, and duty cycle, %.

The results obtained from the study indicated that the observed solar radiation is sufficient to run the electrical tractor. The maximum average PV module power output was 268 W at tilt angle 30°. The daily average energy output was 2.3 kWh/d for 30° tilt angle. The daily average PV conversion efficiency was 13.3% at 30°. There is a liner relationship between duty cycle and motor speed at no-load, and motor speed was varied from 0 to 100% speed ratio.

The output power of solar module changed significantly with solar radiation. The maximum P_{output} of 265.5 and 301 W were recorded at 13.00 h for 0° and 30° tilt angles, respectively. The daily accumulated energy output was about 1.93 and 2.3 kWh/d for 0° and 30° tilt angles respectively. The daily average PV conversion efficiency was 13.2 and 13.3 % for 0° and 30° tilt angles, respectively.

The proposed speed controller circuit based on PWM was validated experimental. In operation mode 0V (or 0 pulses) will give 0% PWM duty. Increasing duty cycle from 0 to 100% will increase motor speed at same load by adjusting the potentiometer. Results indicated that the frequency was 500 Hz, period time 2ms and rise time 1.58ms during all potentiometer values.

To reach to the maximum efficiency of the PV system powered electric tractor and minimize the effect of the design and environmental parameters, an optimization study must be carried out on different loads and agricultural services.

REFERENCES

1. Bilgen, S.; K. Kaygusuz and A. Sari. 2004. Renewable energy for a clean and sustainable future. *Energy Sources, Part A: Recovery, Utilization, and Environmental Effects* 26(12):1119–1129.
2. Dincer, I. 2001. Environmental issues. II. Potential solutions. *Energy Sources, Part A: Recovery, Utilization, and Environmental Effects*; 23(1):83–92.
3. Eltawil M.A. 2012. *Solar Photovoltaic Powered Cooling System for Potato Storage*" (ISBN 978-3-8484-2379-8). LAP LAMBERT Academic Publishing GmbH & Co. KG, Germany
4. Eltawil, M.A. and Z.M. Imara. 2005. Utilization of photovoltaic array in a multi-tray fruits drying system for rural areas. *Misr J. Ag. Eng.* 22 (4): 820-845.
5. Farhad, S.; M. Saffar-Avval and S. Younessi. 2008. Efficient design of feedwater heaters network in steam power plants using pinch technology and energy analysis. *International Journal of Energy Research* 32:1–11.

6. Fridleifsson, I. B. 2001. Geothermal energy for the benefit of the people. *Renewable and Sustainable Energy Reviews* 5:299–312.
7. Holm-Nielsen, J. B. ; T. Al Seadi and P. Oleskowicz-Popiel. 2009. The future of anaerobic digestion and biogas utilization. *Bioresource Technology*, 100: 5478–5484.
8. Horst, G. H. and A. J. Hovorka. 2009. Fuelwood: the “other” renewable energy source for Africa? *Biomass and Bioenergy* 33:1605–1616.
9. Hughes, A. 2006. *Electric Motors and Drives Fundamentals, Types and Applications*, 3rd Ed., Austin Hughes, Published by Elsevier Ltd.
10. Katsambe, C. T.; V. Luckose and N. S. Shahabuddin. 2017. Effect of pulse width modulation on dc motor speed. *International Journal of Students’ Research in Technology & Management*. 5(2): 42-45.
11. Mohammed, J. A. 2013. Pulse Width Modulation for DC Motor Control Based on LM324. *Engineering & Technology*, part (A), 10 (31): 1882-1896.
12. Okoro, O. I. and T. C. Madueme. 2006. Solar energy: a necessary investment in a developing economy. *International J. of Sustainable Energy*; 25(1): 23–31.
13. Onyegebu, S.O. 1989. Performance of Photovoltaic cell in an Equatorial climate. *Solar & wind Technology*, 6(3): 275-281.
14. Panwar, N. L.; S. C. Kaushikb and K. Surendra. 2011. Role of renewable energy sources in environmental protection: A review. *Renewable and Sustainable Energy Reviews* j. 15 : 1513–1524.
15. Rashid, M. H. 2014. *Power electronics devices, circuits, and applications*. 4th ed. Pearson Education Limited.
16. Shaltout, M. A. M.; A. M. Mahrous; A. E. Ghetas and Y. A. Fattah, 1995. Photovoltaic performance under real desert conditions near Cairo. *Renewable energy*, 6(5-6): 533-536.
17. Shrivastava, S.; J. Rawat and A. Agrawal. 2012. Controlling DC Motor using Microcontroller (PIC16F72) with PWM. *International Journal of Engineering Research*. 1(2), 45-47.
18. Sims, R. E. H. 2004. Renewable energy: a response to climate change. *Solar Energy*. 76: 9–17.
19. Stoppato, A. 2008. Life cycle assessment of photovoltaic electricity generation. *Energy*, 33: 224–232.
20. Thakare S. S. and S. Kompelli 2014. Design and implementation of DC motor speed control based on pic microcontroller. *International Journal of Engineering and Computer Science*. 3(9): 8075-8079.
21. Tiwari G. N. and S. Dubey. 2010. *Fundamentals of photovoltaic modules and their applications*. Centre for Energy Studies, Indian Institute of Technology (IIT) Delhi, New Delhi, India, RSC publishing, 99-100.
22. UNDP. 2000. *World Energy Assessment: Energy and the challenge of sustainability*. New York. (ISBN 9211261260)
23. Youm, I.; J. Sarr; M. Sall and M. M. Kane. 2000. Renewable energy activities in Senegal: a review. *Renewable and Sustainable Energy Reviews*. 4(1):75–89.
24. Zakhidov, R. A. 2008. Central Asian countries energy system and role of renewable energy sources. *Applied Solar Energy*; 44(3):218–223.

تقييم أداء نظام الخلايا الكهروضوئية لتشغيل جرار كهربائي مطور

رامي زكريا عمارة^١، محمد عبد العزيز الطويل^٢، سعيد السيد أبو زاهر^٢،
جمال حسن السيد^١، إسماعيل أحمد عبد المطلب^٢

^١ معهد بحوث الهندسة الزراعية - مركز البحوث الزراعية - الدقي - جيزة - مصر
^٢ كلية الزراعة - جامعة كفر الشيخ - كفر الشيخ - مصر

أجري هذا البحث بغرض تعظيم الاستفادة من الطاقة الشمسية كأحد البدائل المتاحة للوقود الحفري في المجال الزراعي. حيث تم تصميم وتصنيع جرار زراعي كهربائي يعمل بالخلايا الكهروضوئية لأداء العمليات الزراعية الخفيفة. يعتبر الجرار المصمم عبارة عن آلة متعددة الأغراض حيث يتم إنتاج الطاقة الكهربائية وتخزينها في بطاريات لإعادة استخدامها وقت الحاجة. يتكون الجرار من إطار رئيسي من الصلب وإطار لحمل اللوح الشمسي يتميز بمرونة كافية لتوجيه موديول الخلايا الشمسية حسب زاوية الميل المطلوبة. ويتم نقل القدرة من الموتور الرئيسي (٢٤ فولت تيار مستمر-٩٠٠ وات) عن طريق مجموعة نقل الحركة إلى المجموعة الفرعية ومنها إلى عجلات الجرار الخلفية. ويتم توجيهه عن طريق موتور تيار مستمر، كما تم تصميم مجموعة من الدوائر الإلكترونية للتحكم في سرعة الجرار من خلال تطبيق Pulse width modulation للموتور الرئيسي وأيضا لتقليل الطاقة الكهربائية المستخدمة. يوجد أيضا دائرة تحكم في الجرار متصلة بحاسب شخصي محمول (لابتوب) للربط بين حركة أجزاء الجرار كلها. وقد تم تنفيذ هذا البحث على عدة مراحل تضمنت، مرحلة تصميم جرار للأحمال الخفيفة يعمل بالخلايا الشمسية. مرحلة تقييم أداء الخلايا الشمسية للوقوف على مدى قدرتها على توفير الطاقة الكهربائية اللازمة لتشغيل الجرار الشمسي. مرحلة اختبار أداء الخلايا الشمسية عند زاويتي ميل للموديول الشمسي مختلفتين هما ٠° و ٣٠°، ومرحلة دراسة تأثير الظروف البيئية المحيطة على أداء الموديول. أهم النتائج المتحصل عليها: متوسط الطاقة الكهربائية المنتجة ١,٩٣ و ٢,٣ كيلووات ساعة/يوم عند زاوية ميل للموديول الشمسي ٠ و ٣٠ درجة على التوالي. متوسط كفاءة التحويل لخلايا الكهروضوئية ١٣,٢، ١٣,٣ % عند زاوية ميل للموديول الشمسي ٠ و ٣٠ درجة على التوالي، وذلك عند معدل اشعاع شمسي ٧,١ و ٧,٥٥ كيلووات ساعة/م^٢/يوم ودرجة حرارة موديول شمسي ٣٦,٢ و ٣٧,٤ م° عند زاوية ميل للموديول الشمسي ٠ و ٣٠ درجة على التوالي. وجد أن هناك زيادة طفيفة في درجة حرارة الموديول الشمسي عند المنتصف مقارنة بالأركان. وجد أن زيادة درجة حرارة الموديول الشمسي تؤدي إلى انخفاض كفاءة التحويل للموديول. وجد أن الخلايا الشمسية قادرة على توفير القدرة اللازمة لتشغيل الجرار الكهربائي المطور تحت الظروف الحقلية.

APPLE SLICES PROPERTIES AFFECTED BY DIFFERENT DRYING METHODS

KESHEK, M. H. *, M.N. OMAR, * and A.A. SAMAK*

*Agriculture engineering lecturer, Agriculture faculty, Menoufia University.

Abstract

This work conducted to study the effect of air-drying temperature in oven dryer and solar drying systems on some physical and mechanical properties of apple slices. The oven dryer was conducted at temperatures, 40, 50, 60, 70 and 80 °C, meanwhile, the solar drying systems were conducted at direct dryer with solar collector (D.C), direct dryer without solar collector (D), indirect solar dryer (IN.D) and glass cabinet dryer (G). The Apples were cut to slices with thicknesses were 5, 10, 15 and 20 mm, and dried by different dryers. Apple slice with thickness 5mm take the lower drying time 7 hours when dried in oven dryer at 80°C. the apple slices with thickness 5mm had the lest total color changes (ΔE) 10.6 and 11.9 when dried in the oven dryer at temperature 60°C, and indirect solar dryer, respectively. The highest total color changes (ΔE) 29.7 and 28.3 occurred when apple slices with thickness 20mm dried in the direct solar dryer with solar collector and oven dryer with temperature 80°C, respectively. The apple slices with thickness 5mm had the lower firmness 0.72 kg/cm² when dried using the oven dryer with temperature 40°C, and the higher firmness 1.94 kg/cm² occurred when dried the apple slice with thickness 20mm when dried using the oven dryer with temperature 80 °C.

Keywords: Apple, Color, Firmness, Drying, Solar

INTRODUCTION

Drying operations are important steps in the chemical and food processing industries. The basic objective in drying food products is the removal of water in the solids up to a certain level, at which microbial spoilage and deterioration chemical reactions are greatly minimized. The wide variety of dehydrated foods, which today are available to the consumer (snacks, dry mixes and soups, dried fruits, etc.) and the interesting concern for meeting quality specifications and energy conservation, emphasize the need for a thorough understanding of the drying process (Krokida *et al.*, 2003).

Apples are one of the leading fruits produced in the world and apples plantations are cultivated all over the world in many countries. Apples play a significant role in diet as they contain appreciable amount of carbohydrate (12–14%) and about 0.1–0.3% proteins. Approximately 80% of carbohydrates present are the soluble sugars, sucrose (about 2%), glucose (2.4%), and fructose (6.0%). The total fiber content is about 2%. Apples also contain vitamins C and A and important minerals namely calcium, iron, magnesium, phosphorus, potassium, sodium, and zinc (Sinha, 2006).

Apple drying is a highly energy-consuming process. Also, the drying methods have significant effects on the dried apple quality such as nutritional values, color, shrinkage and other organoleptic properties. So far, many works have been performed to study hot air, tray dryer with and without air circulation, fluidized bed, and superheated steam drying of apple pieces of various shapes (Wang *et al.*, 2007).

Color is one of the most important quality components of fresh fruit and vegetables. Fruit ripening is a complex, genetically programmed process that culminates in dramatic changes in

texture, color, flavor and aroma. For instance, the characteristic pigmentation of red, ripe tomato fruit is the result of the *de novo* synthesis of carotenoids, mainly lycopene and β -carotene, which are associated with the change in fruit color from green to red as chloroplasts are transformed to chloroplasts (Pék *et al.* 2010).

Browning in foods is of two types: enzymatic and non-enzymatic. Enzymatic browning is one of the most important reactions that occur in fruits and vegetables, usually resulting in negative effects on color, taste, flavor, and nutritional value. It is a consequence of oxidation reaction of polyphenols catalyzed by polyphenol oxidase enzyme, which facilitate the conversion of phenols to the brown pigment melanin in an oxidation reaction (Guerra *et al.*, 2010).

Color is one of the most relevant attributes with respect to the quality of dried foods (Bonazzi and Dumoulin, 2011).

Other than browning, many reactions can affect color during thermal processing of fruits and vegetables. Among them, the most common is pigment degradation, especially carotenoids and chlorophyll and chemical oxidation of phenols and ascorbic acid. Chemical changes to carotenoids and chlorophyll pigments are caused by heat and oxidation during drying. In general, longer drying times and higher drying temperatures produce greater pigment losses. Other factors affecting color include fruit pH, acidity, fruit cultivar and heavy metal contamination (Mongi, 2013).

Firmness of horticulture products, as measured by mechanical methods, is frequently used to determine their maturity and ripeness (Deell *et al.*, 2001).

Firmness is a good measure of maturity and for many fruit, including apples and pears it is also used as a measure of eating quality. However firmness in the laboratory does not invariably translate into good mouth-feel or texture. It is a complex phenomenon based on the physical characteristics of cells. The cell walls of apple and pear flesh are composed of cellulose that provides strength and pectin substances that make contact with adjoining cells and confer flexibility. This flexibility is essential during fruit development as cells expand and fruit grow larger. These pectin substances are solubilized as fruit ripen causing a loss of cohesion between cells and so affecting general fruit firmness and juiciness (Travers, 2013).

The objective of this study was to find the effect of oven dryer with air drying temperature and solar drying systems on some physical and mechanical properties of apple slices.

MATERIALS AND METHODS

Four identical solar drying systems designed and manufactured by (Mohamed, *et al.* 2010) in the Faculty of Agriculture, Menoufia University and installed on the roof of Agricultural Engineering Department at latitude (30°) The main components of each drying systems were (Solar collector, Drying chamber, Drying trays, Chimney) as shown in Fig.1. These components were combined with each other's to configure the different solar drying systems. These solar drying systems were direct solar dryer with solar collector (DC), covered the drying chamber with black plastic sheet as indirect solar dryer with solar collector (IND), drying chamber with glass as direct dryer without collector (D), and drying chamber designed in the same sizes the previous, with sides change from wood to glass and the glass thickness in 3mm (G). These solar dryers worked in the same time.

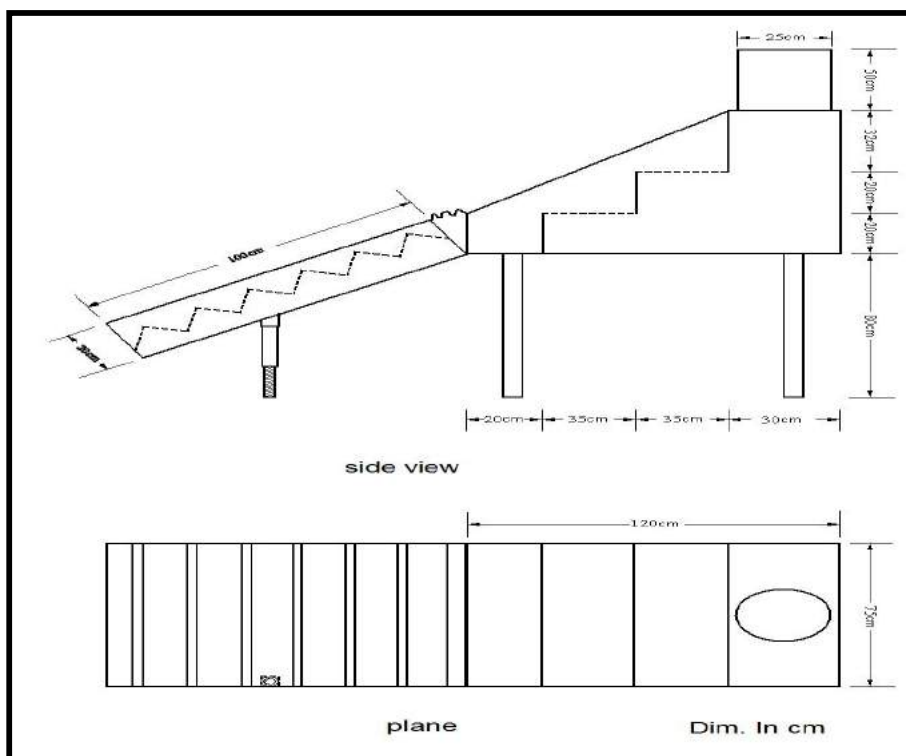


Fig. 1: Schematic diagram of solar drying system (Dim. In cm).

Electric thermal oven dryer:

The specifications of electric oven dryer can show in the Table (1)

Country of manufacture	German-made
Model	Rumo-10878
Using	Drying experiments.
Outside dimensions (W*H*D)	80*70*60 cm.
cavity Dimensions (W*H*D)	50*60*50 cm,
Shelves	Three which put the matter on it
Input power	1500

Apple (Volos) were purchased from a private farm at the city Ashmoun, Menoufia, were stored in the refrigerator at a temperature of 4° °C for one day, apple were washed, peeled and cut normally into slices with thicknesses 5, 10, 15, 20 mm.

The moisture content of initial apple was determined according to Awady *et al.*, (1993) by drying the products in an electrical oven at 70°C for 24 hours.

Surface colour of both fresh and dried apple was measured using a WR-10 Colorimeter to obtain the colour values, which measures three parameters: lightness (L), redness (+a) and yellowness (+b), Fig. 2.

The total colour difference (ΔE) and browning index (Bi) were then determined using the following equations:

$$\Delta E = \sqrt{(\Delta L)^2 + (\Delta a)^2 + (\Delta b)^2} \quad (1)$$

$$Bi = \frac{[100(x-0.31)]}{0.17} \quad (2)$$

$$x = \frac{(a+1.75L)}{(5.645L+a-3.012b)} \quad (3)$$

The fresh apple used as the reference and a higher ΔE represents greater colour change from the reference material (Kamil, 2006).

Lower ΔE show good quality of the apple while the raw apple data tacked as the reference (Tarik, 2007).

Digital instrument Fruit firmness Tester, FHT-1122 Fig. (3) Its armature diameter 7 mm pressed on apple slices by deeply 0.5 cm.



**Fig2: WR10
PortableColorimeter**



**Fig. 3: Photographic of
penetrometers.**

RESULTS AND DISCUSSION

In order to achieve the goals of this research, some drying characteristics and some properties of apple slices (color and firmness) were studied, and we can clear the results of this study as follow,

Figs. 4(a, b, c, d) show the variations in moisture content of different apple slice thickness as a function with drying time at various drying air temperatures.

Results accentuate the initial moisture content 86 % (wet base) decreases continually with drying time. Drying curves illustrate the drying air temperatures and slices thicknesses had a major impact on the moisture content of the apple slices. In other words, as increasing the drying air temperature and decreasing of apple slice thickness lead to drying time decreases to reach equilibrium moisture in the different drying methods.

The drying time to reach equilibrium moisture content of the apple slice thicknesses of 5 mm were 26, 20, 11, 9 and 7 hours at the drying air temperatures of 40, 50, 60, 70 and 80°C, respectively. Corresponding values for the apple thickness of 10 mm were 32, 25, 16, 14 and 12 hour at the same drying air temperatures, respectively. Meanwhile, results show that the drying time varied from 37 to 19 hours for apple slices thickness of 15 mm and from 47 to 24 hours at the apple slices thickness of 20 mm.

Data illustrated that increasing the air temperatures from 40° to 80°C decreased the drying time by about 73%, 62.5%, 48.6%, and 48.9%, at the apple thickness of 5, 10, 15, and 20 mm, respectively.

The decreasing in drying time of apple slices with increasing the drying air temperature has been observed by (Ramaswamy and van Nieuwenhuijzen, 2002) and (Wang and Chao, 2002).

The increasing in drying time with the increase in the slices thickness due to increase moisture transmission distance and increase the surface area exposed with constant diameter. Similar results have been noted by (Wang and Chao, 2002) for apple slices.

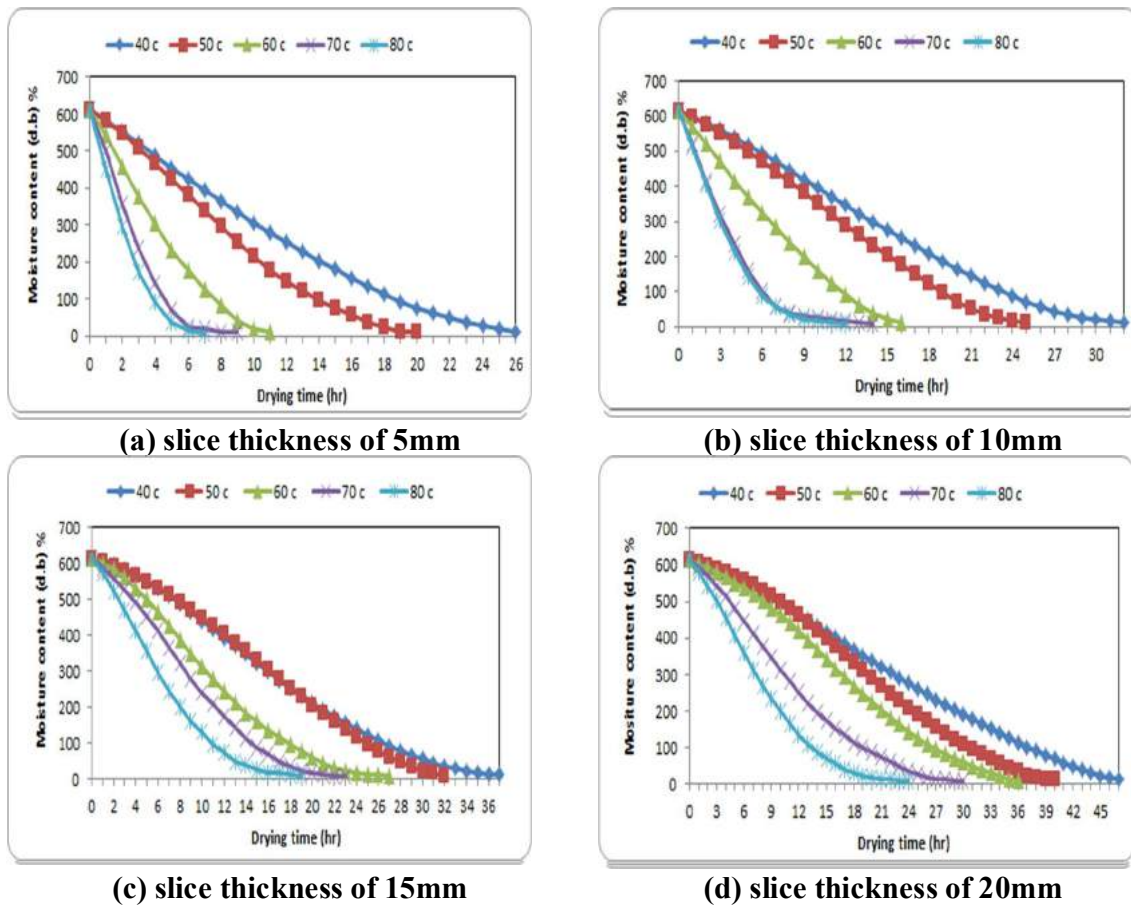


Fig.4: Moisture content curves of dried apple slices with drying time oven at different temperatures and different thicknesses.

Figs. 5(a, b, c, d) describe the variations in moisture content of apple slices as a function with drying time in different solar drying systems. The drying time to reach the final moisture content of apple slices thicknesses 5, 10, 15 and 20 mm in the direct solar dryer with solar collector were 12, 18, 24 and 32 hour, respectively. The similar results were obtained for the glass dryer chamber system; this is due to the convergence of the temperature inside the drying chambers.

Meanwhile, results show that the drying time varied from 34 to 14 hours in the direct dryer without solar collector system and from 42 to 18 hours for the indirect system at the all apple slices thicknesses.

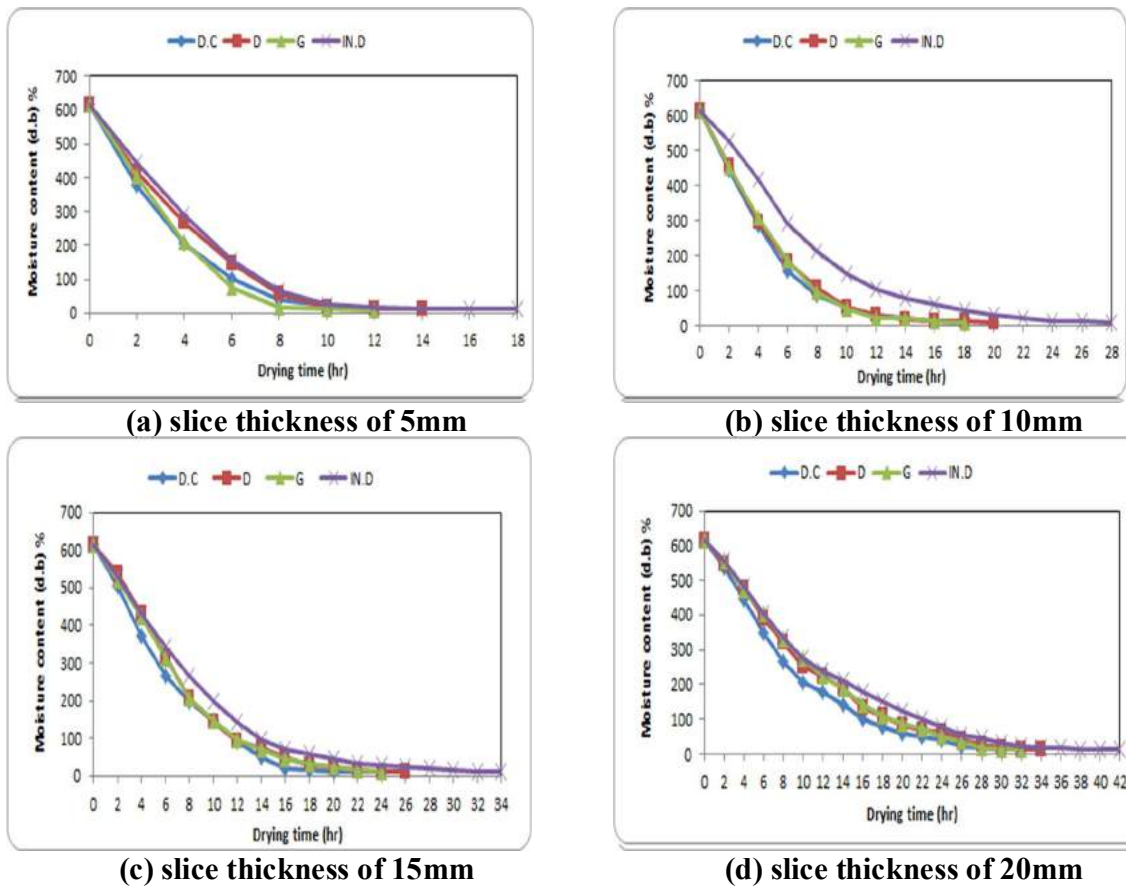


Fig.5: Moisture content curves of dried apple slices with drying time in solar drying systems for different thicknesses.

From, the value of (L) was change from 68.5 of apple slices thicknesses 15mm and drying air temperature 50°C (this is the lowest value in change compared to the fresh sample) to 48.7 of apple slices thicknesses 20mm and drying air temperature 70°C (this is the highest value in change compared to the fresh sample).

The value of (a) was change from 0.9 of apple slices thicknesses 5mm and drying air temperature 60°C (this is the lowest value in change compared to the fresh sample) to 15.3 of apple slices thicknesses 20mm and drying air temperature 80°C (this is the highest value in change compared to the fresh sample).

The value of (b) was change from 21.8 of apple slices thicknesses 5mm and drying air temperature 60°C (this is the lowest value in change compared to the fresh sample) to 37.3 of apple slices thicknesses 20mm and drying air temperature 80°C (this is the highest value in change compared to the fresh sample).

The total color change values (ΔE) varied from 10.6 of apple slices thicknesses 5mm and drying air temperature 60°C (this is the lowest value in change compared to the fresh sample) to 28.3 of apple slices thicknesses 20mm and drying air temperature 80°C (this is the highest value in change compared to the fresh sample).

Data illustrated that decreasing the apple slice thickness from 20 to 5 mm the total color change decreased by about 36%, 38%, 49%, 45% and 31% for the different drying air temperature 40, 50, 60, 70 and 80°C, respectively.

Fig.6 shows the effect of drying temperature and slices thickness on total color change. From this the total color change increased with increasing slices thickness and when drying temperature increased from 40 to 60°C the total color change decreased and when it increased from 60 to 80°C the total color change increased.

These results clear that the less total color change occurred in slices thickness 5 mm and drying temperature 60°C, the (L) value decreased from 70.2 (fresh sample) to 60.7 (white color decreased), the (a) value increased from -1.3 (green) to 0.9 (red) and (b) value increased from 17.7 to 21.8 (yellow color increased). The highest total color change occurred in slices thickness 20 mm and drying temperature 80°C, the (L) value decreased from 70.2 (fresh sample) to 58.3 (white color decreased), the (a) value increased from -1.3 (green) to 15.3 (red) and (b) value increased from 17.7 to 37.3 (yellow color increased).

The value of L was change from 68.3 of apple slices thicknesses 5mm and direct solar drying system (this is the lowest value in change compared to the fresh sample) to 47.8 of apple slices thicknesses 20mm and indirect solar drying system (this is the highest value in change compared to the fresh sample).

The value of a was change from 3.6 of apple slices thicknesses 5mm and indirect solar drying system (this is the lowest value in change compared to the fresh sample) to 18.4 of apple slices thicknesses 20mm and solar glass drying chamber (this is the highest value in change compared to the fresh sample).

The value of b was change from 25.6 of apple slices thicknesses 10mm and indirect solar drying system (this is the lowest value in change compared to the fresh sample) to 40 of apple slices thicknesses 15 and 20mm and solar glass drying chamber (this is the highest value in change compared to the fresh sample).

The total color change values (ΔE) varied from 11.9 of apple slices thicknesses 5mm and indirect solar drying system (this is the lowest value in change compared to the fresh sample) to 33.4 of apple slices thicknesses 20mm and solar glass drying chamber (this is the highest value in change compared to the fresh sample).

Fig.7 shows the effect of solar drying systems and slices thickness on total color change. From this figure, the total color change increased with increasing slices thickness and when increased exposure to solar rays the total color change increased.

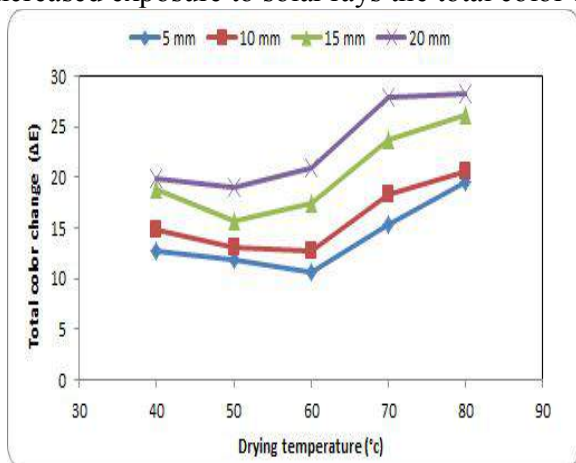


Fig. 6: Effect of drying temperature on total color change of apple slices.

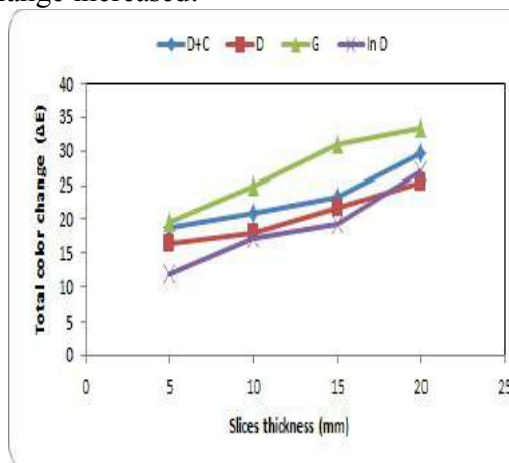


Fig. 7: Effect of solar drying systems on total color change of apple slices.

Figs. (8, 9, 10, 11 and 12) were clear that color changes affected by change in the slices thickness at different drying temperature in oven dryer.

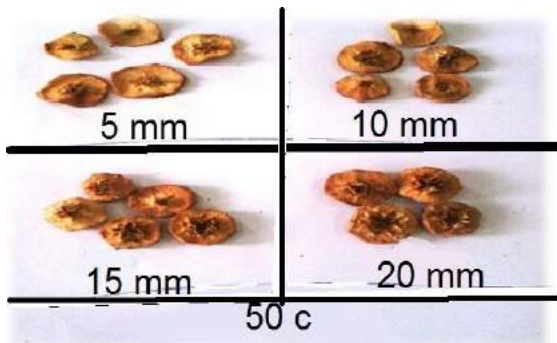


Fig. 8: Apple slices color change by drying inoven at drying air temperature of 50°C for different thicknesses.

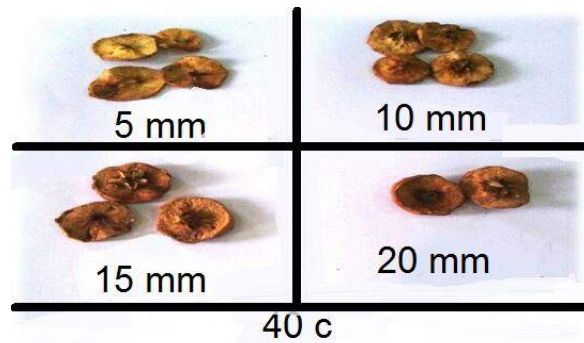


Fig. 9: Apple slices color change by drying inoven at drying air temperature of 40°C for different thicknesses.

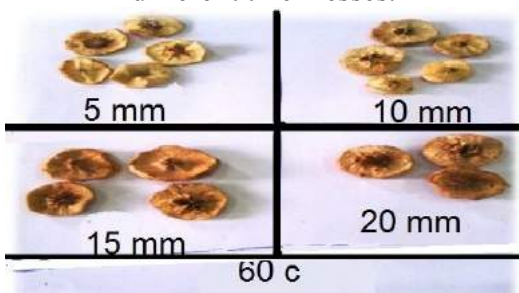


Fig.10 :Apple slices color change by drying inoven at drying air temperature of 60°C for different thicknesses.

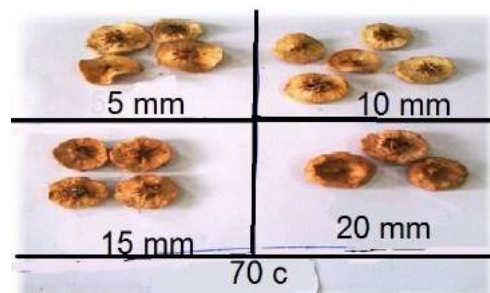


Fig. 11: Apple slices color change by drying inoven at drying air temperature of 70°C for different thicknesses.

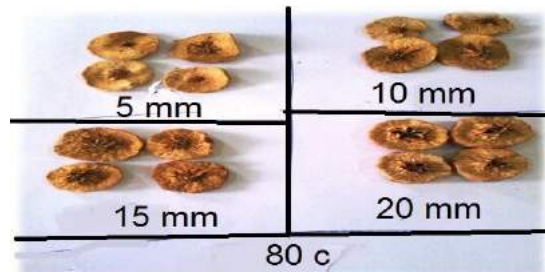


Fig. 12: Apple slices color change by drying inoven at drying air temperature of 80°C for different thicknesses.

From Figs. (13, 14, 15, and 16) were clear that color changes affected by change in the slices thickness at different solar drying systems.

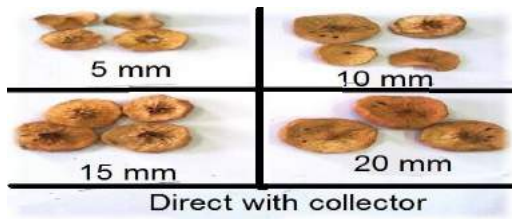


Fig. 13: Apple slices color change by drying in direct with solar collector system for different thicknesses.

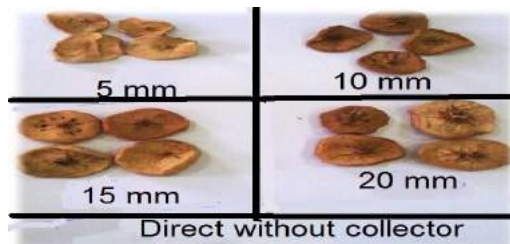


Fig. 14: Apple slices color change by drying indirect without solar collector system for different thicknesses.

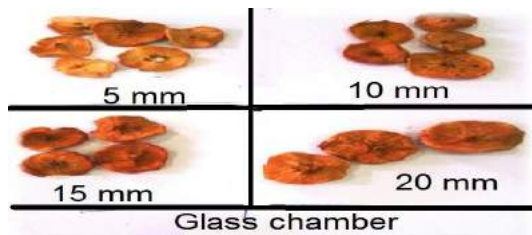


Fig. 15 Apple slices color change by drying in glass drying chamber system for different thicknesses.



Fig.16 Apple slices color change by drying in indirect system for different thicknesses.

Fig.17 shows the effect of slices thickness and drying temperature on browning index. From this browning index increased because of increasing slices thickness and change drying temperature. The lowest value was 44 occurred when used the temperature 60°C and slices thickness 5 mm and higher value was 115 occurred when used the temperature 80°C and slices thickness 20 mm.

Fig.18 shows the effect of slices thickness and solar drying system on browning index. From this browning index increased because of increasing slices thickness. The lowest value was 57 occurred when used indirect solar dryer and slices thickness 5 mm and higher value was 141 occurred when used glass solar dryer and slices thickness 20 mm.

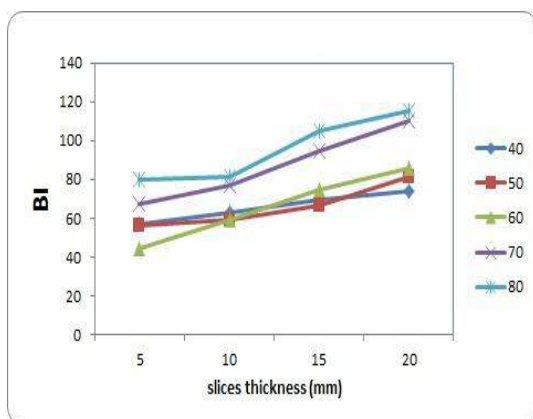


Fig.17: Apple slices browning index because of drying in oven at different temperatures and different thicknesses.

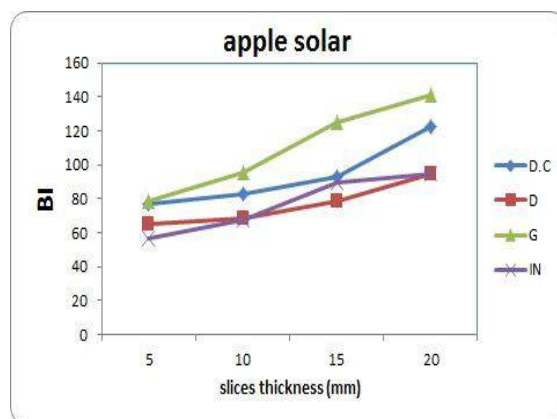


Fig.18: Apple slices browning index because of drying in solar drying systems at different thicknesses.

The fresh apple firmness ranged between 0.33 to 0.44 kg/cm² and then decreased gradually with decrease of moisture content for some time and then it increased even recorded the highest value at the end of the drying time at all drying air temperature in oven drying at all slices thickness. The Table (2) shows the final firmness of apple at all drying air temperature and all thicknesses. The higher value was 1.94 kg/cm² occurred when used the temperature 80°C and slices thickness 20 mm and lowest value was 0.72 kg/cm² occurred when used the temperature 40°C and slices thickness 5 mm.

When used the slice thickness of 5 mm the firmness increase by about 54%, 63%, 67%, 74% and 76% at the drying air temperatures of 40, 50, 60, 70 and 80 °c, respectively. In addition, when used the slice thickness of 10 mm the firmness increase by about 58%, 64%, 69%, 75% and 77% at the drying air temperatures of 40, 50, 60, 70 and 80 °C, respectively.

When used the slice thickness of 15 mm the firmness increase by about 53%, 58%, 62%, 73% and 74% at the drying air temperatures of 40, 50, 60, 70 and 80 °c, respectively. Moreover, when used the slice thickness of 20 mm the firmness increase by about 56%, 58%, 66%, 74% and 77% at the drying air temperatures of 40, 50, 60, 70 and 80 °c, respectively.

Table (2): The final firmness of fresh and dried apple by oven drying				
Firmness (kg/cm²)				
drying temperature(°C)	apple slices thickness(mm)			
	5	10	15	20
fresh	0.33	0.33	0.44	0.44
40°	0.72	0.78	0.94	1.00
50°	0.89	0.94	1.06	1.06
60°	1.00	1.06	1.17	1.28
70°	1.28	1.33	1.61	1.72
80°	1.39	1.44	1.72	1.94

At the beginning of the solar drying the firmness remain almost constant for some time and then increases after that until you reach to a higher value at the end of the drying time at all solar drying systems at all slices thickness. the Table (3) shows the final firmness of apple at all solar drying systems and all thicknesses.

The higher value was 1.39 kg/cm² occurred when used the solar drying system (glass drying chamber) and slices thickness 20 mm and lowest value was 0.83 kg/cm² occurred when use the solar drying system (indirect) and slices thickness 5 mm.

When used the slice thickness of 5 mm the firmness increase by about 64% at the solar drying systems (direct with solar collector and direct without solar collector), 67% at the glass drying chamber system and 60% at the indirect system.

When used the slice thickness of 10 mm the firmness increase by about 73% at the solar drying systems (direct with solar collector and glass drying chamber), 72% at the direct without solar collector system and 69% at the indirect system.

When used the slice thickness of 15 mm the firmness increase by about 64% at the solar drying systems (direct with solar collector, direct without solar collector and glass drying chamber), 62% at the indirect system.

When used the slice thickness of 20 mm the firmness increase by about 66% at the solar drying systems (direct with solar collector and direct without solar collector), 68% at the glass drying chamber system and 62% at the indirect system.

Table (3): The final firmness of fresh and dried apple by solar drying systems:				
Firmness (kg/cm ²)				
solar drying systems	apple slices thickness (mm)			
	5	10	15	20
fresh	0.33	0.33	0.44	0.44
DC	0.94	1.22	1.28	1.28
D	0.94	1.17	1.22	1.28
G	1.00	1.22	1.22	1.39
IND	0.83	1.06	1.17	1.17

CONCLUSION

From the previous study, we can concluded that it is preferred to dry the apple slices with thickness 5mm by oven dryer with temperature 60 °C and indirect solar dryer with collector because they gave the best results for drying time and some quality parameters such as (the total color change ΔE and firmness) compared to the other treatments.

REFERENCES

1. Awady, M.N.; S.A. Mohamed; A.S. El-Sayed and A.A. Hassanain (1993) "Utilization of solar energy for drying processes of agricultural products". *Misr, J. Ag. Eng.*, 10(4):794-804.
2. Bonazzi, C. and E. Dumoulin, (2011). Quality Changes in Food Materials as Influenced by Drying Processes. In: *Drying Technology, 3: Product Quality and Formulation*, First Edition (Edited by Tsotsas, E., Arun, S. and Mujumdar, A.S). Wiley-VCH Verlag GmbH & Co. KGaA. Published. : 1-20.
3. Deell, J.R., S. Khanizadeh, F. Saad, D.C. Ferree, (2001). Factors affecting apple fruit firmness: a review. *J. Am. Pomol. Soc.*: 55, 8–27.
4. Guerra, M. P., Kudo, T., Kon, T. and Holderbaum, D. F. (2010). Enzymatic browning, polyphenol oxidase activity and polyphenols in four apple cultivars: dynamics during fruit development. *Hortscience* 45(8): 1150 - 1154.
5. Kamil, S. and Ahmet K. (2006). The thin layer drying characteristics of organic apple slices. *Journal of Food Engineering* (73): 281–289.
6. Krokida, M. K.; V. T. Karathanos; Z. B. Maroulis; and D. Marinos-Kouris (2003) "Drying kinetics of some vegetables". *Journal of Food Engineering* 59: 391:403
7. Mongi, R.J. (2013): Solar drying of fruits and vegetables: dryers' thermal performance quality and shelf life of dried mango, banana, pineapple and tomato, Ph.D. Thesis., sokoine university of agriculture. Morogoro, Tanzania.

8. Pék, Z., Helyes, L., &Lugasi, A. (2010). Color changes and antioxidant content of vine and postharvest-ripened tomato fruits. *HortScience*, 45(3): 466–468.
9. Ramaswamy, H. S. and N. H. van Nieuwenhuijzen, (2002). Evaluation and modeling of two-stage osmo-convective drying of apple slices. *Drying Technology*, 20(3): 651–667.
10. Sinha NK: (2006). *Hand book of fruits and fruit processing*. USA: Blackwell Publishing; : 265–78.
11. Tark, D. (2007). Determination of effective parameters for drying of apples. School of Engineering and Sciences of İzmir Institute of Technology, Master of science. Urla, İzmir, Turkey.
12. Travers, S., (2013): Dry matter and fruit quality manipulation in the field and evaluation with nir spectroscopy, Ph.D. Thesis., Dept. of Food Science, Faculty of Science and Technology, Aarhus University, Denmark.
13. Wang, J. and Y. Chao, (2002). Drying characteristics of irradiated apple slices. *Journal of Food Engineering*, 52(1): 83–88.
14. Wang, Z., J. Sun, X. Liao, F. Chen, G. Zhao, J. Wu and X. Hu, (2007). Mathematical modeling on hot air drying of thin layer apple pomace. *Food Research International* 40 (1): 39–46.

خواص شرائح التفاح المتأثرة بطرق التجفيف المختلفة

محمود حسن كشك*، محمد نبيه عمر* عبد اللطيف عبد الوهاب سمك*

* مدرس الهندسة الزراعية-قسم الهندسة الزراعية-كلية الزراعة -جامعة المنوفية.

يعتبر التجفيف من الطرق المستخدمة بكثرة في حفظ الخضار والفاكهة وتعرف عملية التجفيف بأنها إزالة الرطوبة إلى الحد الذي لا يسمح بنمو الكائنات الحية الدقيقة، وعملية التجفيف لها تأثير كبير على الخواص الطبيعية والميكانيكية للمنتجات الزراعية، حيث أن عملية التجفيف تؤدي إلى تغير في خواص المنتجات مثل اللون والصلابة، وهذه الخواص تستخدم في تقدير جودة المادة الغذائية المجففة. ولتحقيق الهدف من هذا البحث أجريت هذه الدراسة بقسم الهندسة الزراعية – كلية الزراعة – جامعة المنوفية سنة ٢٠١٥ م.

واشتملت الدراسة على الآتي:

- (١) استخدام أنظمة مختلفة لعملية التجفيف مثل:
 - أ) التجفيف بالفرن الحراري تحت مستويات مختلفة من درجات الحرارة (٨٠° ، ٧٠° ، ٦٠° ، ٥٠° ، ٤٠° م).
 - ب) مجفف شمسي مباشر ملحق به مجمع شمسي.
 - ت) مجفف شمسي مباشر غير ملحق به مجمع شمسي.
 - ث) مجفف شمسي غير مباشر ملحق به مجمع شمسي.
 - ج) مجفف شمسي زجاجي مماثل للمجففات السابقة وغير ملحق به مجمع شمسي.
- (٢) تجفيف شرائح التفاح بسمك شرائح مختلفة (٥، ١٠، ١٥، ٢٠ مم) بأنظمة التجفيف المختلفة.
- (٣) دراسة سلوك منحنيات التجفيف للتفاح تحت أنظمة التجفيف المختلفة.
- (٤) دراسة تأثير أنظمة التجفيف المختلفة على بعض الخواص الطبيعية والميكانيكية (اللون – الصلابة) لشرائح التفاح وكانت أهم النتائج المتحصل عليها: -
- (١) أوضحت النتائج أن أقل وقت أستغرق في تجفيف شرائح التفاح كان ٧ ساعات عند درجة حرارة ٨٠° م وسمك شرائح ٥ مم، حيث انخفض المحتوى الرطوبي من ٦١٤ جم ماء/جم مادة جافة على أساس جاف الى المحتوى الرطوبي المتوازن ١١ جم ماء/جم مادة جافة على أساس جاف.
- (٢) كان أعلى قيمة لمتوسط معدل التجفيف خلال زمن التجفيف الكلي ٠,٨٦٥ جم ماء/جم مادة جافة*ساعة عند درجة حرارة ٨٠° م وسمك شرائح ٥ مم.
- (٣) كانت أقل قيمة للتغير الكلي في اللون ١٠,٦ عند تجفيف شرائح التفاح على درجة حرارة ٦٠° م وسمك شرائح ٥ مم، بينما كانت أعلى قيمة ٢٨,٣ عند التجفيف على درجة حرارة ٨٠° م وسمك شرائح ٢٠ مم.
- (٤) كانت أقل قيمة للصلابة ٠,٧٢ كجم/سم^٢ عند التجفيف على درجة حرارة ٤٠° م وسمك شرائح ٥ مم، بينما كانت أعلى قيمة ١,٩٤ عند درجة حرارة ٨٠° م وسمك شرائح ٢٠ مم.
- (٥) وكانت أقل قيمة للصلابة ٠,٨٣ كجم/سم^٢ عند استخدام المجفف الشمسي الغير مباشر وسمك شرائح ٥ مم، بينما كانت أعلى قيمة ١,٣٩ كجم/سم^٢ عند استخدام المجفف الشمسي الزجاجي وسمك شرائح ٢٠ مم.

التوصيات

يوصى بتجفيف التفاح بالفرن على درجة حرارة ٦٠° م وسمك شرائح ٥ مم، ويوصى بالتجفيف بالمجفف الشمسي الغير مباشر لشرائح التفاح ذات سمك ٥ مم لأن ذلك يعطي أفضل النتائج.

DEVELOPMENT OF A CHOPPER FOR GREEN CORN-STALK

MERVAT M. ATALLAH

Ag. Eng. Res. Inst., ARC, Egypt.

mervat-tallah@yahoo.com

Abstract

The aim of the present study was to modify and evaluate the stationary thresher machine for chopper green corn-stalk. The studied variables included: five different feed rates of 20, 40, 60, 80 and 100 kg/min., four different cutting-knives speeds of 300, 400, 500 and 600 rpm (12.1, 16.1, 20 and 24.4 m/s), number of blades: 8 and 4 blades and moisture contents of corn-stalk of 45 %. The main results were summarized in the following points: At the optimum conditions from data analysis of developed chopper for green corn-stalk were: Feed rate 100 kg/min, cutting-knives speed 600 rpm (24.4 m/s) and 8 blades. The results obtained at optimum conditions were: The maximum machine productivity of 1360.2 kg/h for cutting length < 5 mm, total maximum production for all cutting length of 4073 kg/h, power requirement of 5.5 kW, specific energy of 8.85 kW.h/ton at 8 blades. The operation and production costs were 74 and 73.25 L.E./h and 18.17 and 35.26 L.E./ton for total maximum production at optimum conditions by using feed rate of 100 kg/min, cutting-knives speed of 600 rpm (24.4 m/s) for 8 and 4 blades respectively. The price of locally fabricated chopping machine reached about fourth of imported machine price.

INTRODUCTION

Egypt, the locally produced forage quantity is not sufficient for feeding the livestock population; the thing which led to a forage gap in the feeding process. There is a gap between the available quantity of green forage and the required amount of animal feed. The gap between the availability and requirement of feed is wide and the estimated shortage is 3.1million tons of total digestible nutrice per year. The forage gap or the feed shortage has been partially narrowed to become 2.42million tons because of using new forage resources (AboSalim and Bendary, 2005 and Bendray *et al.*, 2006).

The best way to remove from agricultural residues cutting and chopping for next operation of waste recycling indifferent industry such as making compost and improvement soil properties, animal feeding, energy source (direct burning, biogas generation) compressed wood and the field of industrial application. Rice and corn are considered among the most important agricultural crops in Egypt. Abo-Habaga and Khader (2005) developed of a combined cutting-unit with harvesting combine machine. They showed the effect of cutting speed on the length of cutting straw. Chou *et al.* (2009) used a chopping system to cut rice straws into smaller sizes (10-5, 5-2 and <2 mm). They indicated that by increasing the rotation speed, the average feed rate increased. The average feed rate increased from 2.3 to 2.5 kg/min by increasing the rotation speed from 620 to 980 rpm for cutting-length straw of 10 mm. El-Hanfy and Shalby (2009) modified and evaluated the Japanese combine chopping-unit. They found that the lowest average of cutting length was obtained at forward speed 0.75 m/sec and cutting speed 550 rpm, meanwhile the highest value was obtained at forward speed 0.35 m/sec and cutting speed 450 rpm. El-Berry *et al.* (2001) mentioned that the quantity of crop residues in Egypt reached about 25 million-ton per year and national income is expected to increase with 1.6 billion L.E/year if residues are recycled.

They evaluated Hematol chopper and compared it with Balady thresher in rice straw. El-Iraqi and El-Khawaga (2003) designed and evaluated a machine for cutting crop residues. The maximum percentage in cut length of less than 5 cm of 87.80 % and 92 % were obtained for rice straw and corn stalks residues respectively. Meanwhile, the energy requirement was found to be 6.36 and 6.17 kW.h/ton for rice straw and corn stalks residues respectively. The maximum operating cost was 5.10 L.E/h or 6.61 L.E/ton for cut rice straw residues. Ebaid (2006) used corn Sheller for chopping cotton and corn stalks and mentioned that: Farmers can use the corn sheller for chopping crop residues. The optimum performance was at feed rate of 750 kg/h (0.750 ton/h) , 500 kg/h (0.50 ton/h) for corn and cotton stalks residues respectively, chopping drum speed of 33.5 m/sec (1600 rpm). Cutting length category percentage at these conditions was 63 and 45.40 % in cutting length of <3.35 for corn and cotton stalk residues respectively. It was found that the chop operation cost was 13.33 LE/ton and 20 LE/ton for cutting corn and cotton stalk residues respectively. Tavakoli *et al.* (2009) studied the effects of drum speed, screen size and number of blades on each flange on the power requirement for the size reduction of wheat straw. They reported that the power requirement increased with increases in the drum speed (from 500 to 800 rpm) and decreases in screen size (from 4 cm to 2.5 cm) and number of blades (from 8 to 4) in each flange. The power requirement for the size reduction of wheat straw ranged between 0.985-5.377 kW and the average power requirement was 2.763 kW. Arfa (2007) studied the stationary thresher machine for chopping residues and indicated that by increasing feed rate from 0.5 ton/h to 1.5 ton/h, the percentage cutting-length of rice straw for first category (<3.5 cm) decreased from 78.5 to 70.2 %. Meanwhile the percentage cutting-length of rice straw for second and third categories (3.5 -10 cm and <10 cm) was increased from 16.2 to 20.7 % and 5.3 to 9.1% at 4 cm² oval slots concave, 18.3m/s drum speed, 14.3 % moisture content and 3 cm drum-concave clearance. Basiouny and Ghanem (2010) showed the effect of cylinder speed and feed rate on the unthreading percentage of green rice straw at three different concave clearance ratios. From the figure, it can be generalized that trend of the unthreading percentage of green rice straw decreased by increasing the concave clearance ratio. At feed rate of 200 kg/h and cylinder speed of 16.28m/s, the unthreading percentage of green rice straw decreased from 4.47 to 3.53% when the concave clearance ratio was increased from 0.333 to 1.0. Abo-Habaga *et al.* (2015) mentioned that the decreasing of average cutting-length of rice straw and percentage of rice-straw size less than 8 cm by increasing cutting-knives speed and number of knives is due to increasing number of impacts of flail knives to rice stalks. Meanwhile, the increasing of average cutting-length of rice straw and percentage of rice-straw size more than 8 cm by increasing platform tilt-angle is due to increasing feeding rate of rice straw according to increasing the weight of rice straw bale on claws drum. So, the mean of the present research directed to developing, constructing and testing a chopper to improve its performance and minimize the operational cost.

MATERIALS AND METHODS

The developed chopper:

The thresher drum was replaced by the fan with cutting-knives for chopping the green corn-stalk. The frame of chopper was manufactured by iron sheet of 1.5mm thick. The chopper was 130 cm length, 65 cm width and 85 cm height.

The developed chopper of green corn-stalk was fabricated by using a local materials and the experiments were carried out in Khadra Village, El-Bagour Center, Minofiea Governorate, Egypt, during summer seasons of 2016, 2017. The photographs of developed chopper are shown in [Fig.](#)

1. The overall dimensions are: total length of 124 cm, width of 80 cm and height 66 cm. The developed chopping machine consists of the following parts: 1- Feed opening, 2- Outlet 3- Fan with cutting-knife.



Fig. 1: Photograph of the developed chopping machine of green corn-stalk.

Feed opening: Feed opening was made of iron sheet with length of 46 cm, width of 25, 35cm and thickness of 5 mm in (Fig. 2).



Fig. 2: Photograph of the feed opening

Feeding mechanism

Feeding mechanism consists of two drums :

- 1- **Upper** feeding drum has 20 cm length, 25 cm diameter and 8 blades with drum of 20 length, 8 cm height and 5 mm thickness which welded with the drum to guide the green corn-stalks towards the cutting mechanism (Fig. 3).
- 2- **Lower** drum with diameter of 25 cm and 20 cm length. The lower drum rotates in inverse direction for first drum.



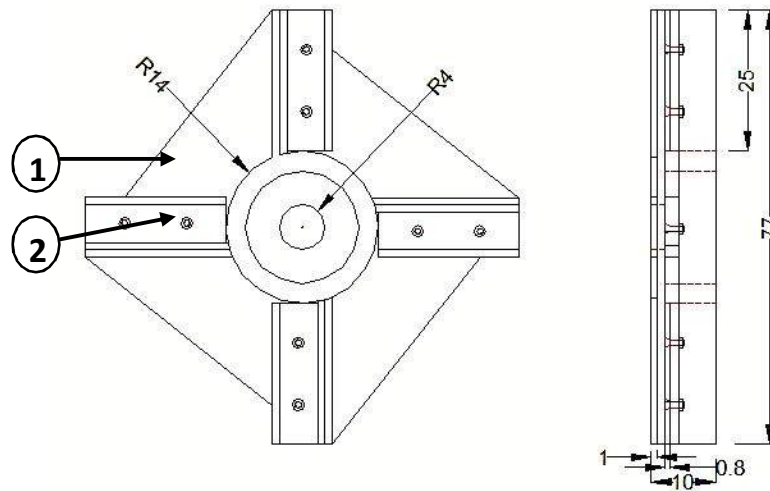
Fig. 3: Photograph of the feeding drum.

Fan:

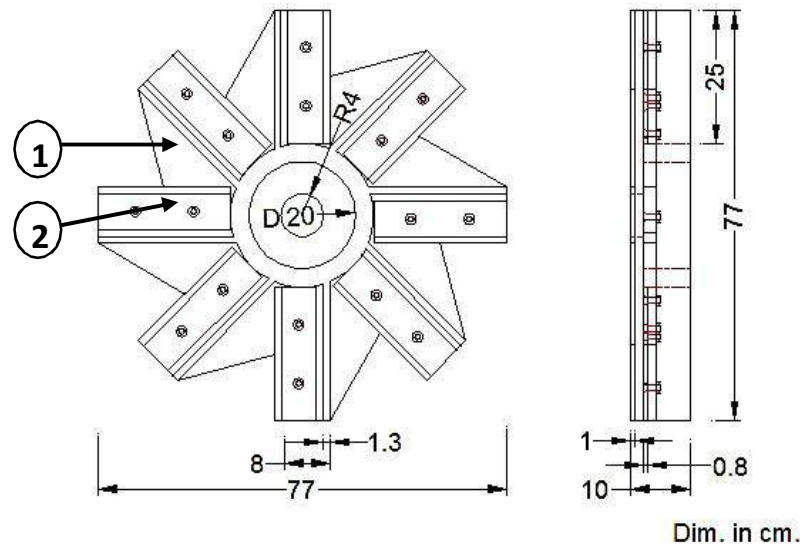
Four and eight blades fan were made of cast iron (**Fig. 4-A and -B**). Every fan blade has a shape upright angle with 25 cm length, 10 cm width, 12 mm thickness. Four or eight parts (paddles) welded with fan blade. The paddle has a shape upright triangle, with dimensions of 12 x 22 x 25 cm and 12 mm thickness. The paddles help the fan to push the chopping green corn the outlet direction.

Rotating cutting-knives :

Eight cutting-knives was made of carbon steel with length of 25 cm, width of 8 cm, thickness of 8 mm and edge sharpness angle of 28°. The cutting-knives were bolted with fan blades by two



(A) 4 knives



(B) 8 knives

1- Paddle, 2- Cutting-knife

Fig. 4: Assembly views of the cutting-knives (A-4 knives, B-8 knives) with fan.

bolts with diameter of 12 mm. Each knife has 2 holes with 12 mm diameter. Rotating cutting-knives cut green corn-stalks and push the chopped materials through the outlet.

The fixed knife :

The horizontal fixed blade was made of carbon steel with 34 cm length, 6 cm width and 12 mm thickness. The fixed knife is fixed behind lower drum at height of 11 cm from the center of lower drum and fixed to the frame of the machine by two bolts. A clearance between rotating and fixed cutting-knives was zero mm. This clearance allows the chopper to cut the corn-stalks like scissors, (Fig. 5). Fig. 6 shows the sketch of feeding and cutting mechanism of green corn-stalk.

Outlet:

The Outlet Made of iron tube with diameter of 160 mm and thickness of 3 mm. The Bottom part, has length of 100 cm and the top part, has length of 150 cm. Outlet is setting above the fan.

Power transmission system:

The power is transmitted from tractor of 50 kW (65 hp). The drive pulley (55cm) which installed on the end of universal joint of the tractor P.T.O. by V-belt to the driven pulley (12cm) thereafter, motion will transmit to the fan. The transmission system details were shown in Fig. 7.

Physical properties of green corn-stalk:

1-Green corn-stalk: Type: variety Giza 310, stalk diameter 23: 26 mm, average 290 mm stalk length and (45 %) moisture content for stalk.

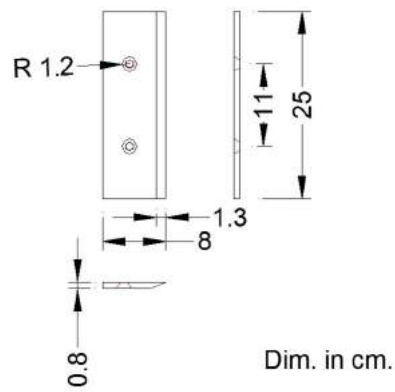
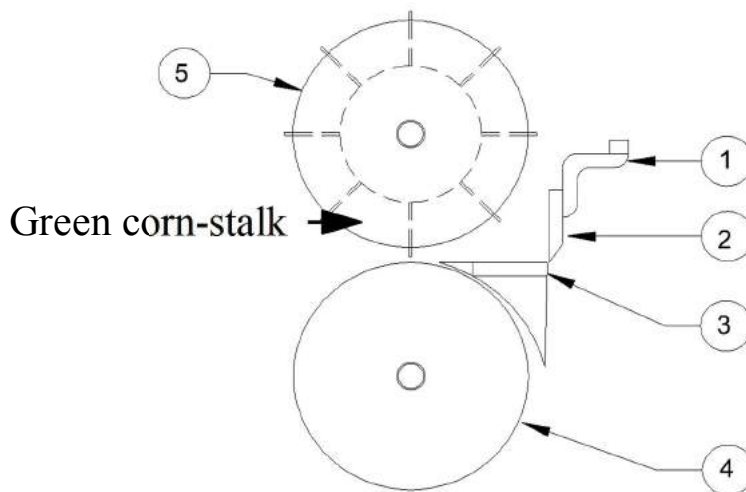


Fig. 5 : Views of the fixed knife.



- 1- Fan blade
- 2- Cutting-knife 3- Fixed knife

- 4-Lower feeding drum 5-Upper feeding drum

Fig. 6 : Sketch of the feeding and cutting mechanism of green corn-stalk.

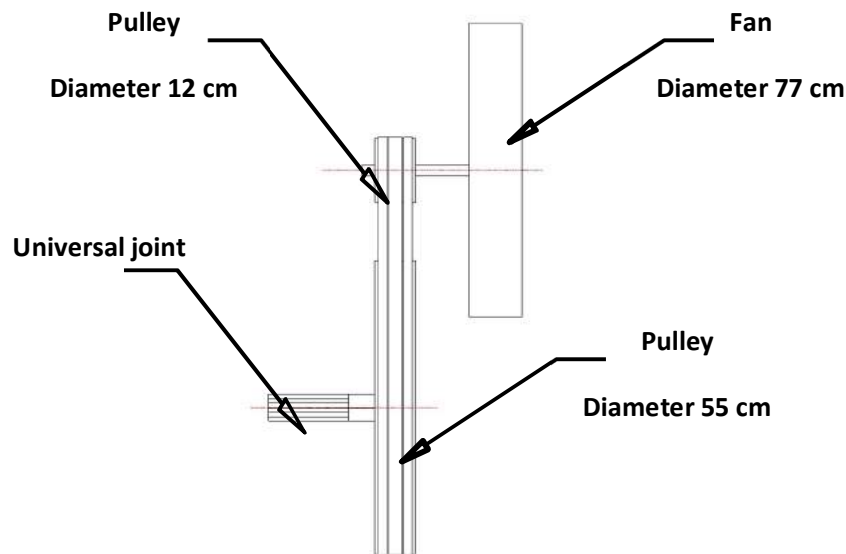


Fig. 7 : Transmission system.

Test procedures on the experimental Stationary chopping green corn-stalk machine:

The following factors were investigated to show their effect on chopping effectiveness:

- 1-**Feed rate:** five different feed rates were tested 20, 40, 60, 80 and 100 kg/min.
- 2-**Cutting-knives speed, rpm. :** Four different cutting-knives speed were tested 300, 400, 500 and 600 rpm (12.1, 16.1, 20 and 24.4 m/s).
- 3- **Number of blades:** 4 or 8 blades, corn-stalk chopping experiments were conducted by varying the number of blades on the fan.

Equipment and Instruments:

- 1-**Tractor:** The source of power for the field experiments was Nasr tractor 65 hp, diesel engine and (2-WD), P.T.O speed 540, 1000 and 1500 r.p.m was used to drive the machine.
- 2-**Hand tachometer:** A hand tachometer was used to measure the rotation speed in three ranges. First range: 40 – 500 rpm., second range: 400 –5000 rpm., and third range: 4000 – 50000 rpm direct reading, with accuracy of ± 1% .
- 3-**Electronic balance:** An electronic balance (made in Japan). Its scale ranged from 0 to 5 kg, and accuracy of 0.2 g was used to weight the chopped samples of corn-stalk.
- 4-**Spring balance:** A spring balance was used to weight corn-stalk. The corn-stalk was collected in bundles before starting the chopping process. It had a range up to 75 kg, and 0.5 kg accuracy.
- 5-**Oven:** to determine the moisture content of corn under test.
- 6-**Hay-moisture tester:** Model (HTM-1) ranged from 13 to 50% was used to measure the moisture content of the corn-stalk.

Measurements:

- 1-**Machine productivity:** was calculated by using the following formula
By mady, 1999.

$$P= W \times 3600 / t \dots\dots\dots(1)$$

Where:

P = productivity in ton/h. W= mass of output in ton.
 T = time in sec.

2-length of cutting: was assessed by taking a sample of 1 kg from corn-stalk chopping material into laboratory. Each cutting length in the sample was weighed and calculated as a percentage from the total weight of the output (**El-Iraqi and Khawaga, 2003**).

3-Cutting-knives speed: Peripheral cutting-knives speed was calculated:

$$S = (22 \times n \times d) / (7 \times 60) \dots\dots\dots (2)$$

Where:

S= Peripheral cutting-knives speed, m/s n =rotational speed, (r.p.m).
 d=cutting-knives diameter, m

4-power requirements: The power consumption requirements were calculated according to the formula of **Hunt, 1984** as follows:

Required power =

$$(F_c \times 1/3600) \rho F \times L.C.v. \times 427 \eta_{Th} \times \eta_m \times 1/75 \times 1/1.36, kW\dots (3)$$

Where:

F_c = the fuel consumption rate, L/h
 ρF = density of the fuel, kg/ L(for solar fuel, kg/ L)
 L.C.v. = lower calorific value of fuel. Kcal/ kg (average Lcv for solar fuel is 10000 kcal/ kg
 427 =thermo-mechanical equivalent, kg .m / kcal
 η_{Th}= thermal efficiency of engine (assumed as 40% for diesel engine) and η_m= mechanical efficiency of the engine (considered to be about 80 % for diesel engine)

5-Specific energy : *It was calculated by using the following equation:*

$$\text{Specific energy (E)} = P \times 1000 / P_p , kW.h/ton \dots(4)$$

Where: P = Total power, kW; P_p = productivity; kg/h.

6- Total cost, LE/h:

-Estimation the costs of using the machine:

Cost of operation is calculated according to equation given by **Awady (2003)**, which has the following form:

$$C = P/H(1/y + i/2 + t + m) + (A. k. f. u) + S/144 \dots(5)$$

Where:

C = Total hourly cost, P = Price of machine LE, H = Estimated yearly-operating hours, y = Estimated life-expectancy of machines in years, i = Interest rate/year , t = Taxes and overhead rates, %; m = Maintenance and repairs ratio,% ; A = Ratio of rated power and lubrication related to fuel cost; K = Power in kW or hp (65 hp), f = Specific fuel-consumption in L/kW.h or L/hp.h; u = Price of fuel per LE ; S = Monthly salaries , LE; and 144 = Estimated working hours per month.

-Total cost requirements of the chopping machine include fixed and operating costs. Declining balance method was used to determine the depreciation (**Hunt, 1983**). The unit operating cost could be estimated from the following formula:

Operating cost (L.E./ton) =

$$\text{machine cost (LE/h) / machine productivity(ton/h), . \dots(6)}$$

RESULTS AND DISCUSSION

Effect of feed rate, cutting-knives speed and number of blades on the cutting-length percentage of green corn-stalk.

Number of blades 8 blades **Fig. 7** showed that the maximum percentage of cutting-length of 46 % was obtained by using feed rate of 100 kg/min, cutting-knives speed of 600 rpm (24.4 m/s). Meanwhile, the minimum percentage of cutting-length of 10.45% was obtained by using feed rate of 100 kg/min, cutting-knives speed of 300 rpm (12.1 m/s) for cutting length < 5 mm. The maximum percentage of cutting-length of 38.5% was obtained by using feed rate of 100 kg/min, cutting-knives speed of 300 rpm (12.1 m/s). Meanwhile, the minimum percentage of cutting-length of 9.68 % was obtained by using feed rate of 100 kg/min, cutting-knives speed of 600 rpm (24.4 m/s) for cutting length >15 mm.

It can be noticed that the decreasing of cutting-length percentage of green corn-stalk by increasing cutting-knives speed is due to increasing number of hits of cutting-knives to green corn-stalk.

Number of blades 4 blades **Fig. 8** showed that the maximum percentage of cutting-length of 41.2 % was obtained by using feed rate of 100 kg/min, cutting-knives speed of 600 rpm (24.4 m/s). Meanwhile, the minimum percentage of cutting-length of 11.3 % was obtained by using feed rate of 100 kg/min, cutting-knives speed of 300 rpm (12.1 m/s) for cutting length < 5 mm. The maximum percentage of cutting-length of 39.2% was obtained by using feed rate of 100 kg/min, cutting-knives speed of 300 rpm (12.1 m/s). Meanwhile, the minimum percentage of cutting-length of 12.29 % was obtained by using feed rate of 100 kg/min, cutting-knives speed of 600 rpm (24.4 m/s) for cutting length >15 mm.

Effect of feed rate, cutting-knives speed and number of blades on machine productivity of green corn-stalk.

Number of blades 8 blades **Fig. 9** showed that the maximum machine productivity of 1360.2 kg/h was obtained by using feed rate of 100 kg/min, cutting-knives speed of 600 rpm (24.4 m/s). Meanwhile, the minimum machine productivity of 455 kg/h was obtained by using feed rate of 20 kg/min, cutting-knives speed of 300 rpm (12.1 m/s), for cutting length < 5 mm. The total maximum machine productivity for all cutting length (<5 mm., <8 mm., <10 mm. and >15 mm) of 4073 kg/h was obtained by using feed rate of 100 kg/min, cutting-knives speed of 600 rpm (24.4 m/s). Number of blades 4 blades **Fig. 10** showed that the maximum machine productivity of 693.68 kg/h was obtained by using feed rate of 100 kg/min, cutting-knives speed of 600 rpm (24.4 m/s). Meanwhile, the minimum machine productivity of 232.1 kg/h was obtained by using feed rate of 20 kg/min, cutting-knives speed of 300 rpm (12.1 m/s), for cutting length < 5 mm. The total maximum machine productivity for all cutting length (<5 mm., <8 mm., <10 mm. and >15 mm) of 2077.7 kg/h was obtained by using feed rate of 100 kg/min, cutting-knives speed of 600 rpm (24.4 m/s). It can be noticed that the increasing of machine productivity by increasing cutting-knives speed is due to decreasing of cutting time. Meanwhile, the increasing of machine productivity by increasing number of blades is due to increasing the cutting-stalk mass and decreasing of cutting time. The fit curve can be illustrating the effect of cutting-knives speed and feed rate (**F**) on machine productivity (**P**) for number of blades 8,4 blades are the linear curve. The best linear equations can be shown in the following equations :

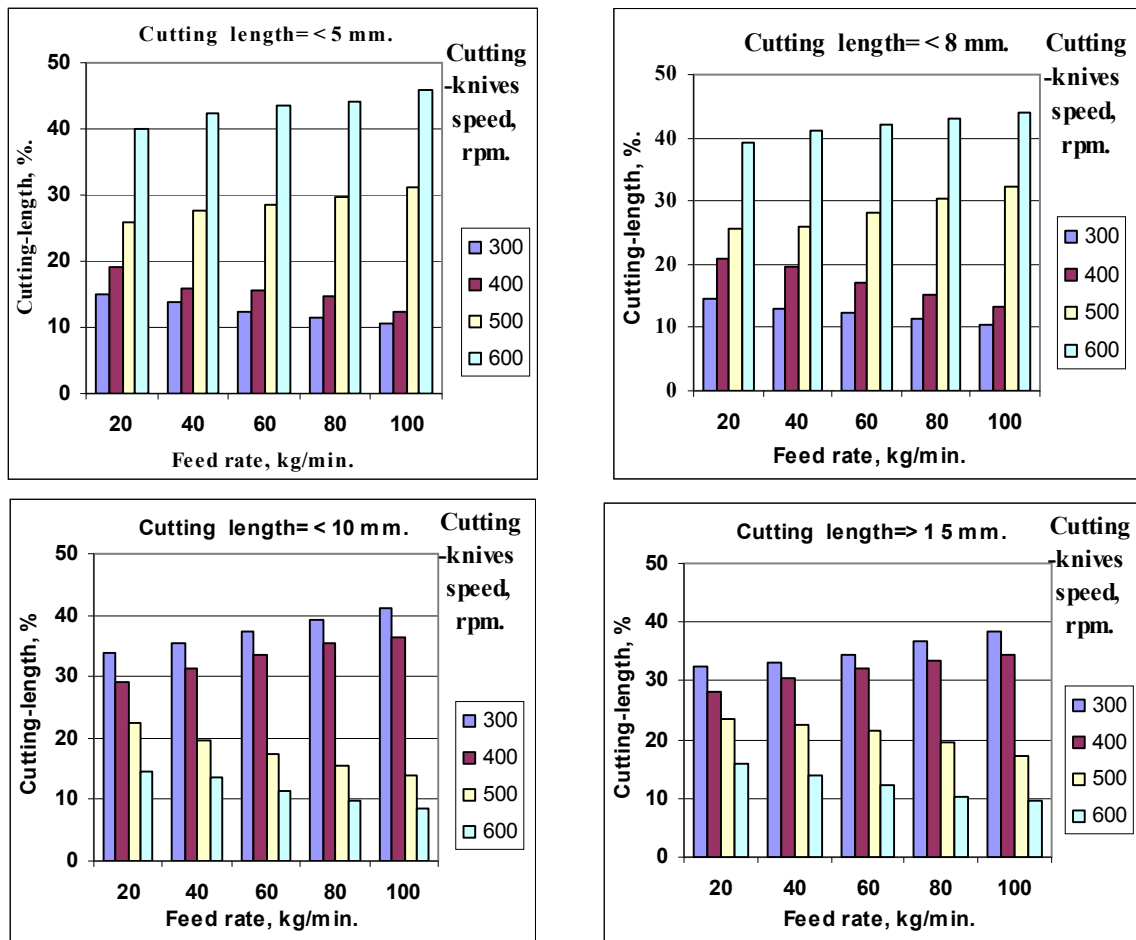


Fig. 7: Effects of feed rate and cutting-knives speed on percentage of cutting-length of green corn- stalk for number of blades 8 blades.

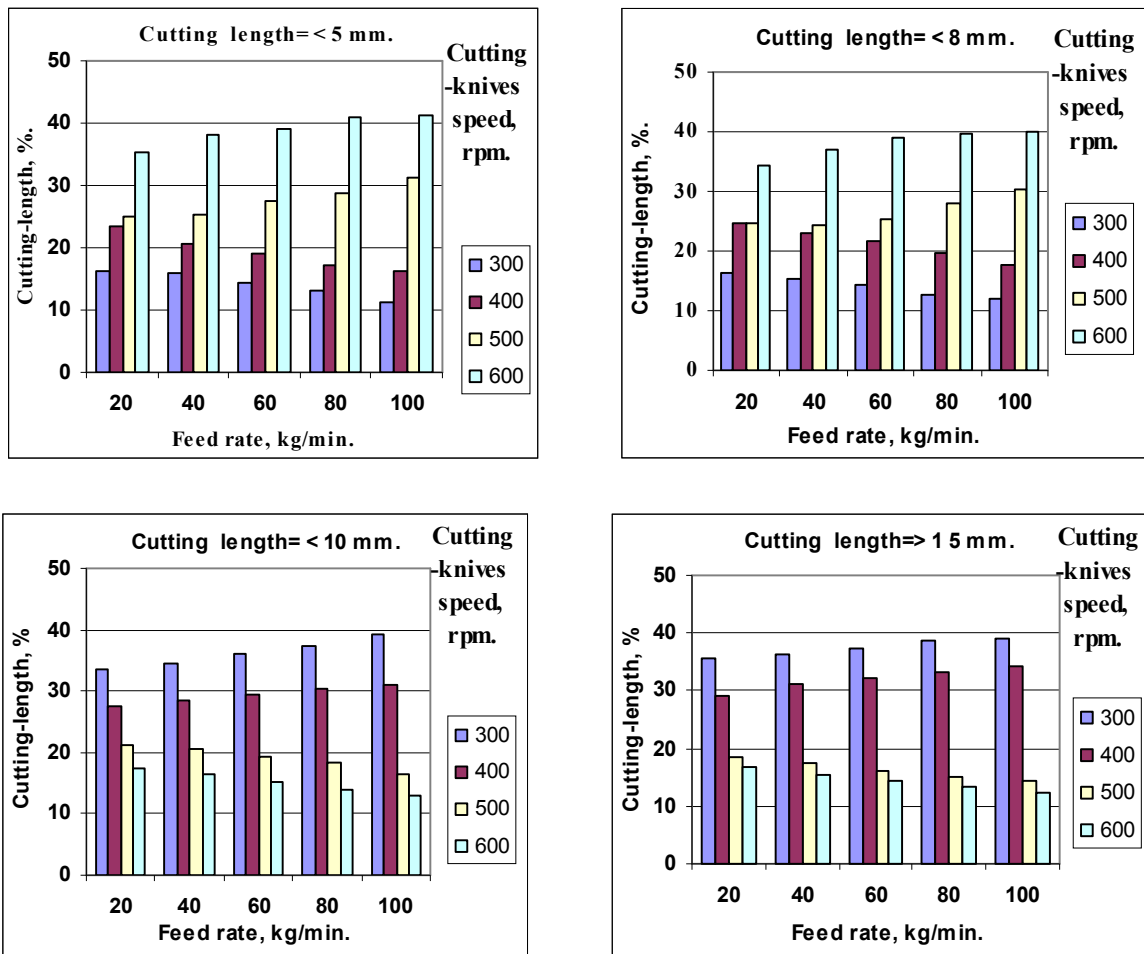


Fig. 8: Effects of feed rate and cutting-knives speed on percentage of cutting-length of green corn-stalk for number of blades 4 blades.

number of blades	cutting-knives speed	The best linear equations	Sum of Squares (R^2)
8 blades	300 rpm	$P = 0.532 4x + 0.85$	$R^2 = 0.94$
4 blades	600 rpm	$P = 0.426 x + 0.72$	$R^2 = 0.92$

The multiple regression analysis of the relation between cutting-knives speed (**S**), feed rate (**F**) and number of blades (**N**) on machine productivity (**P**) give by the following equations :

$$P = 0.78 + 0.57 S + 0.34 F + 0.62 N, R^2 = 0.96$$

From the above equation it can be clear that machine productivity (**P**) is a direct relationship between cutting-knives speed, feed rate and number of blades. Also, the analysis of variance for the data of machine productivity (**P**) at 600 rpm (24.4 m/s) speed, 100 kg/min feed rate and 8 blades indicated a highly significant differences between the treatments with " $R^2 = 0.96$ ".

Effect of feed rate, cutting-knives speed and number of blades on power requirement and specific energy of green corn-stalk.

Fig. 11 showed that the maximum power requirement of 5.5 kW was obtained by using feed rate of 100 kg/min, cutting-knives speed of 600 rpm (24.4 m/s). Meanwhile, the minimum power requirement of 4.03 kW was obtained by using feed rate of 20 kg/min, cutting-knives speed of 300 rpm (12.1 m/s), for 8 blades. The maximum power requirement of 4.79 kW was obtained by using feed rate of 100 kg/min, cutting-knives speed of 600 rpm (24.4 m/s). Meanwhile, the minimum power requirement of 3.5 kW was obtained by using feed rate of 20 kg/min, cutting-knives speed of 300 rpm (12.1 m/s), for 4 blades. It can be noticed that the increasing of power requirement by increasing cutting-knives speed is due to decreasing of cutting time. **Fig. 12** showed that the maximum specific energy of 8.85 kW.h/ton was obtained by using feed rate of 20 kg/min, cutting-knives speed of 300 rpm (12.1 m/s). Meanwhile, the minimum specific energy of 4.05 kW.h/ton was obtained by using feed rate of 100 kg/min, cutting-knives speed of 300 rpm (12.1 m/s) for 8 blades. The maximum specific energy of 15.08 kW.h/ton was obtained by using feed rate of 20 kg/min, cutting-knives speed of 300 rpm (12.1 m/s). Meanwhile, the minimum specific energy of 6.9 kW.h/ton was obtained by using feed rate of 100 kg/min, cutting-knives speed of 600 rpm (24.4 m/s) for 4 blades.

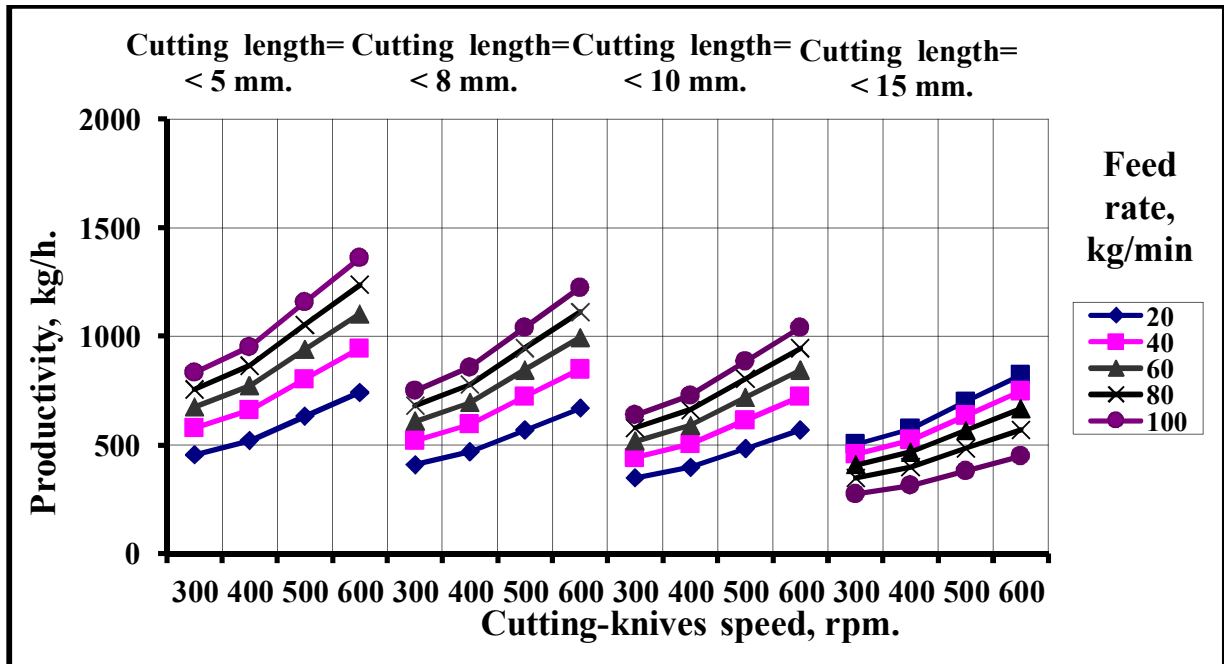


Fig. 9 : Effects of feed rate and cutting-knives speed on productivity, kg/h. of green corn-stalk for number of blades (8 blades).

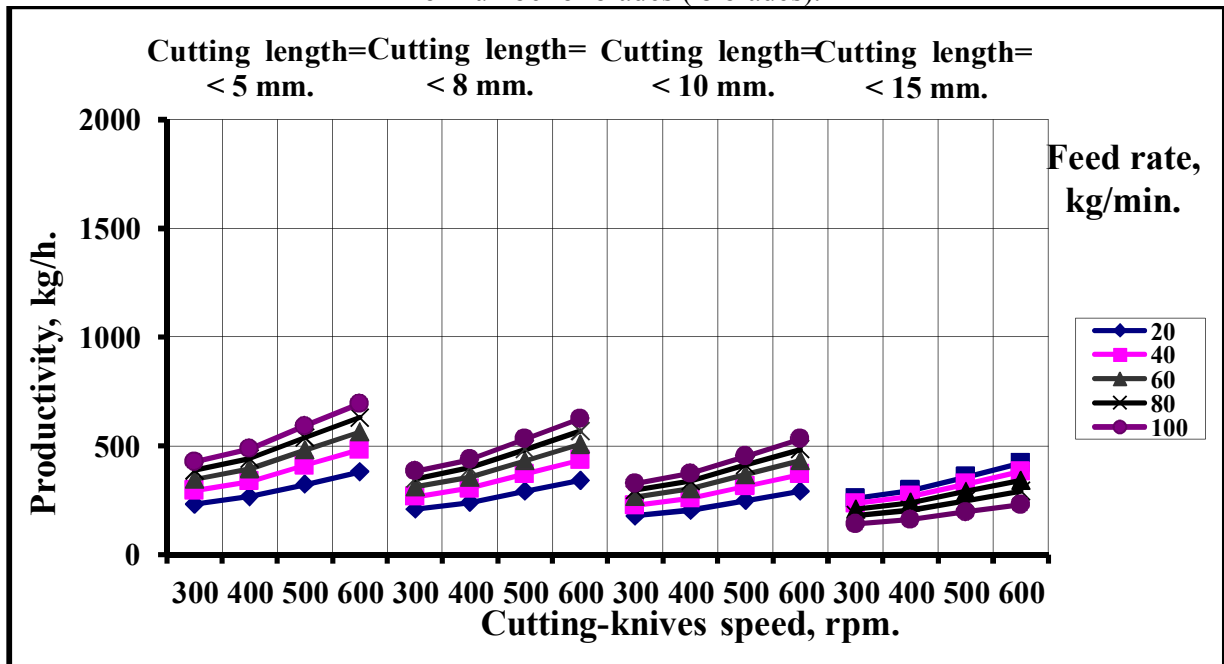


Fig. 10 : Effects of feed rate and cutting-knives speed on productivity, kg/h. of green corn-stalk for number of blades (4 blades).

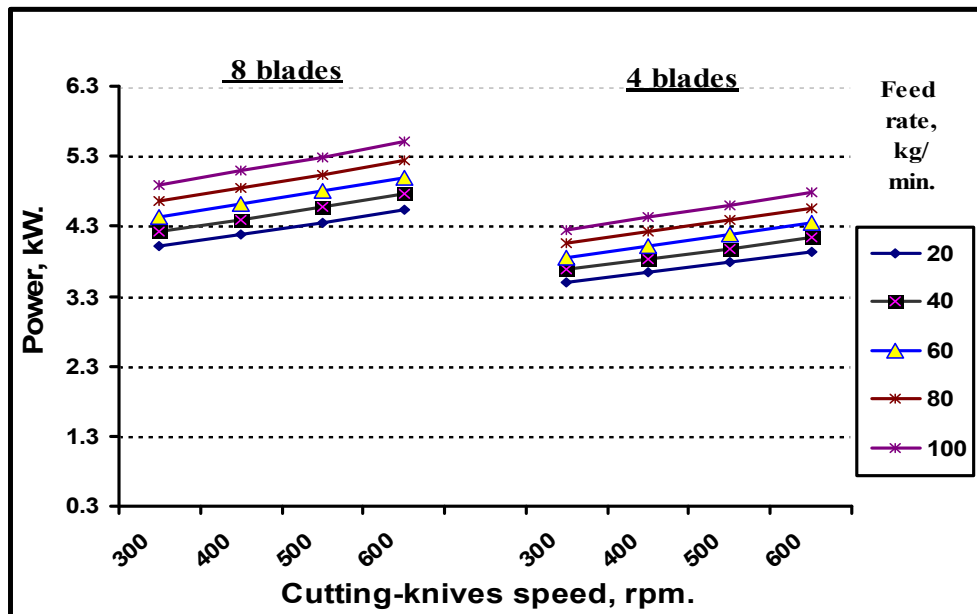


Fig. 11 : Effects of feed rate, cutting-knives speed and number of blades on power requirement kW of green corn-stalk.

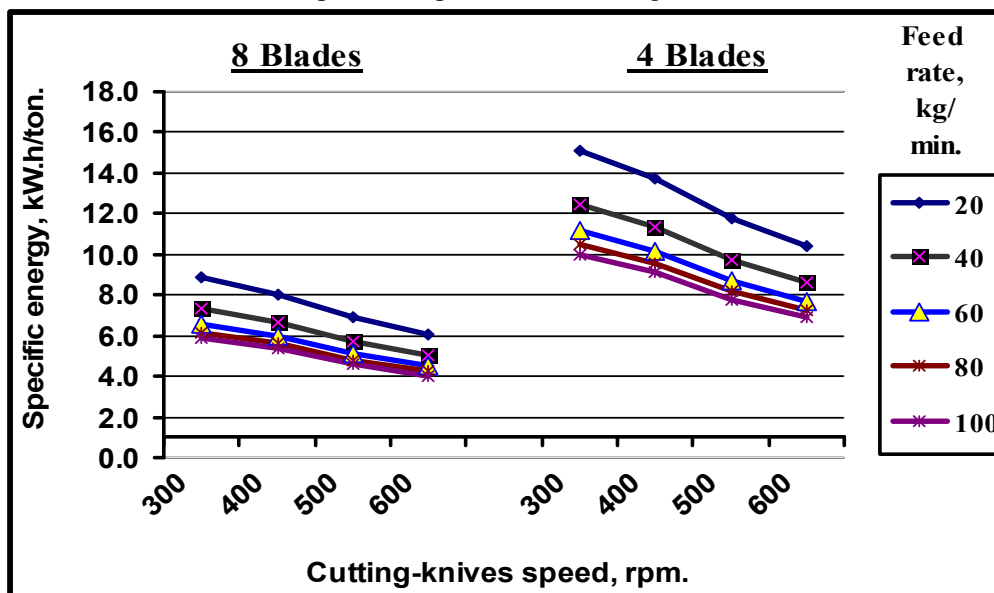


Fig. 12 : Effects of feed rate, cutting-knives speed and number of blades on specific energy kW.h/ton of green corn-stalk.

Production costs for chopping green corn-stalk.

The operation and production costs were 74 and 73.25 L.E./h and 18.17 and 35.26 L.E./ton for total maximum production at optimum conditions by using feed rate of 100 kg/min, cutting-knives speed of 600 rpm (24.4 m/s) for 8 and 4 blades respectively,.

CONCLUSION

The optimum conditions from data analysis of developed chopper for green corn-stalk were: Feed rate 100 kg/min, cutting-knives speed 600 rpm (24.4 m/s) and 8 blades. The results obtained at optimum conditions were: The maximum for: Total machine productivity of 4073 kg/h,

power requirement of 5.5 kW and specific energy of 4.5 kW.h/ton for 8 blades. The operation and production costs were 74 and 73.25 L.E./h and 18.17 and 35.26 L.E./ton for 8 and 4 blades respectively,. The price of locally fabricated chopping machine reached about fourth of imported machine price.

REFERENCES

1. Abo-Habaga, M.M and M.O. Khader (2005). Developed of a combined cutting unit with rice harvesting combine machine for utilization in field waste. *J. Agric. Sci. Mansoura Univ.*, 30(3):1481-1487.
2. Abo-Habaga, M. M. ; I. Yehia and G. A. Abo-Elasaad (2015). Development of a rice straw bales Chopper. *J. Soil Sci. and Agric. Eng., Mansoura Univ.*, 6 (10) :1249 - 1262,
3. AboSalim, I. A. and M. M. Bendary (2005). Forage supplies in Egypt-resources-maximizing its utilization. *Proc. 2nd Conf. Anim. Prod. Res. Inst., Sakha 27-29, Sep.*, : 57-67.
4. Arfa, G. K., (2007). Subdual of stationary thresher machine for chopping residues. *Misr J. Ag. Eng.*, 24(3): 504-521.
5. Awady, M.N., I. Yehia, M. T.Ebaid, and E. M. Arif, (2003). Development and theory of rice cleaner to reduce impurities and losses. *Misr J. Agric. Eng.*, 20 (4): 53 – 68.
6. Basiouny, M.A. and G. H. A. Ghanem. (2010). Modifying a thresher for ensiling the Green rice straw by shredding. *Misr J. Ag. Eng.*, 27(2): 482 – 500.
7. Chou, C. S.; S. H. Lin and W. C. Lu (2009). Preparation and characterization of solid biomass fuel made from rice straw and rice bran, *Fuel Processing and Technology*, 90: 980-987.
8. Ebaid M. T. (2006). Possibility of utilizing corn sheller for chopping cotton and corn stalks. 1 st Agric. Eng. Conference, Mansoura Univ., 31(7): 121-130.
9. EL-Berry, A.M; M.A. Baiomy; H.A. Radwan and E.M. Arif (2001). Evaluation of (Hemtol) machine in rice straw chopping. 9th-Conf. of Misr Society of Agr. Eng., : 65-76.
10. El-Hanfy, E. H, and S. A. Shalby (2009). Performance evaluation and modification of the japanese combine chopping unit. *Misr J. Ag. Eng.*, : 1021- 1035.
11. EL-Iraqi, M. and S. El-Khawaga (2003). Design and test erformance of cutting machine for some crop residues (a). *Misr J. Ag. Eng.*, 20(1): 85-101.
12. Hunt, D. (1984). *Farm power and machinery management*. 8th Ed. Iowa state Univ., Press Ames, U.S.A., :364-368.
13. Tavakoli, H., S. S. Mohtasebi, A. Jafari and D. Mahdavinejad, (2009). Power requirement for particle size reduction of wheat straw as a function of straw threshing unit parameters. *American Journal of Crop Science*, 3(4), 231-236.

تطوير آلة لفرم سيقان الذرة الخضراء

ميرفت محمد عطاالله

معهد بحوث الهندسة الزراعية - مركز البحوث الزراعية - الدقى - جيزة

تعتبر الأعلاف الخضراء هي الأساس الفعلى في تغذية حيوانات المزرعة، فلا يمكن الاستغناء عنها طوال السنة سواء أكانت على صورتها الخضراء أو بعد معاملتها بأحدى الطرق مثل الكمر (السيلاج) أو التجفيف. مع العلم أن كمية الأعلاف المنتجة محليا بمصر ليست كافية لتغذية حيوانات المزرعة مما أدى إلى وجود فجوة بين المتاح والمطلوب من تلك الأعلاف، لذا يهدف البحث الى إستخدام عيدان الذرة الأخضر وتقطيعه للإستفادة منه بعد كمره واستخدامه كعلف.

يهدف هذا البحث إلى تطوير ماكينة دراس قديمة لدى المزارعين (التي أصبحت ليس لها فائدة بعد انتشار الآت الدراس والتذرية الحديثة) لفرم وتقطيع المحاصيل الحقلية الخضراء (عيدان الذرة الأخضر) بعد الحصاد مباشرة وذلك بإستبدال إسطوانة الدراس بمروحة طرد مزودة بسكاكين لفرم وتقطيع عيدان الذرة الأخضر ذو المحتوى الرطوبى ٤٥ % ، ودراسة تأثير بعض العوامل المؤثرة على أداء آلة الفرمة لإختبار أنسب ظروف تشغيل لها بعد التعديل. تتكون الآلة من إطار ، فتحة لتقييم تحنوى على درفيلين لسحب عيدان الذرة إلى الداخل، سكين ثابتة، مروحة دوارة صممت بشكل يعمل على طرد أجزاء عيدان الذرة الأخضر بعد عملية القطع إلى خارج الماكينة، المروحة ذات ريش مثبت علي كل ريشه للمروحة سكين قطع ، حيث تعمل المروحة والسكاكين على فرم وطردهم الفش الى الخارج، يتم شبك الآله بجرار.

كانت عوامل الدراسة كالتالى : خمس معدلات تغذية : ٢٠ ، ٤٠ ، ٦٠ ، ٨٠ ، ١٠٠ كج / د ، أربع سرعات لسكاكين القطع : ٣٠٠ ، ٤٠٠ ، ٥٠٠ ، ٦٠٠ لفة/د (١،١٢،١، ١٦،١، ٢٠، ٢٤،٤ م/ث). عدد السكاكين المتحركة ٤ ، ٨ سكين. وكانت أهم النتائج المتحصل عليها عند أنسب المعاملات المستخدمة من خلال تحليل البيانات كالتالى :

معدل تغذية ١٠٠ كج/د ، وسرعة سكاكين القطع ٦٠٠ لفة/د (٢٤،٤ م/ث) ، عدد السكاكين المتحركة ٨ ، كانت أعلى إنتاجية للآلة هي ١٣٦٠،١ كج/ساعة عند أطوال قطع أقل من ٥ مم . وأعلى إنتاجية كلية للآلة لكل اطوال القطع هي ٤٠٧٣ كج/ساعة وأعلى قدرة هي ٥،٥ كيلوات وأن أعلى طاقة نوعية هي ٨،٨٥ كيلوات/س/طن . تكلفة تشغيل الآلة والجرار ٧٤ و ٧٣،٢٥ جنيه/ساعة وتكاليف الإنتاج هي ، ١٨،١٧ و ٣٥،٢٦ جنيه/طن بإستخدام المروحة ذات السكاكين المتحركة ٨ ، ٤ سكين على التوالى.

EXPERIMENTAL SIMULATION OF SOLAR CHIMNEY SYSTEM USING FINE-BUBBLE TECHNIQUE

KAMEL, REHAM M.¹, M.M. EL-KHOLY¹,
S.E. ABOUZAHER² and I.A. ABDELMOTALEB²

1. *Agricultural Engineering Research Institute (AEnRI), Dokki, Giza, Egypt.*
 2. *Faculty of Agriculture, Kafrelsheikh University, Kafrelsheikh, Egypt.*
-

Abstract

Natural ventilation driven by a solar chimney attached to single-space structure was studied experimentally using a fine bubble technique in which fine hydrogen bubbles simulated the thermal buoyancy effect in the chimney caused by temperature differences. Parameters studied in the experiments were the chimney depth, buoyancy flux, inlet areas for the chimney and structure and chimney height. Similarity between the experimental model and suggested prototypes was used to determine and calculate air velocity of two different prototypes under kafrelsheikh conditions. Similarity results of the suggested prototypes showed that the system in winter is more effective than in summer. It also showed that the values of high air velocity reached the recommended values during winter season. However, the maximum value of the low air velocity was less than the recommended for broilers.

INTRODUCTION

Ventilation is the supply of fresh outdoor air to a space to dilute and remove indoor air contaminants. Natural ventilation occurs due to two causes: wind driving force, or thermal buoyancy driving force (stack effect) or both of them. Use of solar energy can create such a large temperature difference, and hence improve the thermal buoyancy effect for space natural ventilation. The solar chimney is an effective practical way to enhance space natural ventilation by thermal buoyancy. Solar energy heats up the air inside the chimney. As a result of the temperature difference in air, a density gradient between the inside and outside of the chimney is obtained that in turn induces a natural upwards movement of air. The application of solar chimney concept is considered more reliable in single-space structures such the case in most agricultural structures.

Although full-scale modelling of building ventilation systems promises to provide the most accurate and reliable information, its feasibility is still very limited due to the high construction and operation cost. Consequently, laboratory small-scale visualization and modeling systems have been widely used for understanding and evaluating natural ventilation in buildings. (Etheridge and Sanderberg, 1996). Chen *et al.* (2001a) developed a fine bubble technique for buoyancy driven natural ventilation in buildings. The main idea of their modelling technique is to use fine bubble-generated buoyancy plumes in water to simulate the thermal buoyancy-driven flows induced by temperature differences in buildings. In the present work, natural ventilation driven by a solar chimney attached to a single-space structure was studied through an experimental simulation. The experiments were performed using a developed fine-bubble technique in which fine hydrogen bubbles are produced electrolytically in a salt solution to simulate the buoyancy effect caused by temperature differences obtained by the existing of a solar chimney.

From the previous studies (Chen *et al.*, 2001a; Chen *et al.*, 2001b; Li *et al.*, 2003), it was seen that natural ventilation and stratification phenomenon in a single-zone building can be successfully simulated by the fine hydrogen-bubble technique. Since no heating elements are involved in the system, the set-up and operation for the fine-bubble method are simple. Unlike the

brine-water modelling system, bubble plumes have positive buoyancy. Therefore, buoyancy flows in the model are upwards, just as in reality. Further, since the bubbles leave the free water surface during the experimental process, the properties of the bulk liquid will not change throughout the experiments. Consequently, the fine-bubble system does not require a big liquid reservoir and a compact modelling system can be easily constructed.

Therefore, the main objective of the present study was to investigate thermal buoyancy natural ventilation through a solar chimney system attached to a single-space structure. The specific objectives were as follows:

- 1- To study the effect of chimney depth, buoyancy flux, chimney height and inlet areas on the performance of solar chimney as a natural ventilation system by thermal buoyancy.
- 2- To determine and calculate the simulated ventilation parameters namely air velocity, throughout an entire year for suggested prototypes under kafrelsheikh conditions.

MATERIALS AND METHODS

The model was submerged in a large glass tank filled with a salt-water solution. Current passing through a copper wire cathode, positioned along the height of the inner surface of the outer chimney wall. It produced a plume of fine bubbles, which simulated the buoyancy effect within the chimney due to solar radiation. The density between the bubble plume and the ambient fluid simulated density differences caused by temperature differences produced by solar radiation. Fig. 1 depicts a schematic of the experimental set-up. The experimental system was fabricated and constructed in the Electrical and Electronics Lab (of Rice Mechanization Center (RMC) at Meet El-Deeba, Kafrelsheikh governorate, Egypt. The experimental work was executed from December 2008 to March 2009.

The small-scale model was comprised of a solar chimney attached to a single space structure. Single space structure had dimensions of 0.2 cm (Wide) \times 0.1 cm (long) \times 0.2 cm (high). Fig. 2 illustrates isometric of the whole model. The inner tank (small-scale model) was situated in a large tank with a clearance of 65 mm above the bottom floor of the large tank. The large tank, with dimensions of 0.9 m (wide) \times 0.345 m (long) \times 0.6 m (high), represented a static environment surrounding the building. Tap water was filtered before being poured into the tank to eliminate particles that could damage the cathode. Salt was then stirred into the water tank, producing a salt-water solution, approximately 6.6% by weight. This percentage was decided through a pre-experimental as appropriate for the polystyrene particles to be suspended within the water. Salt was added to increase electrical conductivity as well.

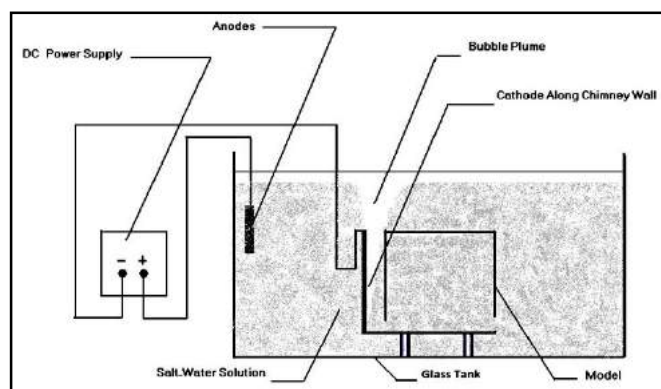


Fig. (1): Schematic view of experimental set-up.

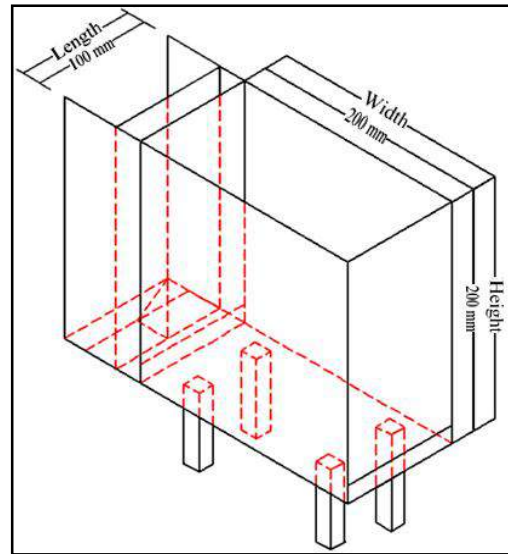


Fig. (2): Isometric of the scale model

In the present study fine hydrogen bubbles were produced by a copper wire array cathode located on the inner surface of the outer chimney wall and provided buoyancy forces in the chimney. When the electric circuit was closed, the current traveled from a graphite anode, through the salt-water, and to the copper wire array cathode, from which hydrogen bubbles were generated. Sixteen solid-cylindrical shaped graphite anodes each one has approximately 40 mm (high) 3.6 mm (diameter).

The buoyancy flux (B), produced by the bubble plume, was calculated using the following equation (Chen *et al.*, 2001a):

$$B = gQ_g \frac{(\rho_s - \rho_g)}{\rho_s} \tag{1}$$

where Q_g is the gas flow rate from the cathode (m^3/s), which is determined by the current, and ρ_s and ρ_g are the densities of the salt-water and hydrogen gas (kg/m^3), respectively. The effect of incident heat flux on the chimney was investigated by varying the buoyancy flux of the bubble plume produced by the copper wire cathode. The buoyancy flux was varied simply by varying the current through the cathode; i.e. by increasing the current, the hydrogen flow rate (Q_g) was increased and, in turn, the buoyancy flux (B). The buoyancy flux is proportional to the heat flux from the source (S), as follows (Chen *et al.*, 2003):

$$B = \frac{gSwH}{\rho C_p T_{amb}} \tag{2}$$

Where (H) the chimney height (m) is, S is the heat flux (W/m^2), ρ is air density (kg/m^3), C_p is specific heat density at ambient temperature ($J/kg \cdot K$), w is chimney width (m), and T_{amb} is the ambient temperature (K). Buoyancy flux for prototypes B and C under Kafrelsheikh conditions for the 21st day in each month of the year was also calculated and listed in Table (1).

Table 1: Buoyancy flux for prototype B and C under Kafrelsheikh conditions for the 21st day in each month throughout an entire year.

Buoyancy flux (m ⁴ /s ³)	Month											
	Jan	Feb	Mar	Apr	May	June	July	Aug	Sep	Oct	Nov	Dec
Prototype B	0.024	0.467	0.369	0.246	0.164	0.129	0.107	0.238	0.300	0.448	0.013	0.032
Prototype C	0.819	0.729	0.076	0.380	0.206	0.201	0.246	0.372	0.000	0.701	0.802	0.832

In this work, a convenient method for measuring the flow velocity due to the fact that the experiments were performed in salt-water and low flow velocities was encountered. It was finally decided according to spencer (2001) the best available method was the particles tracking technique. In which neutrally buoyant particles were timed, and hence the velocity could be determined, as they passed through the ventilated space. A specific particle entering the model inlet was traced by recording images as a video tracking. Then this video could be transformed to cut frames. The images were played back frame-by-frame, and the number of video frames that the particle took to travel a distance between the model inlet and chimney were determined. Knowing that the video played back at 30 frames per second by using Ulead VideoStudio 11 Plus Program.

Experimental treatments:

Four factors namely solar radiation flux incident on the vertical solar chimney, inlet and outlet air space areas, solar chimney height, and solar chimney channel gap, were investigated. Regarding solar radiation, it should be remembered that it will be represented in terms of buoyancy flux as indicated before. The whole treatments are indicated as follows;

- Solar radiation incident on the solar chimney wall, at buoyancy fluxes of 122, 244, 367 and 489 cm⁴/s³;
- Ventilated space and chimney inlet area, four different opening as defined in Table 2 were studied as different four models;
- Solar chimney height, for 200 and 400 mm;
- Solar chimney channel gap, from 4 to 32 mm for the 200 mm chimney and from 8 to 48 mm for the 400 mm chimney.

Table 2: Defining of the four different models and chimney inlet areas.

Model	Area (mm ²)	
	Single-space structure inlet	Chimney inlet
I	1500	1500
II	3000	1500
III	1500	3000
IV	3000	3000

Similarity towards suggested prototypes:

A scale model I was used to physically simulate the real system of the different suggested prototypes. The model was constructed to simulate:

- A single-space structure representing a poultry house of 4 m long, 8 m wide, and 3.5 m high (prototype B);
- A single-space structure representing a poultry house of 5 m long, 10 m wide, and 3.5 m high (prototype C). The configurations of the suggested prototypes are shown in Figs. (3 and 4).

Scale factors are applied to measurements taken from the small-scale test to obtain full-scale quantities. However, this can be done only if the flows in the model and the prototype are dynamically

and geometrically similar. The dynamic similarity requires the dimensionless differential equations and boundary conditions describing both flows be identical. In other words, the ratio of forces acting on the model and the prototype must be constant and in the same direction. If both flows are to have the same dimensionless boundary conditions, then they must be geometrically similar. Also all solid surface boundaries of the model must be the same shape as the prototype and scaled by a constant factor (**Spencer, 2001**). He added that depending upon non-dimensionalizing the governing differential equations and boundary conditions of the two flows, certain coefficients, or similarity parameters, will appear in the dimensionless form of the equations. Therefore, if the similarity condition is to be satisfied (i.e. identical dimensionless governing equations describing both flows) the similarity parameters must have the same value for both the model and the prototype.

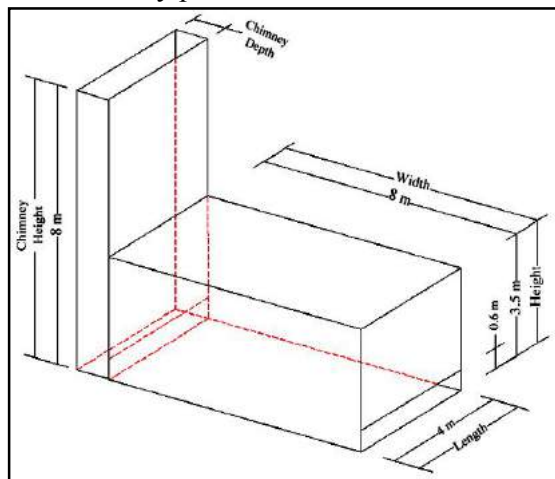


Fig. (3): Isometric of the prototype B.

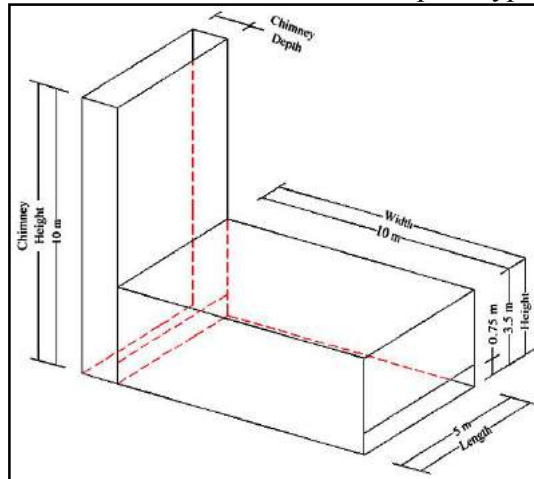


Fig. (4): Isometric of the prototype C.

Similarity analysis:

According to (**Etheridge and Sandberg, 1996**) buildings ventilated by means of natural convection, the appropriate similarity parameters are the Rayleigh (Ra) and the Prandtl (Pr) numbers, (or Schmidt number for natural convection driven by temperature differences). However, in turbulent dominated flows with sufficiently large Rayleigh numbers, buoyancy dominates and viscous effects become negligible; consequentially, the requirements for the Rayleigh and Prandtl numbers become unnecessary and the flow in the model and the prototype will be similar. Turbulent flow dominates when $Ra \geq 10^{13}$. The Rayleigh number generated by a heat source, is given by

$$Ra = \frac{g\beta qL^2}{k\nu D_T} \tag{3}$$

where q is heat flow from the heat source (W), β is the thermal expansion coefficient (1/K), L is the characteristic length of the system (m), k is the thermal conductivity (W/m K), ν is the kinetic viscosity (m^2/s) and D_T is the thermal diffusivity (m^2/s). Since the buoyancy flux (B) from a heat source in a building is given by equation (8). Then β could be expressed as $1/T_{amb}$ and k could be expressed as $\rho C_p D_T$ (ASHRAE, 2009), equation (3) can be rewritten as:

$$Ra = \frac{BL^2}{\nu D_T^2} \tag{4}$$

According to Chen *et al.* (2001a) Rayleigh number for the three prototypes was calculated to reach a reasonable dynamic similarity between the experimental model and the corresponding

prototype. These Rayleigh numbers were calculated through an entire year represented as twelve values corresponding to the twelve months per year depending on the value of B for each month and each prototype. Inserting the above values into equation (4) gives Rayleigh numbers as given in Table 3 for prototypes B and C.

Table 3: Rayleigh number for prototype B under Kafrelsheikh conditions for the 21st day in each month throughout an entire year.

Rayleigh number ($\times 10^{15}$)	Month											
	Jan	Feb	Mar	Apr	May	June	July	Aug	Sep	Oct	Nov	Dec
Prototype B	4.167	3.519	2.780	1.755	1.072	0.801	0.974	1.477	2.242	2.98	3.598	4.081
Prototype C	10.17	8.576	6.776	4.293	2.289	1.949	2.385	3.607	5.475	7.284	8.784	9.966

Rayleigh number for the experimental model was calculated at each buoyancy flux corresponding to different applied electrical currents. This procedure was done by using equation (4). In which B and L depended upon the specifications of the model and the applied electrical currents. On the other hand the values of ν and D_T in the equation for the ambient air replaced by the corresponding values for the intended media. However the kinematic viscosity (ν_m) was considered for the water while the diffusivity D_m was considered for the hydrogen fine bubbles in the water. This procedure was followed by **Chen *et al* (2001a)**. As an example the following procedure illustrates the methodology to calculate the Rayleigh number for the model:

$$Ra = \frac{BL^2}{\nu_m D_m^2} \tag{5}$$

For:

$$B = 122 \text{ cm}^4/\text{s}^3$$

$$L = 0.2 \text{ m}$$

$$\nu_m = 1 \times 10^{-6} \text{ m}^2/\text{s}, \text{ the kinematic viscosity of water at temperature } 298 \text{ K.}$$

$$D_m = 5.10 \times 10^{-9} \text{ m}^2/\text{s}, \text{ taken as the diffusivity of fine bubbles in water equal to that of hydrogen in water at mean water temperature of } 298 \text{ K.}$$

Rayleigh number will be $Ra = 1.88 \times 10^{15}$. Table 4 shows the calculated Rayleigh numbers for experimental model.

The free plume height (L) in equation (6) can be calculated by rearranging equation (5):

$$L = \sqrt{\frac{Ra D_m^2 \nu_m}{B}} \tag{6}$$

Considering the minimum value for the buoyancy flux (B) and a Rayleigh number of $Ra = 10^{13}$, corresponding to the critical value for turbulent flow, equation (6) i.e. the free plume height should be less than 15 mm. Unfortunately this could not be observed during the experiments. However, according to **Chen *et al.* (2001a)** and compared with the model height of 200 mm this could be existed. Therefore the similarity analysis introduced by **Chen *et al* (2001a)**, **Chen *et al.* (2001b)** and **Spencer (2001)** was followed in the present study.

Table 4: Calculated Rayleigh number for experimental model at four different applied currents and buoyancy fluxes.

Applied Current (I) (A)	Buoyancy Flux (B) cm ⁴ /s ³	Rayleigh Number (Ra) (× 10 ¹⁵)
1	122	1.88
2	244	3.76
3	367	5.64
4	489	7.52

The main objective of the similarity analysis in the present study is to confirm the similar behavior between the model and the corresponding prototype as the real situation. The represented similarity was led to the determination of air velocity within a suggested single-space structure. When the similarity between the model and its corresponding prototype is achieved, the following dimensionless relationships may be obtained (Chen *et al.*, 2001a):

$$\left(\frac{B}{L^4\theta^{-3}}\right)_{PT} = \left(\frac{B}{L^4\theta^{-3}}\right)_M \tag{7}$$

Where θ is the characteristic time scale, i.e. the time that the system takes to undergo a specific change (ASHRAE, 2009), or

$$\left(\frac{B_{PT} L_M^4}{B_M L_{PT}^4}\right) = \left(\frac{\theta_M}{\theta_{PT}}\right)^3 \tag{8}$$

The subscriptions PT and M in equations (7) and (8) point to prototype and model respectively. The term, θ_M/θ_{PT} in equation (8) can be determined from known parameters of B_{PT} , B_M , L_{PT} , L_M . Therefore, velocity (u) and for the prototypes may be obtained by the following expressions, respectively (Chen *et al.* 2001a):

$$\frac{u_{PT}}{u_M} = \left(\frac{L_{PT}}{L_M}\right) \left(\frac{\theta_M}{\theta_{PT}}\right) \tag{9}$$

RESULTS AND DISCUSSION

In this work, the effect of chimney width, buoyancy flux, chimney height and ventilation inlet area on the ventilation flow rate were investigated. The effect of inlet was tested for four different ventilation openings, known as modes, at a buoyancy flux of 367cm⁴/s³. The opening models are categorized according to combination of inlet areas to the room and chimney; see Table 2. The effect of buoyancy fluxes of 122, 244, 367 and 489 cm⁴/s³ was investigated while the inlet area was fixed at Model (I). The effect of chimney height was investigated for heights of 200 and 400mm at opening Model (I) and a buoyancy flux of 367cm⁴/s³.

Performance of solar chimney system

Effect of chimney depth and buoyancy flux:

Fig. 5 shows the effect of chimney depth and buoyancy flux on air exchange rate (ACH). It reveals that, as the chimney depth increased from 4 mm, the air exchange rate in the structure gradually increased until the chimney depth reached about 12 mm. As the chimney depth increased beyond this point, the air change rate decreased. The maximum air exchange rate (optimum level) occurred at a chimney depth of 12 mm. With a further increase in the chimney depth (greater than the optimum depth) there was a significant reversal flow or back flow and consequentially a

reduction in the net flow through the system. This is in agreement with the data published by numerous researchers (Sparrow and Azevedo, 1985; Aboulnaga, 1998; Gan, 1998; Zhai *et al.*, 2004; Miyazaki *et al.*, 2006).

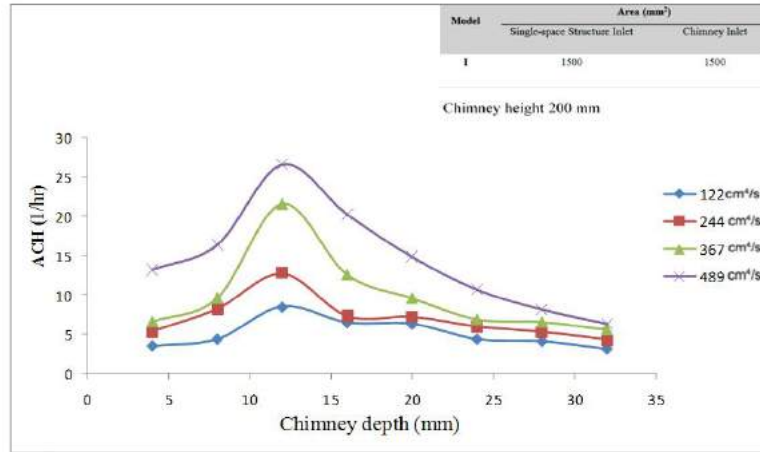


Fig. (5): The effect of chimney width and buoyancy flux on ventilation rate.

It can be seen that increasing the buoyancy flux in the chimney caused a general increase in flow rate through the system. This is expected, because of increasing the heat flux into the chimney increases the temperature of fluid within the chimney and, hence, the temperature difference between the chimney and the outside fluid. This, in turn, increases the driving pressure by thermal buoyancy and the air flow rate. There are other factors to be considered in solar chimney design that affect the optimum chimney depth, i.e. inlet areas and chimney height, which will be discussed later in the following sections.

Effect of Inlet Area:

Variation of the room and chimney inlet areas had a significant affect on both the ventilation flow rate and the optimum chimney width. From Fig. 6, it is seen that much higher flow rates could be achieved with opening Models (III) and (IV), compared to Models (I) and (II). This suggests that increasing the chimney inlet area is more effective than increasing the room inlet area. Further inspection of Fig. 6 reveals a shift in optimum chimney width, it becoming significantly larger for Model (III) and (IV) at 16mm. At model (II), the optimum is about the same as it is at Model (I), occurring at 12mm.

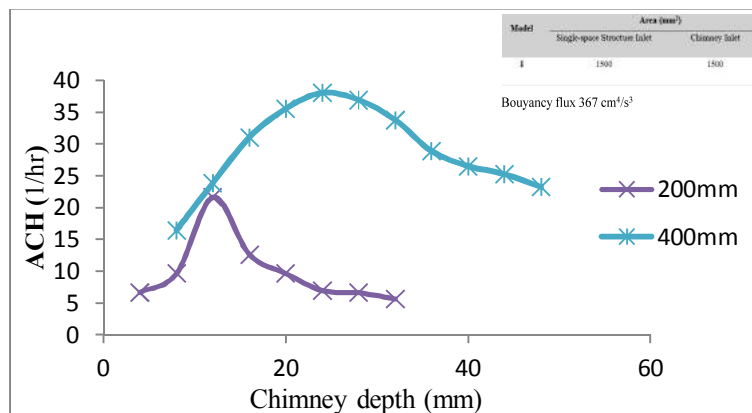


Fig. (6): The effect of ventilation inlet area on ventilation rate.

Effect of Chimney Height:

To evaluate the effect of the chimney channel height, tests were performed for heights of 200mm and 400mm. The tests were carried out at a buoyancy flux of $367 \text{ cm}^4/\text{s}^3$ and at Model (I). The results are shown in Fig. 7. It can be seen that the optimum chimney width occurs at around 24mm for the 400mm chimney; twice the width encountered for the 200mm chimney. Such results imply a linear relationship between the chimney height and the optimum chimney width as shown in Fig. 7. In other words, the optimum aspect ratio (chimney height: optimum chimney width) remained fixed. This is in agreement the data published by Bouchair (1994).

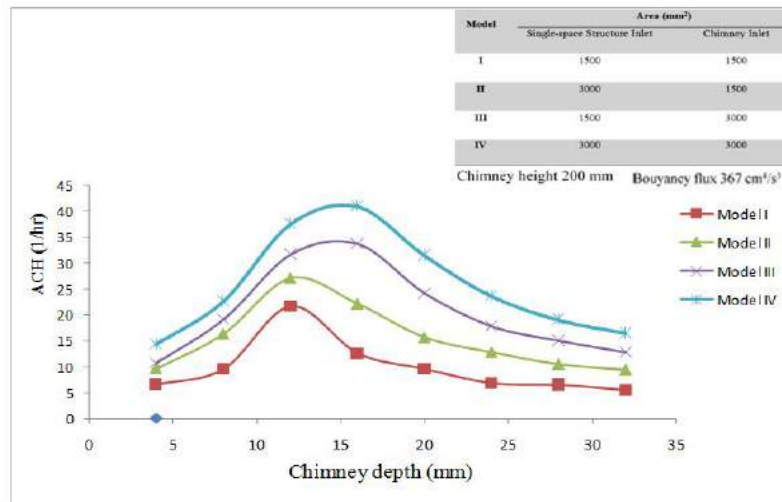


Fig. (7): The effect of chimney height on the ventilation rate.

Referring again to Fig. 7, it is noted that the air change rate measured at the optimum chimney width for 400mm chimney is almost twice that measured for the 200mm chimney. Therefore, it appears that doubling the chimney height doubles the obtainable ventilation flow rate. These results suggest that increasing the chimney height is an effective way of increasing flow rate. The direct relationship between the ventilation rate and chimney height is confirmed by Gan (1998) and Afonso and Oliveira (2000).

Simulated air velocity for suggested prototypes

The air velocity was simulated and determined at both cases that achieve high and low flow rate. As shown before in Fig. 5, it was noted that the highest and lowest flow rates of model I for buoyancy fluxes of 122, 244, 367 and $489 \text{ cm}^4/\text{s}^3$ occurred at 12 mm and 32 mm chimney depth, respectively. Consequently, the corresponding values for prototype B and C at high flow rate were at 0.48 m and 0.6 m chimney depth, and low flow rates at 1.28 m and 1.6 m chimney depth. The values of the highest and lowest air velocity for prototypes B, and C through an entire year are illustrated in Figs (8 and 9), respectively. It should be mentioned that each point on each curve represents the value of air velocity at the day of 21st of each month of the year.

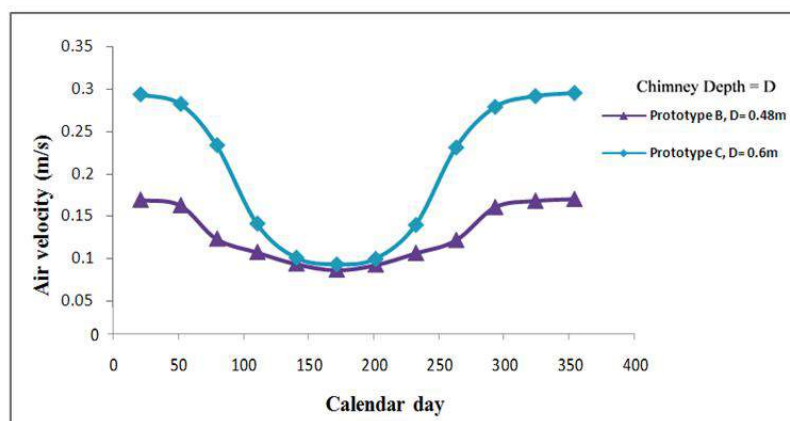


Fig. (8): Highest air velocity variations within the prototypes B and C throughout an entire year.

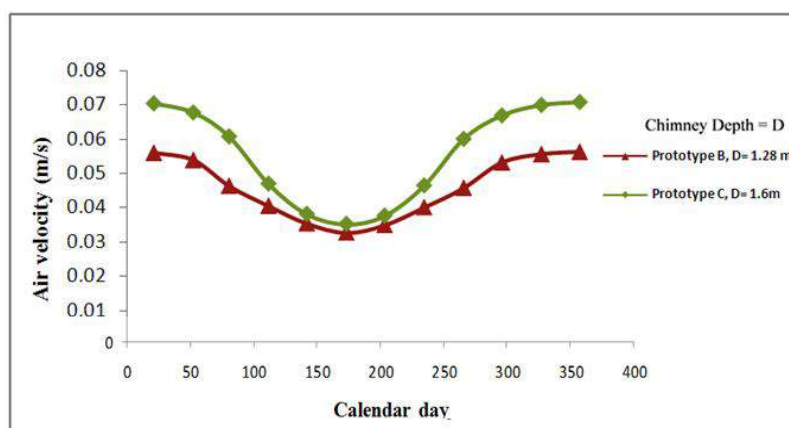


Fig. (9): Lowest air velocity variations within the prototypes B and C throughout an entire year.

As shown in Fig. 8, the high air velocity decrease gradually with the increase of the day number until it reaches the minimum values of about 0.087 and 0.093 m/s for prototypes B and C, respectively at the day number of 172 (June 21st). Then it tends to increase gradually until it reaches the maximum values of about 0.170 and 0.295 m/s respectively, at the day number of 355 (December 21st). The simulated data of high air velocity for prototypes B and C were in the ranges of 0.162-0.170 and 0.282-0.295 m/s respectively throughout the winter season (December 21st – February 21st). In summer season (June 21st – August 21st) the ranges were 0.087-0.106 and 0.093-0.140 m/s for prototypes B and C, respectively.

This means that the values of high air velocity in summer and winter seasons for prototype C were higher than that for prototype B by about 15.55% and 73.68%, respectively. Moreover, it appears that the system in winter is more effective than in summer. From the present study and referring to the recommended air velocity at bird level (0.2-0.3 m/s) (Allam, 1986 and El-Hadidi, 1989), it seems that the suggested system for prototype B and C will be able to achieve the recommended values of air velocity during winter season. However it is recommended to increase chimney height to enhance its performance during summer season or increasing chimney inlet area which is more effective than increasing the prototype inlet.

On the other hand for the values of the lowest air velocity Fig. 9 shows that, low air velocity decrease gradually with the increase of calendar day until it reaches the minimum values of about

0.032 and 0.035 m/s for prototypes B and C respectively, at the day number of 172 (June 21st). Then it tends to increase gradually until it reaches the maximum values of about 0.056 and 0.070 m/s respectively, at the day number of 355 (December 21st). The simulated data of low air velocity for prototypes B and C were in the ranges of 0.053-0.056 and 0.067-0.070 m/s throughout the winter season (December 21st – February 21st), respectively. While in summer season (June 21st – August 21st) the ranges were 0.032-0.040 and 0.035-0.046 m/s for prototypes B and C, respectively.

This means that the values of low air velocity in summer and winter seasons for prototype C were higher than that for prototype B by about 9.51% and 25.82%, respectively. It can be seen that the maximum value of low air velocity in summer and winter season for the prototypes B and C was 0.07m/s. This value is less than the recommended for broiler. Therefore, air velocity could be increased by decreasing chimney depth until it reached the optimum one that gives the highest air velocity values.

CONCLUSION

The experiments were performed using developed fine-bubble technique in which fine hydrogen bubbles are produced electrolytically in salt solution to simulate the buoyancy effect in the chimney caused by temperature differences. Results of the experimental model showed that there was an optimum depth at which maximum ventilation rate can be achieved. The ventilation rate increased with increasing the buoyancy flux and ventilation inlet areas. It was also found that, at moderate to large chimney depth, the effect of chimney inlet area on the ventilation rate was more significant than the effect of structure inlet area. Furthermore, when the chimney height was doubled, the highest ventilation rate was almost doubled as well. Similarity results of the suggested prototypes showed that the system in winter is more effective than in summer. It also showed that the values of high air velocity reached the recommended values during winter season. However, the maximum value of the low air velocity was less than the recommended for broilers.

REFERENCES

1. AboulNaga, M.M. (1998). A roof solar chimney assisted by cooling cavity for natural ventilation in buildings in hot arid climates: an energy conservation approach in Al-Ain city. *Renewable Energy*, 14(1-4): 357–363.
2. Afonso, C. and A. Oliveira (2000). Solar chimney: simulation and experiment. *Energy Buildings*, 32(1): 71-79.
3. Allam, S. (1986). *Poultry Breeding and its Care*. 7th Edition. The Egyptian Anglo library. (In Arabic).
4. ASHRAE (2009). *Handbook of fundamentals*. Atlanta, ga. 30329: American society of heating, refrigerating and air-conditioning engineers.
5. Bouchair, A. (1994). Solar chimney for promoting cooling ventilation in southern Algeria. *Building Services Engineering Research and Technology*, 15(2): 81-93.
6. Chen, Z.D; P. Bandopadhyay; J. Halldorsson; C. Byrjalsen; P. Heiselberg and Y. Li (2003). An experimental investigation of a solar chimney model with uniform wall heat flux. *Building and Environment*, 38(7): 893-906.
7. Chen, Z.D; Y. Li and J. Mahoney (2001a). Experimental modelling of buoyancy-driven flows in buildings using a fine-bubble technique. *Building and Environment*, 36(4): 447-455.
8. Chen, Z.D; Y. Li, and J. Mahoney (2001b). Natural ventilation in an enclosure induced by a heat source distributed uniformly over a vertical wall. *Building and Environment*, 36 (4): 493-501.

9. El-Hadidi, Y.M.S. (1989). Mechanization on poultry farms. Unpub. Ph. D. Thesis Agricultural Mechanization Department, Faculty of Agriculture, Mansoura University, Egypt.
10. Etheridge, D.W. and M. Sanderberg (1996). Building ventilation: Theory and measurements. John Wiley & Sons Ltd, : 90-91, 206-209, 649-667.
11. Gan, G. (1998). A parametric study of Trombe walls for passive cooling of buildings. *Energy and Buildings*, 27(1): 37-43.
12. Li, Y; V.C.W. Shing and Z. Chen (2003). Fine bubble modelling of smoke flows. *Fire Safety Journal*, 38(3): 285–298.
13. Miyazaki, T; A. Akisawa and T. Kashiwagi (2006). The effect of solar chimneys on thermal load mitigation of office buildings under the Japanese climate. *Renewable Energy*, 31(7): 987-1010.
14. Spencer, S (2001). An experimental investigation of a solar chimney natural ventilation system. MSC Thesis, Department of Building, Civil and Environmental Engineering, Concordia University.
15. Sparrow, E.M. and L.F.A. Azevedo (1985). Vertical channel natural-convection spanning between the fully-developed limit and the single-plate boundary-layer limit. *International Journal Heat Mass Transfer*, 28(10): 1847-1857.
16. Zahi, X.Q; Y.J. Dai and R.Z. Wang (2004). Experimental investigation on air heating and natural ventilation of a roof solar-collector. Denver (USA): World Renewable Energy Congress.

محاكاة تجريبية لنظام مدخنة شمسية باستخدام تقنية الفقاعات الدقيقة

ريهام محمد كامل^١، محمد مصطفى الخولي^١، سعيد السيد أبو زاهر^٢، اسماعيل احمد عبد المطلب^٢

- ١ . معهد بحوث الهندسة الزراعية - مركز البحوث الزراعية - الدقي - الجيزة- مصر .
- ٢ . كلية الزراعة - جامعة كفر الشيخ- كفر الشيخ- مصر .

تمت دراسة التهوية الطبيعية الناشئة عن مدخنة شمسية ملحقة بمنشأ أحادي الفراغ باستخدام تقنية الفقاعات الدقيقة وذلك بمحاكاة فقاعات الهيدروجين لتأثير الطفو الحراري الناتج عن اختلاف درجات الحرارة في المدخنة الشمسية. وقد كانت معاملات الدراسة التجريبية كالتالي: عمق المدخنة الشمسية، التدفق الطفوي، مساحات فتحة التهوية لكل من المدخنة والمنشأ وارتفاع المدخنة. تم استخدام تحليل المشابهة بين النموذج التجريبي ونماذج أولية مقترحة لتعيين وحساب سرعة الهواء لهذه النماذج الأولية تحت ظروف مدينة كفر الشيخ. أظهرت نتائج المشابهة للنماذج الأولية المقترحة أن المنظومة في موسم الشتاء أكثر فاعلية مما هي عليه في موسم الصيف. وأظهرت كذلك أن قيم سرعات الهواء المرتفعة بلغت القيم الموصى بها أثناء موسم الشتاء. علي الرغم من أن قيمة الحد الأدنى لسرعة الهواء المنخفضة كانت أقل من الموصى بها لدجاج إنتاج اللحم.

EFFECT OF HIVE BUILDING MATERIAL ON BEE COLONIES

AL-RAJHI M. A.

Agriculture Engineering Research Institute, AEnRI, ARC, El-Dokki – Egypt

Abstract

This study was carried out in a private apiary at Meet Salseel, Eldaqahliyah Governorate, Egypt for four months to compare foam, cement and white brick with common material (wood), in the construction of Langstroth beehive model in a completely randomized design. The evaluation also included three thicknesses of hive sides and three sizes of hives. There were primary measurements on the building materials such as: density, thermal conductivity, water absorption, and rate of water loss. The secondary measurements including: inside hive temperature, number of occupied frames, nest weight, and the production cost. Results indicated that the mean density of foam, cement and white brick samples were about 49, 952 and 811 kg/m³, respectively, while it were 528 kg/m³ for wooden hives. The mean values of thermal conductivity were 0.33, 0.28 and 0.01 W/m²°C for cement, white brick, and foam samples, respectively, while it were 0.18 W/m²°C for wooden hives. The cement, white brick and wood samples absorbed 24, 18, and 14 % of water, while the foam simple didn't absorb any water. Cement and white brick samples absorbed more water and lost it faster than wooden one. The maximum inside hive temperature was recorded in foam hive, while the minimum was recorded in white brick hive. The mean number of occupied frames for foam hives were increased 20.45 % than it in wooden hives, but it were decreased 11.36 and 15.91 % when using cement and white brick hives, respectively. The mean nest weight for foam hives were increased about 24.85 % than it in wooden hives, but it were decreased about 11.7 and 7.41 % when using cement and white brick hives, respectively. There was an increasing in mean internal hive temperatures, number of occupied frames and nest weight by decreasing hive size and increasing side thickness. Foam, white brick and cement cost requirements were 80, 63.3 and 40 % cheaper than the wooden beehive (150 L. E. without the price of the nest). In general, the foam, cement and white brick hives can be easily constructed with a low cost and with similar characteristics as traditional wooden hives.

Keywords: Hive building materials, Thermal conductivity, Temperature, Colonies strength and productivity.

INTRODUCTION

Normally honeybees build their nest in different places like mountains, hollow trees, ground holes and others, trying to protect themselves from wind, rain and enemies. Honeybees are known to control their hive environment to survive drastic changes in the field environment (Jones and Oldroyd, 2007). Bees consume honey to rise inside hive temperature and worker bees contribute to the regulation of brood nest temperature by producing heat while sitting motionless on the caps of brood cells (Marco Kleinhenz, *et al.*, 2003). Several investigators as (Jevtic, *et al.* 2009), has proved positive correlation between stored pollen, brood production and honey yield. The wooden Langstroth beehives offers acceptable conditions, allowing their dispersion worldwide (Wiese, 1974; Dadant and Sons, 1975). But, the Langstroth wooden hive cost is high at the beginning of the honeybee project and didn't encourage the production, especially for small beekeepers at the developed countries. Also the expected life of wooden hives is short and it can be burned. (Hobson, 1983) suggested the ferrocement hive that is more resistant and cheaper than the wooden hive. (Soares and Banwart, 1989), used the Fibercol hive that made of fiberglass despite of its high cost. (Neves, 2002), verified that the brood nest temperature were similar in a

cement vermiculite mortar and wooden hives. (Padilha, *et al.* 2001), obtained that the thermal conductivity of 0.16 to 0.44 W/m/°C in cement-vermiculite mortar (CVM) boards. According to (Stangenhuis, and Paredes 1992), the thermal conductivity of concrete is 1.5 W/m/°C and the mortar cement is 1.15 W/m/°C. Also, it found out that clay hives are easily available and very cheap compared to wooden hives and also more environmentally friendly (F.A.O., 1990). There are little researches about the effect of hive building materials on bee colonies under Egypt conditions. So, the objective of this research is to test the hypothesis that the new hive build materials such as: foam, cement and white brick shows similar results to the wooden hive.

MATERIALS AND METHODS

Langstroth beehives is the most widely used hive in the world (Ojeleye, 1999). To conduct the experimental work, a new Langstroth bee hives were constructed from a local and a valuable cheap materials such as: foam, cement and white brick as illustrate in Fig. (1) and compared with common material (wood). Honeybees (hybrid Carniolan, *Apis mellifera carnica carniolan*) are a single honeybee species adopted by the farmers in Egypt. The honeybees that had been established 8 months prior to the beginning of the experiment were placed on a sunny site in the bee yard, with their entrances far from the common wind direction and rain. Bees were about equal in the strength, food stores (Honey and pollen), queen's age (about 8 months old) and number of combs covered with bees from both sides (5 combs). Colonies were fed with sugar: water solution at 2: 1 percentage during the duration of the study. *Nosema apis* and *Varroa destructor* were monitored every 12 days throughout the study period, and treated whenever necessary. A total of 36 Langstroth enclosure beehives were constructed as following: foam was cut to boards with a suitable dimensions. The foam boards were joined together using adhesive material. The width and the upper edge of the two longitudinal sides were formed to suit the dimensions of Langstroth frames. The wooden beehives were obtained from a local workshop. Cement beehives were built by preparing molds. These molds were easily made, but should followed the dimensions of Langstroth model in its width and height. Before receiving the cement, the molds were previously moistened and coated with oil to facilitate the removal of boards. The cement was gradually filling and compacted in the molds and left to dry for two days without sprinkling water and in the next three days it was sprinkled water twice a day. On the ninth day, it were carefully removed. White brick beehives were made by cutting a valuable and cheap kind of white brick. The boards were joined together by cement, as shown in fig. (1). The slides have to be polished for a better finishing. The Hoffman Bee frames were made of wood. There was a removable top on all of them. There was a piece of sackcloth located under the cover to prevent any foreign insect to inter the hive and absorb vapor from the evaporation process. Beehives standing about 0.5 m above the ground on individual stands. The hives were opened every 12 days to verify possible damages due to the environment and to manage them. The distances between each beehive was 2 meters.

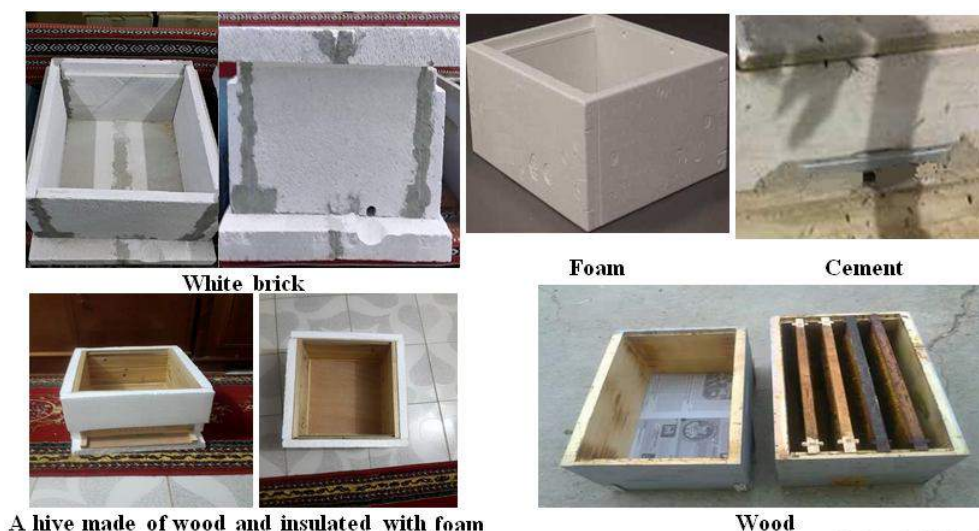


Fig. (1): Different types of beehive materials

Parameters including: four types of hive building materials (white brick, foam, cement and wood), three thicknesses of beehive sides (1, 2, and 3 cm) and three hive sizes (0.057, 0.086 and 0.114 m³) were studied. The present study carried out from 1 December until 30 March. To determine thermal conductivity: three parts of each of foam, wood, cement and white brick were cut and taken as samples. The samples were weighted with electronic balance, with an accuracy of 0.01 grams and the mean mass was obtained. The volumes of white brick, foam, cement and wood were estimated by putting the weighted sample in a measuring flask filled water to its half and estimate the variance of water volume. According to (Rodrigues, 1998) the following equation used to determine thermal conductivity

$$k = 0.0003545 \rho - 0.007146, \text{ W/m}^\circ\text{C} \rightarrow \quad (1)$$

Where: k is thermal conductivity and ρ is the density of samples, which was determined by the following equation,

$$\rho = \frac{m}{V}, \text{ kg/m}^3 \rightarrow (2)$$

Where: m is the mass of broad material in kg and V is the volume of it in m³.

The mass of samples were determined before and after soaking them in water for 30 minutes, the variation between mass indicated water absorption by each material. The samples were dried in an oven at 30°C. The test began at 9:30 a.m. and the mass measurements were taken at 10:00 a.m., 11:00 a.m., 01:00 p.m., 05:00 p.m. and 08:00 a.m. The mean masses for each tested material were obtained and the results were applied by the following equation (Lorenzon, *et al* 2004),

$$W.L.R. = \frac{S.M_{sat}}{S.M_{dry}} \times 100 \rightarrow (3)$$

Where: W. L. R.: water loss, %.

S. M._{sat} : saturated sample mass in gram.

S. M._{dry} : dry sample mass in gram at a given time.

A digital thermometer with an accuracy of 0.1 °C was used to determine internal hive temperatures and in the bee yard. Air temperature outside the hives was taken by a thermometer placed in a shaded place in the apiary. The number of combs covered with bees from both sides was investigated every 12 days throughout the winter season for adding empty new combs. Bees or adult population was estimated at the rate of 2000 adult bees which can cover a comb from both

sides (Hauser and Lensky, 1994). This investigation was carried out every 12 days throughout the winter season of 12 December, 24 December, 5 January, 17 January, 29 January, 10 February, 22 February, 6 March, 18 March and 30 March.

After assembling all types of boxes the empty weight was determined by an electronic balance. The balance had a maximum capacity of 100 kg with an accuracy of ± 30 gram as described by (Meikle *et al.*, 2006). The nearest nests weights were determined by the following equation every 12 days.

$$\text{Nest weight} = \text{whole hive weight} - \text{empty box weight.} \quad \rightarrow (4)$$

The cost for the model Langstroth white brick, foam and cement beehive was estimated and compared with the wooden one.

RESULTS AND DISCUSSION

The mean densities of foam, cement and white brick samples were about 49, 952 and 811 kg/m³, respectively, while it was 528 kg/m³ for wooden hives. The lowest density was obtained with foam material and the highest with cement material. The thermal conductivity of samples were about 0.01, 0.33 and 0.28 W/m/°C for foam, cement and white brick samples, respectively, while it was 0.18 W/m/°C for wooden hives. The lowest thermal conductivity was obtained with foam material and the highest with cement material. In general, the thermal conductivity was decreased by decreasing the density of materials.

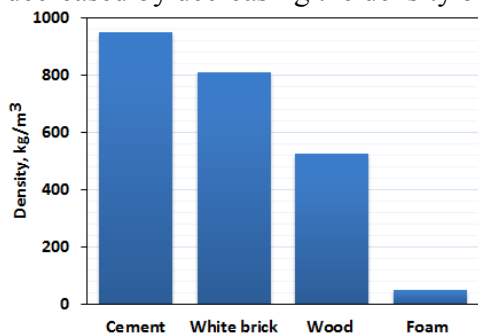


Fig. (2):The density of the used materials

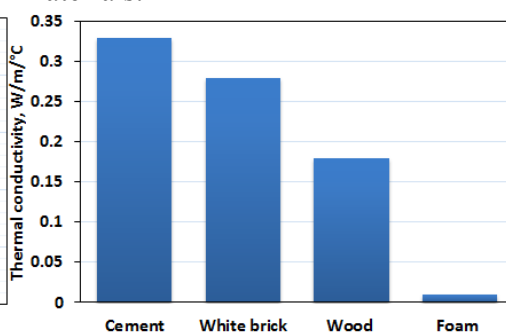


Fig. (3):The thermal conductivity of the used materials

The wood, cement and white brick, samples absorbed 14, 24, and 18 % of water, while the foam simple didn't absorb any water. The cement and white brick samples showed greater loss than wooden sample during the most of the drying time. At the end of the drying process the wooden samples lost much water because the cement and white brick samples were already dried. Generally, cement and white brick samples absorbed more water and lost it faster than wooden one.

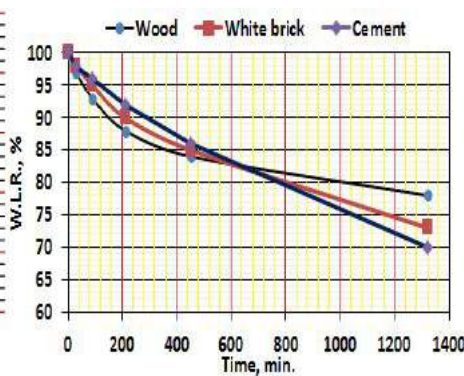
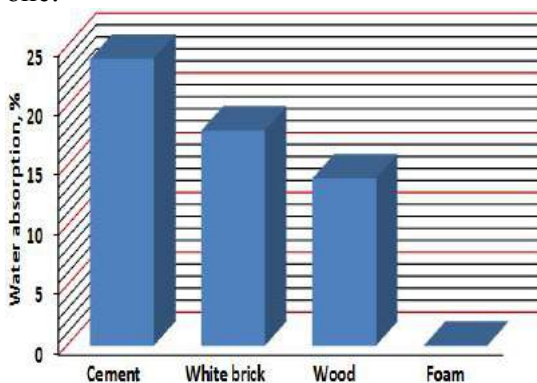


Fig. (4):The water absorption, % Fig. (5):Water loss from white brick and wooden samples

The main inside hive temperature was increased 52.45% than the outside air temperature, because honeybee colonies rise the inside hive temperature to regulate the brood nest temperature.

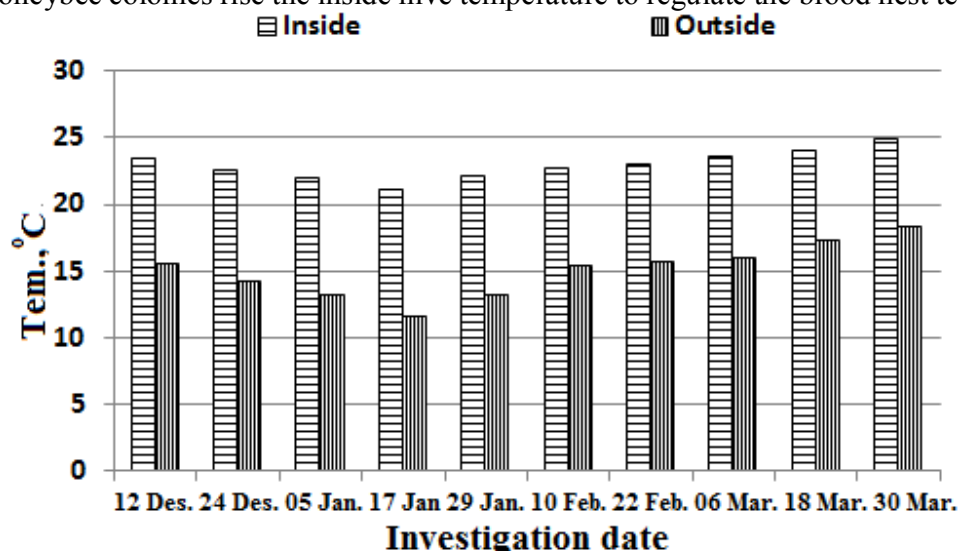


Fig. (6): The inside and outside air temperature, °C during the experiment period

Factors affecting inside hive temperature, °C:-

The mean inside hive temperatures were increased 8.24 % than it in wooden hives for foam hives, but it were decreased 4.34 and 8.29 % when using cement and white brick hives, respectively. There was a little difference in inside hive temperature, °C with reference to the type of material, because honeybee colonies regulated the brood nest temperature for all of foam, wood, cement and white brick hives. This result agrees with (Myerscough, 1993). The mean inside hive temperatures were increased from 21.79 to 24.04 °C when increasing side thickness from 1 to 3 cm, because the rate of heat flux through the hive sides decrease by increasing the sides thicknesses. The mean inside hive temperatures were increased from 21.23 to 24.78 °C when decreasing hive size from 0.114 to 0.057 m³. This due to the small internal environment needed to regulate by the bee worker.

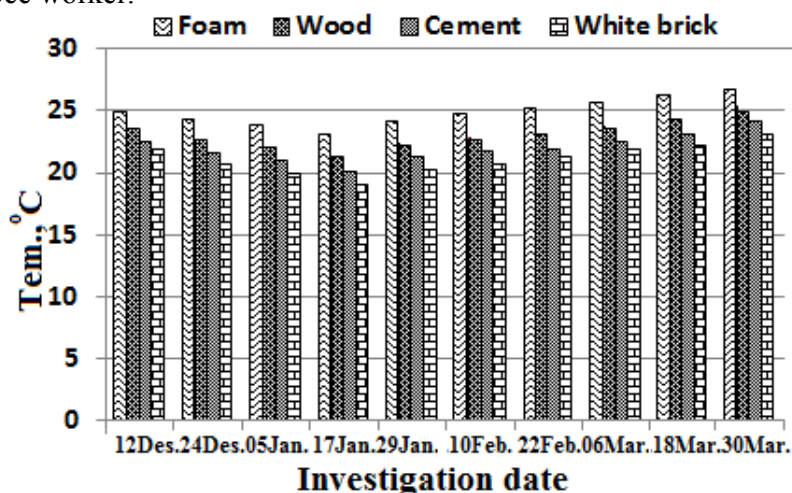


Fig. (7): The effect of hive building materials on inside hive temperature.

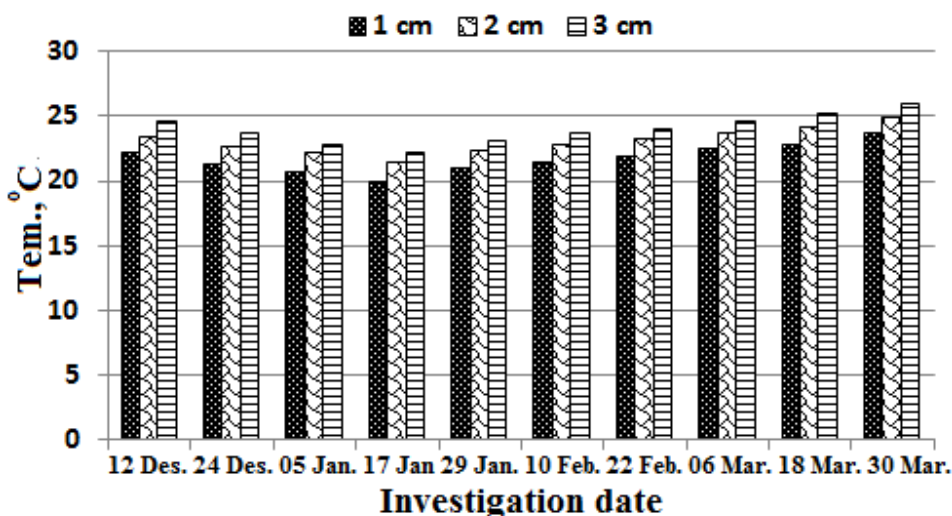


Fig. (8): The effect of the hive sides thicknesses on the inside hive temperature

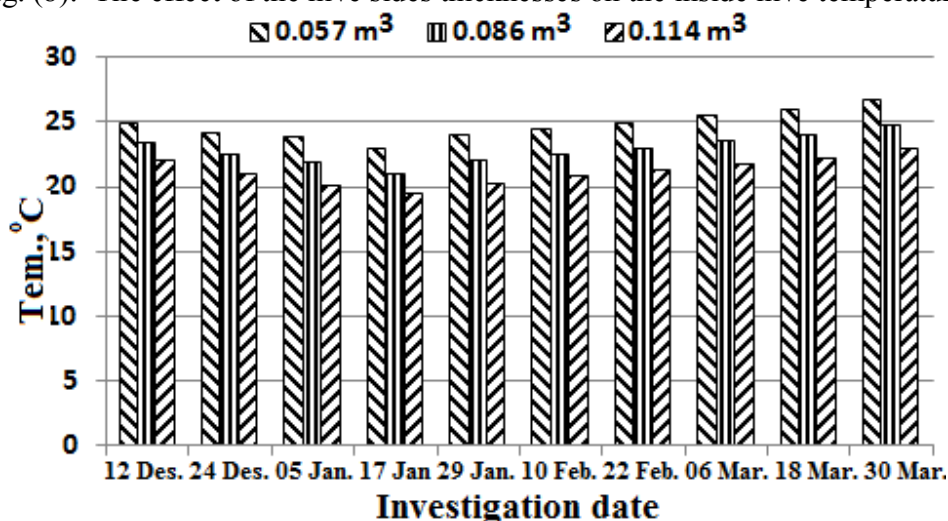


Fig. (9): The effect of hive size on the inside hive temperature.

Factors affecting number of occupied frames:-

The maximum mean number of occupied frames was 8 for foam beehives at the end of March. The minimum number of occupied frames was 2 frames in the middle of January for wood, cement and white brick beehives. The main number of occupied frames for foam were increased 20.45 % than it in wooden hive and decreased 11.36 and 15.91% for cement and white brick, respectively. This is due the higher internal temperature, which improve the colony performance and decrease mortality of worker bees. The mean number of occupied frames were increased from 4 to 5 frames. when increasing side thickness from 1 to 3 cm, due to the improve of the inside hive temperature by increasing the sides thicknesses. The mean number of occupied frames were increased from 4 to 5 frames when decreasing hive size from 0.114 to 0.057 m³. This due to the improve of inside hive temperature and consequently, of the colony performance by decreasing the hive size.

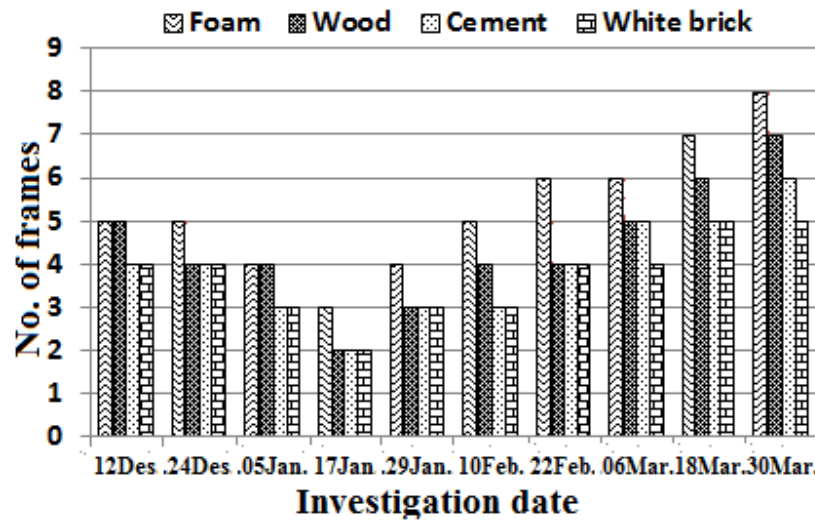


Fig. (10): The effect of hive building materials on the number of occupied frames

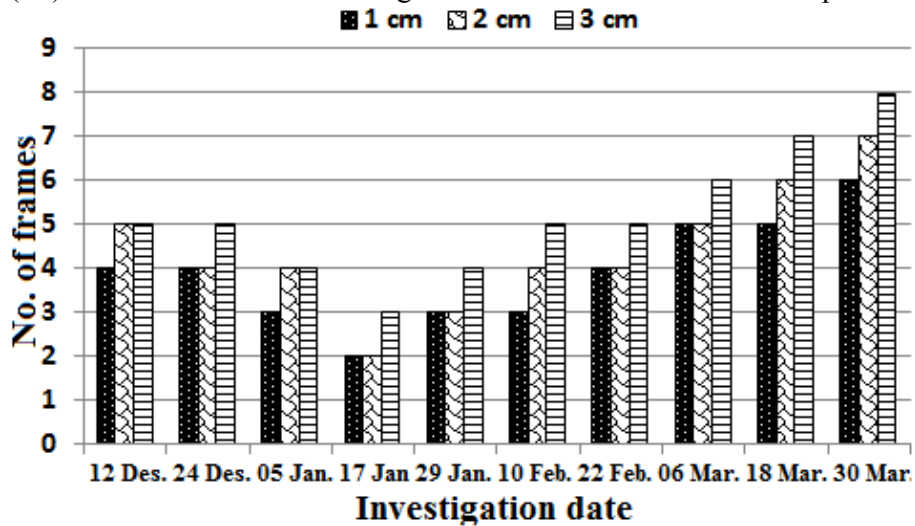


Fig. (11): The effect of the hive sides thicknesses on the number of occupied frames

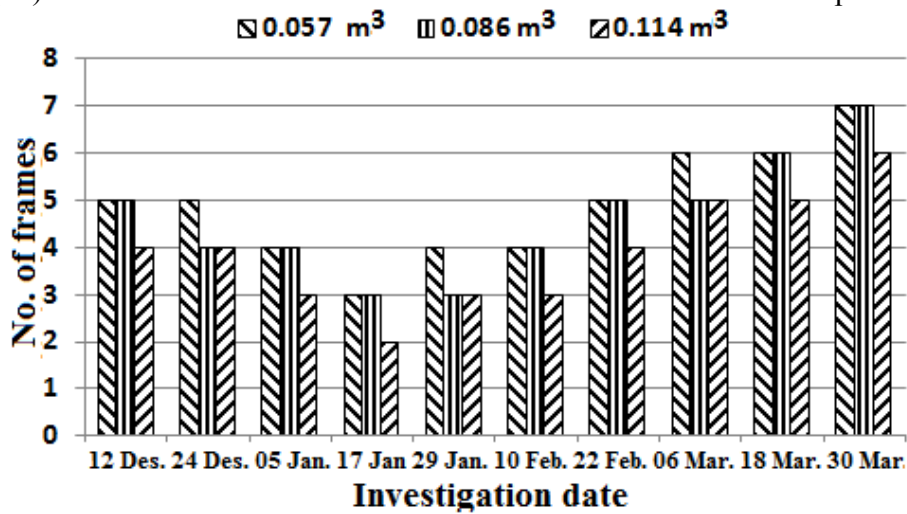


Fig. (12): The effect of hive size on the number of occupied frames

Factors affecting nest weight, kg:

The mean nest weight were increased 24.85 % than it in wooden hives for foam hives, but it were decreased 10.48 and 17.89 when using cement and white brick hives, respectively. This is due the improvement of colony performance and productivity. The mean nest were increased from 5.40 to 6.90 kg when increasing side thickness from 1 to 3 cm, due to the improve of the inside hive temperature by increasing the sides thicknesses. The mean nest weight, kg were increased from 5.43 to 6.75 kg when decreasing hive size from 0.114 to 0.057 m³. This due to the small internal environment needed to regulate by the bee worker.

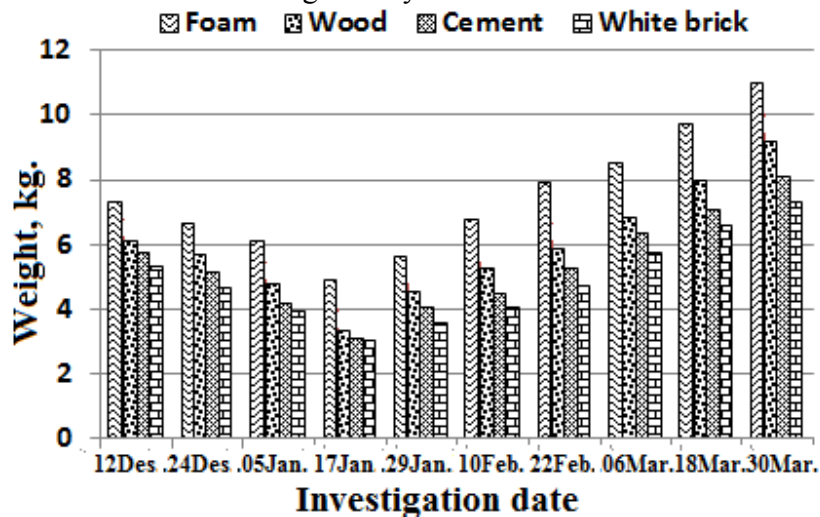


Fig. (13): The effect of hive building materials on nest weight, kg.

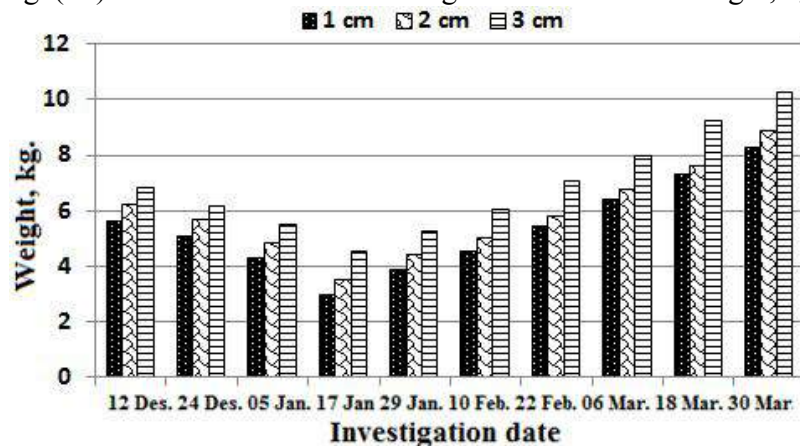


Fig. (14): The effect of the hive sides thicknesses on nest weight, kg.

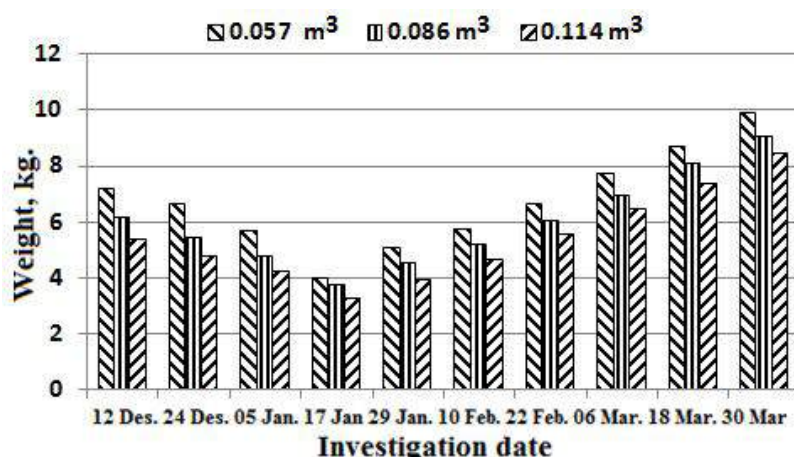


Fig. (15): The effect of hive size on nest weight, kg.

It was noticed that the main inside hive temperature, number of occupied frames, and nest weight, kg increased; with hive building materials, hive sides thicknesses and hive sizes, according to the following descending order (foam > wood > cement > white brick); (3 cm > 2 cm > 1 cm) and (0.057 m³ > 0.086 m³ > 0.114 m³), respectively. In general, the main inside hive temperature, number of occupied frames, and nest weight, kg were decreased for each type of material all levels of hive thicknesses and sizes from, the first day of the experiment (12 December, 2014) up to the nearly middle of January (17 January, 2014) and started to increase from the end of January (29 January, 2015) up to the end of the experiment (30 March, 2015). This is due the effect of changes in ambient temperature during the study. Factors of external ambient conditions are very important to the productivity of honeybees (Cetin, 2004). The main theory to explain why brood production reduces during cold periods is that workers spend more energy in heating the colony than with tasks related to brood production (Engels *et al.*, 1995). Also, ambient temperature has a great effect on foraging activity (Al-Qarni 2006 and Blazyte - Cereskiene *et al.* 2010). In regards to inside hive temperature, number of occupied frames, and nest weight, kg, there was no significant difference between hive material types, hive side thicknesses and hive sizes (P> 0.05). The wooden and foam model could be burned during sterilization by scorching them with a blow lamp compared with cement and white brick model. Wooden hives are more attractive to wax moth (*Galleria mellonella* and *Achroia grisella*). Foam hives are more attractive to rodents and more susceptible to environmental conditions.

Cost estimation: The following table represents a comparison between a complete Langstroth beehive made of wood and foam, cement and white brick hives with a thickness of 2 cm and a size of 0.57 m³.

Table (1): Production cost of foam, wood, cement and white brick hives for one super.

Specification	Price			
	Foam	Wood	Cement	White brick
- Super	15	85	65	45
- Nest from 5 frames	350	350	350	350
- Cover and bottom board	15	65	25	10
- Total hive cost	380 L.E.	500 L.E.	440 L.E.	405 L.E.
- Total hive cost without the price of the nest	30 L.E.	150 L.E.	90 L.E.	55 L.E.

The construction of the new hives (foam, cement and white brick) after subtracting the price of the nest were 80, 40 and 63.3 % reduction in cost relative to the price of wooden hive, that is due to the higher costs of wood Compering with foam, cement and white brick, respectively.

CONCLUSION

Foam is a light-weight, cheap and a valuable material. Cement and white brick materials could be resistant to burnings. The white brick hives needed a certain care while cutting of boards and assembly of it. Some parts like cover and bottom could be cracked by rains or broken during handling, that require more care. Also foam hives have presented gaps, damaging and they were more susceptible to environmental conditions. The expected life of foam hives was about one season, due to the effect of environmental conditions and rodents especially rats. The cement and white brick hives are almost twice as heavy as the mass of wooded one, but it is lighter than the hive constructed by (Lengler *et al.*, 2003) with a mass of 43.55 kg. Even if the white brick presents higher water loss, the internal moisture stability in the colony should be a critical point. wooden hives absorb more water during the periods of rain, so we should protect the outsides of it with a moisture resistant product like foam (figure 1) and the upper cover with a sheet of galvanized steel or put the hives under a shelter during winter season. It was observed that during the studied months, the maximum values of inside hive temperature, number of occupied frames and nest weight were achieved by using foam material, but they have a less expected life and foam can't be sterilized from almost all microorganisms like fungi, bacteria, viruses, and spores by flume without burning hazard. Foam, cement and white brick Langstroth bee hive models were cheaper than the wooden beehive cost. In general, foam, cement and white brick hives can be used by small or poor beekeeping in the countries that imports wood by forging currency like Egypt. On the other hand cement and white brick could provide evaporative cooling by honeybees in the dry period, thus favoring honey maturation and temperature control. Thus, new hives could be performed better in dry climates than humid.

REFERENCES

1. Al-Qarni A. S. (2006). Tolerance of summer temperature in imported and indigenous honeybee *Apis mellifera* L. races in central Saudi Arabia. Saudi J. Biol. Sci. 13: 123–127.
2. Blazyte Cereskiene L., G. Vaitkeviciene, S. Venskutonyte and V. Buda (2010). Honeybee foraging in spring oilseed rape crops under high ambient temperature conditions. Zemdirbyste-Agriculture 97: 61–70.
3. Cetin U. (2004). The effects of temperature changes on bee lost. Uludag Bee J., 4 (4): 171-174.
4. Dadant and Sons (1975). The Beehive and the Melifera Bee. Montevideo: Ed. Southern Hemisphere. 936p.
5. Engels W., P. Rosenkranz, and E. Engels (1995). Thermoregulation in the nest of the Neotropical stingless bee *Scaptotrigona postica* and a hypothesis on the evolution of temperature homeostasis in highly social bees. Studies in Neotropical Fauna and Environment 30 (4): 193–205.
6. F.A.O. (1990). Beekeeping in Africa, Agriculture service bulletin no 68(6), Organization of the United Nations, Rome.
7. Hauser H. and Y. Lensky (1994). The effect of the honeybee (*Apis mellifera* L.) queen age on worker population, swarming and honey yields in a subtropical climate. Apidologie 25, :566-578.
8. Hobson, J. R., J. V. (1983). Ferrocement as a material for hives. Queensl. Agric. Journal 109 (3), :157-160.

9. Jevtic G., M. Mladenovic, B. Anđelković, N. Nedić, D. Sokolović and R. Strbanović (2009). The correlation between colony strength, food supply and honey yield in honeybee colonies. *Biotechnol. Animal Husbandry*, 25: 1141-1147.
10. Jones, J. C., and B. P. Oldroyd (2007). Nest thermoregulation in social insects. *Advances in Insect Physiology*, 33, :153-191.
11. Lengler S.; G. L. Castagrino; C. Kieffer (2003). Evaluation of the internal temperature of beehive and wood beehives. *Informative Zum Zum*, 34, :14-15, 2000.
12. Lorenzon, M. C. A.; R. G. Cidreira; E. H. V. Rodrigues; M. S. Dornelles; and G. Pereira Jr (2004). Langstroth hive construction with cement-vermiculite. *Sci. Agric. (Piracicaba, Braz.)*, 61, (6), :573-578, Nov./Dec. 2004.
13. Marco Kleinhenz, B. B., F. Stefan and T. Jürgen (2003). Hot bees in empty brood nest cells: heating from within. *The Journal of Experimental Biology* 206: 4217- 4231.
14. Meikle, W. G.; Holst, N.; Mercadier, G.; Derouane, F. and James, R. R. (2006). Using balances linked to dataloggers to monitor honey bee colonies. *J. Apic. Res.*, 45: 39-41.
15. Myerscough M. R. (1993). A simple model for temperature regulation in honeybee swarms. *Journal Theor. Biology*, 162 (3), :381-393.
16. Neves J. O. (2002). Hives effect built in mortar cement vermiculite on the performance of Africanized bees (*Apis mellifera* Linnaeus, 1758), in the stretching step. Rio de Janeiro: UFRRJ 2002. 45p. (Dissertation - Master).
17. Ojeleye B. (1999). *Foundation of Beekeeping in the tropics*. CEBRAD press Ibadan, Nigeria: 1-225.
18. Padilha J. A. S.; R. D. T. Filho; P. I. L. Lima; K. Joseph,; and A. F. Leal (2001). Lightweight reinforced mortar with sisal pulp: low thermal conductivity composite for use in rural buildings. *COMBEA*, 2, :1-11.
19. Rodrigues E. H. V. (1998). Development and evaluation of an evaporative system, by intermittent spraying, on aviary cover using distorted scale models. São Paulo: UNICAMP / FEAGRI, 1998. 178p. (Thesis - Doctorate).
20. Soares A. E. E. & L.T. Bannwart (1989). Fibercol a new type of hive for *Apis mellifera*. IN: *Latin-Iberian-American Congress of Beekeeping, III, Annals.* : 300-306.
21. Stangenhuis C. and R. Paredes (1992). Hygrometric comfort, buildings, weights and proposal for humid tropical climate in summer situations. Rio de Janeiro: UFRRJ, 1992. 199p. (Thesis - Master's degree).
22. Wiese, H. (1974). *New Beekeeping*. Porto Alegre: Livraria e Editora Agropecuária Ltda.: 493.

تأثير نوع مادة بناء الخلية علي طوائف النحل

محمد علي إبراهيم الراجحي

معهد بحوث الهندسة الزراعية - مركز البحوث الزراعية - الدقى - جيزة

تمت الدراسة بمنحل خاص بمدينة ميت سلسيل - محافظة الدقهلية - مصر لمدة أربعة أشهر لمقارنة الفوم والإسمنت والطوب الأبيض بالخشب في بناء خلايا من نوع لانجستروس وذلك في تصميم تجريبي من النوع تام العشوائية. تضمنت التقييم ثلاث مستويات من السماكة لجدران الخلية هي ١، ٢، ٣ سم وثلاث أحجام للخلية هي ٠,٠٧٥، ٠,٠٨٦، ٠,١٤٤ م^٣. أجريت التجربة علي ٣٦ خلية من صندوق واحد بهم نحل من النوع الهجين الكرنولي المتساوية في القوة. تم إجراء قياسات أولية علي المواد المستخدمة تضمنت كثافتها والتوصيل الحراري لها وكمية المياه الممتصة ومعدل الفقد لها. أما القياسات الثانوية فتضمنت درجة الحرارة الداخلية للخلية، وعدد البراويز المغطاة بالنحل وكذلك وزن الخلية الصافي وتكلفة تصنيع الخلية من الفوم والإسمنت والطوب الأبيض بالمقارنة بالخشب. كانت كثافة مادة الفوم والإسمنت والطوب الأبيض والخشب هي ٤٩، ٩٥٢، ٨١١ كجم/م^٣ علي الترتيب بينما الخشب ٥٢٨ كجم/م^٣ ومعامل التوصيل الحراري هو ٠,٣٣، ٠,٢٨، ٠,٠١ وات/م^٢ لكل من عينات الإسمنت والطوب الأبيض والفوم علي الترتيب بينما الخشب ٠,١٨ وات/م^٢. لوحظ ان عينات الاسمنت والطوب الأبيض والخشب تمتص ماء بنسبة ٢٤، ١٨، ١٤% بينما الفوم لا يمتص الماء. ولوحظ أن درجات الحرارة المتوسطة داخل الخلية خلال فترة الدراسة الممتدة من ١٢ ديسمبر الي ٣٠ مارس زادت بنسبة ٤٥، ٦٥، ٨٥، ٥٢، ٢٢، ٤٦، ١٩، ٤٠% عن درجة الحرارة بالمنحل لكل من الفوم والخشب والاسمنت والطوب الابيض علي الترتيب. وكانت اعلي درجة حرارة مسجلة داخل الخلية الفوم و اقلها داخل الخلية من الطوب الابيض. زاد متوسط عدد البراويز المغطاة بالنحل الي ٤٥، ٢٠% عنها في الخلية الخشب لكل من الفوم علي الترتيب بينما قلت ٣٦، ١١، ٩١، ١٥% عند استخدام الاسمنت والطوب الأبيض علي الترتيب. وزادت النسبة المئوية لوزن الخلية الصافي بمقدار ٨٥، ٢٤% عنها في الخلية الخشب لكل من الفوم بينما قلت ٧، ٤١، ١١، ٧% عند استخدام الاسمنت والطوب الأبيض علي الترتيب. وكان هناك زيادة في متوسط درجة الحرارة الداخلية للخلية وعدد البراويز المغطاة بالنحل بتقليل حجم الخلية وزيادة سمكها. ولوحظ كذلك ان متوسط درجة الحرارة الداخلية للخلية وعدد البراويز المغطاة بالنحل يقل من بداية التجربة (١٢ ديسمبر) حتي منتصف يناير (١٧ يناير) ثم يبدأ في الزيادة التدريجية حتي نهاية التجربة (٣٠ مارس) ويرجع ذلك لاختلاف الظروف الجوية الخارجية خلال الدراسة. وكانت تكلفة تصنيع الخلية من الفوم والإسمنت والطوب الأبيض أرخص بنسبة ٠، ٨٠، ٠، ٤٠، ٣، ٦٣% من تكلفة تصنيع الخلية الخشبية (١٥٠ جنيه). لذا فان استخدام الخلايا المصنوعة من الفوم والإسمنت والطوب الأبيض يعطي نتائج مشابهه للخلايا الخشبية وبأسعار أقل من الخلايا الخشبية.

DEVELOPMENT OF A WEED CONTROL DEVICE USING WATER STEAM

EL-SAYED, A. S.¹ and G. M. EL-HAMEED²

1. *Agric. Eng. Res. Inst., Arc, Giza, Egypt.*
 2. *Weed Research Central Laboratory (Wrcl), Arc, Giza, Egypt.*
-

Abstract

The aim of this research is to producing and evaluating a new friendly environmental steam weed control system adapting with clean planting without using harmful chemical herbicides and reducing weeds management economic costs at least. So, an electrical steam weed control device was investigated to generates two different kinds of pressurized steam (Damp and superheated one) to exposure cells cytoplasm immediately as, been treated under pressurized levels of steam. Whereas the steam treating period was conducted automatically using an electronic attached system which includes digital twin timer connected with an electrical solenoid to control steam flow rate and pressure stat to adapt steam pressure automatically with the existence weed status. An adequate self-propelled chassis was manufactured with multi adapting levels for its height from the ground and movement speed and direction to move smoothly within crops rows using source power of a friendly AC generator. Two individual field experiments were conducted to study the two generated kinds of steam and compared them (Damp and superheated) under the variables levels of: first four levels of steaming periods (1, 2, 3 and 4 sec) at forward speeds of (1.8, 1.2, 0.9 and 0.72 km/h), second three levels of steaming pressures (3.5, 7 and 10 bar) and third three levels of steaming heights from the ground (10, 15 and 20 cm) to study the following measurements; first on weeds and crop from weeds extermination ratio after treatment for 3 days, weeds re-germination ratio after treatment for 3 weeks, chlorophyll level percentages after treatment for 3 days and crop yield production second on the device from measuring field capacity, field efficiency, and energy requirements third calculating the new weed control system economic costs in exchange for chemical control methods and yield production.

The main results conclude the following; the ability of two kinds of steam damp or superheated one is consider more efficient than the traditional mechanical and chemical weed control methods. The maximum values of weed extermination ratios after 3 days from treatment were 98.84& 97.74% for damp and super-heated steams respectively. Also the chlorophyll percentages after 3 days decreased to 19.38&13.52% for the two kinds of steams at 4 sec of steam exposure period (S_t) (forward speed, 0.72 km/h) for steam pressure (S_p) of 10 bar at steam height from the ground (S_h) 10 cm. However the ability for the superheated steam under pressure for weed control decreased the weeds re-growth ratio to 24.82% after 3 weeks from treatment. Besides the new weed control technique minimized the economic costs at low levels (149.76 L.E/fed) includes fuel consumption, lubrication cost and operator salary instead of the expensive chemical methods due to using water only. The new steam weed control device reaches suitable levels of field capacity and efficiency of 0.61 fed/h at 96.11% field efficiency. Whereas the maximum values of steam device consumed energy (CE, kW.h/fed) reaches from 4.83 to 6.63 Kw.h/fed. So, using the new weed control device is more adequate with the present requirements of the Egyptian planting methods and the global trends of clean cultivation.

Key words: *weed control, steam, elimination ratio, pressurized.*

INTRODUCTION

Weed management is the main yield-limiting factor in production of organic crops. Steaming is a perspective technique for intra-row weed control in no herbicidal row crops of high value, where manual weeding can be very laborious. The thermal weed control technology by high

temperature water steam is a new and very promising one. The essence of the matter is that water steam thermodynamics quality in plant media may change and is accompanied by change of convection heat exchange intensification from 1000 to 2000 times. This unusually big change is decisive for weed control by water steam efficiency and economy. Steam weeding also has the added benefits of improving soil biology and increasing public safety due to elimination of the risk of accidental exposure to dangerous chemicals.

Weeds are natural component of plant communities in cultivated land (Debeljak *et al.*, 2008). All weed control methods reducing weed density are important, therefore they must be used in combination with certain agricultural plant production technologies. Mechanical weeding in row spacing is more common in organic farms and can significantly reduce weed density (Praczyk, 2005). Organic weed control methods include the thermal weed control. Wet steam technology used to control weeds (exposure time 1–2 s) destroys not only plants on the soil surface, but also the seedlings on the topsoil layer (Kerpauskas *et al.*, 2006). The ability to manipulate crop-weed interaction is essential in organic farming system (Rasmussen *et al.*, 2000). Plants are smothering weeds naturally in dense crop due to the lack of light. Various biological preparations often have a different effect on crop yield and weed infestation (Pekarskas *et al.*, 2012). In addition Kruidhof *et al.*, (2008) showed that weeds are a limiting factor in maximization of yields in grain crop production systems. The problem of controlling weeds without synthetic herbicides under the rules of organic agriculture is one of the biggest challenges that organic producers face.

Also, Collins, (1994) showed that steam has the advantage of having greater heat content than boiling water due the latent heat of vaporization, plus a little bit more if superheated. Water at 100°C has 251kj kg of useful heat above the 40°C minimum. Steam at 100°C has 2508kj kg, but occupies 1673 litres kg compared to 1 litre kg for water so as heat content per litre, 100°C water has 251kj L and 100°C steam has 1.5kj. There is difficulty in getting the steam to condense on the plant to make use of the latent heat, requiring trailing covers over the weeds. The apparent advantages of steam are difficult to capture. Maybe the steam could be charged to attract it to the plant, as is done with ultra-low volume spraying. Whereas Ascard. (1998) reported that both steam and flame weeders heat is transferred from the weeder to the plant by 'forced convection' i.e., it is literally blown at the weeds. This is a very fast process taking a few seconds or less to move the heat several feet. However, once the heat reaches a plant's surface, it can only move through the plant's tissues by conduction. This is a tortuously slow process with the heat moving only a fraction of an inch over tens of seconds. This is a problem, because for heat to kill a plant it has to kill all its aerial meristems (buds) (which reside in the leaf axils in dicots and in the center of the stem in monocots. However the hot water method has a great potential to be developed to control weeds in orchards (Kurfess & Kleisinger 2000). In general using flaming by gas in thermal weed control the temperature difference is greater and it reaches 400-900°C. At the same moment the temperature of the water and damp water steam used for weed control is only about 90°C. In spite of high temperature the used method of flaming by gas, the transfused steam q to the tissues of the plant remain 200 times less than condensation water steam and about 5 times less than hot water (the transpiration of a plant is not estimated (Sirvydas & Cesna 2000). However **Sirvydas *et al* (2002)** showed that steam has a high energy density and also a high heat transferring capability. Heat intensity increases 1000-2000 times in comparison to flaming by gas technology. Wet steam surrounding immediately increases temperature of plant surface tissues; the influence is destructive. The biggest yield of barley grain is received after steaming in phase of 2-3 leaves.

Clearly more the thermal weed control for older weeds needs more time that destroys the inner tissues of the weeds of (t 60°C) when reached after some time showed that the heat in the tissues

of plant spreads slowly. The temperature of deeper plant tissues is not reached quickly. So, the speed of moving of equipment as well as its economy decreases (Cesna *et al.*; 2000). In the same manner Edgar, (2000) stated that weeds can be controlled by briefly exposing them to very high temperatures delivered by open flame, infrared heating, steam, or hot water. Thermal methods are considered post-emergence, non-selective, contact methods of weed control. Plant tissue exposed to high temperature is killed by the serious injury caused to the waxy outer cuticle of the tissue, rupture of the cell walls, and the release and abnormal mixing of cell contents. The results of thermal treatments are apparent within a short time after treatment. Also, Kolberg and Wiles (2002), reported that using a prototype steam applicator pulled by a tractor, control was most effective with young weeds (seedling to 4-6 leaf stage) and that resistance to steam treatment exhibited by some species was related to plant structural characteristics such as extensive pubescence. Quantity of steam applied and duration of steam contact with the weeds, factors affected mainly by driving speed, were also important factors in the effectiveness. Weed-control effectiveness was greater at low speed (~1.7 miles/hr) than at high speed (~3.5 miles/hr). Thus several commercial, steam weed-control systems are currently available for agricultural uses with potential to be adapted for landscape and roadside uses; also, a report exists of a steam pressure washer adapted for weed control (Yager, 2004).

kerpeuskas *et al.* (2006) said that damp water steam used for weed control in onion, maize and barley crops it can be successfully used for organic and traditional agriculture. He found that during weed shoot by steam 98% of weeds destroyed after two weed control treatments in an onion field, the crop yield increased up to 10% compared with three times of treatments in maize it was 22% and 10% for barley compared with the not wedded control. He tells that 1 kg of wet water vapor release 2250 KJ of thermal energy to the environment which is 3.7 to 11 times more than of 1 kg of gas in flame weeding technology where the wet water heats the environment with about 2000 times greater efficiency than gaseous medium and the ability of vapor to flow in the direction of colder plants and soil surface. Water vapor condensation reduces its volume 1700 times. The treatment with vapor last from 1-2 seconds to completely destroy the weeds. The beneficial features of wet water vapor present great opportunities for the utilization of wet water vapor devises for ecological weed control. Moreover Banks & Sandral (2007) reported that hot water and steam is very effective at killing annuals, some perennials and some permeable seed near the soil surface. There is virtually a zero risk of non-target plant damage (except when applied on lawn or oval situations) and it is generally more benign to the environment than alternative herbicide options, although it does use more water. Consequently the most vital biological factors in weeds thermal control includes first the weeds size and seconds the degree of exposure of the growing point at the time of thermal treating (Obradovic *et al.*; 2011).

The idea of this research is depend on eliminating weeds using water steam which bursts its cells directly to stop the photosynthesis process during short period not exceeds 5 seconds. Whereas, electrically the developed technique was turned on conversely in other steaming equipment which are generates steam by burning the fuel which is very expensive and make environment pollution.

The main goal of conducting this research is to find a clean resolving method for grown weeds in crops instead of using harmful chemical herbicides and also to minimize the weed control cost and maximizing the national agricultural production.

MATERIALS AND METHODS

The field experiments were carried out at El-Serw, Damietta Governorate during planting season 2016 of beta vagaries crop. The new innovated steam weed control device was designed to

treat weeds in several in row crops. The formed chassis of the steam device had multi options to set its position through and above plant rows to control the grown weeds in rows through the critical plants grown period at the first month of planting. The steam device is self-propelled to facilitate moving through rows with the lowest gas emissions using an electrical motor. The innovated steam control device was formed to generate two different kinds of steam; damp and super-heated steams in several stages of heating water under pressure up to 10 bar by using electrical boiler and extra heaters to super-heated the generated steam. As shown in schematic drawing Fig.1 and Figs (2, 3, 4 and 5) the steam device specifications are listed in table.1 as follows:

Table.1: The innovated steam device specifications.

Power source	7 kW electrical generator 220 V			
Forward speeds	0.72, 0.9, 1.2 and 1.8 km/h			
Chassis dimensions	width	Length	Total height	Height from ground
	75 to 135 cm	163 cm	146 cm	32.5 to 62.5 cm
Operation width	2 rows 75 to 135 cm			
Net weight	165 kg			
Consumed power	7 to 11 Kw.h/fed			
Driving motor	AC 220 V 1/6 hp with gearbox			
Wheels	270 mm dia. solid			

The steam weed control device consisted from the following parts:

First: The power source: Using AC generator as shown in Fig. (3) with specifications as listed in table.(2).

Table.2: The used electrical generator specifications.

Generator			
Model	Lincoln LC 6500 E Chinese	Power factor	1
Standby power	7 KW	Rated of voltage transient	±20-15%
Rated voltage	220 V	Voltage stabilization time	1.5 s
Frequency	50HZ/60HZ	Rated of voltage fluctuations	≤1%
Speed	1500/1800RPM	Dimension (mm) L×W×H	550×430×420
Phase	Single Phase	Net weight (kg)	39
Engine			
Type	GX 200	Capacity of engine oil	0.6
Ignition system	Transistorized magneto	Start system	Mech.
Exclusion of cylinder (cm ³)	196	Capacity of fuel tank (L)	15
The Max. output power (KW/rpm)	4.8/3600(6.5HP)	Consecutive Working (h)	13
Category	Single crock air-cooled four-stroke gasoline engine	Noise (at7m) (dB)	65

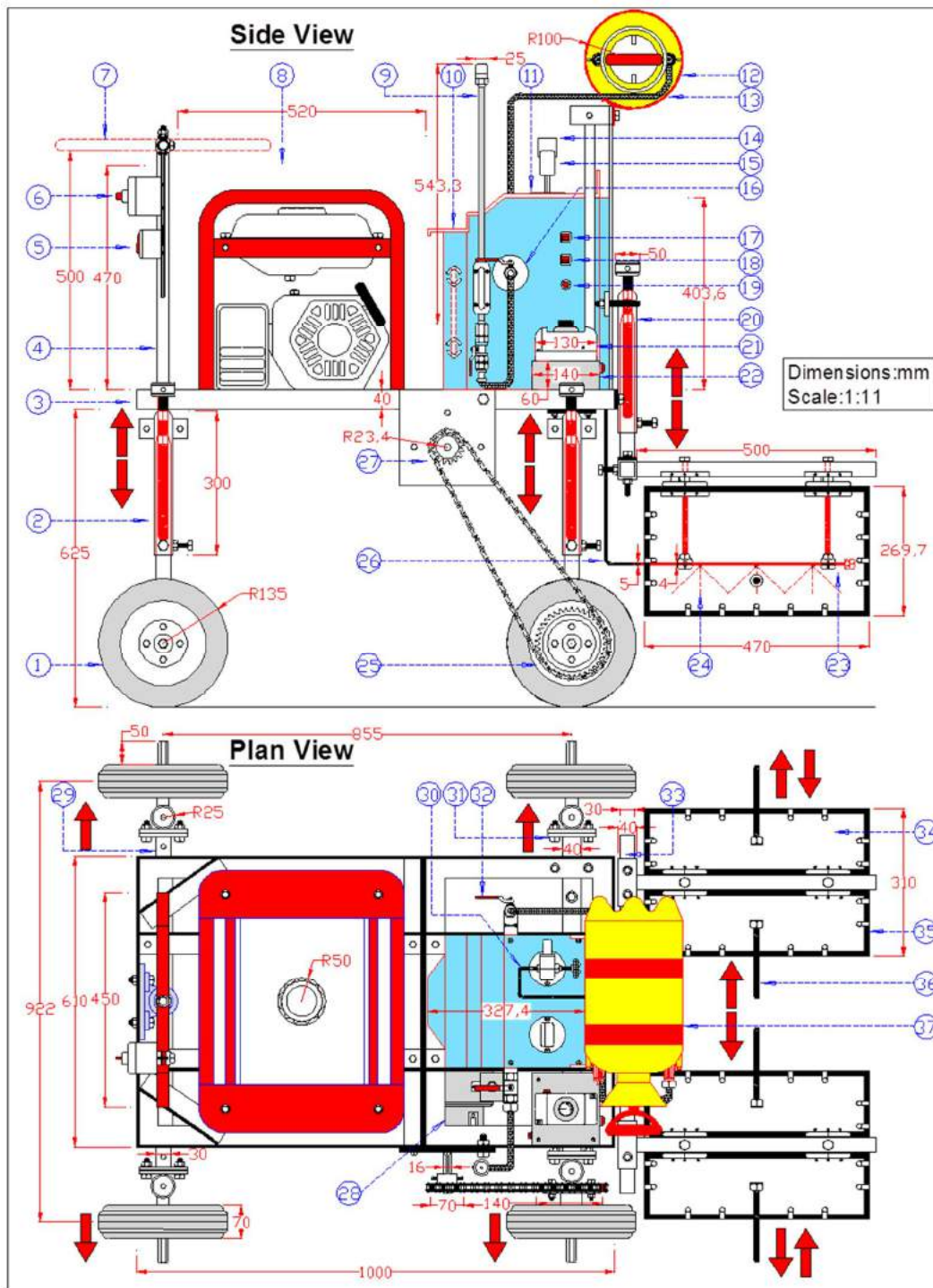


Fig.1: schematic drawing of the innovated steam weed control device:

(1- 27cm Dia. solid wheels, 2- chassis crane, 3- chassis, 4- steering shaft, 5- steam direct press switch, 6- motor on /off/rear/ front switch, 7- steering arm, 8- AC generator 7 Kw 220V, 9- optional steam spray lance, 10- boiler water indicator, 11- boiler, 12- pneumatic water tank, 13- boiler water hose, 14- steam solenoid, 15- pressure manometer (0-10 bar), 16- high pressurized steam valve, 17- solenoid press switch, 18- boiler heater press switch, 19- indicator lamp, 20- steam lines crane,

21- super heater thermostat, 22- twin timer unit, 23- copper steam pipe 4 mm dia., 24- copper steam outlet nozzles 1 mm dia., 25- wheels driven gear 38 teeth, 26- outlet steam thermal hose 5 mm dia., 27- motor driving gear (5, 7, 9 and 14 teeth), 28- driving AC motor (1/6 hp 220 V), 29- rear wheels side slider, 30- outlet steam solenoid, 31- front wheel side slider, 32- boiler water filling valve, 33- steam lines side slider, 34- side steam isolated sheet, 35- thermal isolator, 36- steam angular tighten shaft, 37- water tank holders.)



Second: The steam electrical boiler

As shown in Fig. (6) the electrical boiler is formed locally to generate water steam under pressure from 1-10 bar which used to treat the growing weeds through the planting rows to eliminates weeds by exposure its cells cytoplasm. However, the electrical steam boiler was fixed on the chassis as clear in Fig. (4). The steam boiler has the manufactured specifications as listed in Table (1).

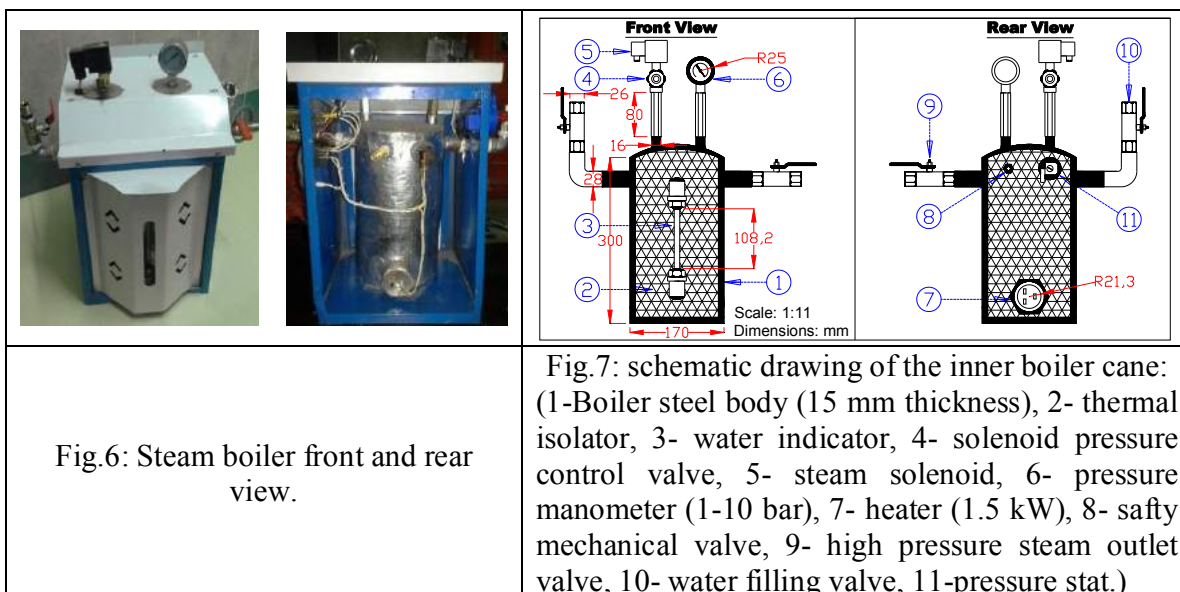


Fig.6: Steam boiler front and rear view.






Fig.7: schematic drawing of the inner boiler cane: (1-Boiler steel body (15 mm thickness), 2- thermal isolator, 3- water indicator, 4- solenoid pressure control valve, 5- steam solenoid, 6- pressure manometer (1-10 bar), 7- heater (1.5 kW), 8- safty mechanical valve, 9- high pressure steam outlet valve, 10- water filling valve, 11-pressure stat.)

Table.3: The used electrical steam boiler specifications.

Boiler capacity	5 liter	Electrical power	1500 Watt-220 V		
Net weight	7 kg	Inner dimensions	Diameter	Height	Thickness
			17 cm	30 cm	15 mm
Pressure	From 1-10 bar	Outer dimensions	Height	Width	Length
			40 cm	28 cm	28 cm

The electrical boiler consists from the following parts:

- 1- The outer boiler chemise:** As shown in Fig.(6) it formed from iron square panted sheets with thickness of 0.6 mm with the dimensions of (28×28×40cm).
- 2- The inner boiler body:** As shown in the schematic drawing (Fig. 7, No.1) it formed as a cylindrical shape from water resistant steel with thickness of 15 mm to stand the inlet large generated pressure and has dimensions of 17 cm dia. and 30 cm length. It was designed to fill with 5 liter's from water which experimentally last for 30 minutes period from continuous operating. Whereas, this chosen size was fits the required consumed energy from the attached AC generator. The inner boiler body was isolated accurately with glass wool to keeps energy from thermal leakage, as shown in (Fig. 7, No.2). A special water indicator from thermal glass tube was fixed frontally to the boiler body to indicate water level, it has length of 10 cm and 10 mm dia. as shown in (Fig. 7, No.3).
- 3- The electrical heater:** With the power of 1500 watt, that formed from brass coils and fixed in the inner bottom of the boiler, as shown in Fig. (8).
- 4- The electrical solenoid:** As shown in Fig. (9) the electrical solenoid has a magnetic inlet coil that open the inlet spike valve; as been the electrical sign turned to it from the direct steam switch or from the timer unit to select the working period. Also, this solenoid has a control valve to choice the needed pressure, as shown in (Fig. 7, No.4). The solenoid works up to 180° C and stand pressure maximum 12 bar.
- 5- The manometer gauge:** As shown in Fig. (10) it has operating range from (1 to 10 bar) to indicates the operating steam pressure. The steam becomes ready from 2 bar pressure and the boiler practically needs 20 minutes to be prepared initially.

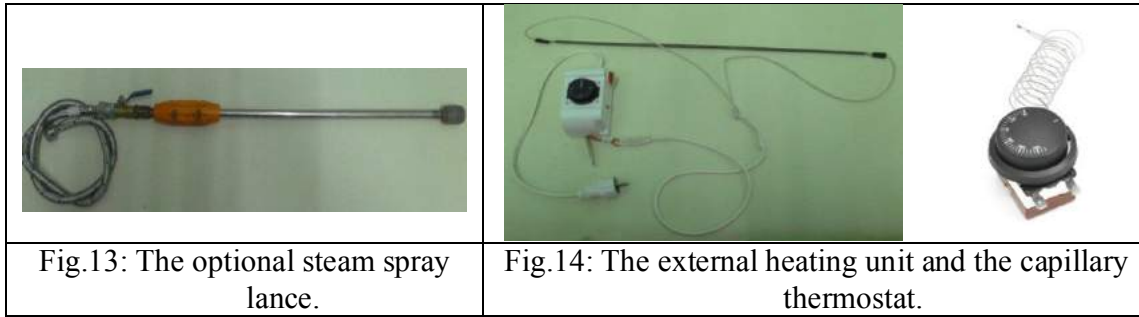
				
Fig.8: The boiler heating element 1500 Watt.	Fig.9: The working solenoid	Fig.10: The pressure manometer.	Fig.11: The safety mechanical valve.	Fig.12: The pressure stat.

- 6- **The safety mechanical spring valve:** As shown in (Fig. 11) which made from brass and stand temperature media of 200° C it has inlet steel calibrated strength spring, which settled to stand pressure up to 10 bar when pressure exceeding its stands it get opened to release the overload pressure to save the boiler from damage(Fig. 7, No.8).
- 7- **The pressure stat:** It was connected through the electrical hot line to connect the electrical power to the heater if the inlet pressure decreased to automatically operate the boiler at the controlled water steam pressure also; it saves the boiler from damage from overheating (Fig. 12).
- 8- **The operating switches:** As shown in (Fig. 1, No. 17&18) two press switches one of them to connect heater with electrical power and the other to connect the solenoid and also there are indicator lamp to indicates boiler working (Fig. 1, No. 19).
- 9- **The boiler valves:** As shown in (Fig.7, No. 9&10) there are two 0.5" valves; the horizontal one is connected to the steam gun and the vertical one is connected to the pneumatic water tank to refill boiler with water.
- 10- **The optional steam spray lance:** As shown in (Fig.1, No.9) and Fig.13 which connected laterally to the boiler outlet high steam pressure valve to be used when the weed treated areas couldn't be reached. It has dimensions of 50 cm length and 13 mm Dia. The steam gun is made from resistant stainless steel and has an isolated operating arm and has a manual valve. The steam gun has adaptable nozzle diameter from 0.5 to 1.5 mm Dia.
- 11- **The pneumatic water tank:** As shown in Fig.2 an attached 10 liters capacity garden sprayer was used to supply the boiler with water to neutralize partly the inlet boiler steam pressure by connecting hoses from it to the filling valve of the boiler. Before using the steam device the pneumatic water sprayer needs to be perpetrated by its manual piston to supply water partly, as the steam consumed.

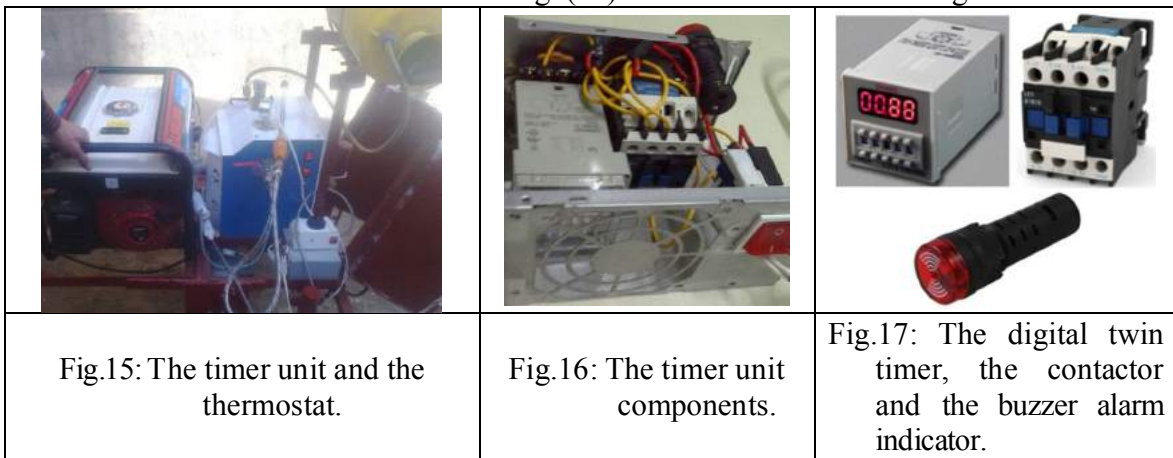
Third: The external heating unit (super- heated steam producing):

As shown in Fig. (14) which produces the second heating act to produce the super-heated steam by heating the brass hosing pipes of steam. This unit consisted from the following:

- 1- **Tubular straight heater:** It made from stainless steel with 60 cm length, 7 mm diameter and 600 W power, as shown in Fig. (14) it have two anodes from both sides positive and negative one when connected with electrical power its fused to reach 250° C. The tubular heater was gathered to the brass holding tube of the steam spray nozzles to super-heated the outlet damp steam from the boiler.
- 2- **Adjustable capillary thermostat:** This has temperature control range from (30-250°) C. It was sited on the chassis beside the boiler as shown in (Fig.1, No.21). It has a tiny 1 mm dia. stainless steel tube and a connecting bulb from its end which contact with the tubular heater when it's containing gas expands it connected within its calibrated temperature range.



Fourth: The timer unit: Which controls the operating periods of the generated steam from the boiler automatically to give multi choices of concludes the perfect weed steaming period for weed control. The timer unit circuit as shown in Fig. (18) consists from the following:



- A- The digital twin timer relay DH48S-S:** As shown in Figs. (16&17) which consists from two timer units housed in a compact case it have settled times; the first one to choose the connecting period for the steam solenoid from (1-5 sec) and the second one to disconnect it also from (1-5 sec). The timer specifications are listed in Table (4).
- B- The contactor:** Which connect the electrical load directly from the power source but it can't connect it until getting the sign from the twin digital timer to its inlet magnetic coils which operated with weak current to save the circuits from overloading, as shown in Fig. (17) and its specifications listed in Table (4).

Table.4: The digital twin timer relay and the connected contactor specifications.

Timer		Contactor	
Operating voltage	AC24~220V. 50Hz, DC24V	Coil Voltage	AC 220V
Delay time range	: 0.1S to 99H	Operating voltage	220 V
Rated load	AC220V 5A COS 1	Operating current	20 A
Dimensions(mm)	48H x 48W x 84D	load	2 hp (1.4914 Kw)
		Overall Size "(L*W*H)	75x45x75 mm

- C- Buzzer alarm indicator:** As shown in Fig. (17) which notice the electrical signal connecting when operating the steaming lines properly at the same adaptable time from the digital twin timer. More clear when the connecting time on this buzzer flashes and lights with the same adapting period tells that the hot steam is out and vice versa it disconnect at the second time. The buzzer had AC 12 V operating voltage and 20 mA operating current.
- D- The steam direct micro switch:** as shown in (Fig.1, No.5) a direct manual connected press switch was connected on the steering arm of the steam device to use it as required.

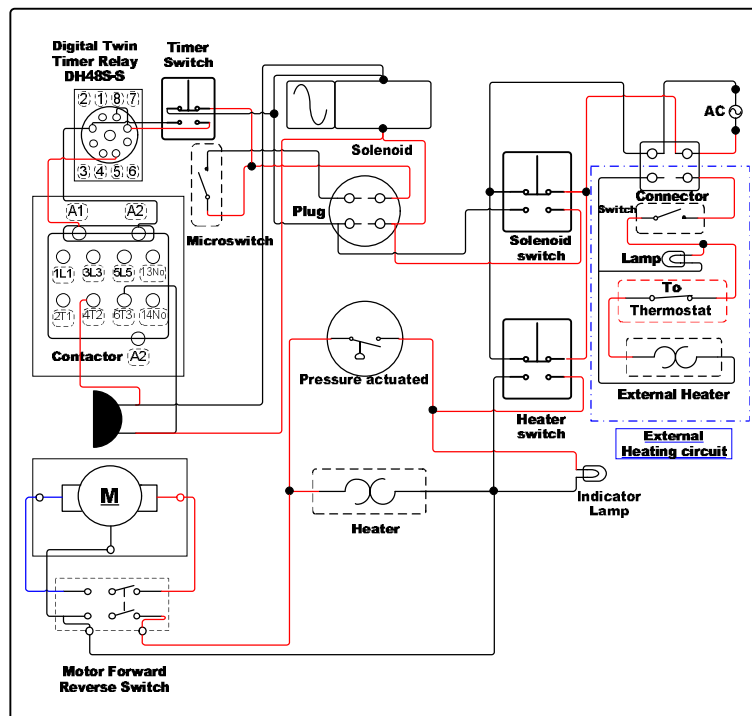


Fig.18: The schematic electrical circuit for the steam device.

Fifth : The weed control device chassis: This part was designed and formed locally to be self-propelled using a driving AC motor with gearbox which move the steam device in front and rear with different forward speeds. The steaming device designed to be frontally moved but it was rear steering by the operator to keep frontally steady steaming operation and easy tracking in narrow places. However the chassis also was assembled to be adaptable with any planting distances for broadcasting besides it could be treats flat soils and terraces. The chassis weight was decreased as possible to protect soil from compacting using suitable wheels. The chassis height from the ground could be settled and also the interference distance between wheels which stands on four adaptable lifting cranes to protect the growing plants lines passing overalls it from 30-62.5 cm height from the lines top as shown in Fig.(1). The treating area was chosen upon the water steam ability of (46×25) cm that equals maximum (0.23 m²) for the two steaming lines with the chosen steaming period. The steaming device has been designed to treat essentially the bottom of growing lines for the in rows crops. The chassis formed from the following:

- 1- **The holding frame:** As shown in Fig. (1) it formed from heavy ironed 1.5" beams with dimensions of (60 W×163 L×146 H cm) to hold the steam boiler, the pneumatic water tank, the driving AC motor and the electrical generator. The frame was merged to fit small areas and easy removing.
- 2- **The chassis cranes:** As shown in (Fig.1, No.2) the chassis had four adaptable wheel cranes to set the chassis height from the ground as the plants tall in the planting lines to pass over it without closing to it. Every crane could be raised from the ground up to 62.5 cm height. The cranes was formed from two telescopic iron square pipes of (2×2×30 cm) with (3×3×30 cm) and gathered internally by inlet screw of (22 mm×30 cm) then an upper manual flange roller was lathed to set the chosen frame height manually. Four wheels with 27 cm diameter were used as shown in (Fig.1, No.1).

- 3- The steering shaft:** It was rear mounted to the chassis and gathered with the rear wheels by 25 mm bearing flange to give rotating angle of 270° to smoothly round the steaming device, as shown in (Fig.1, No.4).
- 4- The driving AC bi-directional gear motor:** This motor was chosen carefully to suits steaming periods that needs low forward speeds from (0.72-1.8 km/h). The motor was electrically directed to keep clean planting from the emissions. The motor rotating speed was decreased using gear box from (1600 to 100 rpm) with reduction ratio of (1:16). The motor specifications listed in Table. (5). Also (5, 7, 9 and 14 teeth) driving gears was hosted on the gearbox shaft to transfer moving to other 38 teeth driven gear that connected to the front right wheel to reduce forward speeds at four variable levels of (0.72, 0.9, 1.2 and 1.8 km/h) as shown in (Fig1.,No 25&27). The motor was controlled using a special switch forward / reverse enclosed IP66 3 pole 20 A square switch suitable for single phase electric motors and attached to the steering shaft to be used by the operator, as shown in Figs. (19&20).



Fig.19: The driving AC gear motor.

Fig.20: The driving AC motor connection.

Table.5: The driving AC motor specifications.

Model	Bison- American-016-242-315	Power	1/6 hp 229 Watt
Operating voltage	220 V AC, 50Hz	Rotating speed	From 1600 to 100 rpm
Operating current	1.0 A	Reduction ratio	1:16
Torque	91 In-LBS		

- 5- The steam lines:** This part was fabricated to cover the bottom of two parallel adjacent rows. A twin steaming adapting concaved shaped plates with a changeable angle from 45° to 90° was formed to suit the various planting distances to gauge the steam flow only over the weed infected areas far away from plants rows, as shown in Figs. (21&22). Whereas the steaming concaves was quilted by a thermal glass wool layer to prevent the crops from heat leakage (Fig.1, No. 35). However the twin steam concaves were hinges to the frame by a crane (Fig.1, No. 20) to set its height over the rows and also were formed to be slipped latterly on the telescopic square pipes (Fig.1, No. 33) to suit planting distances between rows. The steam lines consisted from the following:

A- The concave plates: As shown in (Fig.1, No. 34) which were formed from 1mm thickness of galvanized plates to resist oxidize with dimensions of (46×25 cm) and gathered by two hinges from every side, as shown in Fig.(22) to a square iron pipes of (2×2 cm) with the length of 50 cm that covers this length virtually with steam. Every steaming concave line was quilted from inside by a thermal glass wool layer. The concaved angle was settled by 10 mm screw bolt with length of 50 cm, as shown in (Fig.1, No. 36).

B- The brass steam pipes: As shown in Fig. (21) this formed from brass with the thermal conductivity K of 109 W/m².K with diameter of 4 mm and length of 45 cm which connected to the boiler by an isolated thermal 5 mm dia. hoses. Three steam spraying nozzles of 1 mm dia. were assembled in every steam spraying line at equal distances from them of 15 cm to

make spraying integrated cones to spray all the under area of bottom line. Every brass pipe was hinged to the holding square pipe by another 20 cm length adaptable screw bolt (10 mm dia.) to gauge the distance between ground and the flowed steam.

C- The concaves holding crane: As shown in (Fig1, No. 20) it was attached to the frame to set the concaves height over the plating rows. It was made from two telescopic iron square pipes of (2×2×30 cm) with (3×3×30 cm) and gathered by inlet 22 mm dia. screw with length of 30 cm and have a manual roller to set its height manually.



The steam device operation: Generally operating the steam device needs followed steps to eliminates weeds perfectly from setting the chassis height width and height then set the steam heights, periods, pressures at the forward speeds. Whereas as shown in Figs. (23, 24&25) cleared the steam elimination effect on weeds directly and after 3 days.



Test factors

Clearly two kinds of steam were produced in two water heating stages and had a specifications according to the standard steam tables and diagram, as shown in Table. (6).

Table. (6): The used saturated damp and super-heated steams specifications.

Saturated damp steam					
Pressure bar	Temperature °c	Latent heat KJ/kg	Steam specific enthalpy KJ/kg	Water specific enthalpy KJ/kg	Steam specific volume m ³ /kg
3.5	148.017	2119.83	2743.52	623.692	0.412757
7	170.482	2047.05	2768.37	721.319	0.23995
10	184.123	1999.28	2780.71	781.434	0.177232
Super-heated steam					
Pressure bar	Temperature °c	Steam specific enthalpy KJ/kg	Steam specific volume m ³ /kg	Steam specific heat KJ/kg.K	Steam viscosity mPas
3.5	398.017	3268.91	0.682247	2.09106	0.0243569
7	420.482	3310.93	0.395766	2.12253	0.0252869
10	434.123	3335.78	0.292855	2.14453	0.0258533

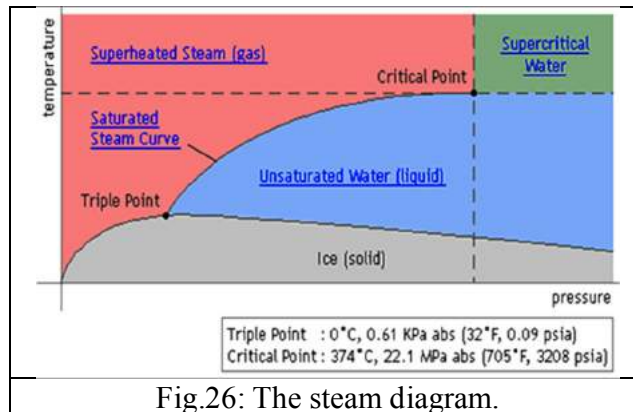


Fig.26: The steam diagram.

For optimizing the affecting factors of the investigated steam device, field experiments were done using the steam device to test the following affecting factors to compare the two different generated steam kinds (damp steam and super-heated steam) under the following variables levels:

- 1) **Steaming periods (S_t):**
Four steaming periods of (1, 2, 3 and 4 sec) using the twin digital timer at four settled equivalent forward speeds of (1.8, 1.2, 0.9 and 0.72 km/h).
- 2) **Steaming pressure (S_p):**
Three steam pressures were chosen (3.5, 7 and 10 bar) by rotating the adapting the pressure stat.
- 3) **Steaming height (S_h):**
Three steaming heights from the ground were used of (10, 15 and 20 cm) using the steam lines lifting crane.

Measurements and instrumentation

Pre-laboratory experiments were conducted to calibrate the needed time for preparing the water boiler for generating pressurized steam and the affecting period for weed elimination process for the best height over weeds from the ground. However the field experiments were carried out on the beta vagaries crop as season 2016. The measurements were as follows:-

- 1) Weed extermination ratio, (EX.R) %: After treatment, two and three days. It was assumed by the following equation:-

$$EX.R = \frac{\text{weeds mass in rows before steam treated, g/ m}^2}{\text{weeds mass in rows after steam treted, g/ m}^2} \times 100 \dots\dots\dots (1)$$

- 2) Chlorophyll level percentage, (ch) %: After treatment, two and three days. It was estimated by the following equation:-

$$ch = \frac{\text{weed leaves chloropyll percentage after treatment,mg/ cm}^2}{\text{weed leaves chloropyll percentage before treatment, mg/cm}^2} \times 100 \dots\dots\dots (2)$$



Fig.27: Digital Chlorophyll Meter model atLEAF.

The weeds chlorophyll level percentage was calculated using: atLEAF+ Digital Chlorophyll meter with software model PN/0131 made in USA (3VDC-0.2 A+ 5V USB).

- 3) Weeds re-growth, (GR) %: For treated weeds per one, two and three weeks. It was calculated by the following equation:-

$$GR = \frac{n.of\ germinated\ weeds,\ stalk}{n.of\ weeds\ after\ treatment,\ stalk} \times 100 \dots\dots\dots (3)$$

4) Yield production ratio Y %: It was assumed by the following equation:-

$$Y = \frac{trated\ area\ crop\ yield,\ ton/fed}{control\ crop\ yield,\ ton/fed} \times 100 \dots\dots\dots (4)$$

5) Field capacity, (FC) fed/h: by using the following equation:-

$$FC = \frac{trated\ area,\ fed}{time\ of\ treatment,\ h} Fed/h \dots\dots\dots (5)$$

6) The machine efficiency (Fe), %: It was measured according to *Kepner et al. (1982)*.

$$Fe = \frac{T_{th}}{T_{ac}} \times 100 \dots\dots\dots (6)$$

Where: Fe: machine efficiency, %, T_{th}: theoretical time per fed, h T_{ac}: the actual operating time, h.

7) The fuel consumption (F), lit/min:

Fuel consumption was determined by measuring the volume of fuel consumed during the operation time for each run and calculated in liter per hour. It was measured by completely filling the fuel tank then before each end run and refilling the fuel tank using a scaled container. The fuel consumption rate was calculated from the following equation:

$$F = \frac{V}{T} \quad L/h \dots\dots\dots (7)$$

Where: F: rate of fuel consumption, L/h, V: rate of consumed fuel, L T: time, h

8) Specific energy consumption, CE (kW.h/fed):

The electrical energy consumption (kW) was determined for each test by taking the readings of both line current and voltage, using super clamp meter (700-k type) that connected to the steam device cables. Hence the consumed electrical power (kW) for each treatment was estimated according to (*Kurt, 1979*) as follow:

$$Ep = I * V * \eta * \cos \phi / 1000 \dots\dots\dots (8)$$

Where: EP = electrical consumed power under different machine loads;

I = line current strength in Amperes; V = potential difference (voltage) being equal to 220 V; η = mechanical efficiency (assumed as 80 %); cos φ = power factor (was taken as 0.7).

Consequently, the specific energy consumption (kWh/fed) for each treatment could be calculated using the following equation:

Specific energy consumption = **consumed power (kW.h) / Machine field capacity (fed/h).**

9) Total costs, (C) L.E./fed: comparing to the traditional methods were estimated: using the following equation (*Awady et al., 2003*):

$$C = \frac{P}{h} \left[\frac{1}{a} + \frac{I}{2} + T + r \right] + (W.e) + \frac{m}{144} \dots\dots\dots (9)$$

Where :C: hourly cost, L.E./h; P: price of the machine, L.E.;
 h: yearly working hours, h/year; a: life expectancy of the machine, year;
 I: interest rate per year; T: tax overheads ratio;
 r: repair and maintenance ratio; W: power of motor, kW;
 e: hourly cost/kW.h. m: the monthly average wage ,
 L.E.; 144: the monthly average working hours.

The operating cost was determined using the following formula:

$$\text{Operating cost (L.E / fed)} = \frac{\text{Machine hourly cost, (L.E./h)}}{\text{Actual field capacity (fed / h)}} \text{L.E / fed} \dots\dots\dots (10)$$

The experimental plots were arranged in a three way completely randomized factorial experiment with three replicates and analyzed statistically and the significance according to the probability ($P < 0.05$) was evaluated by the CoStat program (Oida, 1997).

RUSULTS AND DISCUSSION

The main results could be discussed as follows:

1- Factors affecting weeds extermination ratio, (Ex.R %):

The relationships compared between the damp and superheated steams at the different steam exposure periods (S_p , sec) to the weeds extermination ratios (EX.R, %) (after steam exposure, 2 days and 3 days) at the different steam pressures (S_p , bar) are illustrated in Figs. (28 & 29). Actually increasing the S_t for the two different kinds of steam; damp and superheated respectively increases the weeds extermination ratios (EX.R) with increasing the treatment of the (S_p) in a direct relationships. The maximum values of (EX.R 1,2&3) for damp and super-heated steams were {(91.89, 94.0, and 95.84) & (93.69, 95.94 and 97.74) %}, respectively at 4 sec of the S_t for S_p of 10 bar, on the other hand the minimum values of the (EX.R 1,2&3) for damp and super-heated steams were {(72.49, 74.44 and 76.30) & (74.41, 76.33 and 78.51) %}, respectively for of the 1 sec of S_t at S_p of 3.5 bar.

Thus, as shown in Figs. (30&31), the maximum values of the (EX.R 1,2&3) for damp and super-heated steams were {(91.35, 93.40 and 95.43) & (93.34, 95.44 and 97.27) %} respectively, for S_t of 4 sec at 10 cm of the steam height from the ground (S_h), when the minimum values of the (EX.R 1,2&3) for damp and super-heated steams were {(72.97, 74.95 and 76.95) & (75.01, 76.74 and 78.92) %}, respectively for the 1 sec S_t at 20 cm of S_h .

These results may be owned to by increasing the exposure periods of steaming weeds the extermination ratios increased relatively as exposure the weeds cells due to overheating limits that exceeds 180°C by using the damp steam when using the superheated steam increases the heating levels over 400°C that rapid the weeds death. However, using the pressurized steam levels from 3.5 to 10 bar increases the weeds death acting under the chosen steam heights at the first ages of weeds. Statically there are high significant effects for the total interaction between different treatments with ($P < 0.05$) for the (EX.R 1, 2&3) values respectively. Also ANOVA analysis indicated highly significant differences between the treatments. A simple power regression analysis applied to relate the change in (EX.R 1, 2&3) with the change in the tested factors for all treatments. The obtained regression equations were in the form of:

	Damp steam	Super-heated steam
Ex. R1 %	67.169 +6.015 St +0.175 SP- 0.075 Sh R ² = 0.9864 C.V=1.181	68.415+5.941 St + 0.229 SP-0.046 Sh R ² =0.9998 C.V=0.140
Ex. R2 %	68.256 + 6.01 St +0.24 SP-0.048 Sh R ² =0.9997 C.V=0.175	70.153 + 6.09 St + 0.206 SP -0.047 Sh R ² =0.9997 C.V=0.154
Ex. R3 %	70.328 + 5.60 St +0.228 SP-0.0491Sh R ² =0.9996 C.V=0.189	72.46 + 5.948 St + 0.217 SP -0.048 Sh R ² =0.9998 C.V=0.121

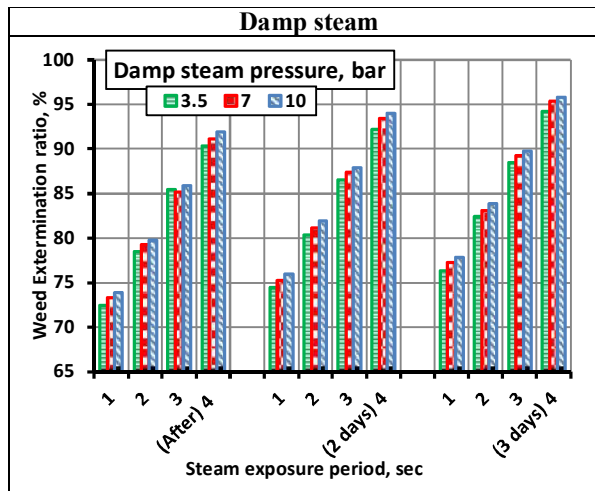


Fig. 28: Effect of damp steam exposure periods on the weeds extermination ratios at the different steam pressures.

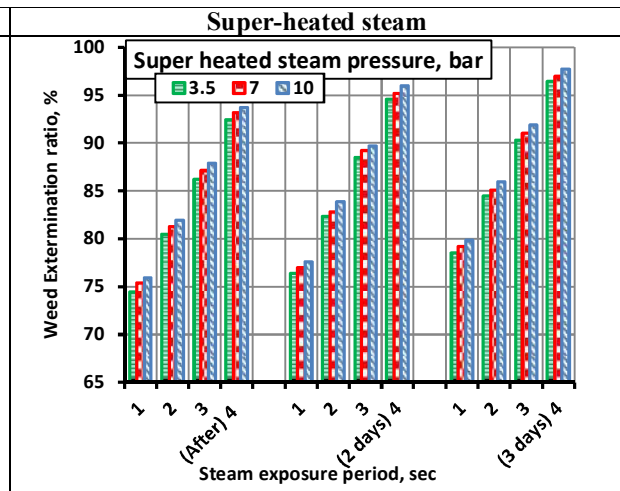


Fig. 29: Effect of super-heated steam exposure periods on the weeds extermination ratios at the different steam pressures.

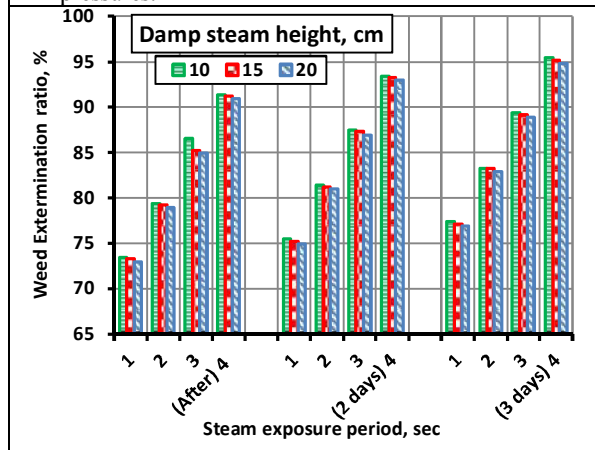


Fig. 30: Effect of damp steam exposure periods on the weeds extermination ratios at the different steam heights.

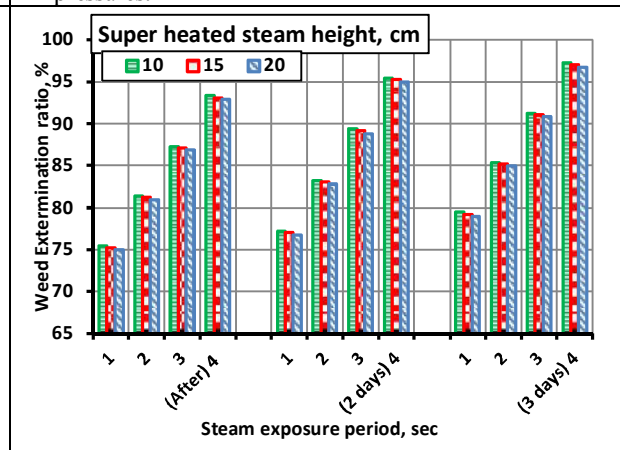


Fig. 31: Effect of super-heated steam exposure periods on the weeds extermination ratios at the different steam heights.

2- Factors affecting weeds chlorophyll percentage (Ch, %)

The graphs which describes the effect of the damp and superheated steams on the weeds chlorophyll percentages (EX.R, %) (After steam exposure, 2 days and 3 days) at the different steam exposure periods (S_p , sec) to with different steam pressures (S_p , bar) are shown in Figs. (32 & 33). As well, increasing the S_t for the two different kinds of steam damp and superheated respectively decreases the weeds chlorophyll percentages (Ch, %) with increasing the treatment of the (S_p) in adverse relationships. The maximum values of (Ch 1,2&3) for damp and super-heated steams were {(74.68, 43.92 and 19.38) & (59.55, 29.24 and 13.52) %}, in arrangement at 4 sec of the S_t for S_p of 10 bar, during the lowest values of the (Ch 1,2&3) for damp and super-heated steams were {(55.83, 20.73 and 6.90) & (40.86, 10.63 and 2.64) %}, respectively for of the 1 sec of S_t at S_p of 3.5 bar.

In that manner, the highest values of the (Ch 1,2&3) for damp and super-heated steams were {(73.23, 42.72 and 18.22) & (58.19, 27.82 and 12.58) %} respectively, as shown in Figs. (33&34) for S_t of 4 sec at 10 cm of the steam height from the ground (S_h), where the lowest values of the (Ch 1,2&3) for damp and super-heated steams were {(56.93, 21.89 and 8.97) & (42.13, 11.77 and 3.48) %}, respectively for the 1 sec S_t at 20 cm of S_h .

To be ascribable these results by reason of; by increasing the exposure period of steaming weeds the chlorophyll percentages decreased because of decreasing the moisture content of the weeds cells and stopped the photosynthesis operations as a proof of exterminated the weeds. Statically the total interactions between different treatments have high significant effects with ($P < 0.05$) for the (Ch 1, 2&3) values respectively. Too ANOVA analysis indicated highly significant differences between the treatments. A simple power regression analysis applied to relate the change in (Ch 1, 2&3) with the change in the tested variables for all treatments. The obtained regression equations were in the form of:

	Damp steam	Super-heated steam
Ch1 %	$80.129 - 5.08 St - 0.589 SP + 0.117 Sh$ $R^2=0.9993$ C.V=0.302	$64.649 - 4.989 - 0.565 SP + 0.116 Sh$ $R^2=0.9990$ C.V=0.452
Ch2 %	$48.937 - 6.417 St - 0.544 SP + 0.12 Sh$ $R^2=0.9993$ C.V=0.689	$34.463 - 4.988 St - 0.55 SP + 0.115 Sh$ $R^2=0.9992$ C.V=1.012
Ch3 %	$22.776 - 2.61 St - 0.76 SP + 0.145 Sh$ $R^2=0.9964$ C.V=2.03	$17.231 - 2.655 St - 0.49 SP + 0.11 Sh$ $R^2=0.9971$ C.V=2.521

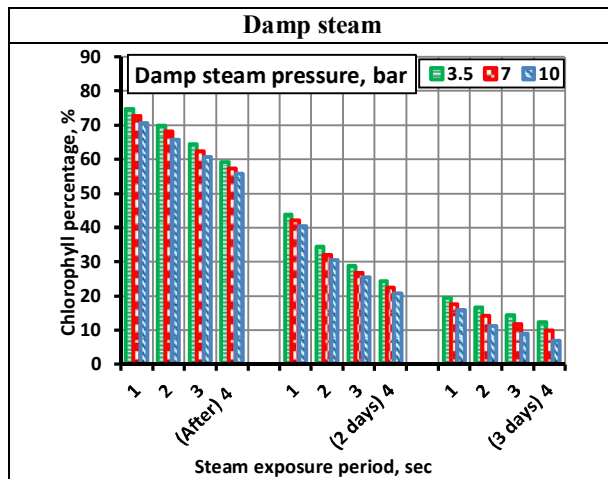


Fig. 32: Effect of damp steam exposure periods on the weeds chlorophyll percentages at the different steam pressures.

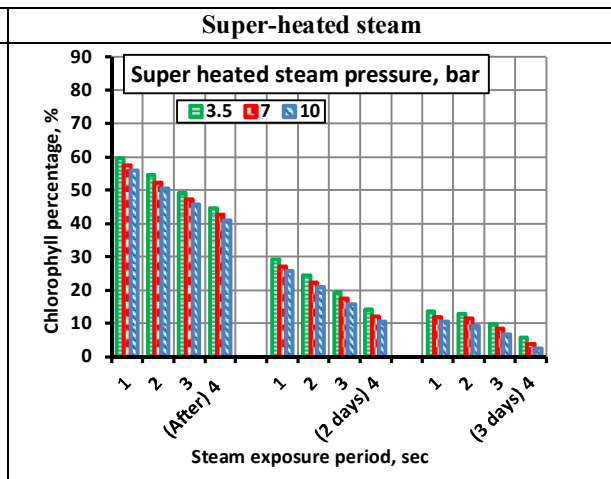


Fig. 33: Effect of super-heated steam exposure periods on the weeds chlorophyll percentages at the different steam pressures.

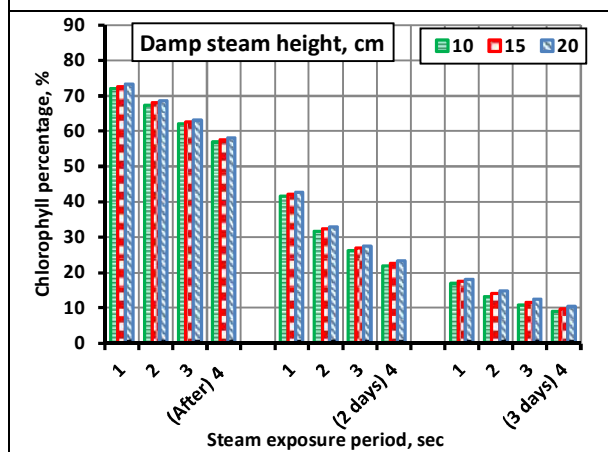


Fig. 34: Effect of damp steam exposure periods on the weeds chlorophyll percentages at the different steam heights.

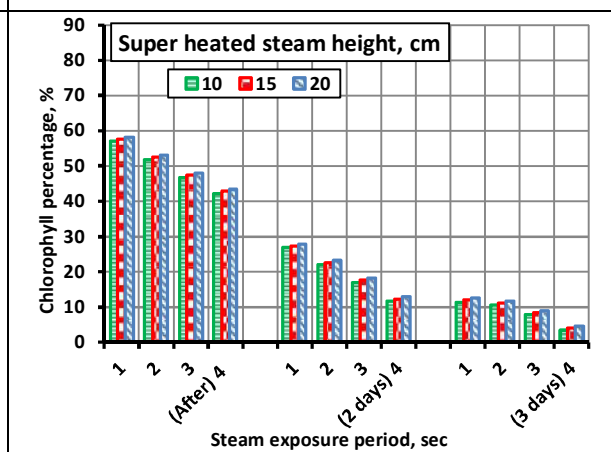


Fig. 35: Effect of super-heated steam exposure periods on the weeds chlorophyll percentages at the different steam heights.

3- Factors affecting weeds re-growth ratio (Gr, %)

Likewise Figs. (36 & 37) describe the effect of damp and superheated steams at the different steam exposure periods (S_p , sec) on the weeds regrowth ratios (Gr, %) (After steam exposure, 2 weeks and 3 weeks) with the different steam pressures (S_p , bar). Furthermore, increasing the S_t for the two different kinds of steam damp and superheated respectively decreases the weeds re-growth ratios (Gr, %) with increasing the treatment of the (S_p) in opposite trends. The maximum values of (Gr 1,2&3) for damp and super-heated steams were {(24.87, 26.88 and 28.77) & (20.90, 22.63 and 24.82) %}, in arrangement at 1 sec of the S_t for S_p of 3.5 bar, as the lowest values of the (Gr 1,2&3) for damp and super-heated steams were {(5.08, 7.08 and 9.31) & (1.08, 3.33 and 5.40) %}, respectively for of the 4 sec of S_t at S_p of 10 bar.

Too, as shown in Figs. (38 & 39), the maximum values of the (Gr 1,2&3) for damp and super-heated steams were {(24.33, 26.37 and 28.12) & (20.32, 22.26 and 24.27) %} respectively, for S_t of 1 sec at 20 cm of the steam height from the ground (S_h), despite the minimum values of the (Gr 1,2&3) for damp and super-heated steams were {(5.30, 7.59 and 9.84) & (1.69, 3.79 and 5.83) %}, respectively for the 4 sec S_t at 10 cm of S_h .

These results in view of increasing the exposure periods between treating weeds it gives chances to regrow the weeds again, but it still under the acceptable un-harmful degrees of weeds infections. However using the superheated steam treatment not affects only the weeds but also affect its seeds in the soil which minimize the weeds regrowth ratios at least. Statically there are high significant effects for the total interaction between different treatments with ($P < 0.05$) for the (Gr 1, 2&3) values respectively. Whereas, ANOVA analysis indicated highly significant differences between the treatments. A simple power regression analysis applied to relate the change in (Gr 1, 2&3) with the change in the tested factors for all treatments. The obtained regression equations were as follows:

	Damp steam	Super-heated steam
Gr1 %	29.304 - 6.091St + 0.234 SP - 0.046 Sh R ² =0.9999 C.V=0.592	25.169 - 6.069 St + 0.243 SP - 0.0463 Sh R ² =0.9998 C.V=1.007
Gr2 %	31.411 - 6.114 St + 0.23 SP - 0.045 Sh R ² =0.9997 C.V=0.802	27.155 - 5.997 St + 0.231 SP - 0.048 Sh R ² =0.9998 C.V=0.848
Gr3 %	32.925 - 5.969 St + 0.245 SP - 0.046 Sh R ² =0.9998 C.V=0.549	29.355 - 6.026 St + 0.22 SP - 0.047 Sh R ² =0.9998 C.V=0.735

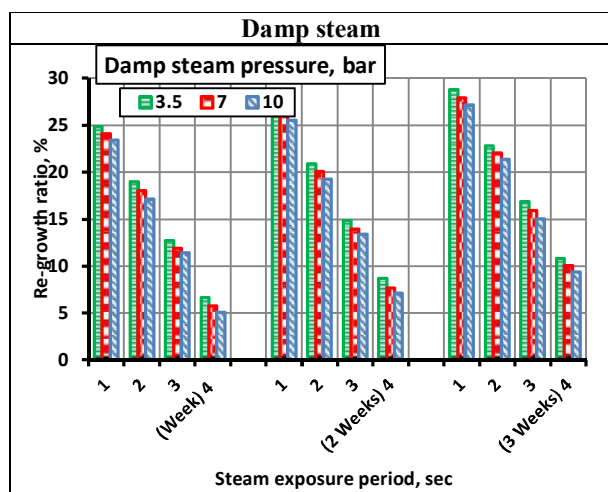


Fig. 36: Effect of damp steam exposure periods on the weeds re-growth ratios at the different steam pressures.

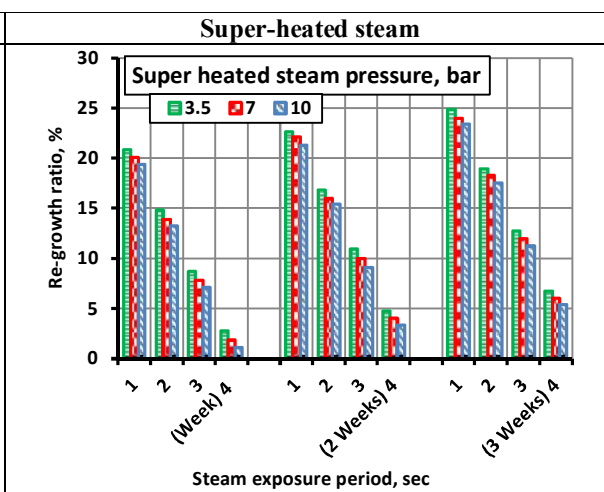


Fig. 37: Effect of super-heated steam exposure periods on the weeds re-growth ratios at the different steam pressures.

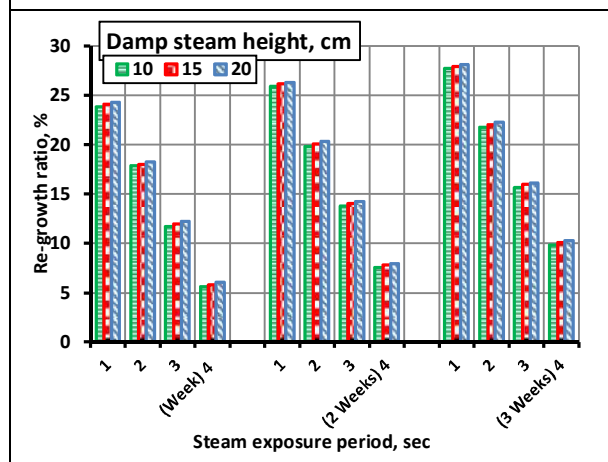


Fig. 38: Effect of damp steam exposure periods on the weeds re-growth ratios at the different steam heights.

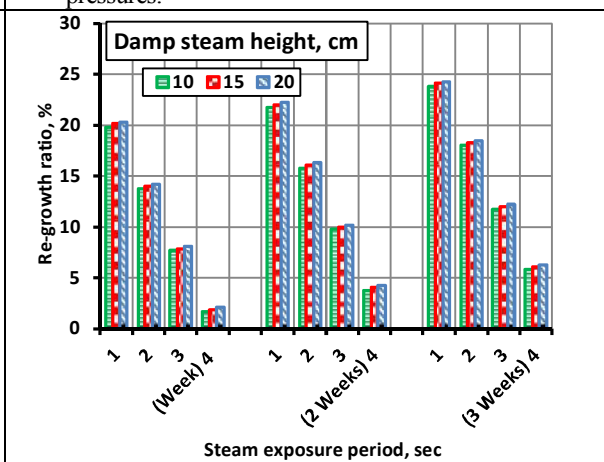


Fig. 39: Effect of super-heated steam exposure periods on the weeds re-growth ratios at the different steam heights.

4- Factors affecting yield increasing ratio (Y, %):

Figs. (40 & 41) are illustrated in the relationships compared between the damp and superheated steams at the different steam exposure periods (S_p , sec) to the weeds regrowth ratios (Y, %) at the different steam pressures (S_p , bar). Besides, increasing the S_t for the two different kinds of steam damp and superheated respectively increases the yield increasing ratios (Y, %) to the control with increasing the treatment of the (S_p) in direct relationships. The maximum values of (Y, %) for damp and super-heated steams were (45.41 and 49.57 %) over control (12 ton/fed), respectively at 4 sec of the S_t for S_p of 10 bar, while the lowest values of the (Y) for damp and super-heated steams were (33.64 and 40.60 %), respectively for of the 1 sec of S_t at S_p of 3.5 bar.

During, the maximum values of the (Y) for damp and super-heated steams were (44.82 and 49.14 %) over control (12 ton/fed) respectively, as shown in Figs. (42&43) for S_t of 4 sec at 10 cm of the steam height from the ground (S_h), when the minimum values of the (Y) for damp and super-heated steams were (31.10 and 39.58 %), respectively for the 1 sec S_t at 20 cm of S_h .

These results may be attributed to by increasing the exposure periods of treating weeds using the two different steams minimizes the chances of grow weeds that led crop yield increases over the control

because of finishing the competition between the crop and the weeds on the light and feed . Statically there are high significant effects for the total interaction between different treatments with ($P < 0.05$) for the Y values respectively. Also ANOVA analysis indicated highly significant differences between the treatments. A simple power regression analysis applied to relate the change in (Y) for damp and superheated steams with the change in the tested factors for all treatments. The obtained regression equations were in the form of:

	Damp steam	Super-heated steam
Y %	$31.242 + 3.0986 S_t + 0.324 S_p - 0.065 S_h$ $R^2=0.9957$ C.V=0.722	$39.057 + 2.322 S_t + 0.235 S_p - 0.059 S_h$ $R^2=0.9958$ C.V=0.471

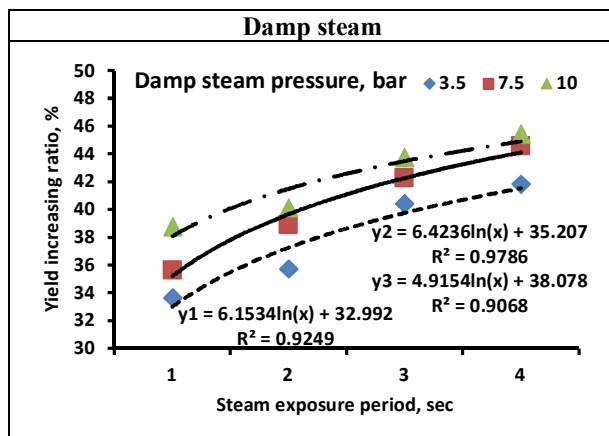


Fig. 40: Effect of damp steam exposure periods on the yield increasing ratio at the different steam pressures.

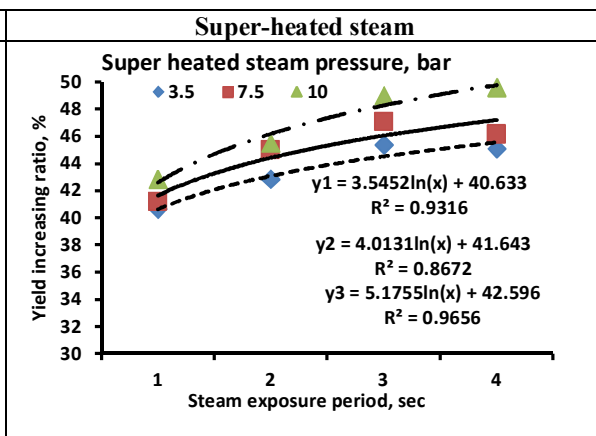


Fig. 41: Effect of super-heated steam exposure periods on the yield increasing ratio at the different steam pressures.

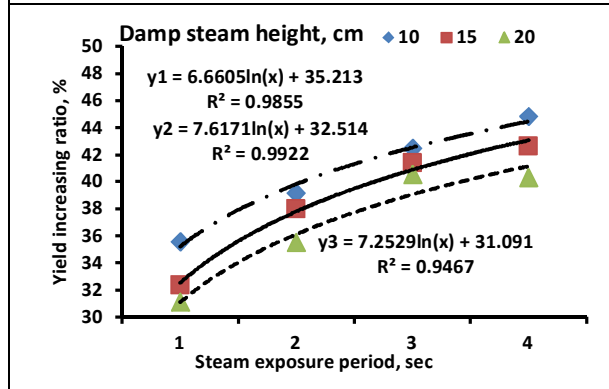


Fig. 42: Effect of damp steam exposure periods on the yield increasing ratio at the different steam heights.

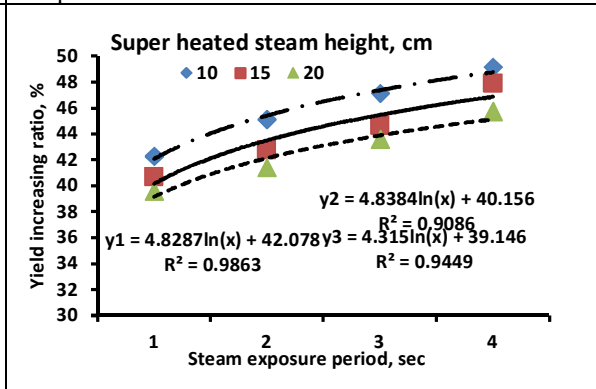


Fig. 43: Effect of super-heated steam exposure periods on the yield increasing ratio at the different steam heights.

5- Factors affecting the steam device field efficiency (Fe, %):

The relationships compared between the damp and superheated steams at the different steam exposure periods (S_p , sec) to the steam device field efficiency (F_e , %) at the different steam pressures (S_p , bar) are illustrated in Figs. (44 & 45). Generally, increasing the forward speed (FV) at the different S_t for the two different kinds of steam damp and superheated respectively increases the device field efficiency (F_e , %) with increasing the treatment of the (S_p) in direct relationships. The maximum values of (F_e , %) for damp and super-heated steams were (96.11 and 94.12 %), respectively at 1 sec of the S_t (1.8 km/h) for S_p of 10 bar, while the lowest values of the (F_e) for damp and super-heated steams were (85.59 and 83.47 %), respectively for of the 4 sec of S_t (0.72 km/h) at S_p of 3.5 bar.

While, the maximum values of the (Fe) for damp and super-heated steams were (95.97 and 93.73 %) respectively, as shown in Figs. (46&47) for S_t of 1 sec (1.8 km/h) at 10 cm of the steam height from the ground (S_h), where the minimum values of the (Fe) for damp and super-heated steams were (83.06 and 82.16 %), respectively for the 4 sec S_t (0.72 km/h) at 20 cm of S_h .

These results may be attributed to by increasing the forward speed of the steam device the field efficiency increases relatively but its values for damp steam were increased than the super-heated steam because consumed more time for generating the super-heated steam. However the maximum value of steam pressure 10 bar with the minimum close steam height 10 cm from the ground achieves the maximum efficient variables setting. Statically there are high significant effects for the total interaction between different treatments with ($P < 0.05$) for the Fe values respectively. Also ANOVA analysis indicated highly significant differences between the treatments. A simple power regression analysis applied to relate the change in (Fe) for damp and superheated steams with the change in the tested factors for all treatments. The obtained regression equations were in the form of:

	Damp steam	Super-heated steam
Fe %	$97.149 - 2.922 S_t + 0.318 S_P - 0.065 S_h$ $R^2=0.9988$ C.V=0.161	$95.184 - 2.934 S_t + 0.319 S_P - 0.064 S_h$ $R^2=0.9991$ C.V=0.140

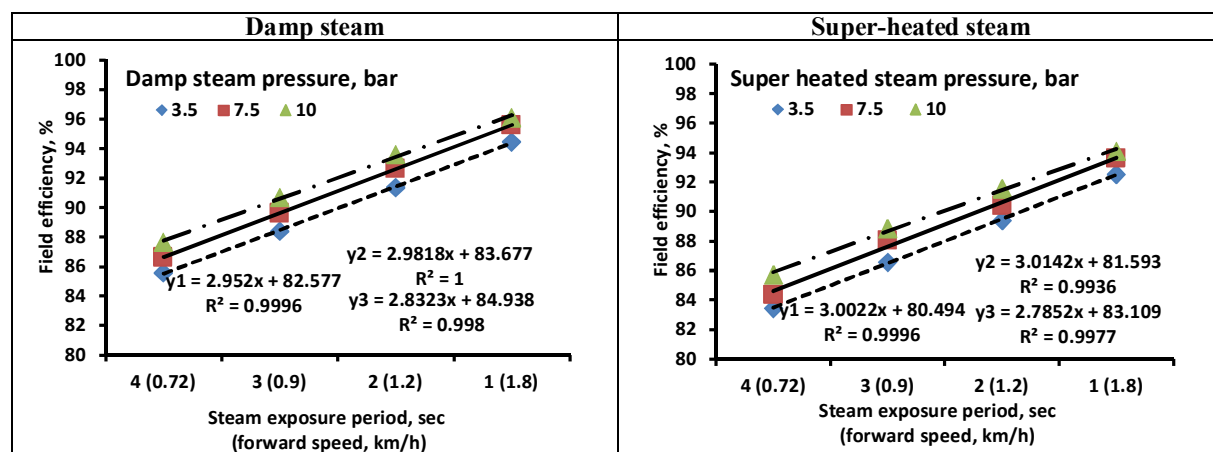


Fig. 44: Effect of damp steam exposure periods (forward speeds) on the field efficiency at the different steam pressures.

Fig. 45: Effect of super-heated steam exposure periods (forward speeds) on the field efficiency at the different steam pressures.

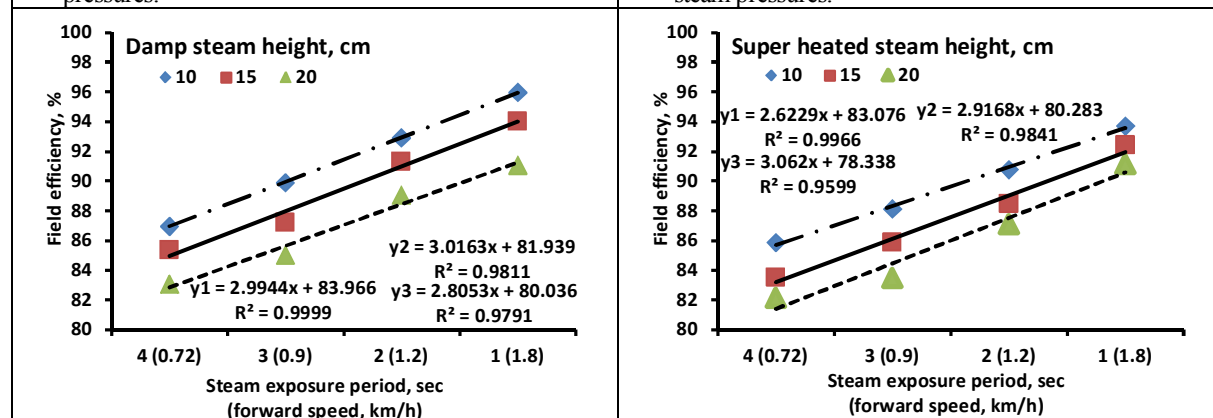


Fig. 46: Effect of damp steam exposure periods (forward speeds) on the field efficiency at the different steam heights.

Fig. 47: Effect of super-heated steam exposure periods (forward speeds) on the field efficiency at the different steam heights.

6- Factors affecting the steam device field capacity, (FC, fed/h):

The relationships compared between the damp and superheated steams at the different steam exposure periods (S_p , sec) to the steam device field efficiency (FC, fed/h) at the different steam pressures (S_p , bar) are illustrated in Figs. (48 & 49). Generally, increasing the forward speed (FV) at the different S_t for the two different kinds of steam damp and superheated respectively increases the device field efficiency (FC, fed/h) with increasing the treatment of the (S_p) in direct relationships. The maximum values of (FC, fed/h) for damp and super-heated steams were (0.61 and 0.59 fed/h), respectively at 1 sec of the S_t (1.8 km/h) for S_p of 10 bar, while the lowest values of the (FC) for damp and super-heated steams were (0.21 and 0.20 fed/h), respectively for of the 4 sec of S_t (0.72 km/h) at S_p of 3.5 bar.

While, the maximum values of the (FC) for damp and super-heated steams were (0.59 and 0.59 fed/h) respectively, as shown in Figs. (50 & 51) for S_t of 1 sec (1.8 km/h) at 10 cm of the steam height from the ground (S_h), where the minimum values of the (FC) for damp and super-heated steams were (0.20 and 0.18 fed/h), respectively for the 4 sec S_t (0.72 km/h) at 20 cm of S_h .

These results may be attributed to by increasing the forward speed of the steam device the field capacity increases also at the adequate operating width for the steam device. However the field capacity values are low but the steam treating for the weeds needs time to do the effective extermination operation properly. Statically there are high significant effects for the total interaction between different treatments with ($P < 0.05$) for the FC values respectively. Also ANOVA analysis indicated highly significant differences between the treatments. A simple power regression analysis applied to relate the change in (FC) for damp and superheated steams with the change in the tested factors for all treatments. The obtained regression equations were in the form of:

	Damp steam	Super-heated steam
FC	$0.649 - 0.119 S_t + 0.001 S_P - 0.000244 S_h$	$0.624 - 0.116 S_t + 0.001 S_P - 0.000247 S_h$
Fed/h	$R^2=0.9999$ C.V=0.169	$R^2=0.9999$ C.V=0.173

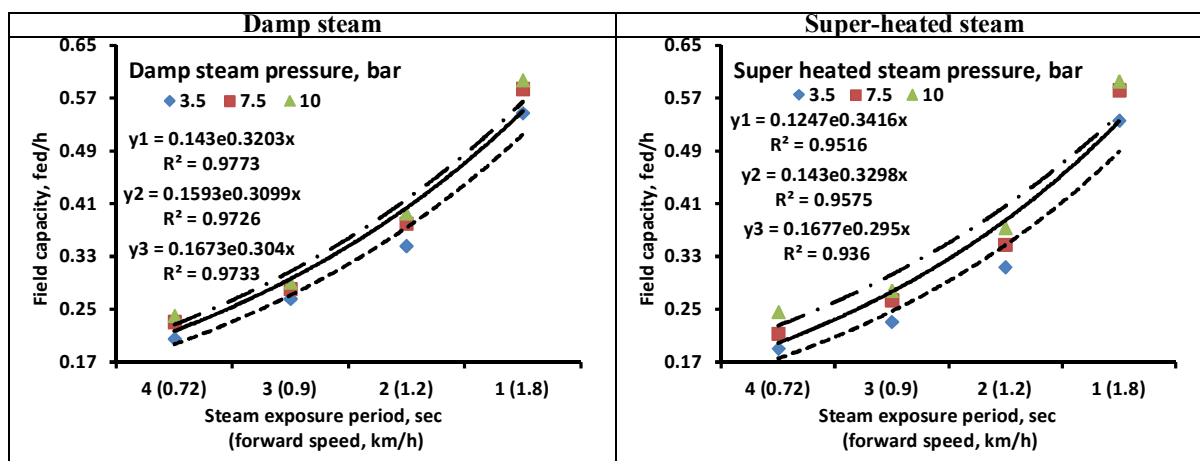


Fig. 48: Effect of damp steam exposure periods (forward speeds) on the field capacity at the different steam pressures.

Fig. 49: Effect of super-heated steam exposure periods (forward speeds) on the field capacity at the different steam pressures.

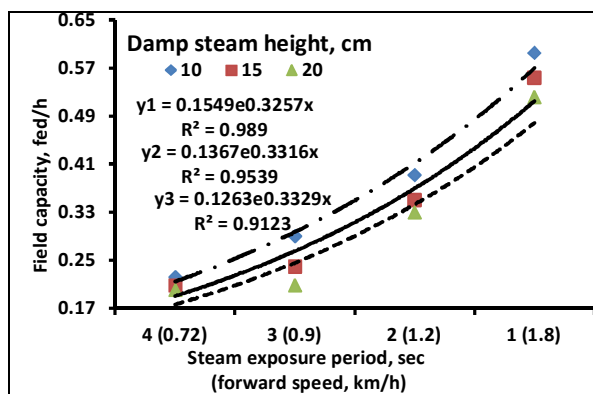


Fig. 50: Effect of damp steam exposure periods (forward speeds) on the field capacity at the different steam heights.

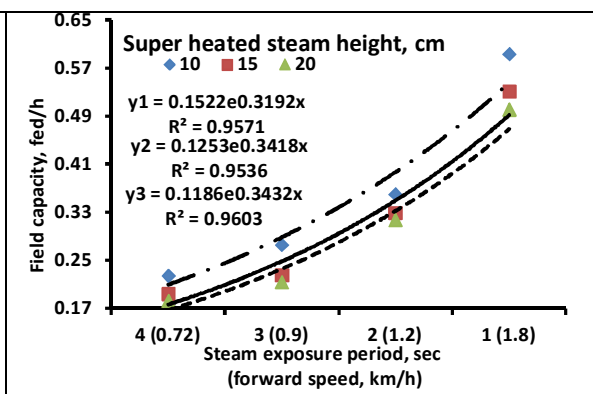


Fig. 51: Effect of super-heated steam exposure periods (forward speeds) on the field capacity at the different steam heights.

7- Factors affecting fuel consumption, (F, lit/h):

The relationships compared between the damp and superheated steams at the different steam exposure periods (S_p , sec) to the steam device fuel consumption (F, lit/h) at the different steam pressures (S_p , bar) are illustrated in Figs. (52 & 53). As well, increasing the forward speed (FV) at the different S_t for the two different kinds of steam damp and superheated respectively increases the device fuel consumption (F, lit/h) with increasing the treatment of the (S_p) in direct relationships. The maximum values of (F, lit/h) for damp and super-heated steams were (1.61 and 1.87 lit/h), respectively at 1 sec of the S_t (1.8 km/h) for S_p of 10 bar, while the lowest values of the (F) for damp and super-heated steams were (0.87 and 1.04 lit/h), respectively for of the 4 sec of S_t (0.72 km/h) at S_p of 3.5 bar.

While, the maximum values of the (F) for damp and super-heated steams were (1.57 and 1.83 lit/h) respectively, as shown in Figs. (54 & 55) for S_t of 1 sec (1.8 km/h) at 10 cm of the steam height from the ground (S_h), where the minimum values of the (F) for damp and super-heated steams were (0.93 and 1.10 lit/h), respectively for the 4 sec S_t (0.72 km/h) at 20 cm of S_h .

These results may be attributed to by increasing the forward speed of the steam device the fuel consumption levels increases directly but its less also from any other mechanical control treatment for weeds like hoeing operations because of using 6.5 hp merged friendly gasoline motor to the AC generator which consumed minor level of fuel. Also the fuel consumption increases for the super-heated steam operations at the high steam pressure level for the closest steam height than the damp steam operations due to more electrical power consumed by the external heater. Statically there are high significant effects for the total interaction between different treatments with ($P < 0.05$) for the F values respectively. Also ANOVA analysis indicated highly significant differences between the treatments. A simple power regression analysis applied to relate the change in (F) for damp and superheated steams with the change in the tested factors for all treatments. The obtained regression equations were in the form of:

	Damp steam	Super-heated steam
F lit/h	$1.702 - 0.192 S_t + 0.0209 S_P - 0.0048 S_h$ $R^2=0.9982$ C.V=0.896	$1.931 - 0.215 S_t + 0.0227 S_P - 0.0052 S_h$ $R^2=0.9988$ C.V=0.743

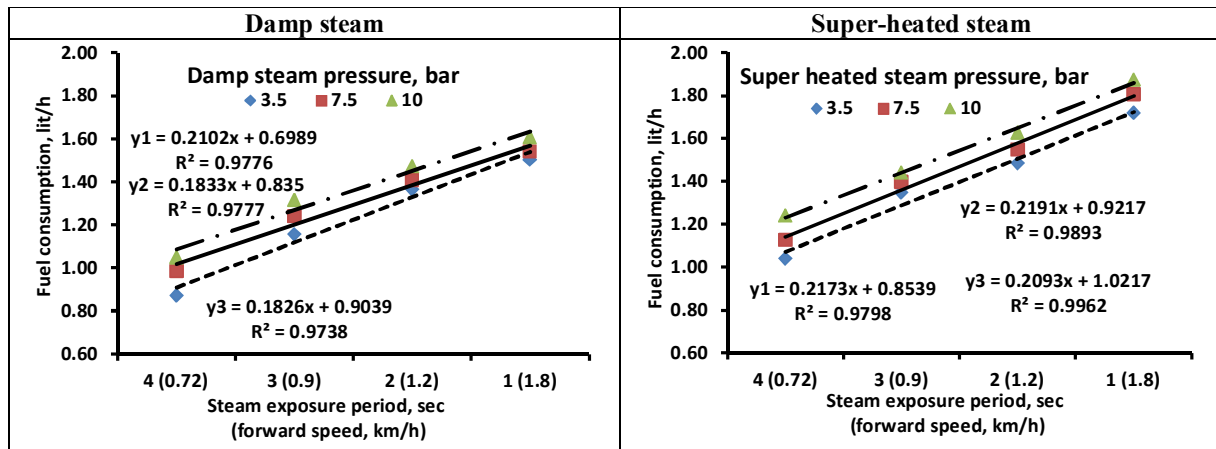


Fig. 52: Effect of damp steam exposure periods (forward speeds) on the fuel consumption at the different steam pressures.

Fig. 53: Effect of super-heated steam exposure periods (forward speeds) on the fuel consumption at the different steam pressures.

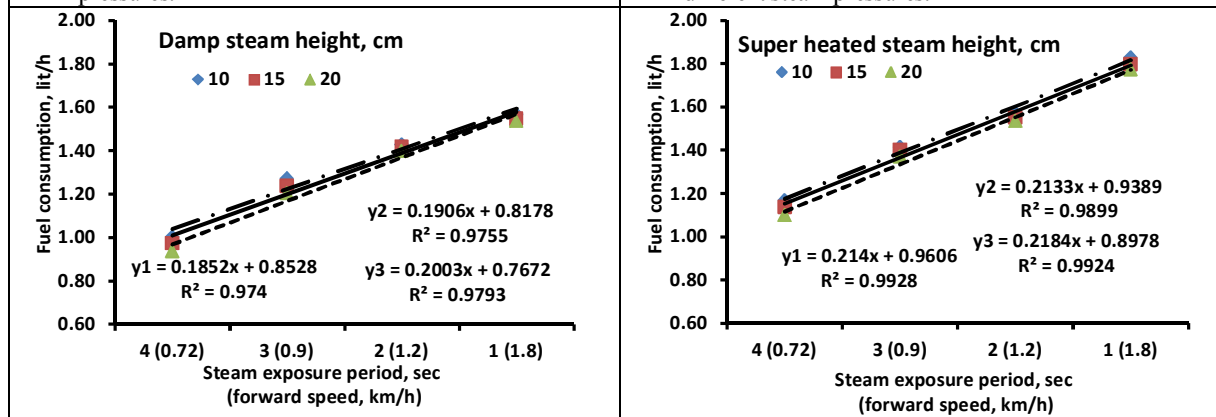


Fig. 54: Effect of damp steam exposure periods (forward speeds) on the fuel consumption at the different steam heights.

Fig. 55: Effect of super-heated steam exposure periods (forward speeds) on the fuel consumption at the different steam heights.

8- Factors affecting the steam device consumed energy, (CE, kW.h/fed):

The relationships compared between the damp and superheated steams at the different steam exposure periods (S_p , sec) to the steam device consumed energy (CE, kW.h/fed) at the different steam pressures (S_p , bar) are illustrated in Figs. (56 & 57). As well, increasing the forward speed (FV) at the different S_t for the two different kinds of steam damp and superheated respectively decreases the device consumed energy (CE, kW.h/fed) with increasing the treatment of the (S_p) in opposite relationships. The maximum values of (CE, kW.h/fed) for damp and super-heated steams were (4.83 and 6.63 Kw.h/fed), respectively at 4 sec of the S_t (0.72 km/h) for S_p of 10 bar, while the lowest values of the (CE) for damp and super-heated steams were (1.72 and 2.36 Kw.h/fed), respectively for of the 1 sec of S_t (1.8 km/h) at S_p of 3.5 bar.

While, the maximum values of the (CE) for damp and super-heated steams were (4.80 and 6.58 kW.h/fed) respectively, as shown in Figs. (58&59) for S_t of 4 sec (0.72 km/h) at 10 cm of the steam height from the ground (S_h), where the minimum values of the (CE) for damp and super-heated steams were (1.73 and 2.36 kW.h/fed), respectively for the 1 sec S_t (1.8 km/h) at 20 cm of S_h .

These results due to for higher forward speeds the consumed energy decreases in opposite relationship logically and vice versa for lowest forward speeds. However, the consumed energy values for super-

heated steam were greatest than the damp stem because of consuming more power to rise the steam temperature. Statically there are high significant effects for the total interaction between different treatments with ($P < 0.05$) for the CE values respectively. Also ANOVA analysis indicated highly significant differences between the treatments. A simple power regression analysis applied to relate the change in (CE) for damp and superheated steams with the change in the tested factors for all treatments. The obtained regression equations were in the form of:

	Damp steam	Super-heated steam
CE, kW.h/fed	$0.732+1.0137S_t - 0.0119 S_P + 0.0024 S_h$	$1.124+1.385 S_t - 0.0174 S_P + 0.0037 S_h$
	$R^2=0.9999$ C.V=0.182	$R^2=0.9999$ C.V=0.183

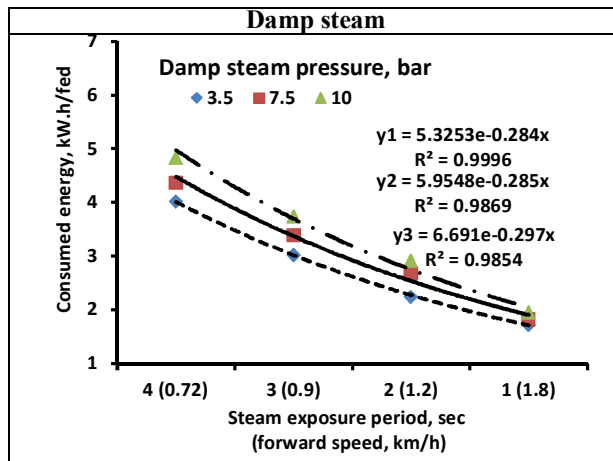


Fig. 56: Effect of damp steam exposure periods (forward speeds) on the consumed energy at the different steam pressures.

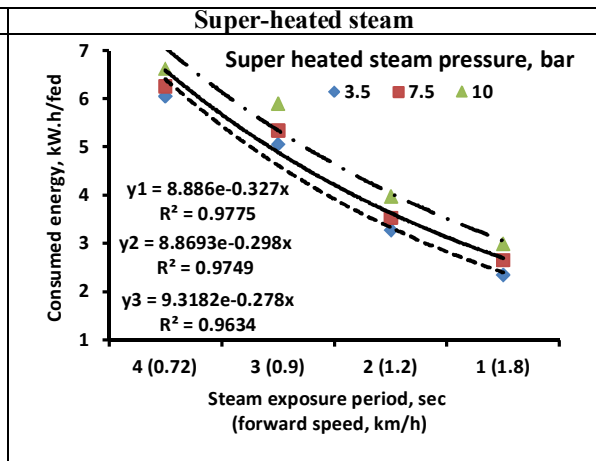


Fig. 57: Effect of super-heated steam exposure periods (forward speeds) on the consumed energy at the different steam pressures.

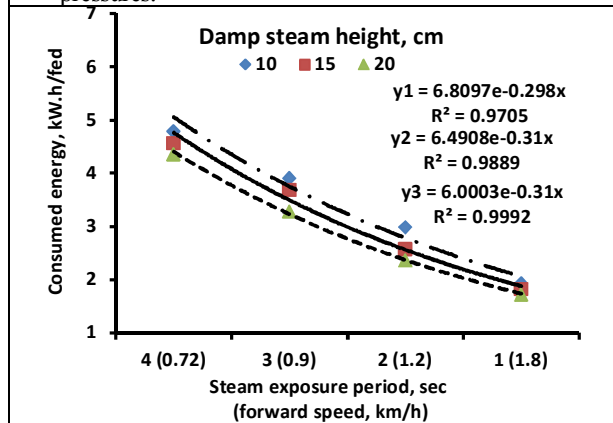


Fig. 58: Effect of damp steam exposure periods (forward speeds) on the consumed energy at the different steam heights.

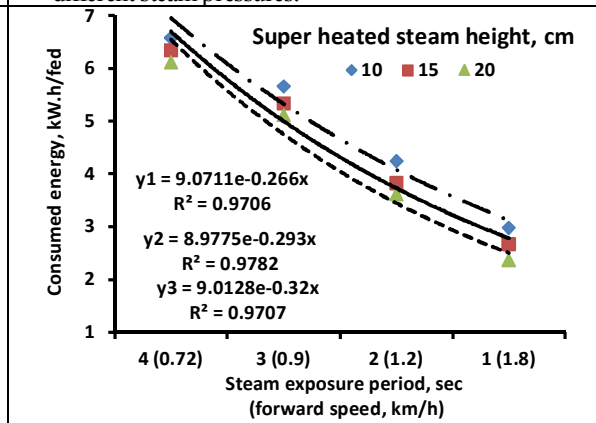


Fig. 59: Effect of super-heated steam exposure periods (forward speeds) on the consumed energy at the different steam heights.

9- Factors affecting steam device operating cost, (C, L.E/fed):

The relationships compared between the damp and superheated steams at the different steam exposure periods (S_p , sec) to the steam device operating cost (C, L.E/fed) at the different steam pressures (S_P , bar) are illustrated in Figs. (60 & 61). As well, increasing the forward speed (FV) at the different S_t for the two different kinds of steam damp and superheated respectively decreases the device operating cost (C, L.E/fed) with increasing the treatment of the (S_P) in opposite relationships. The maximum values of (C, L.E/fed) for damp and super-heated steams were (121.70 and 149.76 L.E/fed), respectively at 4 sec of

the S_t (0.72 km/h) for S_p of 3.5 bar, while the lowest values of the (C) for damp and super-heated steams were (43.35 and 53.13 L.E/fed), respectively for of the 1 sec of S_t (1.8 km/h) at S_p of 10 bar.

While, the maximum values of the (C) for damp and super-heated steams were (120.78 and 148.55 L.E/fed) respectively, as shown in Figs. (62&63) for S_t of 4 sec (0.72 km/h) at 20 cm of the steam height from the ground (S_h), where the minimum values of the (C) for damp and super-heated steams were (43.56 and 53.35 L.E/fed), respectively for the 1 sec S_t (1.8 km/h) at 10 cm of S_h .

These results due to by increasing the forward speeds the operating costs decreased because of using high forward speeds is economic to save the lasted times so the operating costs decreased. However operating steam device with the super-heated steam is more expensive than using the damp steam but its more efficient. Statically there are high significant effects for the total interaction between different treatments with ($P < 0.05$) for the C values respectively. Also ANOVA analysis indicated highly significant differences between the treatments. A simple power regression analysis applied to relate the change in (C) for damp and superheated steams with the change in the tested factors for all treatments. The obtained regression equations were in the form of:

	Damp steam	Super-heated steam
C, L.E/fed	$18.425 + 25.519 S_t - 0.294 S_P + 0.061 S_h$ $R^2=0.9999$ C.V=0.175	$25.406 + 31.273 S_t - 0.398 S_P + 0.0835 S_h$ $R^2=0.9999$ C.V=0.157

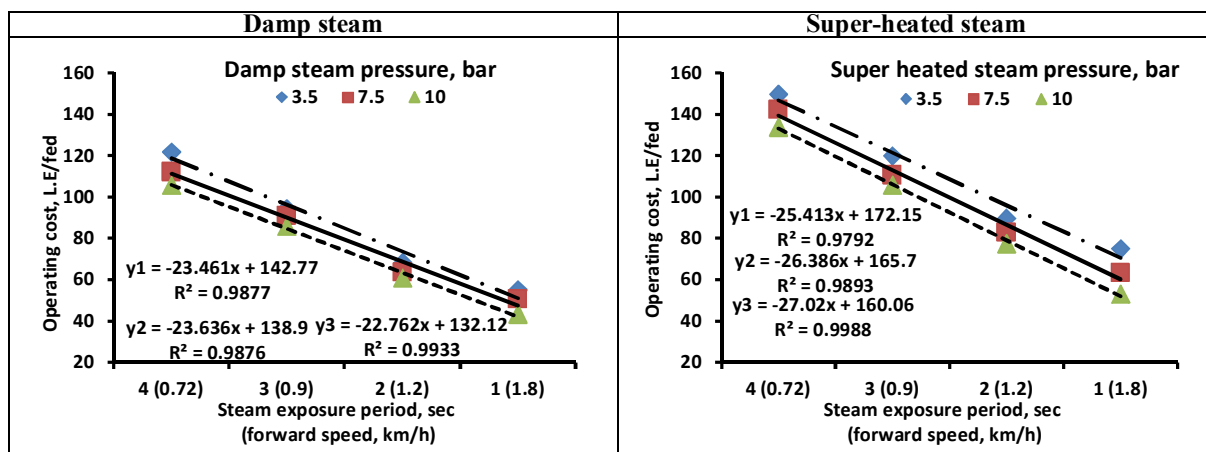


Fig. 60: Effect of damp steam exposure periods (forward speeds) on the operating cost at the different steam pressures.

Fig. 61: Effect of super-heated steam exposure periods (forward speeds) on the operating cost at the different steam pressures.

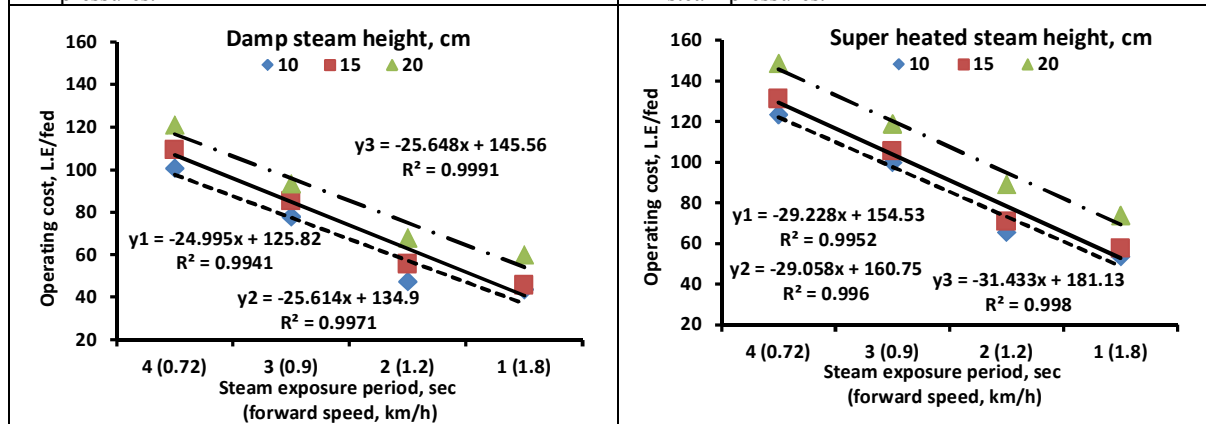


Fig. 62: Effect of damp steam exposure periods (forward speeds) on the operating cost at the different steam heights.

Fig. 63: Effect of super-heated steam exposure periods (forward speeds) on the operating cost at the different steam heights.

The total fabrication cost of the steam device including workshop manufacturing and attaching devices costs was about 8000 LE at 2017 price level. The steam device can decrease the costs of weed control from (1500 to 150 L.E/fed) as about 90.0 % cost reduction ratio. The internal rate of return (IRR) after considering depreciation, alternative chance costs, the amount costs of fuel and lubricants, and the rental rate calculated found (25 to 30 L.E/h). The internal rate of return (IRR) with release year was calculated found 36%. This rate is visible compared with the current interest rate of 17% due to the capital return which was about 3 years. An economic analysis had been done to evaluate the new technique of control weeds in comparison for using the usual control methods to eliminate weeds from mechanical methods like hoeing and chemical control using herbicides. The yield production cost of beta vagaries crop by using the steam device was calculated to the control and the total spending to the net earn was as the following table:

Table.7: The steam device assumed cost criteria

System	Control	Damp steam	Superheated steam
Yield production (ton/fed)	12	17.45	17.95
Yield cost (L.E/fed)	3840	5584	5744
Weed control cost (L.E/fed)	1500	120	150
Soil preparation cost (L.E/fed)	350	350	350
Planting cost (L.E/fed)	250	250	250
Irrigating cost (L.E/fed)	300	300	300
Labor cost (L.E/fed)	250	250	250
Net earn (L.E/fed)	1190	4314	4444
Increasing ratios using device %		72.42 %	73.22 %

CONCLUSION

The main results are summarized as follow:

- 1- The maximum values of weed extermination ratios after treatment, after 2 days and 3 days (EX.R 1,2&3) for damp and super-heated steams were {(91.89, 94.0, and 95.84) & (93.69, 95.94 and 97.74) %}, respectively at 4 sec of steam exposure period (S_t) (forward speed, 0.72 km/h) for steam pressure (S_p) of 10 bar at steam height from the ground (S_h) 10 cm.
- 2- The maximum values of chlorophyll percentages after treatment, after 2 days and 3 days (Ch 1,2&3) for damp and super-heated steams were {(74.68, 43.92 and 19.38) & (59.55, 29.24 and 13.52) %}, respectively at 4 sec of steam exposure period (S_t) (forward speed, 0.72 km/h) for steam pressure (S_p) of 10 bar at steam height from the ground (S_h) 10 cm.
- 3- The maximum values of weeds re-growth ratios after week, after 2 weeks and 3 weeks (Gr 1, 2&3) for damp and super-heated steams were {(24.87, 26.88 and 28.77) & (20.90, 22.63 and 24.82) %}, respectively at 1 sec of steam exposure period (S_t) (forward speed, 1.8 km/h) for steam pressure (S_p) of 3.5 bar at steam height from the ground (S_h) 20 cm.
- 4- The maximum values of yield increasing ratios (Y%) over control for damp and super-heated steams were (45.41 and 49.57 %), respectively at 4 sec of steam exposure period (S_t) (forward speed, 0.72 km/h) for steam pressure (S_p) of 10 bar at steam height from the ground (S_h) 10 cm.
- 5- The maximum values of steam device field efficiency (F_e , %) for damp and super-heated steams were (96.11 and 94.12 %), respectively at 1 sec of the S_t (1.8 km/h) for S_p of 10 bar at (S_h) 10 cm.
- 6- The maximum values of steam device field capacity (FC, fed/h) for damp and super-heated steams were (0.61 and 0.59 fed/h), respectively at 1 sec of the S_t (1.8 km/h) for S_p of 10 bar at (S_h) 10 cm.

- 7- The maximum values of fuel consumption (F, lit/h) for damp and super-heated steams were (1.61 and 1.87 lit/h), respectively at 1 sec of the S_t (1.8 km/h) for SP of 10 bar at (S_h) 10 cm.
- 8- The maximum values of steam device consumed energy (CE, kW.h/fed) for damp and super-heated steams were (4.83 and 6.63Kw.h/fed), respectively at 4 sec of the S_t (0.72 km/h) for S_p of 10 bar at (S_h) 10 cm.
- 9- The maximum values of steam device operating costs (C, L.E/fed) for damp and super-heated steams were (121.70 and 149.76 L.E/fed), respectively at 4 sec of the S_t (0.72 km/h) for S_p of 3.5 bar at (S_h) 20 cm.

REFERENCES

- 1) Ascard. J, (1998) Comparison of flaming and infrared radiation techniques for thermal weed control .Weed Research 38,; 69-76.
- 2) Awady, M. N.; E.Y. Ghoniem and A. I. Hashish (1982). A critical comparison between wheat combine harvesters under Egyptian conditions. Res. Bul. 1920, Fac. of Agric. Ain Shams Univ.: 13.
- 3) Banks. J and G. Sandral (2007) "report on weed control using hot water / steam and herbicides in the city of Joondalup, Scientific article PP.1-13. Available at www.joondalup.wa.gov.au/files/.
- 4) CESNA. J., A. SIRVYDAS, P. KERPAUSKAS and R. VASINAUSKIENE (2000) Investigation of thermal weed control in high-temperature media. Environmental Engineering. VIII, Nr 1,; 28-35.
- 5) Collins. M, (1994)" THERMAL WEED CONTROL, A TECHNOLOGY WITH A FUTURE?" Twelfth Australian Weeds Conference17, :s25-28.
- 6) Debeljak M., G. R. Squire, D. Demšar, M. W. Young and S. Džeroski (2008) Relations between the oilseed rape volunteer seedbank, and soil factors, weed functional groups and geographical location in the UK. Ecological Modelling, 212, : 138–146.
- 7) Edgar, R. (2000). Evaluation of infrared treatments for managing roadside vegetation. Final report. SPR 376. Oregon Dept. Transportation, Salem, Ore.
- 8) Kepner, R. A.; R. Bainer and E.L. Barger (1982). Principles of farm machinery. 3rd ed. avi pub Co. West part, Connecticut. USA. : 464 – 468.
- 9) Kerpauskas, P., A. Sirvydas, P. Lazauskas, R. Vasinauskienė and A. Tamošiūnas (2006). Possibilities of weed control by water steam. Agronomy Research, 4 (Special issue), : 222–225.
- 10) Kolberg, R.L. and L.J. Wiles. (2002) "Effect of steam application on cropland weeds". Weed Tech. 16(1):43-49.
- 11) Kruidhof, H.M., L. Bastiaans, and M.J. Kopf (2008) Ecological weed management by cover cropping: effects on weed growth in autumn and weed establishment in spring. Weed Research 48, 492–502.
- 12) KURFESS. W and S. KLEISINGER (2000) Effect of hot water on weeds. (in German with English summary).Proceedings 20th German conference on weed biology and weed control. Stuttgart, Hohenheim, Germany, 14 -16 March, 2000, Zeitschrift für Pflanzenkrankheiten, Pflanzenschutz 17, :473-477.
- 13) Kurt , G. (1979). Engineering formulas. Third Ed. McGraw - Hill book Company. New York St. Louis San Francisco Montreal – Toront.
- 14) Obradovic, A., A. Datta, R. Wilson and S.Z. Knezevic (2011) Economic Analysis of Various Weed Control Treatments in Corn, Soybean, and Sunflower. Proceedings of 66th

- Annual Meeting of the North Central Weed Science Society: 10. Milwaukee, Wisconsin, USA.
- 15) Oida, A. (1997). Using personal computer for agricultural machinery management. Kyoto University. Japan. JICA publishing.
 - 16) Pekarskas, J., A. Raškauskienė, J. Sinkevičienė and V. Genys (2012) Ekologiškų žeminių rūšių auginimas ekologinės gamybos ūkyje be ariminių žemdirbystės būdu. Žmogaus ir gamtos sauga: 18-osios tarptautinės mokslinės-praktinės konferencijos medžiaga. : 75–78.
 - 17) Praczyk, T. (2005) Zwalczenie chwastów. Rozdział w: Technologia produkcji rzepaku. Wydawnictwo Wieś Jutra, Warszawa, : 97–107.
 - 18) Rasmussen, J. and J. Ascecard (1995) Weed control in organic farming systems. In: Ecology and integrated Farming Systems // IACR-Long Ashton Research Station. Bristol (UK): John Wiley Sons Ltd, : 49–67.
 - 19) Sirvydas A. P. and J. Cesna (2000) Energy processes modeling in weed tissues and weed control. Agricultural engineering, Research papers 32, Raudondvaris, : 53-72.
 - 20) Sirvydas. A, P. Lazauskas, R. Vasinauskienė, and P. Kerpauskas (2002) "Thermal weed control by water steam" 5th EWRS Workshop on Physical Weed Control 253 Pisa, Italy, : 2553-262.
 - 21) Yager, L. (2004) Landa® hot water pressure washer. The Invasive Species Initiative. The Nature Conservancy. Accessed at <http://mcweeds.ucdavis.edu/tools/hotsteam.html>.

تطوير جهاز لمقاومة الحشائش باستخدام بخار الماء

أحمد شوقي السيد السيد^١ و جلال محمد عبدالحميد^٢

١ . معهد بحوث الهندسة الزراعية – مركز البحوث الزراعية – مصر.

٢ . المعمل المركزي لبحوث الحشائش – مركز البحوث الزراعية – مصر.

يهدف هذا البحث إلى استحداث وتقييم نظام صديق للبيئة لمكافحة الحشائش بالبخار يتوافق مع الزراعة النظيفة بدون استخدام المبيدات الكيماوية الضارة وكذلك تقليل تكاليف مكافحة الحشائش للحد الأدنى. لذلك تم ابتكار جهاز لمكافحة الحشائش بالبخار لتوليد نوعين من البخار تحت ضغط النوع الأول بخار ماء رطب تصل درجة حرارته إلي ١٨٤ درجة سيليزيوس والنوع الثاني بخار محمص تصل درجة حرارته إلي ٤٣٤ درجة سيليزيوس وذلك باستخدام غلاية بخارية تعمل بمولد كهربائي صديق للبيئة تم استخدامه كمصدر للطاقة الكهربائية لتسخين المياه بها وتوليد بخار تحت ضغط يصل الي ١٠ بار حيث تم تزويد الغلاية بمانومتر لقياس ضغط البخار بالإضافة الي تسخين البخار الرطب الخارج منها تحت ضغط باستخدام وحدة تسخين خارجية مزودة بسخان أفقي وثرموستات هوائية لتقوم بتحميص البخار الرطب الخارج من الغلاية وذلك لتفجير محتوى السيتوبلازم لخلايا الحشائش حاليا بمجرد تعرضها لمستويات البخار تحت ضغط. حيث تم التحكم أوتوماتيكيا في زمن المعاملة بالبخار بواسطة جهاز إلكتروني ملحق يحتوي علي تايمر ديجيتال ثنائي الأزمنة متصل بسولونيد كهربائي للتحكم في معدل تدفق البخار وريوستات ضغط لضبط ضغط البخار أليا مع حالة الحشائش الموجودة . حيث تم تصنيع شاسيه مناسب ذاتي الحركة متعدد مستويات الضبط من إمكانية ضبط ارتفاعه عن سطح الأرض وعرض التشغيل بين الخطوط وسرعته الأمامية واتجاهها ليتحرك بسلاسة خلال صفوف المحاصيل المزروعة حيث تم عزل خطوط رش البخار بطبقة من الجلد الحراري والصوف الزجاجي وذلك لحماية النباتات المزروعة من تسرب البخار أثناء المعاملة .

تم اجراء تجربتين حقليتين منفردتين لدراسة نوعي البخار المتولدين والمقارنة بينهما (البخار الرطب والبخار المحمص) تحت مستويات عوامل الدراسة الآتية: ١- أربعة مستويات من زمن التعرض للبخار (١، ٢، ٣، ٤ ثانية) وذلك عند أربعة سرعات أمامية لجهاز البخار (٨، ١، ٢، ٩، ٠، ٧٢، ٠، ٧٢ كم/الساعة) ٢- ثلاثة مستويات من ضغط البخار (٥، ٣، ٧، ١٠ بار) ٣- ثلاثة ارتفاعات للبخار عن سطح الارض (١٠، ١٥، ٢٠ سم) وذلك لدراسة القياسات التالية: أولا علي الحشائش والمحصول من نسبة الإيابة للحشائش بعد المعاملة ولمدة ثلاثة أيام وكذلك نسبة استعادة الحشائش بعد المعاملة لمدة ثلاثة أسابيع ونسبة مستوي الكلوروفيل بعد المعاملة ولمدة ثلاثة أيام وغلة المحصول ثانيا قياسات علي الجهاز من قياس السعة والكفاءة الحقلية واحتياجات الطاقة ثالثا حساب التكاليف الاقتصادية في مقابل استخدام طرق مكافحة الكيماوية وعلي زيادة غلة المحصول.

واشتملت أهم النتائج علي التالي علي قدرة البخار سواء الرطب أو المحمص لمقاومة الحشائش النامية في المحاصيل المنزرعة علي خطوط تعتبر فعالة وأمنة وصديقة للبيئة بالمقارنة بالطرق المكافحة التقليدية الأخرى سواء الميكانيكية أو الكيماوية. حيث كانت أعلى نسبة إيابة للحشائش في محصول البنجر باستخدام جهاز البخار كانت ٩٥،٨٤ و ٩٧،٧٤ % لنوعي البخار الرطب والمحمص علي الترتيب، كذلك انخفضت نسبة الكلوروفيل بعد ٣ أيام من المعاملة لتصل الي ١٩،٣٨ و ١٣،٥٢ % لنوعي البخار عند استخدام زمن تعرض للبخار ٤ ثواني عند ضغط ١٠ بار وارتفاع للبخار ١٠ سم عن سطح الارض بينما كانت السرعة الامامية لجهاز البخار ٠،٧٢ كم/ الساعة. كذلك كانت قدرة البخار المحمص تحت ضغط لمكافحة الحشائش قللت من معدل انبثاقها لتقل هذه النسبة الي ٢٤،٨٢ % فقط وذلك بعد مرور ٣ أسابيع من المعاملة. إن تقنية مكافحة الحشائش الجديدة بالبخار قللت من التكلفة الاقتصادية لمستويات منخفضة ١٤٩،٧٦ جنيه/الفدان تضمنت استهلاك الوقود وتكلفة التزييت وأجر العامل بدلا من نظم مكافحة الكيماوية الغالية نتيجة لاستخدام الماء فقط. حقق الجهاز الجديد لمكافحة الحشائش بالبخار مستويات مناسبة من السعة والكفاءة الحقلية من انجاز ٠،٦١ فدان/ الساعة بمستوي كفاءة حقلية ٩٦،١١ % . بينما كانت معدلات استهلاك الطاقة مناسبة حيث وصلت أقصاها من ٤،٨٣ إلي ٦،٦٣ كيلووات ساعة/الفدان. لذلك ان استخدام الجهاز الجديد لمكافحة الحشائش يناسب المتطلبات الحالية لظروف الزراعة المصرية والاتجاهات العالمية الحالية للزراعة النظيفة.

DEVELOPMENT OF MACHINE TO REMOVE AQUATIC WOVEN "*GIANT REED*" IN FRESH WATER LAKES

REFAAY, M. M. * and A. S. EL_SAYED

*

*Agric. Eng. Res. Institute, ARC, Egypt

Abstract

Scientifically cutting woven under water surface let water penetrates its stalks down into their root that rots the woven weeds and this action eliminates woven successfully. A special front mower with adequate operating width of 1.20 m was modified and hinged on a floating boat to cut the woven under the water and gathering it beside the boat to use it in the different industries. The cutting knives of the mower were galvanized to wear oxidization due to the water. However a special mechanical holding mechanism was fabricated locally to attach the mower on the boat and control its height and depth under the water by a screw crane. The source of power which rotates the mower was 13 hp gasoline engine fixed on the boat surface. The plunger depth of the boat and the different loads through operating the mower was calculated to keep the operational stability under high percentage from the safety factor. The aquatic experiments were carried out to study the interaction and the suitable adapting for the following variables: first; three levels of the speed ratios between the mower knife linear speed and the forward speeds of the boat of (0.66, 0.67 and 0.68) at forward seeds of (1, 1.5 and 2 km/h); second: three levels of the mower operating widths of (0.6, 0.9 and 1.2 m) third; three levels from water depths of (0 level on the water surface, 0.25 and 0.50 m under the water). The measurements included the following the mowing efficiency, the machine efficiency, the field capacity, the fuel consumption, the mowing regrowth's ratio after 1 month, the consumed energy and the operating costs. The main results included that the mowing efficiency reached high levels of 94.31 % at field capacity of 0.27 fed/h at machine efficiency of 94.95% at the highest speed ratio of 0.68 for operating width 1.2 m and operating depth of 0.5 m. However the minimum consumed energy was 32.94 kW.h/fed at the maximum levels of the tested variables. The minimum operating cost of mowing the giant reed was 110.59 L.E/fed which is lower than any traditional control methods. So using this control system for giant reed seems to solve an important problem which needs to be published at the local levels through the Egyptian costal governorates.

Key words: *mower, giant reed, re-growth, aquatic.*

INTRODUCTION

Giant reed, (*Arundo donax*), is a plant that has long been valued by many and, more recently, despised by others. The dense thickets dry out and remain standing in the winter, creating a fire hazard. Even when green, giant reed thickets are fire-prone. Mechanical control (e.g., digging up the roots and/or repeated mowing) may be somewhat effective. Prescribed burning, either alone or combined with herbicide applications, may be effective if conducted after flowering but if small fragments of root are left in the soil, they may regrow. Once giant reed thickets have been reduced sufficiently, native plants may be seeded or transplanted at the treated site.

Giant reed (*Arundo donax*L.) is currently one of the greatest invasive threats to river ecosystems in Mediterranean-type climate regions worldwide (Coffman, 2007). Control of aquatic weeds can be subdivided into four general categories: (1) prevention, (2) mechanical and physical, (3) biological, and (4) herbicides. Often a combination of these practices is necessary for adequate control. Various types of weed harvesters have been used, including a cutting device on a floating barge. As the weeds are cut, they are brought up on a conveyor and deposited on the barge. Devices

such as these are expensive and disposal of the wet, heavy plant material is a problem. Generally (Wells & Clayton 2005) they mentioned that mechanical digger have most value in artificial canals and areas that are shallow and close enough to lake shorelines to allow access for a digger. Costs can vary, depending on the width of canals and extent of weed infestation. From disadvantages of this method include removal of large amounts of benthic fauna and fish, particularly eels, and causing high turbidity and sometimes anoxia. In addition, machines widen and deepen drains, which may encourage weed growth. They may also spread weeds from one waterway to another. However (Clayton *et al.*, 2000) evaluated the mechanical weed cutters and stated that these can target a specified area and cut to a nominated depth. This can also have the benefit of removing nutrients from the waterway. Weed cutting and disposal is priced at \$2,000–4,000 per hectare, although costs can vary considerably, depending on the density of aquatic weeds and the distance to a disposal site. A disadvantage is the quick re-growth to nuisance levels, because cutting stimulates the plant to re-grow. Cutting may have to be repeated two or three times in a growing season. A further disadvantage is the potential spread of aquatic weeds, even when fragments are collected and bagged, as some viable plant fragments inevitably escape. Also (Tremblay 2004) evaluated both biological and chemical control methods for giant reed and stated that the biological control agents available, the Grass Carp *Ctynopharyngodon idella* (Valenciennes) is most widely used as an aquatic weed control agent. It feeds on a range of submerged and floating weeds, but prefers soft plant tissues. However use of herbicides is easier and cheaper, when compared to mechanical methods, and many are harmless to aquatic organisms at concentrations required for aquatic weed control. The main disadvantage is that a chemical is in water as residue for a period of time. Therefore, not all herbicides can be used in aquatic environments. Besides that (Datta 2009) evaluated the mowing process and tells that this process consists of cutting the weeds close to the ground with the help of manual or power operated mowing machines. Mowing is effective on tall growing plants. Repeated mowing not only prevents seed production of emergent weeds but may also starve the underground parts which store carbohydrate reserves and provides energy to vegetative reproductive organs. The best time to mow is when carbohydrate reserves are low. For many species it is when the active growth phase is over and the time of flowering initiation starts. Repeated mowing hastens carbohydrate depletion and slow death of plants. Generally, this practice effectively controls emergent weeds on canals, water reservoirs etc. banks. Also (Boland 2008) showed that mechanical removal involves collecting and destroying the stems and all below-ground rhizomes, which is labor and machinery intensive. Mechanical removal is prohibitively expensive except on small areas, with costs reaching \$8,100 per acre (Lawson *et al.* 2005).

On the other hand from the researches that benefits from this aquatic weed in some industries as follows; (García-Ortuño *et al.*, 2011) studied the feasibility of using giant reed particles to manufacture particleboard and obtained panels suitable for general use and for furniture manufacturing. This research demonstrated that giant reed can be easily transformed into a low-cost and sustainable material for the manufacturing of containers for the fruit and vegetable industry. Also (Vamvuka and Sfakiotakis, 2011) stated that giant reed particleboard, as a raw material, complies with the requirements of the packaging and packaging waste directive because it is biodegradable and renewable (Ceotto and Di Candilo, 2010).

The aim of this research is to develop a friendly control method for mowing the giant reed weeds aquatically in fresh lakes by innovating a floating cutter mower. The mowed giant reed

gathered by the developed mower laterally on floating grid which connecting with another parallel boat to move it by adequate quantities due to its heavy wetted weight to the shore.

MATERIALS AND METHODS

A developed mechanical control method for mowing the aquatic giant reed was modified locally to remove giant reed from the fresh water lakes in Egypt; specially El-Manzalla Lake; which the experiments were conducted there. A floating mowing mechanical system was developed and hinged in a boat to chop the giant reed stalks under water to eliminate it to let water penetrates its chopped stalks into roots to rot its rhizomes and kills it gradually from May to September before flowering. The developed floating mechanical control unit consisted from the following: as shown in the isometric drawing Fig. (1) and Figs. (2 to 9). The new machine specifications are listed in Table (1).

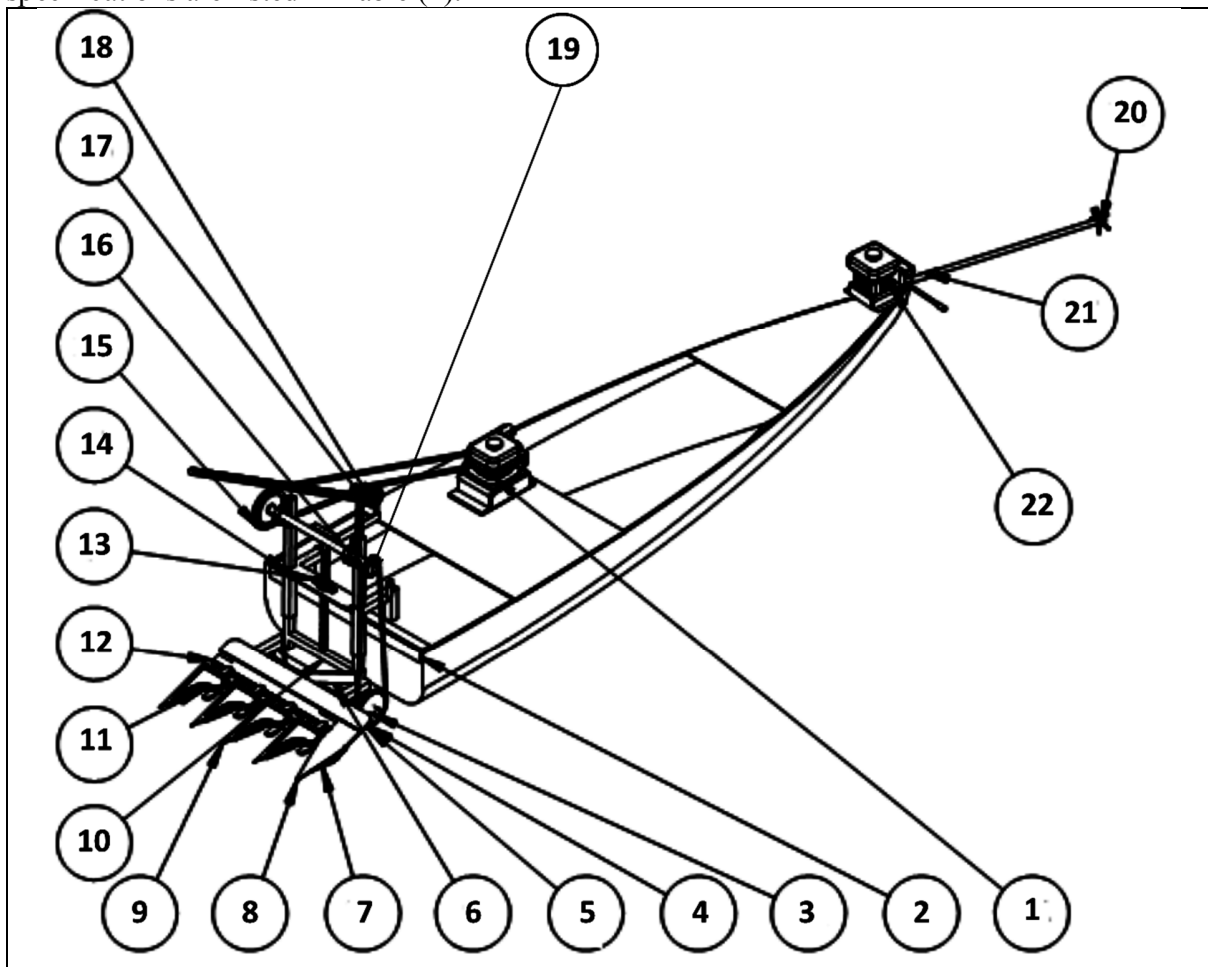


Fig. 1: The isometric drawing of the giant reed mowing system:

(1- mower gasoline motor (13 hp), 2-The boat, 3- the lowest gear (38T) 4- the chain 5- the mower sliding sheet 6- the three hitching points, 7- the mower left guide, 8- the front penetration arm, 9- the mower star roller, 10- the telescopic square pipes, 11- the cutter knife, 12- the moving fingers chain, 13- the crane, 14- the sliding square pipes, 15- the mower power transmitting pulley (13 cm Dia.), 16- the bearing flanges (25 mm Dia.), 17- the belt tension pulley, 18- belt (2050×17 mm), 19- the upper gear (15T), 20- the boat moving fan, 21- the boat propeller shaft and 22- the moving gasoline motor (6.5 hp).

Table.1: The new machine specifications.

1	Power source	13 hp gasoline engine		
2	Forward speed	6.5 hp gasoline engine 1, 1.5 and 2 km/h		
3	Boat dimensions	width	Length	height
		150 cm	5.40 cm	50 cm
4	Mowing Operation width	120 cm		
5	Net weight	280 kg		
6	Machine capacity	630 to 1050 m ² /h		
7	Consumed power	32 to 68 Kw.h/fed		



Fig.2: The aquatic mower operation.



Fig.3: The aquatic mower side view.



Fig.4: The aquatic mower front view.



Fig.5: The aquatic mower through moving.



Fig.6: The boat forward motor.



Fig.7: The mower hitching and transmission system.

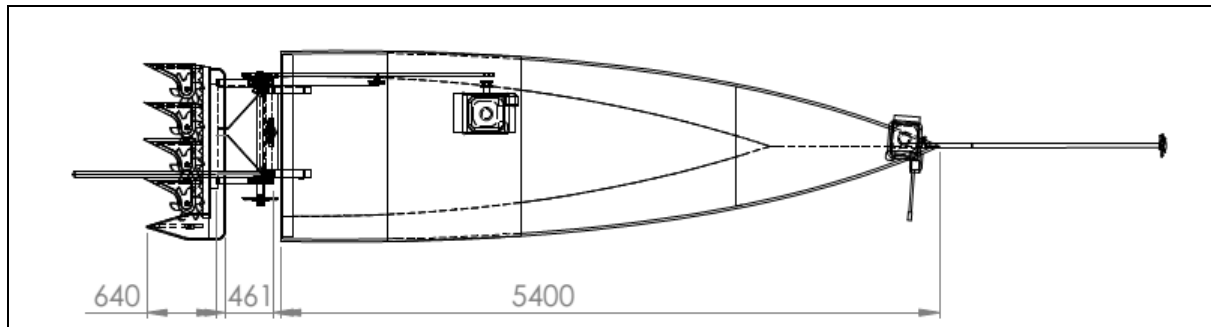


Fig. 8: Plan view of the aquatic mowing system. (Dimensions: mm & Scale:1:11)

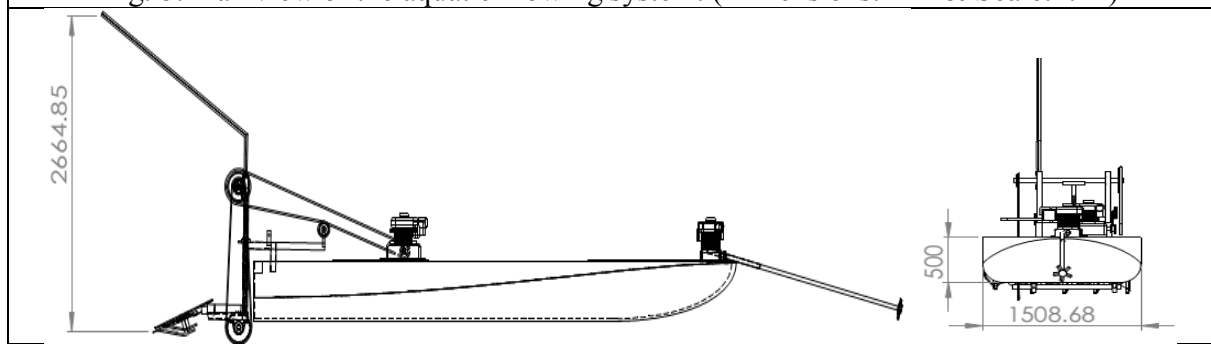


Fig. 9: Side and rear views of the aquatic mowing system. (Dimensions: mm & Scale:1:11)

The aquatic mechanical mowing system parts are, as the following:

A- Power source: two different gasoline motors (13 & 6.5 hp) were used on the boat; the first one was used for operating the aquatic mower. However the second one was used for moving the boat. The gasoline motors Figs (5&6) specifications are listed in Table (2):

Table.2: The gasoline engine specifications.

Motor specifications	Mower motor	Boat Forward motor
1 Power	13 hp (9.694 Kw)	6.5 hp (4.847 Kw)
2 Net weight	31 kg	20 kg
3 Torque	22 N.m	11 N.m
4 Speed	3500 rpm	2000 rpm
5 Model	Kopel (China)	Kopel (China)

B- The Aquatic mower modification: as shown in Fig. (10) The front cutter mower for wheat crop was used and developed to be attached externally on floating wooden boat and settled to be depth control using a manual crane to cut woven at the water surface and under its surface at adequate depths from 1 to 50 cm under water (Fig.11). The modification process achieved through four main steps, as the following:

- 1- **The knife:** was galvanized with nickel chrome to resist wearing.
- 2- **The bearings:** all the used were replaced using fiber wrenches to save the moving flanges.
- 3- **The mower diving parts:** the main parts of the mower were painted with anti-oxidize paint.
- 4- **The mower gearbox:** oil seals were putted at it to save gears from water.

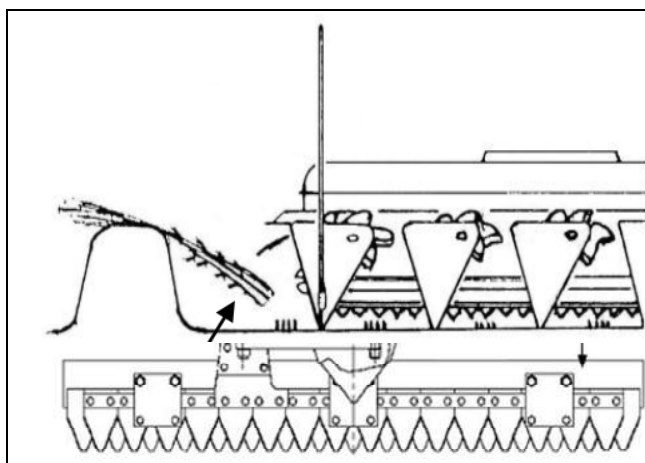


Fig.10: The used mower and its knife.

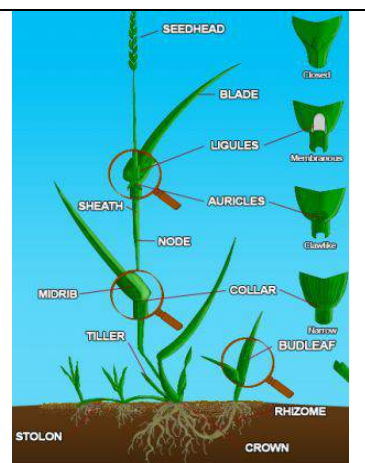


Fig.11: The giant reed parts.

C- The mower chassis: A powerful chassis was manufactured and formed to attach the modified mower on the boat. The chassis was formed to be pivoted to maintain the mower as needed and facilities moving the boat. The chassis formed from the following:

- 1- **The fixing point:** twin of this part was formed to be attached from the external side of the boat which contains 4 bolts with 24 mm Dia, as shown in Fig. (7).
- 2- **The crane:** with dimensions of 75 cm length and 40 mm Dia. with the topes' 50 mm dia. flange with metal solid manual arm which positioned to set the mower height and depth from the water surface. The crane was hinged on two telescopic square metal pipes of (5×5 cm) within (6×6 cm) (Fig. 1, No.14).
- 3- **The three hitching points:** as shown in (Fig. 1, No. 6) which was formed to attach the mower at the perpendicular mode to move the mower parallel to the back surface of the boat to easy penetrate water through the mowing operation.
- 4- **The pivoting system:** as shown in Fig. (7) four flanges were welded at the frame within solid shaft of 50 mm. Dia with length of 50 cm to left the mower through moving. Besides that a manual arm was used to height the mower through moving, as shown in Fig. (5).

D- The transmission system: as shown in Fig.(1) a pulley with 6 cm dia. and 17 mm thickness on the motor shaft was used to transmit the rotating moving to other 13 cm Dia. However an attached manual tension arm with a small pulley tension (6 cm Dia.) was used with the operating belt to connect and disconnect the transmitted power from the motor, as shown in (Fig.1, No. 17). The upper idler shaft with Dia. of 27 mm with length of 70 cm length holding on two bearing flanges of 25 mm Dia which fixed into tensioned paths to control chain tightening. Then 15 teeth of 6 cm Dia. to another gear of 38 teeth of 16 cm Dia. on another lower idler shaft to the inner side 15 teeth gear then to the deferential gear of 18 teeth of 8 cm Dia. The rotating speeds for the aquatic mower are listed in the following table:

Table. 3: The transmission system speeds.

Mower motor Speed (rpm)	Mower pulley 13 cm (rpm)	Idler top gear 15 T (rpm)	Gearbox gear 18 T (rpm)	Knife Crank speed (rpm)	Knife speed (m/sec)
1200	554	219	183	92	0.184
1850	854	337	281	140	0.28
2500	1154	456	380	190	0.38

E- The boat modifying: the external boat surface was supported with 70 cm beam with width of 10 cm with using fiber parts to prevent boat from the vibrations and shocks. However the boat was driven externally using rear steering system by using 6.5 hp gasoline motor to push the

boat at the forward speed levels. Also the driving gasoline motor with 13 hp (30 kg) was fixed accountably at the center of gravity of the boat to equalize the load of the mower weight of 80 kg (30+80=110 kg) however the front of the boat stands the operator weight of 90 kg and 20 kg (90+20= 110 kg).

The floating mower operation:

Reciprocating reaping method is suited to right angled quadrilateral long and narrow zones, as shown in Fig. (12). However reaping method of left turn is the aquatic standard operation method, as shown in Fig. (13). Then the shopped giant reed gathered laterally on floating grid connected to another boat to move it to the shore.

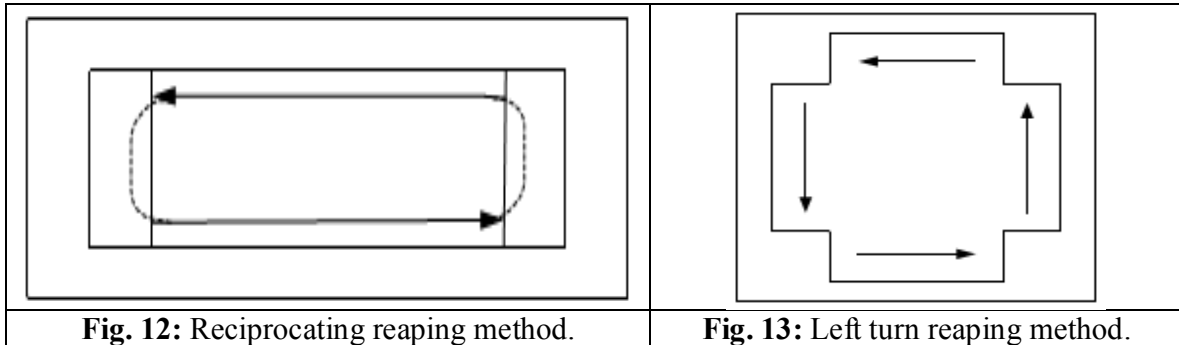


Fig. 12: Reciprocating reaping method.

Fig. 13: Left turn reaping method.

The tested variables:

Three different variables and their levels were chosen and tested aquatically in the El-Manzalla Lake. The experiments were replicated three times. The data were statistically analyzed to determine the significant effect of the mentioned variables under the study according to the probability (P < 0.05) by the CoStat Program (Oida, 1997). The tested factors were, as the following:

A- The speed ratio (Sr): three levels were used (0.66, 0.67 and 0.68) (1:1.52, 1: 1.5 and 1: 1.47) between the oscillating speeds of the mower knife of (0.184, 0.28 and 0.38 m/sec) to the forward speeds of (0.28, 0.42 and 1.47 m/sec or 1, 1.5 and 2 km/h). The knife speed was calculated from the following equation:

$$\{V_k = S n / 30\} \dots \dots \dots (1)$$

Where (V_k: the knife speed m/sec, S: length of knife stroke m, n: crank speed rpm).

B- The operating width (W): three levels of it as (0.6, 0.9 and 1.2 m) by adapting the operating width.

C- The operating depth (D): three levels of it as (0.0 water surface, 0.25 and 0.5 m under water) by adapting the operating depth from the manual lifting crane of the mower.

Measurements:

1- The cutting efficiency (Cη)%: it calculated from the following equation:

$$\{C\eta = W1 - W2 / W1 \times 100\} \dots \dots \dots (2)$$

Where: Cη: the cutting efficiency, %, W1: number of plants before cutting, W2: number of plants after cutting.

The number of giant reed stalks by unit area was observed by average 35 stalks/m².

2- The machine efficiency (Mη) %: It was measured according to Kepner *et al.* (1982).

$$M\eta = \frac{T_{th}}{T_{ac}} \times 100 \dots \dots \dots (3)$$

Where: Mη : machine efficiency, %, T_{th} : theoretical time per m², h T_{ac} : the actual operating time, h.

3- The field capacity (FC) fed/h: was calculated as follows:

$$FC = \frac{S \times W \times Fe}{4.2}, \text{ fed/h.} \dots\dots\dots (4)$$

Where: **F.C:** the field capacity, fed/h, **S:** speed of travel, Km/h, **W:** rated width of implement, m, and **Fe:** field efficiency, %.

4- The fuel consumption (F), lit/h:

Fuel consumption was determined by measuring the volume of fuel consumed during the operation time for each run and calculated in liter per hour. It was measured by completely filling the fuel tank then before each end run and refilling the fuel tank using a scaled container. The fuel consumption rate was calculated from the following equation:

$$F = \frac{V}{T} \quad L / h \dots\dots\dots (5)$$

Where: **F:** rate of fuel consumption, L/h, **V:** rate of consumed fuel, L ; **T:** time, h

5- The machine consumed energy (CE), kW.h/fed: It was estimated by using the following equation: **(Hunt, 1983)**

$$CE = \left(\frac{Fs \times \rho_f \times C.V}{3600} \right) \times \left(\frac{427 \times \eta_{th} \times \eta_m}{75 \times 1.36 \times FC} \right) (kW .h / fed) \dots\dots\dots (6)$$

Where: **CE:** machine requirements, (kW.h/fed);
F_s: fuel consumption rate, (L/h);
ρ_f: density of fuel, kg/L, (for diesel = 0.85 kg/L);
C.V: calorific value of fuel, (Kcal/kg);
427: thermal-mechanical equivalent, (kg.m/Kcal);
η_{th}: thermal efficiency of the engine, assumed 40 % for diesel engine;
η_m: mechanical efficiency to engine, assumed 80 % for diesel engine;
F_c: actual field capacity, m²/h.

6- The cost estimation (C), L.E/h: The operating cost was determined using the following formula:

$$\text{Operating cost}(L.E / fed) = \frac{\text{Machine hourly cost}(L.E / h)}{\text{Actual machine capacity}(fed / h)} \dots\dots\dots (7)$$

The labor cost was estimated actually according to the currently labors wage which was about 30 L.E/fed includes fuel consumption, lubrication costs and maintenance costs.

7- Giant reed re-growth ratio, (GR) %: For mowing giant reed after period of one month. It was calculated by the following equation:-

$$GR = \frac{\text{n.of germinated giant reed, stalk}}{\text{n.of giant reed stalks after mowing, stalk}} \times 100 \dots\dots\dots (8)$$

RESULTS AND DISCUSSION

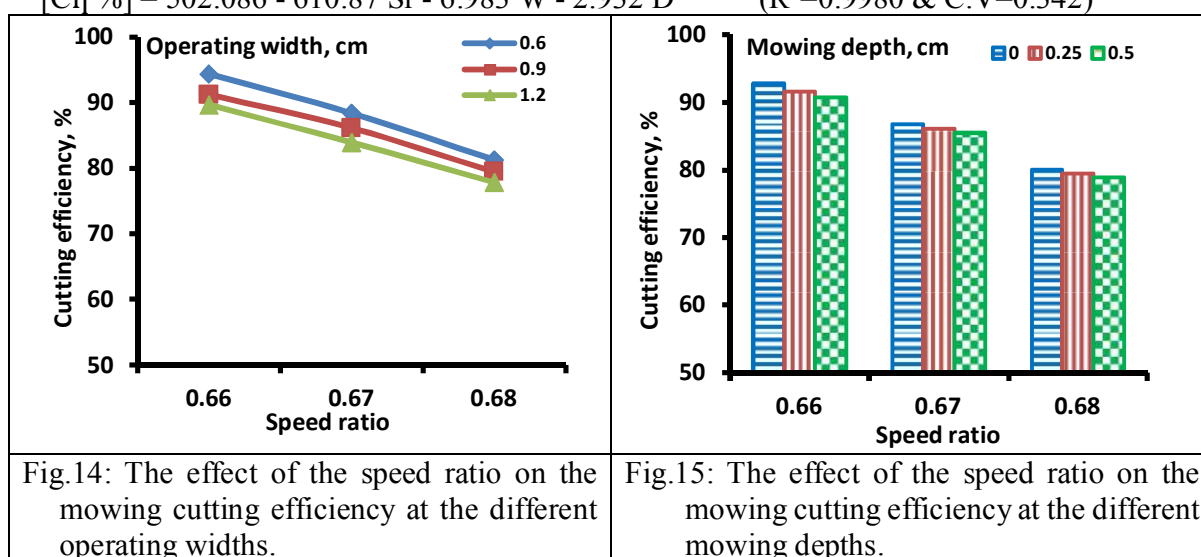
1- Factors affecting mowing cutting efficiency, C_η%:

The relationships affecting the mowing cutting efficiency (C_η, %) to the different speed ratios (Sr) at the different operating widths (W, m) and depths (D, m) are illustrated in Figs. (14 & 15). Generally, increasing the speed ratio (Sr) decreases the mowing cutting efficiency (C_η, %) with increasing the treatments of the (W&D) in opposite relationships. The maximum value of (C_η, %) was (94.31 %) at Sr (0.66) for W of 0.6 m, while the lowest value of the (C_η, %) was (77.82 %) for 0.68 of Sr at W of 1.2 m, as shown in Fig. (14).

On the contrary, the maximum value of the ($C\eta$, %) was (92.77 %), as shown in Fig. (15) for Sr of 0.68 at 0 m of the water surface (D), where the minimum value of the ($C\eta$, %) was (78.93 %) for 0.68 of Sr at 0.5 m of D.

These results may be attributed to by increasing the speed ratios between the knife oscillating and the forward speeds decreases the available time for mowing the giant reed which decreases relatively the cutting efficiency. However adapting the mower at narrow operating width improves the cutting efficiency and vice versa at the operating depths because at the deepest one the stalks of the giant reed becomes weakest than its top parts which minimizes the cutting efficiency for the deepest mowing depth. Statically there are high significant effects for the total interaction between different treatments with ($P < 0.05$) for the $C\eta$ values. Too ANOVA analysis indicated highly significant differences between the treatments. A simple power regression analysis applied to relate the change in ($C\eta$) with the change in the tested factors for all treatments. The obtained regression equation was in the form of:

$$[C\eta \text{ \%}] = 502.086 - 610.87 Sr - 6.983 W - 2.932 D \quad (R^2=0.9980 \ \& \ C.V=0.342)$$



2- Factors affecting the machine efficiency $M\eta$ %:

Figs. (16 & 17) are illustrated the relationships affecting the machine efficiency ($M\eta$, %) to the different speed ratios (Sr) at the different operating widths (W, m) and depths (D, m). Obviously, increasing the speed ratio (Sr) increases the machine efficiency ($M\eta$, %) with increasing the treatments of the (W&D) in direct relationships. The maximum value of ($M\eta$, %) was (94.95 %) at Sr (0.68) for W of 1.2 m, when the lowest value of the ($M\eta$, %) was (75.70 %) for Sr of 0.66 at 0.6 m of W, as shown in Fig. (16).

During, the maximum value of the ($M\eta$, %) was (94.02 %), as shown in Fig. (17) for Sr of 0.68 at 0.5 m of D, where the minimum value of the ($M\eta$, %) was (77.25 %) for 0.66 of Sr at 0.0 m of D.

These results may be owing to by increasing the speed ratios the consumed time decreases which maximizing the machine field efficiency at the lowest depth and the maximum operating width too. Statically there are high significant effects for the total interaction between different treatments with ($P < 0.05$) for the $M\eta$ values. Also ANOVA analysis indicated highly significant differences between the treatments. A simple power regression analysis applied to relate the change in ($M\eta$) with the change in the tested factors for all treatments. The obtained regression equation was in the form of:

$$[M\eta \text{ \%}] = -430.025 + 759.463 Sr + 7.31 W + 3.0 D \quad (R^2=0.9985 \ \& \ C.V=0.362)$$

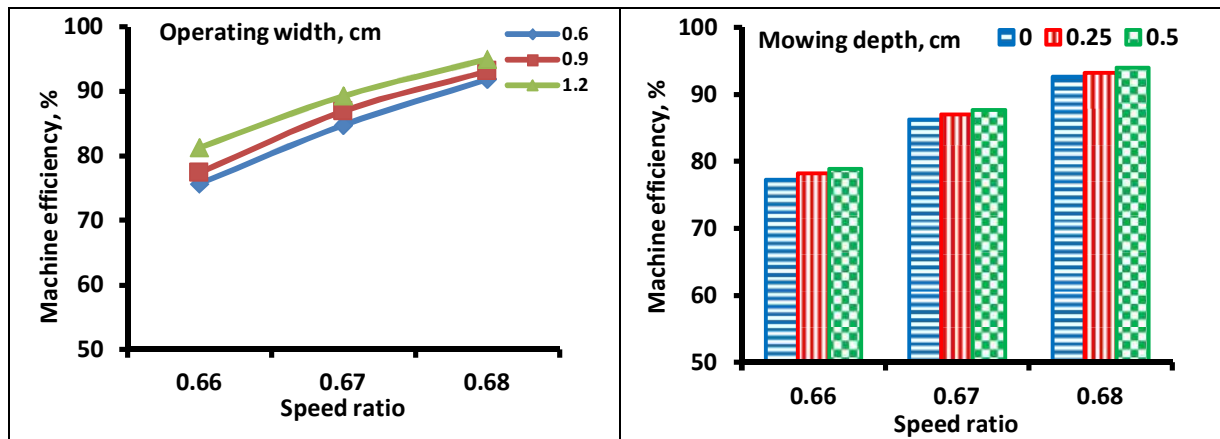


Fig.16: The effect of the speed ratio on the machine efficiency at the different operating widths.

Fig.17: The effect of the speed ratio on the machine efficiency at the different mowing depths.

3- Factors affecting the machine field capacity FC, fed/h:

Nerveless the relationships affecting the machine field capacity (FC, fed/h) to the different speed ratios (Sr) at the different operating widths (W, m) and depths (D, m) are illustrated in Figs. (18 & 19). In that manner, increasing the speed ratio (Sr) increases the machine field capacity (FC) with increasing the treatments of the (W&D) in direct relationships. The maximum value of (FC) was (0.27 fed/h) at Sr (0.68) for W of 1.2 m, while the lowest value of the (FC, fed/h) was (0.11 fed/h) for Sr of 0.66 at 0.6 m of W, as shown in Fig. (18).

Too the maximum value of the (FC) was (0.20 fed/h), for Sr of 0.68 at 0.5 m of D, where the minimum value of the (FC) was (0.17 fed/h) for 0.66 of Sr at 0.0 m of D, as shown in Fig. (19).

These results may be ascribable by increasing the speed ratios the mowing area increases which enlarging the field capacity at the tested variable levels. Statically there are high significant effects for the total interaction between different treatments with (P < 0.05) for the FC values. Thus ANOVA analysis indicated highly significant differences between the treatments. A simple power regression analysis applied to relate the change in (FC) with the change in the tested factors for all treatments. The obtained regression equation was in the form of:

$$[FC, \text{ fed/h}] = -1.085 + 1.596 Sr + 0.22 W + 0.0069 D \quad (R^2=0.9998 \ \& \ C.V=0.475)$$

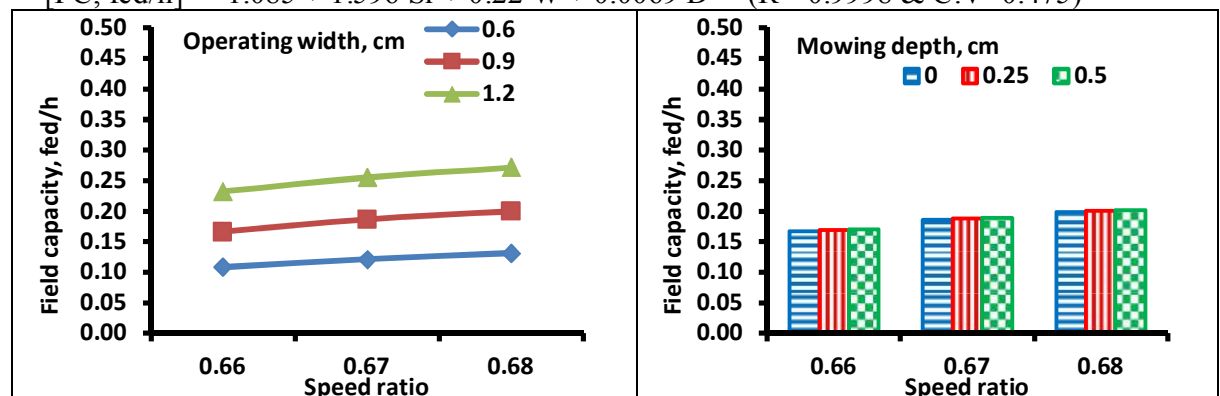


Fig.18: The effect of the speed ratio on the field capacity at the different operating widths.

Fig.19: The effect of the speed ratio on the field capacity at the different mowing depths.

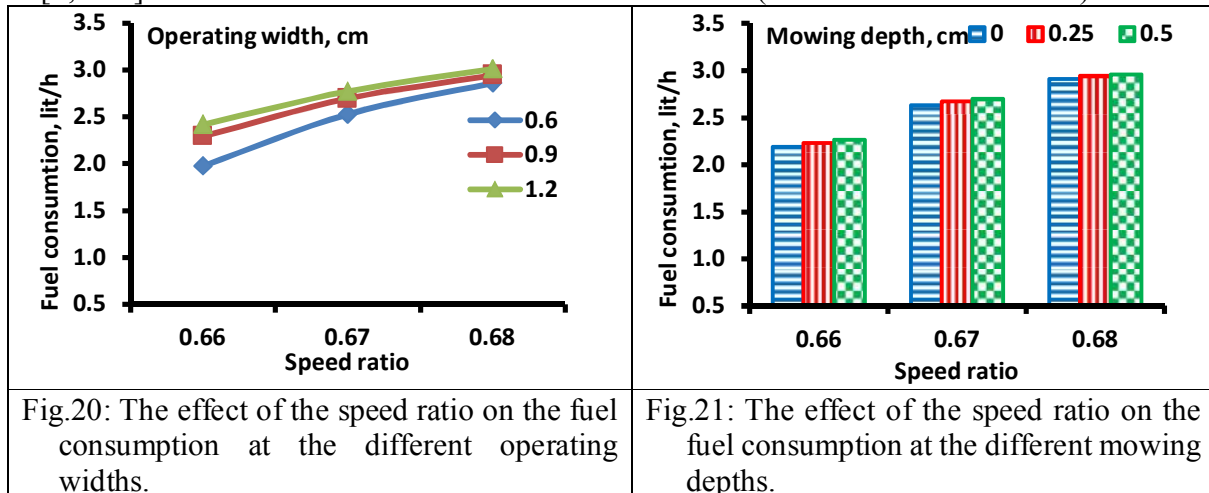
4- Factors affecting the fuel consumption F, lit/h:

Clearly the relationships affecting the machine fuel consumption (F, lit/h) to the different speed ratios (Sr) at the different operating widths (W, m) and depths (D, m) are illustrated in Figs. (20 & 21). Too, increasing the speed ratio (Sr) increases the machine fuel consumption (F) with increasing the treatments of the (W&D) in direct relationships. The maximum value of (F) was (3.01 lit/h) at Sr (0.68) for W of 1.2 m, while the lowest value of the (F, lit/h) was (1.97 lit/h) for Sr of 0.66 at 0.6 m of W, as shown in Fig. (20).

As shown in Fig. (21) the maximum value of the (F) was (2.96 lit/h), for Sr of 0.68 at 0.5 m of D, where the minimum value of the (F) was (2.18 lit/h) for 0.66 of Sr at 0.0 m of D.

These results may in consequence of increasing the speed ratios the gasoline motors consumed more fuel to increases relatively the forward speed and the mowing speed also at the maximum operating width and depth. There are high significant effects for the total interaction between different treatments statically with (P < 0.05) for the F values. As well ANOVA analysis indicated highly significant differences between the treatments. A simple power regression analysis applied to relate the change in (F) with the change in the tested factors for all treatments. The obtained regression equation was in the form of:

$$[F, \text{lit/h}] = -21.631 + 35.5 \text{ Sr} + 0.468 \text{ W} + 0.139 \text{ D} \quad (R^2=0.9943 \ \& \ C.V=1.136)$$



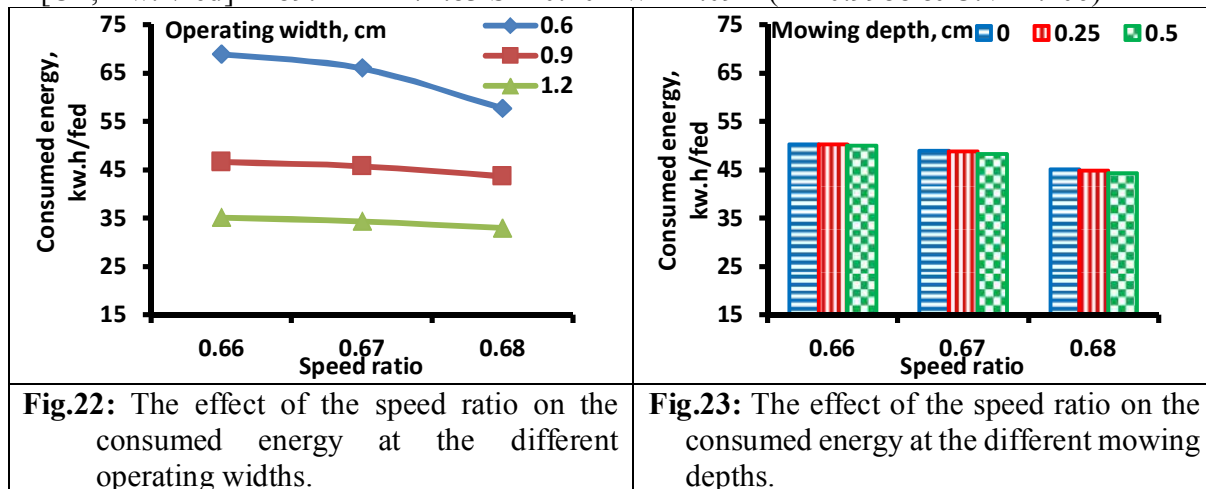
5- Factors affecting the consumed energy CE, kW.h/fed:

The relationships affecting the machine consumed energy (CE, kW.h/fed) to the different speed ratios (Sr) at the different operating widths (W, m) and depths (D, m) are shown in Figs. (22 & 23). Furthermore, increasing the speed ratio (Sr) decreases the machine consumed energy (CE) with increasing the treatments of the (W&D) in opposite relationships. The maximum value of (CE) was (68.89 kW.h/fed) at Sr (0.66) for W of 0.6 m, while the lowest value of the (CE) was (32.94 kW.h/fed) for Sr of 0.68 at 1.2 m of W, as shown in Fig. (22).

Also the maximum value of the (CE) was (50.31 kW.h/fed), as shown in Fig. (23) for Sr of 0.66 at 0.0 m of D, where the minimum value of the (CE) was (44.39 kW.h/fed) for 0.68 of Sr at 0.5 m of D.

These results may be owing to by increasing the speed ratios the consumed fuel increases also and vice versa the consumed energy decreased because of increasing the field capacity. Statics showed that there are high significant effects for the total interaction between different treatments with (P < 0.05) for the F values. Furthermore ANOVA analysis indicated highly significant differences between the treatments. A simple power regression analysis applied to relate the change in (CE) with the change in the tested factors for all treatments. The obtained regression equation was in the form of:

$$[CE, Kw.h/fed] = -89.414 + 271.83 Sr - 0.104 W + 1.09 D (R^2=0.9988 \& C.V=1.106)$$



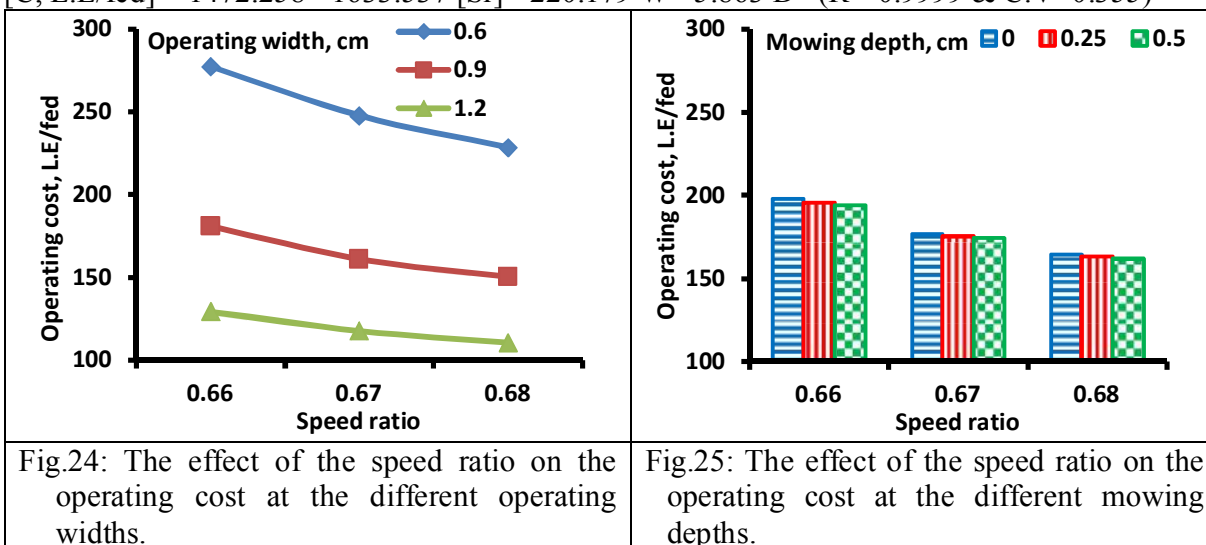
6- Factors affecting the machine operating cost C, L.E/fed:

Figs. (24 & 25) are illustrate the relationships affecting the machine operating cost (C, L.E/fed) to the different speed ratios (Sr) at the different operating widths (W, m) and depths (D, m). Too, increasing the speed ratio (Sr) decreases the machine operating cost (C) with increasing the treatments of the (W&D) in opposite relationships. The maximum value of (C) was (277.43 L.E/fed) at Sr (0.66) for W of 0.6 m, while the lowest value of the (C) was (110.59 L.E/fed) for Sr of 0.68 at 1.2 m of W, as shown in Fig. (24).

Moreover, the maximum value of the (C) was (197.73 L.E/fed), for Sr of 0.66 at 0.0 m of D, where the minimum value of the (C) was (162.0 L.E/fed) for 0.68 of Sr at 0.5 m of D, as shown in Fig. (25).

These results may be espoused of by increasing the speed ratios the consumed fuel increases also and vice versa the operating costs decreased because of increasing the field capacity. Statically there are high significant effects for the total interaction between different treatments with (P < 0.05) for the F values. So ANOVA analysis indicated highly significant differences between the treatments. A simple power regression analysis applied to relate the change in (C) with the change in the tested factors for all treatments. The obtained regression equation was in the form of:

$$[C, L.E/fed] = 1472.258 - 1633.537 [Sr] - 220.179 W - 5.863 D (R^2=0.9999 \& C.V=0.355)$$



7- Factors affecting the giant reed re-growth ratio Gr, %:

The relationships affecting the machine operating cost (Gr, %) to the different speed ratios (Sr) at the different operating widths (W, m) and depths (D, m) are illustrated in Figs. (26 & 27). In addition, increasing the speed ratio (Sr) increases the giant reed regrowth ratio after one month of mowing it (Gr) with increasing the treatments of the (W&D) in direct relationships. The highest value of (Gr) was (27.10 %) at Sr (0.68) for W of 1.2 m, while the lowest value of the (C) was (17.70 %) for Sr of 0.66 at 0.6 m of W, as shown in Fig. (26).

Moreover the maximum value of the (C) was (26.24 %), for Sr of 0.68 at 0.5 m of D, where the minimum value of the (C) was (18.35 %) for 0.66 of Sr at 0.0 m of D As shown in Fig. (27).

These results may be in view of increasing the speed ratios the cutting efficiency decreases which let some of the un-mowing giant reed stalks to regrowth again. Statically there are high significant effects for the total interaction between different treatments with (P < 0.05) for the F values. Despite ANOVA analysis indicated highly significant differences between the treatments. A simple power regression analysis applied to relate the change in (Gr) with the change in the tested factors for all treatments. The obtained regression equation was in the form of:

$$[Gr \%] = -216.543 + 350.09 Sr + 4.123 W + 1.555 D \quad (R^2=0.9979 \ \& \ C.V=0.783)$$

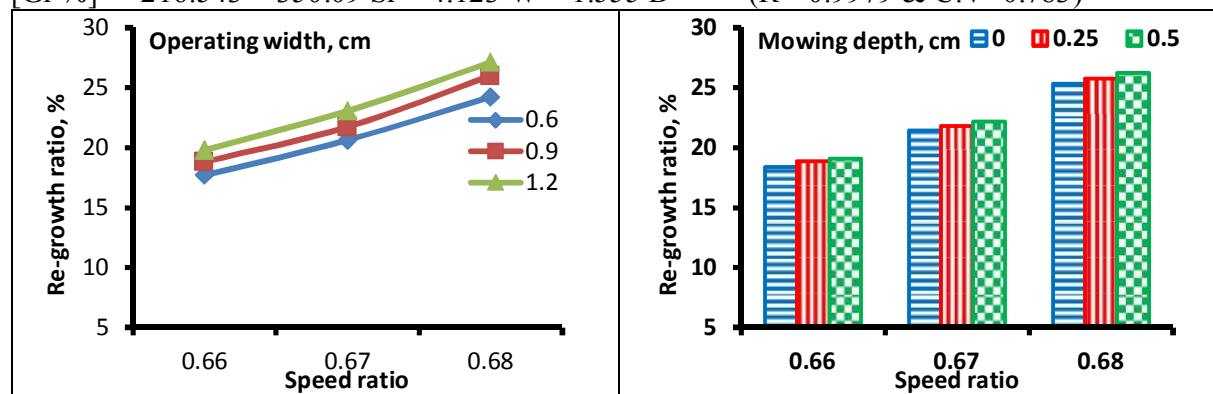


Fig.26: The effect of the speed ratio on the giant reed regrowth ratio after 1 month at the different operating widths.

Fig.27: The effect of the speed ratio on the giant reed regrowth ratio after 1 month at the different mowing depths.

CONCLUSION

The main results could be summarized as follows:

- 1- The maximum value of the cutting efficiency of the giant reed (C_η, %) was (94.31 %) at speed ratio Sr (0.66) for operating width W of 0.6 m at the water surface of 0.0 m for the operating depth W.
- 2- The maximum value of the machine efficiency (M_η, %) was (94.95 %) at speed ratio Sr (0.68) for operating width W of 1.2 m at 0.5 m for the operating depth W.
- 3- The maximum value of the field capacity (FC) was (0.27 fed/h) at speed ratio Sr (0.68) for operating width W of 1.2 m at 0.5 m for the operating depth W.
- 4- The maximum value of the fuel consumption (F) was (3.01 lit/h) at speed ratio Sr (0.68) for operating width W of 1.2 m at 0.5 m for the operating depth W.
- 5- The minimum value of the consumed energy (CE) was (32.94 kW.h/fed) at speed ratio Sr (0.68) for operating width W of 1.2 m with 0.5 m for the operating depth W.
- 6- The minimum value of the operating cost (C) was (110.59 L.E/fed) at speed ratio Sr (0.68) for operating width W of 1.2 m at 0.5 m for the operating depth W.

7- The minimum value of the giant reed re-growth ratio after month (Gr) was (27.10 %) at speed ratio Sr (0.68) for operating width W of 1.2 m at 0.5 m for the operating depth W.

REFERENCES

- 1) Boland, J. M. (2008). "The roles of floods and bulldozers in the break-up and dispersal of *Arundo donax* (giant reed)." *Madroño* 55 (3): 216–222.
- 2) Ceotto, E., and M. Di Candilo. (2010). Shoot cuttings propagation of giant reed (*Arundo donax* L.) in water and moist soil: The path forward *Biomass and Bioenergy* 34:1614-1623.
- 3) Clayton, J.S; D.E. Hofstra and K. D. Getsinger (2001). Evaluation of selected herbicides for the control of exotic submerged weeds in New Zealand: II. The effects of turbidity on diquat and endothal efficacy. *Journal of Aquatic Plant Management* 39: 25–27.
- 4) Coffman, G.C. (2007). Factors Influencing Invasion of Giant Reed (*Arundo donax*). In: *Riparian Ecosystems of Mediterranean-type Climate Regions*. Doctoral Thesis. Environmental Health Sciences. University of California. Los Angeles, California, USA. :282 .
- 5) Datta, S. (2009). 2nd year project Report on Studies on Safe and Effective Chemical Control Measures for Floating and Submerged Aquatic Weeds Affecting Aquaculture. Submitted to CIFE, Mumbai. : 54.
- 6) Garcia, R., and F. Freire (2011). Comparative assessment of environmental life-cycle based tools: an application to particleboard. *International Symposium on Sustainable Systems and Technology (IEEE-ISSST)*, Chicago, Illinois, USA. DOI: 10.1109/ISSST.2011.5936915.
- 7) Hunt, D. (1983). *Farm power machinery management* Eighth edition Iowa State Univ Press Ames. : 3-6.
- 8) Kepner, R. A., R. Bainer and E.L. Barger (1982). *Principles of farm machinery*. 3rd ed. avi pub Co. West part, Connecticut. USA. : 464 – 468.
- 9) Lawson, D. M., J. A. Giessow, and J. H. Giessow (2005). "The Santa Margarita River *Arundo donax* control project: development of methods and plant community response." Pp. 229–244 In: *USDA Forest Service Gen. Tech. Rep. PSW-GTR-195*. Albany, CA.
- 10) Oida, A. (1997). *Using personal computer for agricultural machinery management*. Kyoto University. Japan. JICA publishing.
- 11) Tremblay, L.A. (2004). Biomarkers in eel to evaluate effects of diquat in a Christchurch river. *Australasian Journal of Ecotoxicology* 10: 53-56.
- 12) Vamvuka, D., and S. Sfakiotakis (2011). Effects of heating rate and water leaching of perennial energy crops on pyrolysis characteristics and kinetics. *Renewable Energy* 36:2433-2439.
- 13) Wells, R.D.S. and J.S. Clayton (2005). Mechanical and Chemical Control of Aquatic Weeds: Costs and Benefits. In: *Encyclopedia of Pest Management* DOI: 10.1081/E-EPM-120024643.

تطوير آلة للتخلص من البوص ببخيرات المياه العذبة

* د/ محمد منصور شلبي رفاعي و * د/ أحمد شوقي السيد السيد

*معهد بحوث الهندسة الزراعية- مركز البحوث الزراعية- مصر.

يهدف هذا البحث إلي تطوير نظام ميكانيكي لحش حشيشة البوص مائيا باستخدام محشة ترددية أمامية لتناسب عملية حش وقطع حشيشة البوص تحت سطح المياه بأعماق مختلفة بالبخيرات العذبة بصفة عامة وببحيرة المنزلة بصفة خاصة بهدف تسهيل حركة المياه بها وبالتالي زيادة الثروة السمكية بالبحيرة. علميا إن حش البوص تحت سطح المياه يجعل المياه تخترق سوقه نزولا الي الجذور مما يسبب تعفن البوص والقضاء عليه بنجاح. تم استخدام محشة أمامية بعرض تشغيل مناسب ١,٢٠ م حيث تم تعديلها وتعليقها علي قارب عائم لحش البوص تحت سطح الماء وتجميعه بجانب القارب لاستخدامه في الصناعات المختلفة. تم جلفنه سكاكين المحشة لمقاومة الصدا بسبب المياه. كذلك تم تصنيع نظام تعليق ميكانيكي محليا لتعليق المحشة والتحكم في ارتفاعها بواسطة شداد. تم استخدام موتور بنزين ١٣ حصان كمصدر للقدرة ليعطي الحركة للمحشة وتم تثبيته علي سطح القارب. تم حساب عمق الغاطس للقارب والأحمال المختلفة أثناء تشغيل المحشة وذلك لتوفير الاتزان عند التشغيل وذلك تحت معامل أمان كبير نسبيا. تم إجراء التجارب المائية لدراسة التفاعل والضبط المناسب للعوامل الآتية: أولا: ثلاثة سرعات نسبية (٠,٦٧, ٠,٦٨, ٠,٦٨) بين ثلاثة سرعات خطية لسكينة المحشة مع ثلاثة سرعات أمامية للقارب وهي (٠,١, ٠,٥, ١,٠) ثانيا: ثلاثة مستويات من عرض تشغيل المحشة (٠,٦, ٠,٩, ١,٢ متر) ثالثا: ثلاثة مستويات مختلفة من أعماق الحش (٠ علي سطح الماء , ٠,٥٠, ٠,٥٠ متر تحت سطح الماء). وتضمنت القياسات علي الآتي: كفاءة الحش، كفاءة الآلة، السعة الحقلية، معدل استهلاك الوقود و معدل استعادة نمو البوص بعد شهر من عملية الحش، بالإضافة الي حساب احتياجات الطاقة و تكاليف التشغيل. تضمنت أهم النتائج علي الآتي: وصلت كفاءة الحش الي ٩٤,٣١% بينما كان معدل أداء الآلة ٠,٢٧ فدان/الساعة بكفاءة حقلية وصلت نسبتها الي ٩٤,٩٥% عند نسبة سرعة ٠,٦٨ أي سرعة أمامية ٢ كم/الساعة وعرض تشغيل ١,٢٠ م وعمق حش تحت الماء ٠,٥ م. بينما كان أقل استهلاك للطاقة ٣٢,٩٤ كيلووات ساعة/ الفدان عند أقصى مستويات من العوامل تحت الدراسة. كذلك كانت أقل تكلفة تشغيل ١١٠,٥٩ جنية/الفدان باستخدام المحشة المائية وهي أقل من تكلفة أي نظام مكافحة آخر. لذلك نوصي باستخدام هذا النظام لمكافحة البوص حيث أنه يقوم بحل مشكلة هامة والتي تحتاج لتعميم هذه الفكرة علي المستوى المحلي خصوصا للمحافظات الساحلية في جمهورية مصر العربية.

DEVELOPMENT OF A SPEAKING ELECTRONIC DEVICE FOR PROBLEM DIAGNOSING IN RICE COMBINE HARVESTERS

EL_SAYED, A.S. * M.E. EL_IRAQI* and W. F. EL_METWALLY*

* *Agric. Eng. Res. Inst. ARC, Egypt.*

Abstract

The main goal of this research is to investigate an attached speaking electronic diagnosing device connected with Japanese rice combine harvesters to be accumulated with its own electrical operating system due to; the daylight brightening and the emitted dusts through harvesting that disrupt operator vision for the combine combination meter. This electronic device was designed to protect both machine and the operator from high noise sounds intensity that exceed the acceptable human ranges (70 dB) using protective wireless headphones which confirm the operator by Arabic recording phrases the break down place with description and the repairing steps to save the maintenance time and the costs which enlarges the machine performance and capacity. The attached electronic speaking wireless device was merged to the combine sensors wiring system to transmits its electrical signal from the combine microcomputer through the transmitting antenna of the investigated device to the operator headphone which synthesized with the transmitting frequency for the recording voices of the following sensors of; (the water temperature alarm, the engine oil pressure alarm, the battery charge indicator, the full grain tank alarm, the main and the treating threshing drums rotating speeds alarm, the returning conveyor rotating speed and the discharging straw chain). The limit of reception the broadcasting signals frequency is about 15 m around combine position which facilitates the monitoring operation remotely.

The field experiments were conducted during rice harvesting seasons 2015& 2016 on three different combine models of; Yanmar 2010 (48 hp), Kubota 2011 (55 hp) and Kubota 2012 (65 hp) and their operators respectively to compare their performance under the following variable levels of; first: three forward speeds of (0.93 km/h slow, 1.5 km/h standard and 1.85 km/h rapid), second: three different times through day of (9.0 am, 12.0 pm and 5.0 pm) and third: two different species of rice with stalk lengths of (55 and 110 cm) at the recommended moisture content of 25 % for harvesting operation. Two main measurement categories were done first on the combine operators from; the exposed noise intensity from combine, the response degree to the combine breakdowns, blood pressure, heart pulse with their weight factor and the hearing level, second for the combine; from field capacity, field efficiency and the net profit comparing with and without using the attached wireless speaking device.

The results concluded the following: using the wireless protective headphones maximized the combine's field capacities and efficiencies by increasing ratios of (24.49, 16.81 and 21.74%) respectively for the three models field capacities due to using the device and vice versa the maintenance costs decreased as their net profit increased of (28.17, 29.63 and 31.62%) respectively than the previous season. However using device maximized the operators responding degree up to 100 % and also saved the operators hearing levels after harvesting season than their companies for the same combine models. The measured sound intensity from combines reached 96 dB which exceeds the human acceptable limits 70 dB. Also using the speaking wireless device reserved the operator's blood pressures and their heart rates around the standard normal limits (120/80 and 100 pulse/min) with the body weight factor. So using the attached electronic speaking wireless device needs to be prevailed to the rice mechanization center to achieve the Egyptian agricultural development.

INTRODUCTION

Rice is very important to economy, society and politics of Egypt. It covers approximately 2 million feddans of cultivated area. Combine harvesters are one of the most economically important labor saving inventions, significantly reducing the fraction of the population that must be engaged in agriculture. The main aim of the automated harvesting of the rice crop is to apply good harvesting methods performance to be able to maximize grain yield, and minimize costs and quality deterioration. And the vast majority of the mechanical harvesting of rice in Egypt has done by the Japanese combines which includes numerous operations arranges, harvesting, threshing, winnowing and filling the grains in following simultaneously operations. So it's important to develop the performance of these machines due to of their importance. Where these equipment were provided with multiple electrical sensors, due to of their high price, so its rough needed to increase their performance continuously.

The studied researches could be explains main two categories as the following:

First: studies related to the physical part:

Obelenis and Malinauskiene (2007) showed that exposure to noise can cause changes in peripheral vascular resistance, in heart rate, blood pressure (BP) and in the urinary concentration of catecholamine's, also they found that noise could damage the cardiovascular system noise and have some effects even on gastrointestinal system, the respiratory system, the immune system, the endocrine system, the reproductive system and the neurogenic system. However, (Singh and Davar , 2004) has strengthened the evidence for an association between noise and adverse effect on blood pressure and also (Sabitoni, 2006) study shows that on-the-job noise contributes to high blood pressure which, in turn, can cause heart disease or stroke.

Besides (Zhao *et al.*, 1991) stated that individuals chronically exposed to continuous noise at levels of at least 85dB have higher blood pressure than those not exposed to noise. In effect the impact of noise on blood pressure is mediated through an intermediate psychological response such as noise annoyance, although this has not been convincingly proved (Lercher *et al*, 1993). The strongest evidence for the effect of noise on cardiovascular system comes from studies of blood pressure in occupational settings (Arndt *et al.*, 1996). Also, (Green *et al.*, 1991) observed a significant increase in systolic and diastolic blood pressure in younger age group (25-44yrs) subjects exposed to more than 85 dB noise as compared to decrease in systolic blood pressure and no effect on diastolic blood pressure in subjects aged 45-65yrs. Where's, (Elise *et al.*, 2002) observed insignificant increase in blood pressure. In a study to observe the effect of exposure to short-term noise on systolic blood pressure and diastolic blood pressure and also (Rashid *et al.*, 2009) indicated that a short-term exposure to noise for 10 minutes produced a significant rise in blood pressure. Both systolic and diastolic blood increased but the rise in diastolic blood pressure was more than the rise in systolic blood pressure. Besides, (Vermeer, 2000) reported noise exposure as constituents of a health risk, by stating sufficient scientific evidence that noise exposure can induce hearing impairment, hypertension, and ischemic heart disease, annoyance, sleep disturbance and decrease performance.

Second: studies related to the combine harvesters performance:

Arnaout (1980) estimated the field capacity and efficiency in rice harvesting using combine harvester and found that the effective field capacities increased by increasing both combine harvesting speed and harvesting area. He also found that field efficiency was highly affected by the lost in both turning time in respect to the forward speed and travel time from field to another whereas, (Zareei *et al.*, 2012) stated that Several other studies have focused on the use of intelligent control systems and according to the complexity of modeling the processes of

harvesting have used artificial neural networks, fuzzy logic and genetic algorithms to control the factors contributing to the loss of combine and forecast the grain loss. And also (Ghonimey and Rostom, 2002) stated that rice crop is considered one of the most important foods and export crops in Egypt. In the last ten years, the annual cultivated area increased from 1.08 to 1.56 million feddans and the grain yield increased from 3.14 to 5.80 million tons. The average grain productivity was 3.42 ton/fed. Besides that (Wei *et al.*, 2009) stated that the structural and operational parameters of combine harvester need to be adjusted accordingly. With the recent advances in sensors, electronics and computational processing power, automated technologies for combine harvester have been made possible in part and there is an urgent need to develop a system which can monitor the separation loss real-time. As well (Fouad *et al.*, 1990) compared the performance of two types of combines in harvesting rice crop in Egypt. The combines were operated at three forward speeds of 0.9, 2.3 and 2.8 km/h for rice combine, and 0.8, 2.1 and 2.9 km/h for the conventional combine. There was a highly significant decrease in total harvesting costs with an increase in operation speed from 0.9 and 0.8 km/h to 2.3 and 2.2 km/h for the rice and conventional combines, respectively and also (El-Haddad *et al.*, 1995) reported that combine harvester gave the lowest cost of about 229.0 L.E/fed in comparison with 283.4 L.E/fed for mounted mower and 300.0 L.E/fed for manual sickle system. Whereas (Helmy *et al.*, 1995) indicated that the effective field capacity increased by decreasing straw moisture content. In addition, increasing forward speed tends to increase the total grain losses with percentage of 10.11 by using Dutz-Fahr combine and 10.43 by using Isaki combine. They found also that increasing combine harvester forward speed from 0.85 to 2.27 km/h tends to decrease harvesting cost from 82.46 to 59.93 L.E/ton for rice (Giza-171) variety and from 57.69 to 37.61 L.E/ton for rice (Giza-175) variety. Also (El-Nakib *et al.*, 2003) used Kubota combine as a mechanical harvester of rice crop (Sakha 102). They found that header, threshing, separating and shoe losses increased with the increase of the forward speed and the decrease of grain moisture content. The optimum operating parameters for harvesting rice crop was, combine forward speed of 4.5 km/h and grain moisture content of 16.5 %. However, (El-Khateeb, 2005) tested multi-purpose combine harvester (Yanmar model CA-760) and found that the maximum value of actual field capacity was 2.90 fed/fed at forward speed of 3.0 km/h and grain moisture content of 18 %. He found also, that the highest value of fuel consumption rate was 7.20 l/fed at forward speed of 1.5 km/h and grain moisture content of 25 %. He recommended that grain moisture content of 22.0 %, forward speed of 1.5 km/h, cylinder speed of 24.0 m/s and baffle plate angle of (90 deg) 1.57rad were the optimum operating conditions for mechanical harvesting rice crop. Also, using combine harvester was the most efficient and economic system (89.70 L.E/fed) compared to manual harvesting and gathering followed by threshing and winnowing (181.60 L.E/fed). Also (El-Sharabasy, 2007) mentioned that using both full and partial mechanization system for harvesting and threshing rice crop at the higher forward speeds and lower grain moisture contents, recorded minimum consumed energy and cost requirements. Also using partial or full mechanization for harvesting rice crop saved time, effort, and total cost requirements and also cleared the rice crop from the field as fast as possible than traditional manual system. As well (Zhou *et al.* 2008) they designed the fuzzy neural network controller of combine harvester threshing drum. Their simulation results show that the fuzzy neural network control method is feasible. Despite many years of attempts to control the harvesters automatically, still the inputs from skilled drivers having much accumulated also, they stated that knowledge is essential for proper adjustment and control of the harvesting machines. The operator knowledge is often in a form that cannot be incorporated in a conventional control system or mathematical equations. Nevertheless, (Gates and Overhults, 1992) evaluated the commercially

available electronic controllers. They classified these units according to enclosure type, analog versus microprocessor based control, power supply, sensors, alarms, control relays and interval timers, outside temperature feedback, and retail price. They found that a great assistance of these controllers indicated several using in the agriculture application technology. Also, (Reid, 2002) studied the assessment of the control and safety needs of autonomous agricultural vehicles and implement systems on farm property by using various sensors and control systems and the relative costs. He found that the implement control which used in autonomous tractors and implement systems that can work on contiguous farm property is more efficient and the cost reduction can be tackled at later stages of progress. So, (Ryan *et al.*, 2011) they consist of an impact plate and a force transducer that converts the net time-averaged impact force into a voltage signal. This type of structure is so simple that impact-type sensors can be easily mounted on combine harvesters and risk of causing an obstruction of the normal threshing process, even when the sensors are damaged, is minimized.

The aim of the research is to improve the efficiency of the Japanese rice combines harvester's performance and protect their operators from noise intensity using the innovated speaking alert diagnosing wireless device.

MATERIALS AND METHODS

A special programmed electronic wireless speaking wireless diagnosing device was smartly attached to the combine electrical system to diagnose the coming signs from the electrical sensors such as: (the water temperature alarm, the engine oil pressure alarm, the battery charge indicator, the full grain tank alarm, the main and the treating threshing drums rotating speeds alarm, the returning conveyor rotating speed and the discharging straw chain).

As shown in Figs. (1 and 2) the innovated programmed electronic circuit was developed to monitor remotely the combine harvester's sensors with less effort from the operator using wireless protective headphones to diagnose the breakdown immediately before increasing it. The electronic programmed circuit of the wireless speaking diagnoses device consists from the following:

- 1- The Monitor:** As shown in (Fig. 2, No.1) the monitor was merged with the electronic circuit to appear immediately the error from seven electrical sensors of the combine harvester to be seen by the operator when the break down occurs to solve it before increasing the problem. However there is small tiny hall with 10 mm dia. in the combine microcomputer, as shown in Fig. (3) which views errors (E1, 2 ex.) and its difficult to observe so the used monitor is widely more to view the errors.
- 2-Programmed IC:** As shown in (Fig. 2, No.2) and Fig. (4) the programmed IC which plays the master role of the circuit from saving the data and connected to the receiving channels from the sensors. Also this IC was programmed to transmit the electrical signal to the memory cards that have the audio record to tell the operator through the wireless headphones the solving of the break down problem before occurred any damage to the combine elements.
- 3- The Receiving Channels:** Seven receiving channels were arranged to connect the combine combination meter and connected to seven diodes to let the electrical signal moves to the circuit in one way only to prevent the circuit from the shortcut, as shown in (Fig. 2, No.3) and Fig. (4). As soon as, any sensor sense the error the own led of the receiving channel lights immediately. Also seven fuses were putted through the path of the electrical current to prevent the electronic circuit from shortcut.
- 4- The audio Saving Units:** as shown in (Fig. 2, No.4) special small seven MP3 with initial memory cards were connected to the transmitting relays which saving the Arabic recording

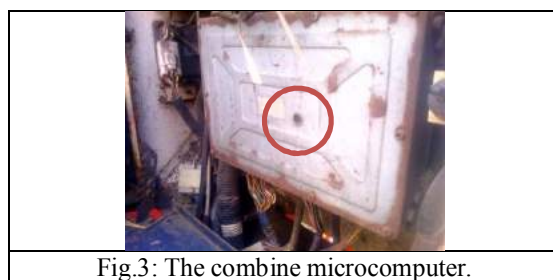
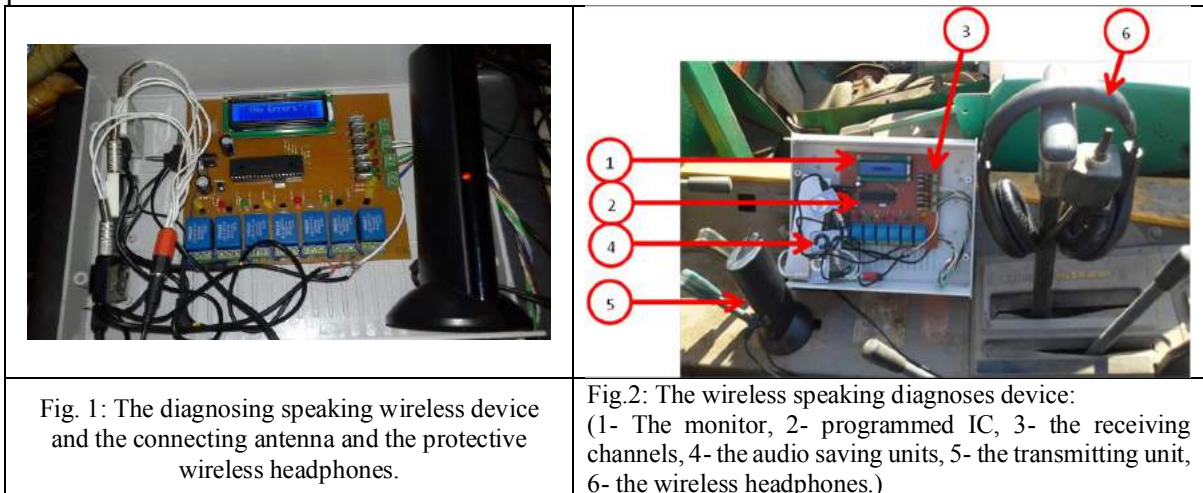
audio files of the solving for the problems and the done steps, that recorded from the experts through the connected wireless headphones of the operator.

5- The Transmitting Unit: As shown in (Fig. 2, No.5) This unit consisted from wireless antenna with the range of transmitting the audio sound signals for 15 meters around the combine position that gives the operator free of moving. However this antenna was connected to seven relays model (Fangke-JZC-23F- 4123) that work with 12V DC and intensity of 5 A to accumulates the device.

6- The Wireless Headphones: As shown in (Fig. 2, No.6) this headphone was made from special kind of materials to prevent the operator ears from the combine noise which synthesis initially at the first use to the transmitting waves frequency.

The programmed electronic circuit operation system

The innovated programmed electronic circuit was connected to the combination meter of the combine harvester electrical system and as been as the electrical signal reaches the alarming unit of the combine it reaches the designed circuit in two sequential restraints the first one to show the operator the problem in the part of the combine on the monitor of the electronic circuit. Second the transmitting channel is ready to send the audio orders to the operator from the memory cards to the wireless antenna to the ears of the operator through the wireless headphones which was tuning previously to receive the waves from the circuit and also this headphones was chosen accurately to save the hearing of the operator to the maximum extent.



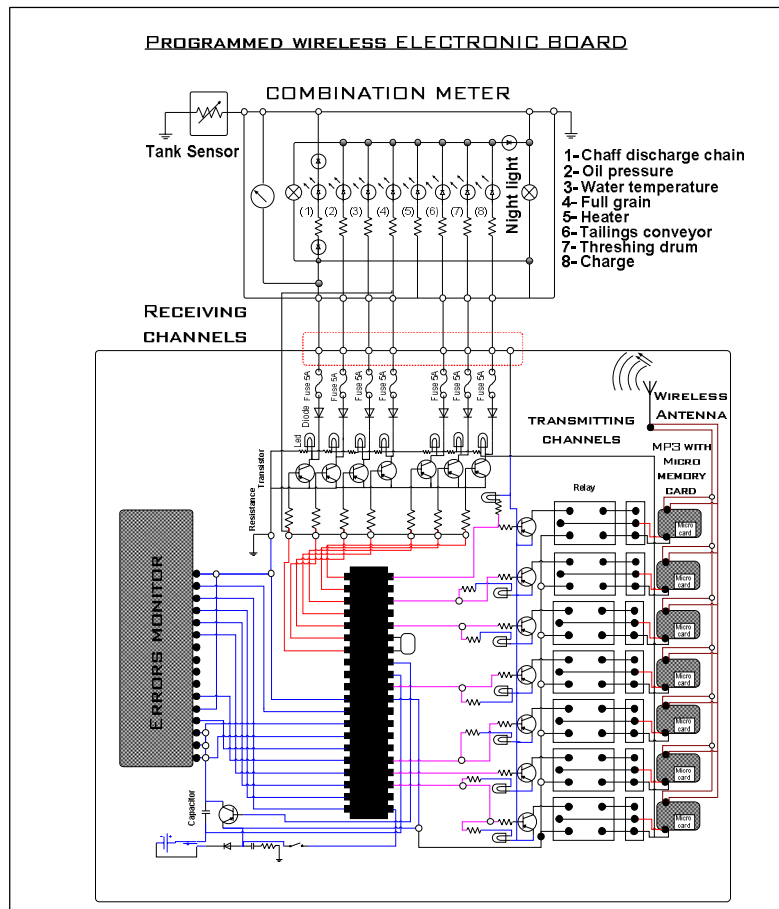


Fig. 4: The wireless speaking diagnoses device circuit.

Test factors

The field experiments were carried out at EL-Serw agricultural research station in Damietta government through seasons 2015&2016 of harvesting rice using three different models of rice combine harvester (mechanical evaluation) and their operators (biological evaluation) (Yanmar 48 hp 2010, Kubota 55 hp 2011 and Kubota 65 hp 2012) using and without using the speaking wireless device to test the following variables: (Tapple 1).

Table.1: The tested combine models and there operators.

Combine model	Production year	Harvesting width, m	Motor rotation rpm	Grain tank capacity, kg
Y.48 hp	2010	1.45	2500	200
K.55 hp	2011	1.50	3000	490
K.65 hp	2012	1.65	3500	550
Operators	Age	Weight	Length	Working years
1 st op.	38	90	1.80	9
2 nd op.	35	81	1.75	5
3 rd op.	33	77	1.77	4

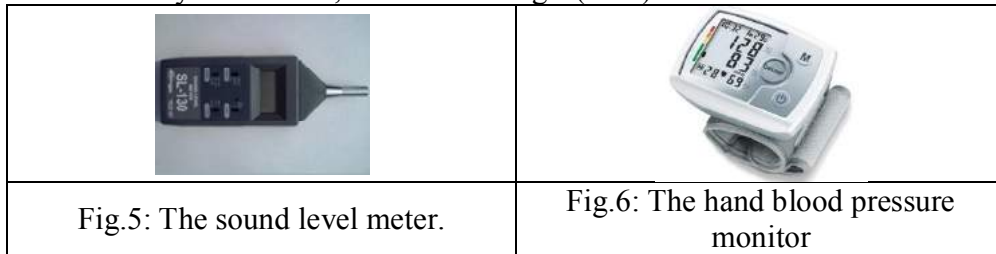
- 1- **Combine harvesters forward speeds (FV, Km/h):** Three levels of the combine forward speeds (0.93 slow, 1.50 standard and 1.85 rapid km/h).
- 2- **Harvesting time (Ht, am&pm):** Three time levels were chosen as (9.00 am, 12.00 pm and 5.00 pm) which these three times affect both the combine due to the weather temperature which practically affected both the combines and the operators performances.
- 3- **Rice species stalk length (R.L, cm):** Two different lengths (55 short and 110 cm long) for Giza 177 and Sakha 101 species were tested.

Measurements and instrumentation

The field experimental units were replicated three times for each treatment on the combine harvesters and the operators. The data were statistically analyzed using the Costat program (Oida, 1997) to determine the effect of the above variables on two main categories of measurements as follows:

A- The biological measurements: To test the operators performance from:

- 1- Noise intensity (db): Using the sound level meter (Pacer- SL-130 digital-USA) in the operator's seats by the db unit, as shown in Figs. (1&5).



- 2- The operators hearing level (HL): using audiograms in the audiogram clinics using a special program which was set-up in the computer system for standard hearing that uses the frequency by hertz through standard headphones to limit the hearing level of each ear for the operator.
- 3- The operators response degree (RD, once/fed): by observing and recording the coming signals from sensors and their response.
- 4- The operators blood pressure (OBP= (SBP/DBP, mm Hg) and heart rate (H.R, pulse/min): using hand blood pressure monitor model (beurer BC3 1- made in Germany), as shown in Fig. (6).

B- The mechanical measurements: To test the combine harvester performance from:

- 1- The combine maintenance time (M, min/fed): using the stop watch.
- 2- The combine field efficiency (Fe), %: It was measured according to Kepner *et al.* (1982).

$$Fe = \frac{T_{th}}{T_{ac}} \times 100 \dots\dots\dots (1)$$

Where: Fe: machine efficiency, %, T_{th}: theoretical time per fed, h T_{ac}: the actual operating time, h.

- 3- The combine field capacity (FC, fed/h) was calculated as follows:

$$FC = \frac{s \ w \ Fe}{4.2} \text{ , fed/h} \dots\dots\dots (2)$$

Where: **F.C**: the field capacity, fed/h, **S**: speed of travel, Km/h, **W**: rated width of implement, m, and **Fe**: field efficiency, %.

- 4- The operating costs (C, L.E/fed) : The operating cost was determined using the following formula:

$$\text{Operating cost (L.E / fed)} = \frac{\text{Machine hourly cost, (L.E./h)}}{\text{Actual field capacity (fed / h)}} \text{L.E / fed} \dots\dots\dots(3)$$

RUSULTS AND DISCUSSION

The evaluation of the speaking wireless device is carried out to investigate the effect of the engineering parameters of the device by analyzing the relative relationships between the various parameters such as the combine harvester forward speed, the harvesting time through the day and the rice stalk length at two main categories; first the combines operators second the combines itself . The results could be discussed as follows:

A- Factors Affecting the combine harvesters operators

1- Factors affecting the combine noise intensity and the operators hearing level:

The relationship between the combine harvester's forward speed (FV, km/h) and its noise intensity (NI, db) at the different harvesting times through the day (Ht) is illustrated in Fig. (7). Clearly increasing the FV for the three different combine models of {Yanmar 48 hp (Y.48), Kubota 55 hp (K.55) and Kubota 65 hp (K.65)} respectively increases the noise intensity (NI) with increasing the treatment of the (Ht) in a direct relationships. The maximum values of (NI) were (98.97, 92.84 and 96.35 db), respectively at FV of 1.85 km/h for Ht of 5.00 pm, while the minimum values of the NI were (81.62, 88.34 and 90.33 db), respectively for 0.93 km/h of FV at Ht of 12.00 pm for the first one and 9.00 am for the two other values.

Whereas, the maximum values of the NI were (89.62, 92.29 and 95.84 db) respectively, as shown in Fig. (8) for FV of 1.85 km/h at 55 cm of the rice stalk length (RL), however the lowest values of the NI were (82.84, 88.56 and 90.55 db), respectively for the 0.93 km/h FV at 110 cm of RL. These results may be attributed to by increasing the combine engine power the outlet sounds intensity from the rotating elements increases relatively and also the harvesting times per day affect the rice straw moisture content which improved as the sunrises and by increasing the weather temperature. Besides that the rice stalk lengths affect the threshing drum that occurs high sounds at the taller species than the shorter ones. Statically the total interactions between different treatments show a high significant effect (P < 0.05) for the NI values respectively. ANOVA analysis indicated highly significant differences between the treatments. A simple power regression analysis applied to relate the change in (NI) with the change in the tested factors for all treatments. The obtained regression equations were in the form of:

NI (db)	NI=		
1 th op.	80.213 + 5.511(FV) -0.304 (Ht) +0.0240 (R.L)	(R ² =0.4784)	(C.V=4.247)
2 nd op.	85.526 +3.547 (FV) -0.0784 (Ht) +0.00605 (R.L)	(R ² =0.9892)	(C.V=0.205)
3 rd op.	86.0559 +5.305 (FV) -0.115 (Ht) +0.0056 (R.L)	(R ² =0.9964)	(C.V=0.170)

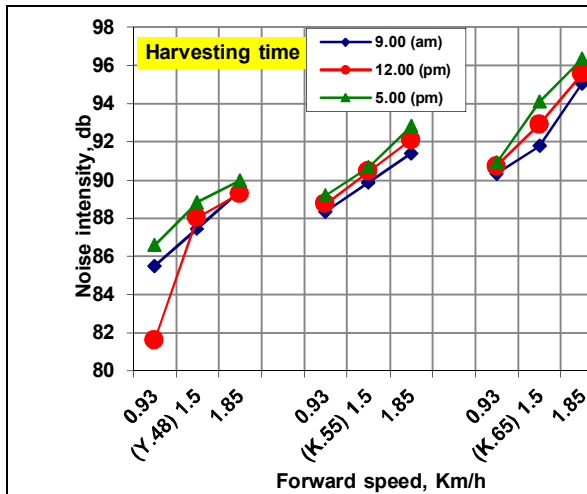


Fig. 7: Effect of the combine forward speeds on the noise intensity at the different harvesting times.

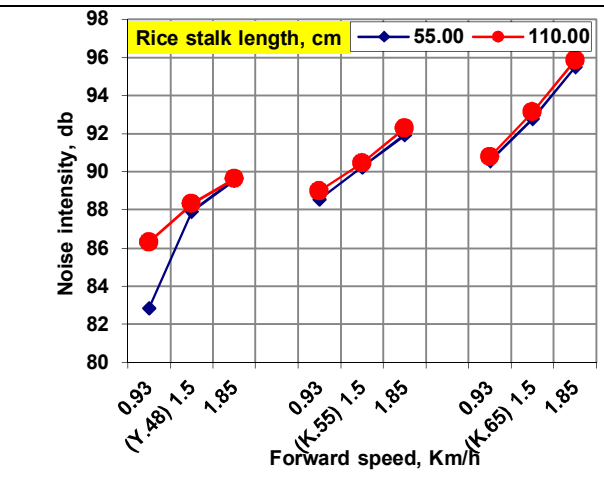


Fig. 8: Effect of the combine forward speeds on the noise intensity at the different rice stalk lengths.

2- Operators Hearing Level:

As been cleared from the audiograms curves Fig.(9) and the Table.(2) of the operators hearing level for the right and left ears its visible that using the protective headphones protect hearing sense from losing according loud noises from combine harvesters or it made significant differences for the hearing level. Sixth operators were tested there hearing level in the hearing clinic and the results showed that the three operators which wear the headphones their hearing levels were normal while the three others were moderated whose didn't wear the headphones.

Table.2: The hearing level for the operators with and without using the wireless protective headphones.

With device	1 st op.	2 nd op.	3 rd op.	Hearing degree
(Right ear) db	2-20	4-20	4-15	Normal
(Left ear) db	5-14	8-14	8-25	Normal
Without device	1 st op.	2 nd op.	3 rd op.	Hearing degree
(Right ear) db	15-33	8-38	19-29	Moderate
(Left ear) db	10-44	15-46	41-45	Moderate

3- Factors affecting the operators response degree:

Figs. (10 & 11) illustrated the relationships compared between the combine harvesters models without attaching the wireless device and using it at the combines forward speed (FV, km/h) to the operators response degree from the combine sensors signals (RD, once/fed) at the different harvesting times through the day (Ht). However increasing the FV for the three different combine models of {(Y.48), (K.55) and (K.65)} respectively minimize the operators response degree (RD) with increasing the treatment of the (Ht) in opposite relationships. The highest values of (RD1&2) were {(9, 5 and 3) & (11, 7 and 5) once/fed}, respectively at 1.85 km/h of the FV for Ht of 5.00 pm except the third value at 12.00 pm, while the lowest values of the (RD1&2) were {(4, 1 and 1) & (6, 2 and 2) once/ fed}, respectively for of the 0.93 km/h of FV at Ht of 9.00 am. The RD increasing ratios from RD2 than RD1 were (18.18, 28.57 and 40.0%) for the maximum values while its values were (33.33, 50.0 and 50.0%) for the minimum RD values.

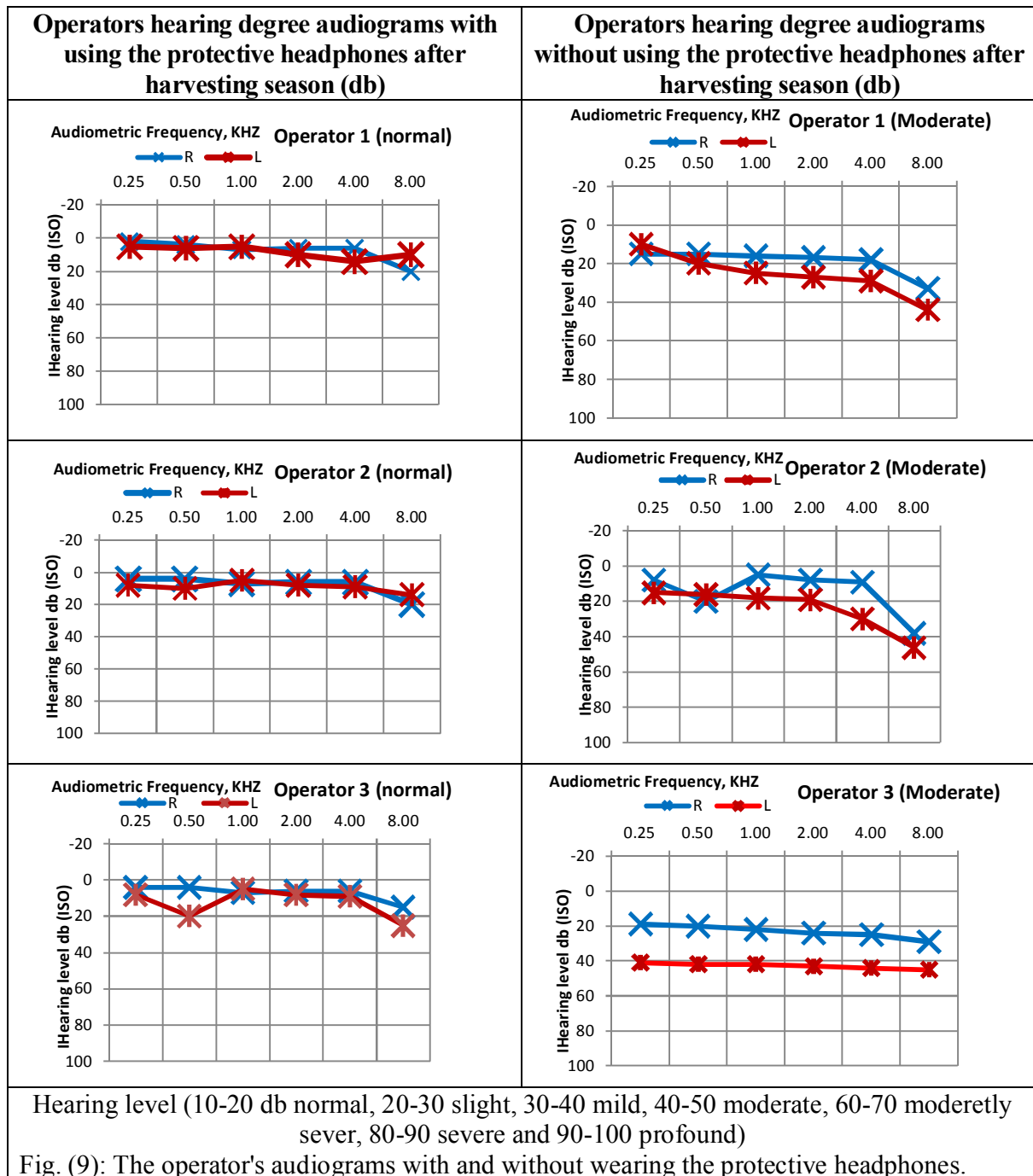


Fig. (9): The operator's audiograms with and without wearing the protective headphones.

As been cleared in Figs. (12&13), the maximum values of the (RD1&2) were {(8, 4 and 3) & (11, 6 and 5) once/fed} respectively, for FV of 1.85 km/h at 110 cm of the rice stalk length (RL), while the minimum values of the (RD1&2) were {(5, 2 and 1) & (6, 3 and 2) once/fed}, respectively for the 0.93 km/h FV at 55 cm of RL except the fourth value at 110 cm of RL. The RD increasing ratios from RD2 than RD1 were (27.27, 33.33 and 40.0%) for the maximum values while its values were (16.67, 33.33 and 50.0%) for the minimum RD values. These results may be due to by increasing the combine forward speed the response degree of the operators decreased as a humans habits lost concentration by increasing the speed and the number of working hours through the day and also the weather temperature play a role

with this. The total interactions between different treatments show a high significant effect ($P < 0.05$) for the RD1&2 values respectively. ANOVA analysis indicated highly significant differences between the treatments. A simple power regression analysis applied to relate the change in (RD) with the change in the tested factors for all treatments. The obtained regression equations were in the form of:

RD (once/fed)	RD1=	RD2 =
1 th op.	$1.4265 + 3.368 \text{ FV} + 0.0075 \text{ Ht} + 0.00135 \text{ R.L}$ ($R^2= 0.8868$) (C.V=11.036)	$2.485 + 4.174 \text{ FV} - 0.0038 \text{ Ht} - 6.734 \text{ R.L}$ ($R^2= 0.8856$) (C.V=9.36)
2 nd op.	$0.243 + 1.861 \text{ FV} + 0.0075 \text{ Ht} + 0.00135 \text{ R.L}$ ($R^2=0.8646$) (C.V=18.252)	$0.213 + 3.181 \text{ FV} - 0.0781 \text{ Ht} + 0.006 \text{ R.L}$ ($R^2= 0.9219$) (C.V=12.267)
3 rd op.	$-0.840 + 1.296 \text{ FV} + 0.0458 \text{ Ht} + 0.0054 \text{ R.L}$ ($R^2=0.7893$) (C.V=24.372)	$-0.323 + 2.342 \text{ FV} - 0.0405 \text{ Ht} + 0.0067 \text{ R.L}$ ($R^2=0.8972$) (C.V=14.007)

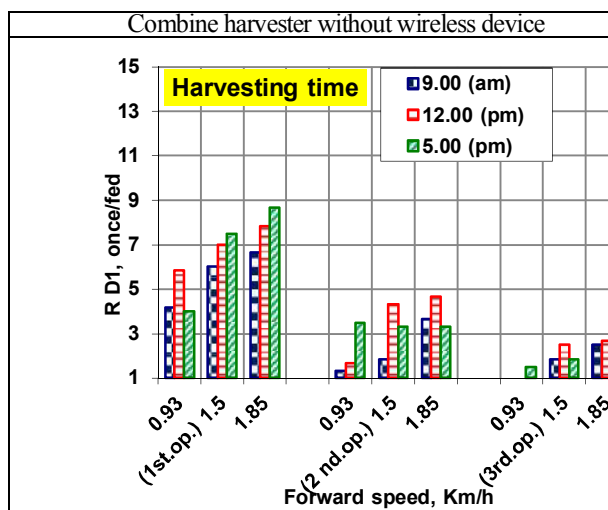


Fig. 10: Effect of the combine forward speeds on the operator response degree at the different harvesting times.

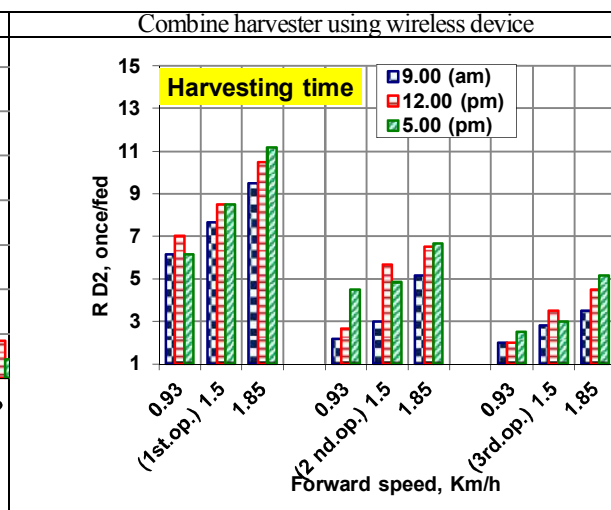


Fig. 11: Effect of the combine forward speeds on the operator response degree at the different harvesting times.

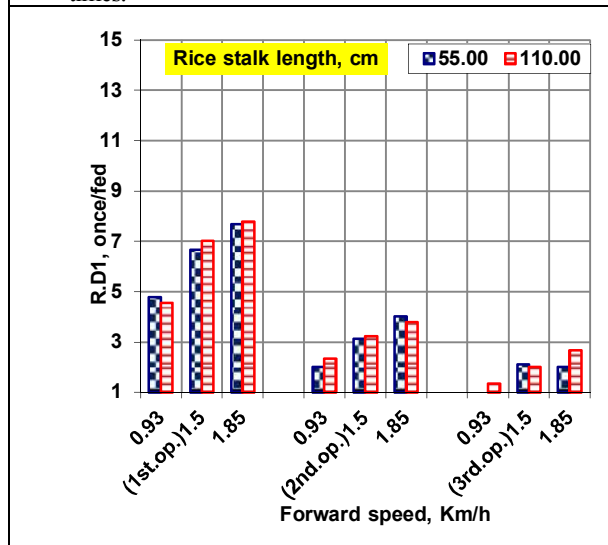


Fig. 12: Effect of the combine forward speeds on the operator response degree at the different harvesting times.

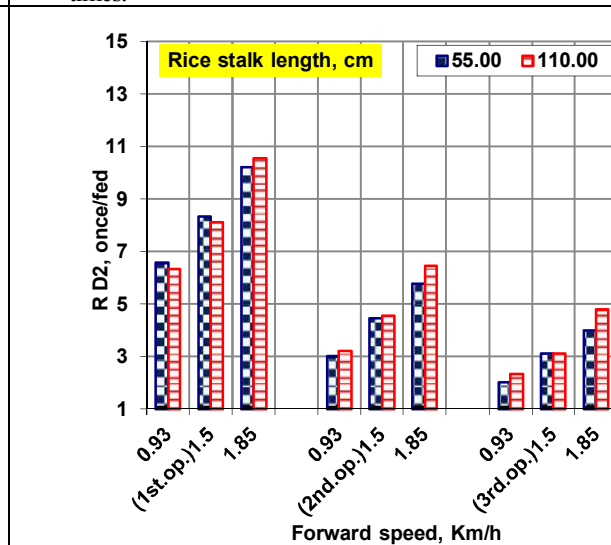


Fig. 13: Effect of the combine forward speeds on the operator response degree at the different rice stalk lengths.

4- Factors affecting the operators blood pressure:

The relationships compared between the combine harvesters models without attaching the wireless device and using it at the combines forward speed (FV, km/h) to the operators blood pressure (OBP, mm Hg) at the different harvesting times through the day (Ht) are illustrated in Figs. (14 & 15) and Table (3). Clearly that Increasing the FV for the three different combine models of { (Y.48), (K.55) and (K.65)} respectively increases the operators blood pressure (OBP) with increasing the treatment of the (Ht) in a direct relationships. The highest values of (OBP and 1&2) were {(137/99, 142/101 and 145/102) & (125/82, 127/85 and 128/86) mm Hg}, respectively at 1.85 km/h of the FV for Ht of 5.00 pm, while the lowest values of the (OBP1&2) were {(121/86, 126/88 and 129/86) & (112/63, 114/66 and 115/67) mm Hg}, respectively for of the 0.93 km/h of FV at Ht of 9.00 am.

Table.3: The operator blood pressure (OBP) values at the interaction between (FV*Ht).

OBP (mm Hg)	Y.48 hp	K. 55 hp	K. 65 hp	FV (km/h)			Ht (am- pm)		
				1.85	1.85	1.85	5.00	5.00	5.00
OBP1 (Max.)	137/99	142/101	145/102	1.85	1.85	1.85	5.00	5.00	5.00
OBP1 (Min.)	121/86	126/88	129/89	0.93	0.93	0.93	9.00	9.00	9.00
OBP2 (Max.)	125/82	127/85	128/86	1.85	1.85	1.85	5.00	5.00	5.00
OBP2 (Min.)	112/63	114/66	115/67	0.93	0.93	0.93	9.00	9.00	9.00

Whereas, the maximum values of the (OBP1&2) were {(136/96, 141/98 and 144/99) & (122/81, 124/84 and 125/85) mm Hg} respectively, as shown in Figs. (16&17) and Table (4) for FV of 1.85 km/h at 110 cm of the rice stalk length (RL), where the minimum values of the (OBP 1&2) were {(123/89, 128/91 and 131/92) & (113/66, 115/69 and 116/70) mm Hg}, respectively for the 0.93 km/h FV at 55 cm of RL.

Table.4: The operator blood pressure (OBP) values at the interaction between (FV*RL).

OBP (mm Hg)	Y.48 hp	K. 55 hp	K. 65 hp	FV (km/h)			RL (cm)		
				1.85	1.85	1.85	110	110	110
OBP1 (Max.)	136/96	141/98	144/99	1.85	1.85	1.85	110	110	110
OBP1 (Min.)	123/89	128/91	131/92	0.93	0.93	0.93	55	55	55
OBP2 (Max.)	122/81	124/84	125/85	1.85	1.85	1.85	110	110	110
OBP2 (Min.)	113/66	115/69	116/70	0.93	0.93	0.93	55	55	55

These results may be owned to by increasing the combine forward speed the operator's blood pressure increased as increasing the adrenalin in the blood and increasing the heart rate according to the weather temperature. While using the investigated device made the operator more confirm by protecting their ears from high sounds which relaxing the operator to minimize the blood pressure to the normal levels. Statically there are high significant effects for the total interaction between different treatments with (P < 0.05) for the OBP 1&2 values respectively. Also ANOVA analysis indicated highly significant differences between the treatments. A simple power regression analysis applied to relate the change in (OBP) with the change in the tested factors for all treatments. The obtained regression equations were in the form of:

OBP (mm Hg)	OBP 1=SBP1/DBP1	OBP 2 = SBP2/DBP2
1 th op.	114.153 +12.042 FV - 0.5 Ht + 0.0189 R.L 85.366 +5.463 FV - 0.219 Ht +0.0047 R.L (R ² =0.9797) (C.V=0.718) (R ² =0.5947) (C.V=4.168)	105.950 +8.32 FV - 0.206 Ht +0.016 R.L 54.42 +14.488 FV - 0.369 Ht +0.0249 R.L (R ² =0.9388) (C.V=1.017) (R ² =0.9757) (C.V=1.551)
2 nd op.	119.153 + 12.042 FV - 0.5 Ht + 0.0189 R.L 87.366 +5.463 FV - 0.219 Ht +0.0047 R.L (R ² =0.9797) (C.V=0.691) (R ² =0.9571) (C.V=1.058)	107.950 +8.32 FV - 0.206 Ht + 0.0162 R.L 57.42 + 14.488 FV - 0.369 +0.025 R.L (R ² =0.5947) (C.V=3.82) (R ² =0.9388) (C.V=1.0)
3 rd op.	122.153 +12.042 FV - 0.5 Ht +0.0189 R.L 88.366 + 5.463 FV - 0.219 Ht +0.0047 R.L (R ² =0.9797) (C.V=0.976) (R ² =0.5947) (C.V=4.036)	108.950 +8.32 FV - 0.206 Ht +0.0162 R.L 58.42 + 14.488 FV - 0.369 Ht +0.025 R.L (R ² =0.9388) (C.V=0.992) (R ² =0.9757) (C.V=1.471)

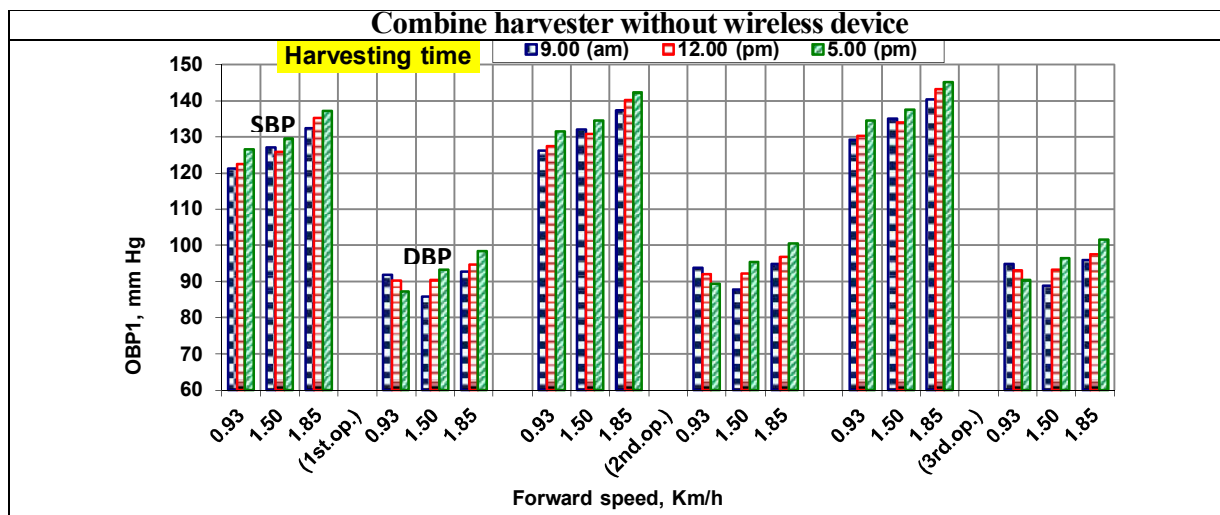


Fig. 14: Effect of the combine forward speeds on the operator's blood pressure at the different harvesting times.

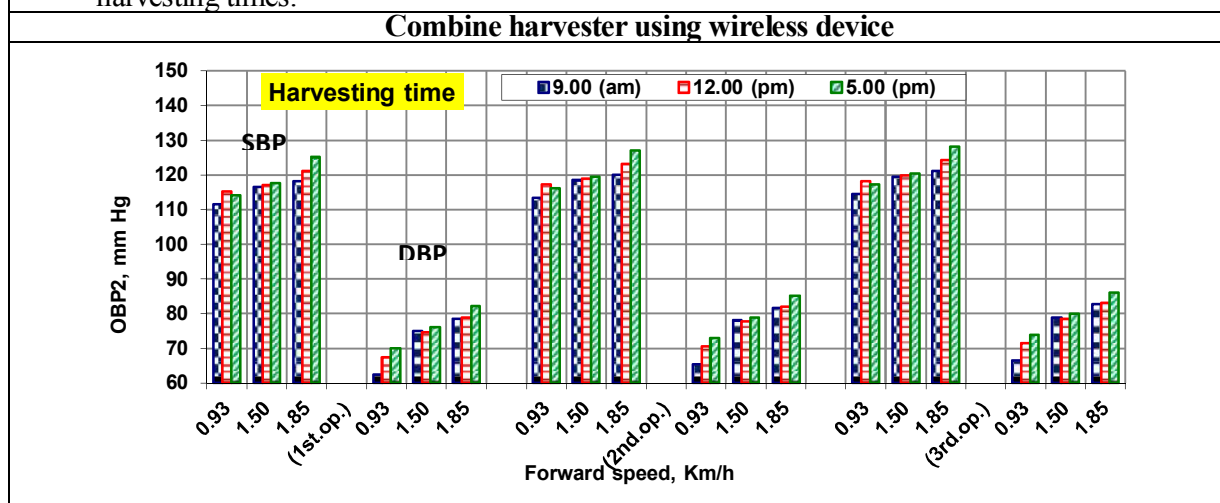


Fig. 15: Effect of the combine forward speeds on the operator's blood pressure at the different harvesting times.

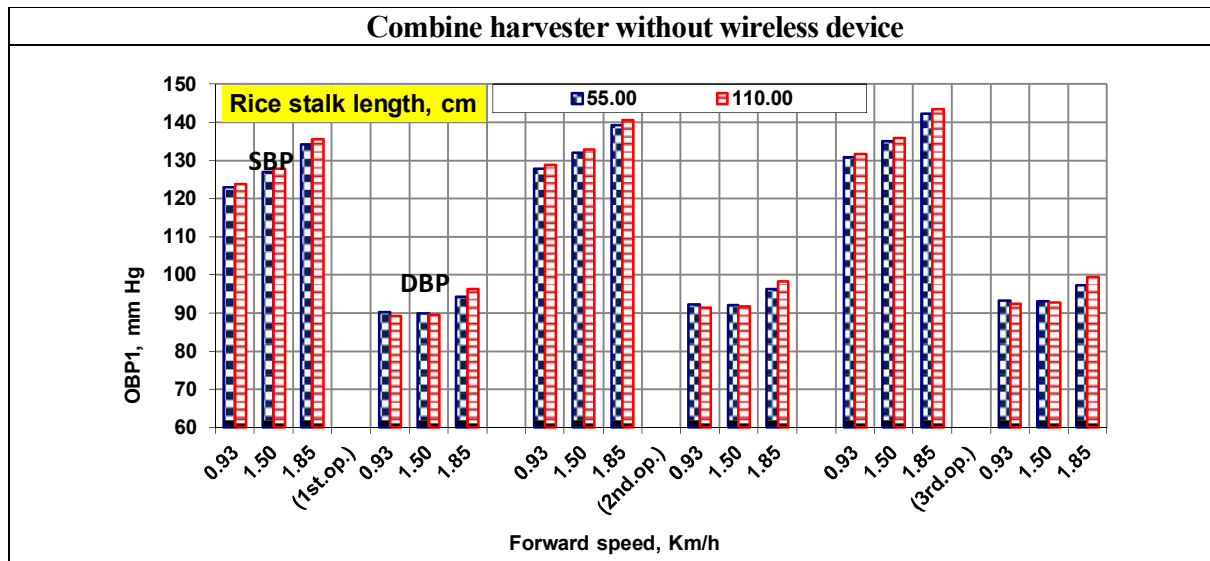


Fig. 16: Effect of the combine forward speeds on the operator's blood pressure at the rice stalk lengths.

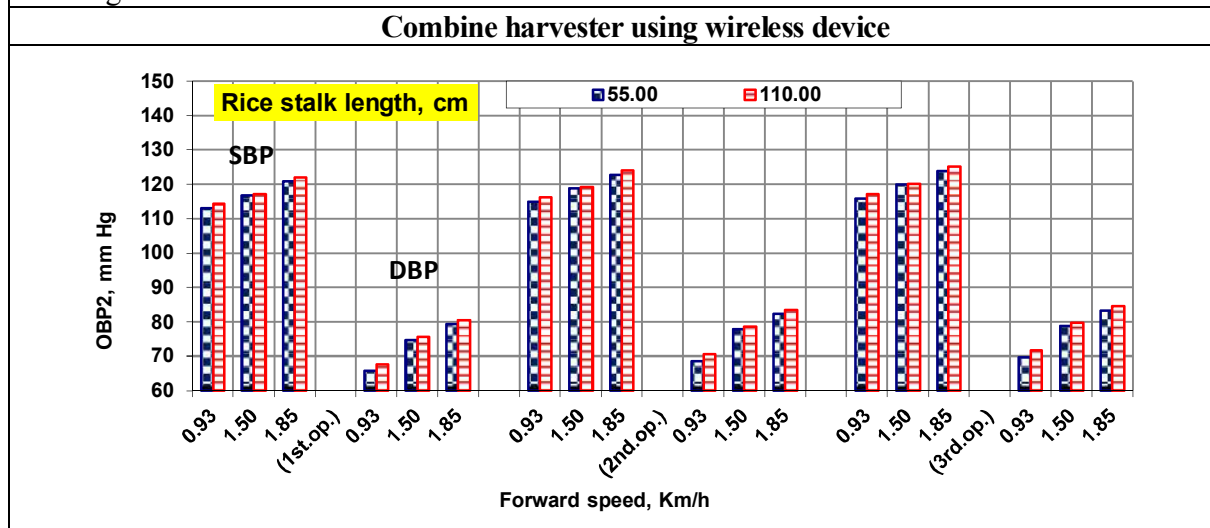


Fig. 17: Effect of the combine forward speeds on the operator's blood pressure at the different rice stalk lengths.

5- Factors affecting the operators heart rate:

Figs. (18 & 19) cleared the relationships compared between the combine harvesters models without attaching the wireless device and using it at the combines forward speed (FV, km/h) to the operators heart rate (HR, pulse/min) at the different harvesting times through the day (Ht). Its visible that maximizing the FV for the three different combine models of { (Y.48), (K.55) and (K.65)} respectively increases the operators heart rate (HR) with increasing the treatment of the (Ht) in a direct relationships. The maximum values of (RD1&2) were {(121, 135 and 146) & (107, 114 and 115) pulse/min}, respectively at 1.85 km/h of the FV for Ht of 5.00 pm, while the lowest values of the (HR1&2) were {(107, 111 and 116) & (76, 82 and 85) pulse/min}, respectively for of the 0.93 km/h of FV(180 plant/m²) at Ht of 9.00 am, as shown in Table (5).

Table. (5): The operators heart rate (HR) values at the interaction between (FV*Ht).

HR (Pulse/min)	Y.48 hp	K. 55 hp	K. 65 hp	FV (km/h)			Ht (am- pm)		
HR1 (Max.)	121	135	146	1.85	1.85	1.85	5.00	5.00	12.00
HR1 (Min.)	107	111	116	0.93	0.93	0.93	9.00	9.00	9.00
HR2 (Max.)	107	114	115	1.85	1.85	1.85	5.00	5.00	5.00
HR2 (Min.)	76	82	85	0.93	0.93	0.93	9.00	9.00	9.00

Also, as shown in Figs. (20&21), the maximum values of the (HR1&2) were {(119, 132 and 146) & (105, 113 and 115) pulse/min} respectively, as for FV of 1.85 km/h at 110 cm of the rice stalk length (RL), where the minimum values of the (HR1&2) were {(107, 114 and 119) & (80, 85 and 88) pulse/min}, respectively for the 0.93 km/h FV at 55 cm of RL, as shown in Table (6).

Table. (6): The operators heart rate (HR) values at the interaction between (FV*RL).

HR (pulse/min)	Y.48 hp	K. 55 hp	K. 65 hp	FV (km/h)			RL (cm)		
HR1 (Max.)	119	132	146	1.85	1.85	1.85	110	110	110
HR1 (Min.)	107	114	119	0.93	0.93	0.93	55	55	55
HR2 (Max.)	105	113	115	1.85	1.85	1.85	110	110	110
HR 2 (Min.)	80	85	88	0.93	0.93	0.93	55	55	55

These results may be owned to by increasing the combine forward speed the the operators heart rate increased as increasing the adrenalin in the blood and increasing the breathing level according to progress in working and also the weather temperature play a role with this . The total interactions between different treatments show a high significant effect (P < 0.05) for the HR1&2 values respectively. ANOVA analysis indicated highly significant differences between the treatments. A simple power regression analysis applied to relate the change in (HR) with the change in the tested factors for all treatments. The obtained regression equations were in the form of:

HR (pulse/min)	HR1=	HR2 =
1 th op.	98.830 +11.427 FV -0.353 Ht +0.0189 R.L (R ² =0.9571) (C.V=1.058)	59.945 +24.939 FV -0.599 Ht +0.0323 R.L (R ² =0.9955) (C.V=0.89)
2 nd op.	99.809 +17.759 FV -0.508 Ht +0.0303 R.L (R ² =0.9935) (C.V=0.595)	62.976 +27.758 FV -0.575 Ht +0.0283 R.L (R ² =0.9932) (C.V=1.123)
3 rd op.	95.985 +26.931 FV -0.624 Ht +0.0424 R.L (R ² =0.9964) (C.V=0.616)	66.0989 +27.83 FV -0.682 Ht +0.0343 R.L (R ² =0.9944) (C.V=1.009)

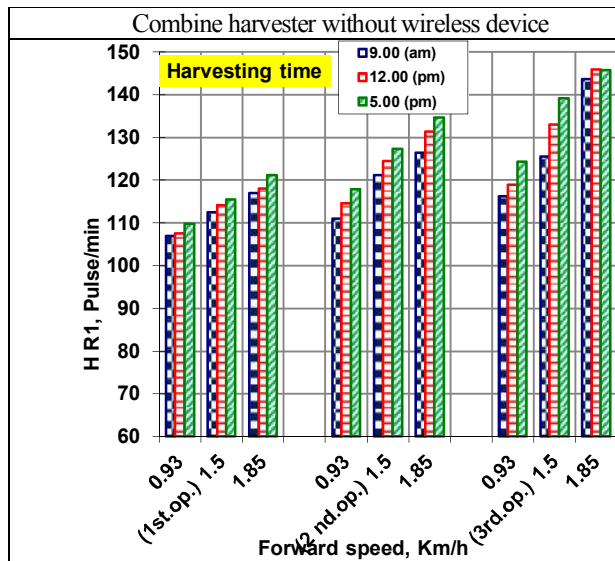


Fig. 18: Effect of the combine forward speeds on the operator's heart rate at the different harvesting times.

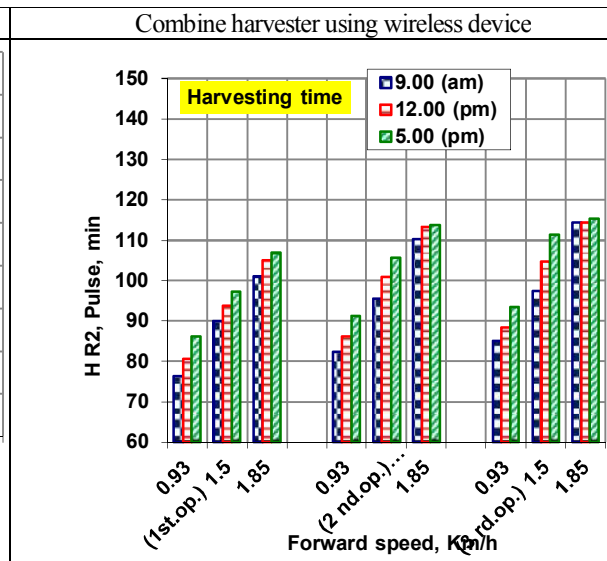


Fig. 19: Effect of the combine forward speeds on the operator's heart rate at the different harvesting times

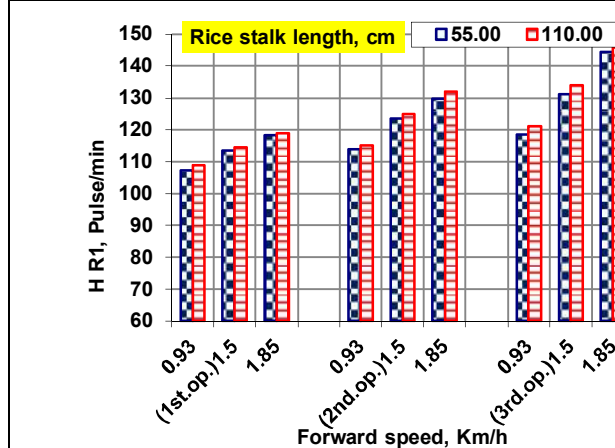


Fig. 20: Effect of the combine forward speeds on the operator's heart rate at the different harvesting times.

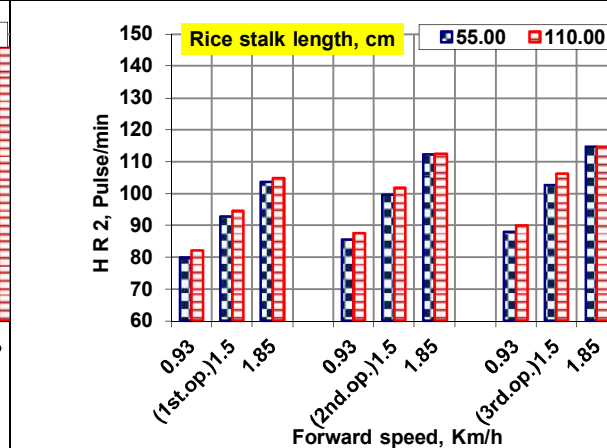


Fig. 21: Effect of the combine forward speeds on the operator's heart rate at the different rice stalk lengths.

B- Factors Affecting the combine harvesters performance

1- Factors affecting the combine harvesters maintenance time:

The relationships compared between the combine harvesters models without attaching the wireless device and using it at the combines forward speed (FV, km/h) to the maintenance time (M, min/fed) at the different harvesting times through the day (Ht) are shown in Figs. (22 & 23). As increasing the FV for the three different combine models of {(Y.48), (K.55) and (K.65)} respectively the maintenance time (M) decreases with increasing the treatment of the (Ht) in opposite relationships. The maximum values of (M1&2) were {(29.50, 28.97 and 29.32) & (16.98, 13.85 and 16.69) min/fed}, respectively at 0.93 km/h of the FV for Ht of 9.00 pm, while the lowest values of the (M1&2) were {(15.58, 13.25 and 13.89) & (1.14, 3.38 and 1) min/fed}, respectively for of the 1.85 km/h of FV at Ht of 5.00 am. The (M) reduction ratios from M2 than M1 were (42.44, 52.19 and 43.07 %) for the maximum values while its values were (42.44, 52.19 and 92.80%) for the minimum M values.

Moreover, the maximum values of the (M1&2) were {(29.20, 27.28 and 28.57) & (16.25, 12.76 and 15.15) min/fed} respectively, as shown in Figs. (24&25) for FV of 0.93 km/h at 55 cm of the rice stalk length (RL) except the sixth value at 110 cm of RL. where the minimum values of the (M1&2) were {(16.90, 14.84 and 15.81) & (3.13, 3.53 and 1.66) min/fed }, respectively for the 1.85 km/h FV at 110 cm of RL. The reduction ratios for (M) from M2 than M1 were (42.44, 52.19 and 43.07 %) for the maximum values while its values were (42.44, 52.19 and 92.80%) for the minimum M values.

These results attributed to by increasing the combine forward speed the maintenance time decreased as the harvesting operation when occurred on lowest forward speeds that mean there are a massive rice density which make more break downs leads to maximizing the consumed time to fix it but using the device confirm the operator about errors immediately which improved these situations and decreases the consumed maintenance time. The total interactions between different treatments show a high significant effect ($P < 0.05$) for the M1&2 values respectively. ANOVA analysis indicated highly significant differences between the treatments. A simple power regression analysis applied to relate the change in (M) with the change in the tested factors for all treatments. The obtained regression equations were in the form of:

M (min/fed)	M1=	M2=
1 th com.	$40.060 - 11.833 FV + 0.198 Ht - 0.0152 R.L$ ($R^2=0.9792$) (C.V=3.846)	$27.107 - 12.499 FV + 0.255 - 0.0144 R.L$ ($R^2=0.9911$) (C.V=0.609)
2 nd com.	$37.982 - 12.494 FV + 0.3292 Ht - 0.0185 R.L$ ($R^2=0.9886$) (C.V=3.127)	$20.693 - 8.988 FV + 0.264 Ht - 0.0176 R.L$ ($R^2=0.9905$) (C.V=2.758)
3 rd com.	$38.474 - 12.501 FV + 0.396 Ht - 0.0155 R.L$ ($R^2=0.9905$) (C.V=0.629)	$26.211 - 13.838 FV + 0.345 Ht - 0.0114 R.L$ ($R^2=0.9929$) (C.V=0.588)

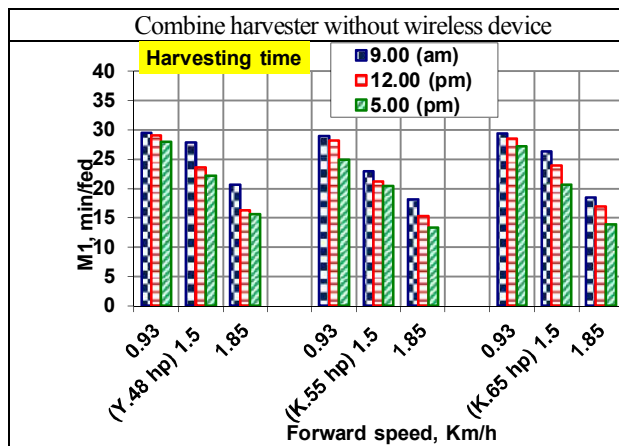


Fig. 22: Effect of the combine forward speeds on the maintenance time at the different harvesting times.

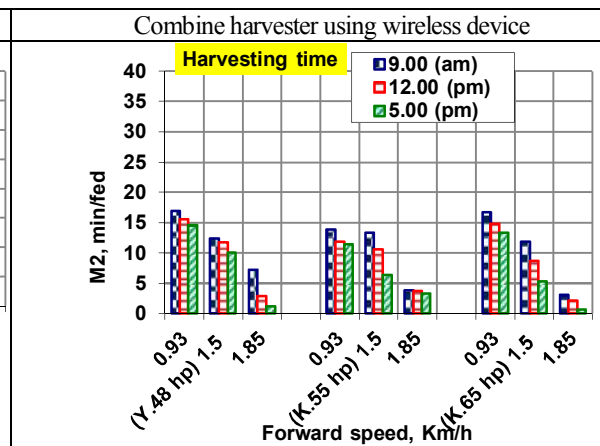


Fig. 23: Effect of the combine forward speeds on the maintenance time at the different harvesting times

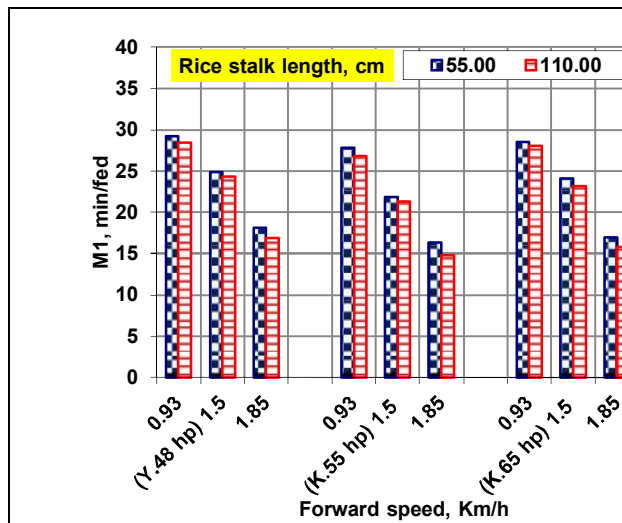


Fig. 24: Effect of the combine forward speeds on the maintenance time at the different harvesting times.

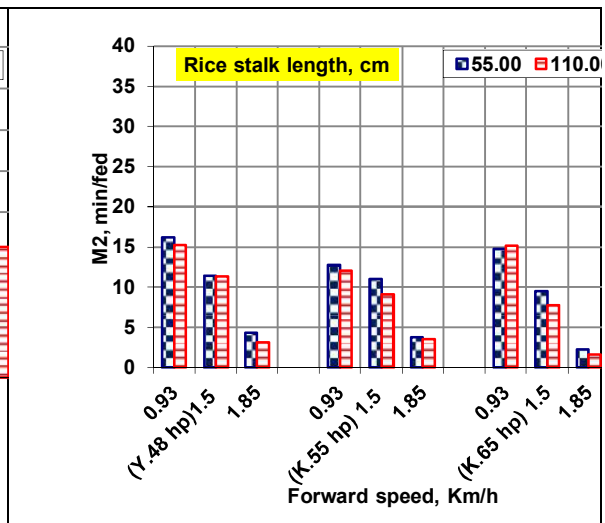


Fig. 25: Effect of the combine forward speeds on the maintenance time at the different rice stalk lengths.

2- Factors affecting the combine harvesters field efficiency

Figs. (26 & 27) explains the relationships compared between the combine harvesters models without attaching the wireless device and using it at the combine's forward speed (FV, km/h) to the combine field efficiency (Fe, %) at the different harvesting times through the day (Ht). Increasing the FV for the three different combine models of {Y.48}, {K.55} and {K.65} respectively increases the field efficiency (Fe) with increasing the treatment of the (Ht) in direct relationships. The highest values of (Fe 1&2) were {(74.03, 77.92 and 76.85) & (98.10, 94.38 and 98.88) %}, respectively at 1.85 km/h of the FV for Ht of 5.00 pm, while the lowest values of the (Fe 1&2) were {(50.83, 51.72 and 51.13) & (71.70, 76.92 and 72.19) %}, respectively for of the 0.93 km/h of FV at Ht of 9.00 am. The Fe increasing ratios from Fe2 than Fe 1 were (24.54, 17.44 and 22.28%) for the maximum values while its values were (29.11, 32.76 and 29.17%) for the minimum Fe values.

However, the highest values of the (Fe 1&2) were {(71.83, 75.27 and 73.65) & (94.79, 94.12 and 97.23) %} respectively, as shown in Figs. (28&29) for FV of 1.85 km/h at 110 cm of the rice stalk length (RL), where the lowest values of the (Fe 1&2) were {(51.33, 53.63 and 52.39) & (72.91, 78.73 and 74.74) %}, respectively for the 0.93 km/h FV at 55 cm of RL except the sixth value at 110 cm of RL. Also the Fe increasing ratios from Fe2 than Fe 1 were (24.22, 20.03 and 24.25 %) for the maximum values while its values were (29.60, 31.88 and 29.90 %) for the minimum Fe values.

These results may be due to by increasing the combine forward speed increases the operating performance specially as increasing the ability gradually ascendant from combine models under the study to maximize the operating rate for the Kubota 65 hp to reach the first level than two other combine models. However using the speaking wireless device improves the performance to increase the field efficiency. The total interactions between different treatments show a high significant effect (P < 0.05) for the Fe 1&2 values respectively. Statically ANOVA analysis indicated highly significant differences between the treatments. A simple power regression analysis applied to relate the change in (Fe) with the change in the tested factors for all treatments. The obtained regression equations were in the form of:

Fe (%)	Fe 1=	Fe 2=
1 th com.	33.233 +19.722 FV -0.330 Ht +0.0253 R.L (R ² = 0.9792) (C.V=1.516)	54.821+20.832 FV -0.424 Ht +0.024 R.L (R ² = 0.9911) (C.V=1.016)
2 nd com.	36.696 +20.822 FV -0.549 Ht +0.0308 R.L (R ² =0.9887) (C.V=1.12)	65.507 +14.981 FV - 0.44 Ht +0.0294 R.L (R ² = 0.9809) (C.V=1.19)
3 rd com.	35.872 +20.836 FV -0.660 Ht +0.0258 R.L (R ² =0.9905) (C.V=1.048)	56.326 +23.062 FV - 0.575 Ht +0.019 R.L (R ² =0.9929) (C.V=1.143)

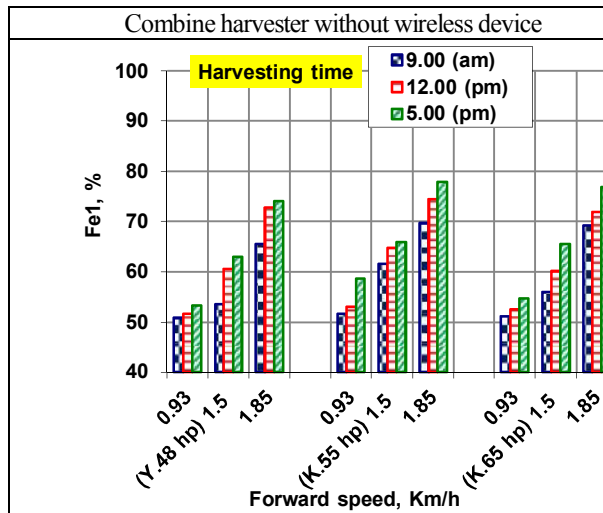


Fig. 26: Effect of the combine forward speeds on the field efficiency at the different harvesting times.

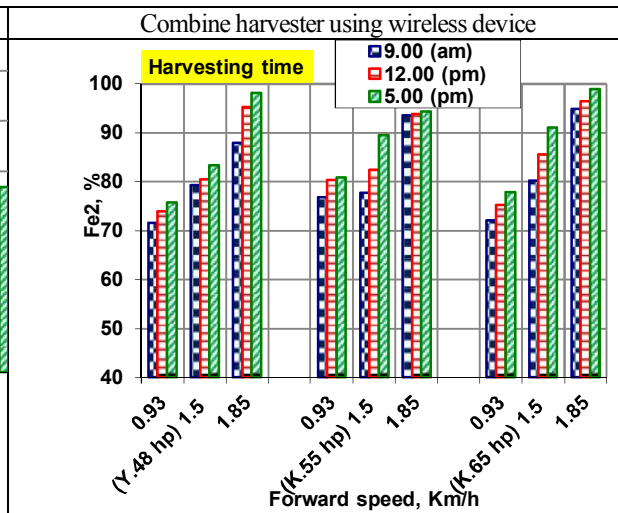


Fig. 27: Effect of the combine forward speeds on the field efficiency at the different harvesting times.

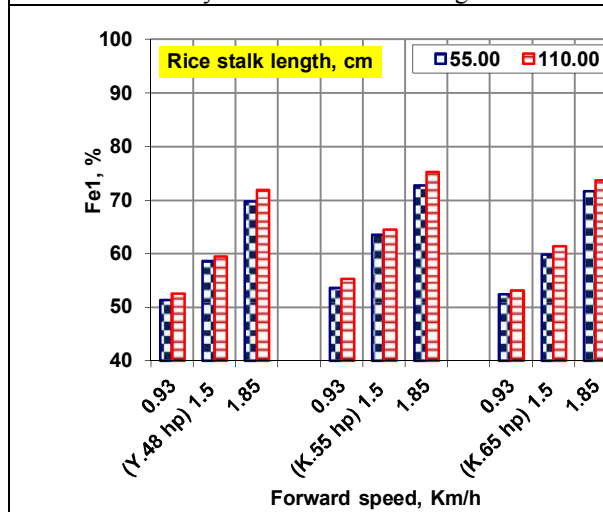


Fig. 28: Effect of the combine forward speeds on the field efficiency at the different harvesting times.

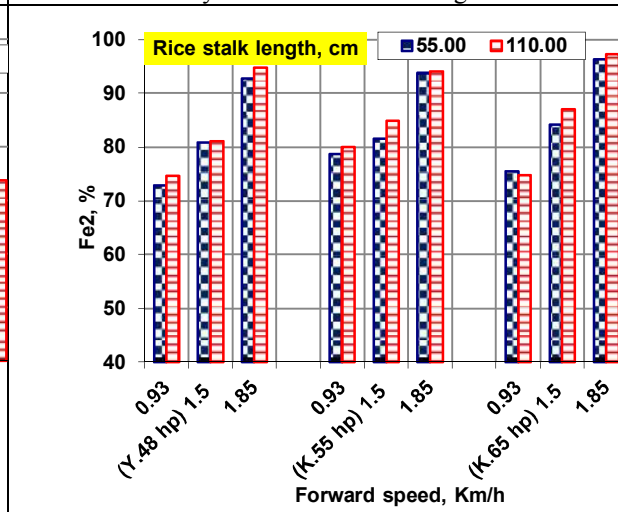


Fig. 29 Effect of the combine forward speeds on the field efficiency at the different rice stalk lengths.

3- Factors affecting the combine harvesters field capacity

The relationships compared between the combine harvesters models without attaching the wireless device and using it at the combines forward speed (FV, km/h) to the e combine field capacity (FC, fed/h) at the different harvesting times through the day (Ht) are illustrated in Figs. (30 & 31). Increasing the FV for the three different combine models of {(Y.48), (K.55) and (K.65)} respectively increases the field capacity (FC) with increasing the treatment of the (Ht) in direct relationships. The maximum values of (FC1&2) were {(0.74, 0.94 and 1.08) & (0.98, 1.13 and 1.38) fed/h}, respectively at 1.85 km/h of the FV for Ht of 5.00 pm, while the minimum values of the (FC1&2) were {(0.51, 0.62 and 0.72) & (0.72,

0.92 and 1.01) fed/h}, respectively for of the 0.93 km/h of FV at Ht of 9.00 am. So the FC increasing ratios from FC2 than FC 1 were (24.49, 16.81 and 21.74 %) for the maximum values while its values were (29.17, 32.61 and 28.71 %) for the minimum FC values.

Clearly, the maximum values of the (FC1&2) were {(0.72, 0.90 and 1.03) & (0.95, 1.13 and 1.36) fed/h} respectively, as shown in Figs. (32&33) for FV of 1.85 km/h at 110 cm of the rice stalk length (RL), where the minimum values of the (FC1&2) were {(0.51, 0.64 and 0.73) & (0.73, 0.94 and 1.05) fed/h}, respectively for the 0.93 km/h FV at 55 cm of RL except the sixth value at 110 cm of RL. Besides the FC increasing ratios from FC2 than FC 1 were (24.21, 20.35 and 24.26 %) for the maximum values while its values were (30.14, 31.91 and 30.48 %) for the minimum FC values.

These results may be due to by increasing the combine forward speed increases the field efficiency according to the rice density but using the investigated device save the operating time to achieve high levels from field capacity. The total interactions between different treatments show a high significant effect ($P < 0.05$) for the FC 1&2 values respectively. ANOVA analysis indicated highly significant differences between the treatments. A simple power regression analysis applied to relate the change in (FC) with the change in the tested factors for all treatments. The obtained regression equations were in the form of:

FC (fed/h)	FC 1=	FC 2=
1 th com.	$0.332 + 0.197 \text{ FV} - 0.0033 \text{ Ht} + 2.532 \text{ R.L}$ ($R^2=0.9793$) (C.V=0.015)	$0.548 + 0.208 \text{ FV} - 0.0042 \text{ Ht} + 2.404 \text{ R.L}$ ($R^2=0.9911$) (C.V=1.226)
2 nd com.	$0.44 + 0.250 \text{ FV} - 0.00658 \text{ Ht} + 3.697 \text{ R.L}$ ($R^2=0.9886$) (C.V=0.013)	$0.786 + 0.180 \text{ FV} - 0.00529 \text{ Ht} + 3.522 \text{ R.L}$ ($R^2=0.9809$) (C.V=1.393)
3 rd com.	$0.502 + 0.292 \text{ FV} - 0.0092 \text{ Ht} + 3.616 \text{ R.L}$ ($R^2=0.9906$) (C.V=0.015)	$0.789 + 0.323 \text{ FV} - 0.008 \text{ Ht} + 2.667 \text{ R.L}$ ($R^2=0.9929$) (C.V=0.014)

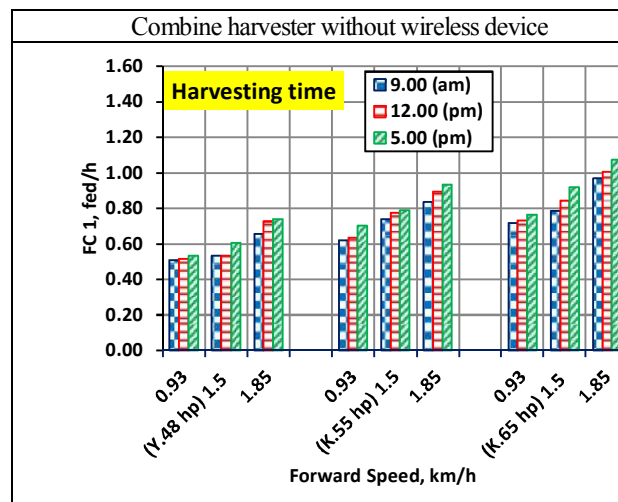


Fig. 30: Effect of the combine forward speeds on the field capacity at the different harvesting times.

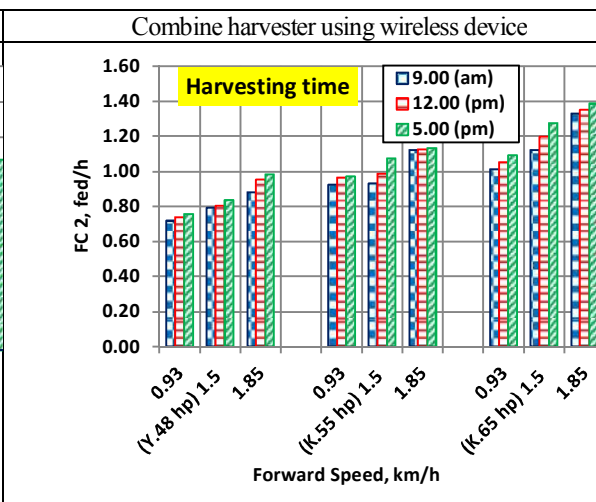


Fig. 31: Effect of the combine forward speeds on the field capacity at the different harvesting times

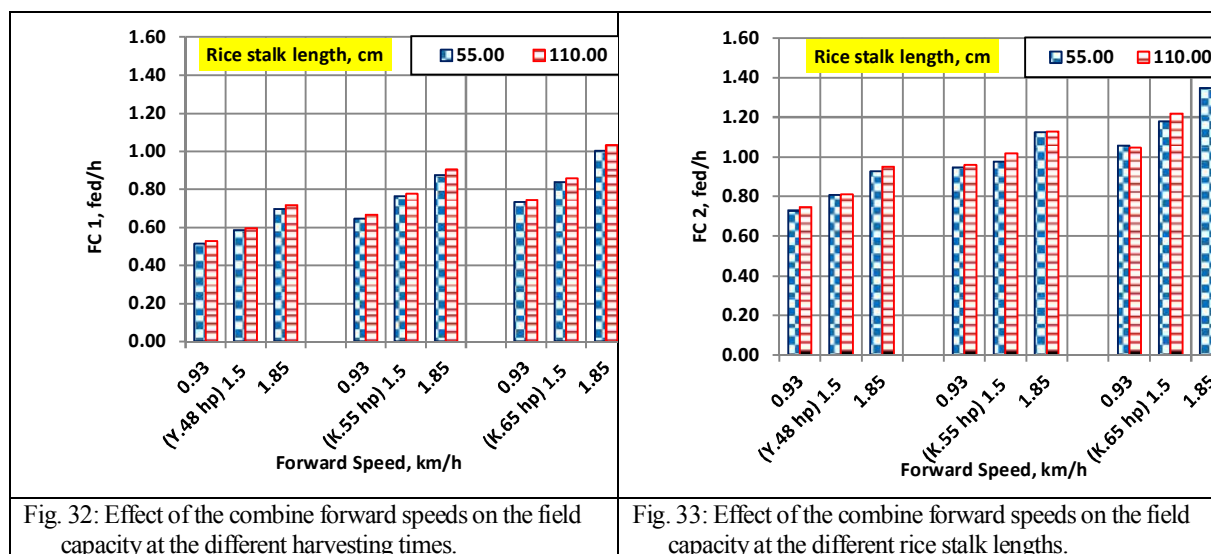


Fig. 32: Effect of the combine forward speeds on the field capacity at the different harvesting times.

Fig. 33: Effect of the combine forward speeds on the field capacity at the different rice stalk lengths.

4- Factors affecting the combine harvesters operating cost

The relationships are illustrated in Figs. (34 & 35) compared between the combine harvesters models without attaching the wireless device and using it at the combines forward speed (FV, km/h) to the combine operating cost (C, L.E/fed) at the different harvesting times through the day (Ht). Increasing the FV for the three different combine models of {(Y.48), (K.55) and (K.65)} respectively increases the operating cost (C) with increasing the treatment of the (Ht) in opposite relationships. The highest values of (C1&2) were {(162.87, 205.70 and 236.68) & (215.82, 49.15 and 304.55) L.E/fed}, respectively at 0.93 km/h of the FV for Ht of 5.00 pm, while the lowest values of the (C1&2) were {(111.83, 136.55 and 157.48) & (157.74, 203.06 and 222.35 L.E/fed)}, respectively for of the 1.85 km/h of FV at Ht of 9.00 am. So the C increasing ratios from C2 than C 1 were (24.53, 17.44 and 22.29 %) for the maximum values while its values were (29.10, 32.75 and 29.17 %) for the minimum C values.

Besides, the maximum values of the (C1&2) were {(158.02, 198.71 and 226.84) & (208.54, 248.46 and 299.47) L.E/fed} respectively, as shown in Figs. (36&37) for FV of 0.93 km/h at 110 cm of the rice stalk length (RL), where the minimum values of the (C1&2) were {(112.93, 141.58 and 161.36) & (160.40, 207.85 and 230.21) L.E/fed}, respectively for the 1.85 km/h FV at 55 cm of RL except the sixth value at 110 cm of RL. The C increasing ratios from C2 than C 1 were (24.23, 20.02 and 24.25 %) for the maximum values while its values were (29.59, 31.88 and 29.91 %) for the minimum C values.

These results may be due to by increasing the combine forward speed the combine operating cost decreased as increasing the performance level under attaching the investigated device to reduce the wasted time in maintenance operations and conform the operators to achieve more harvesting areas in the same unit time. The total interaction between different treatments shows a high significant effect ($P < 0.05$) for the C1&2 values respectively. ANOVA analysis indicated highly significant differences between the treatments. A simple power regression analysis applied to relate the change in (C) with the change in the tested factors for all treatments. The obtained regression equations were in the form of:

C (L.E/fed)	C1=	C2=
1 th com.	73.113+43.389 FV - 0.726 Ht +0.056 R.L (R ² =0.9792) (C.V=2.501)	120.607 +45.83 FV- 0.934 Ht +0.0523 R.L (R ² = 0.9911) (C.V=1.226)
2 nd com.	110.492 +64.175 FV -2.033 Ht +0.0795 R.L (R ² =0.9886) (C.V=1.745)	173.467 +71.0377 FV -1.77 Ht +0.0587 R.L (R ² = 0.9809) (C.V=1.393)
3 rd com.	96.877 +54.972 FV -1.448 Ht +0.081 R.L (R ² =0.9905) (C.V=1.691)	172.95 +39.548 FV -1.163 Ht +0.078 R.L (R ² =0.9929) (C.V=1.143)

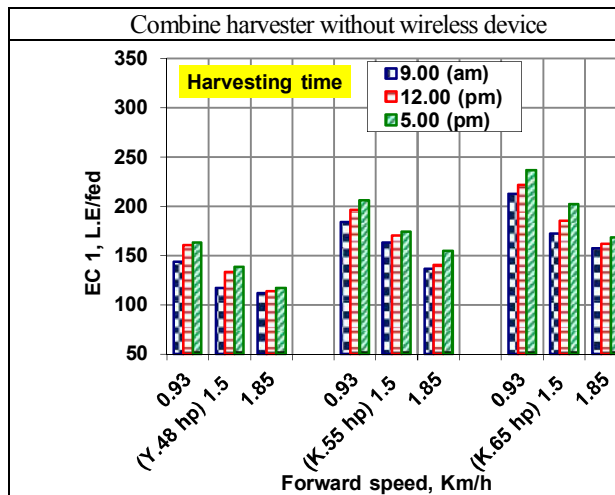


Fig. 34: Effect of the combine forward speeds on the operating costs at the different harvesting times.

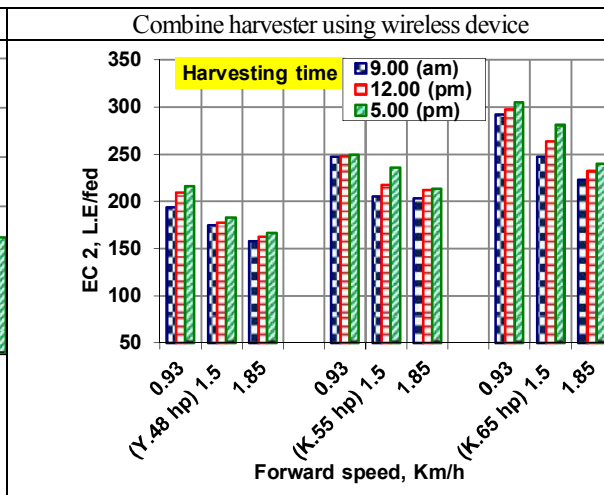


Fig. 35: Effect of the combine forward speeds on the operating costs at the different harvesting times

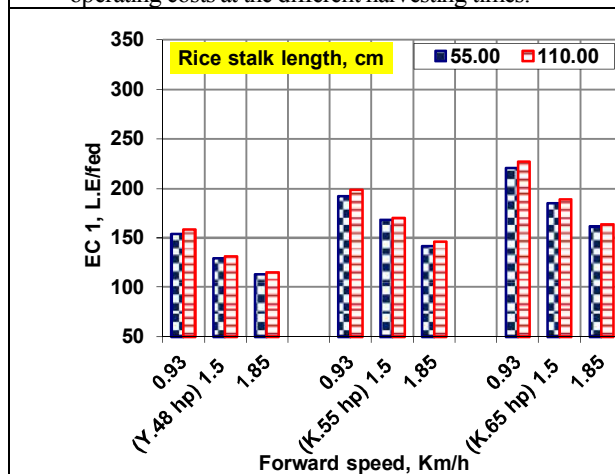


Fig. 36: Effect of the combine forward speeds on the operating costs at the different harvesting times.

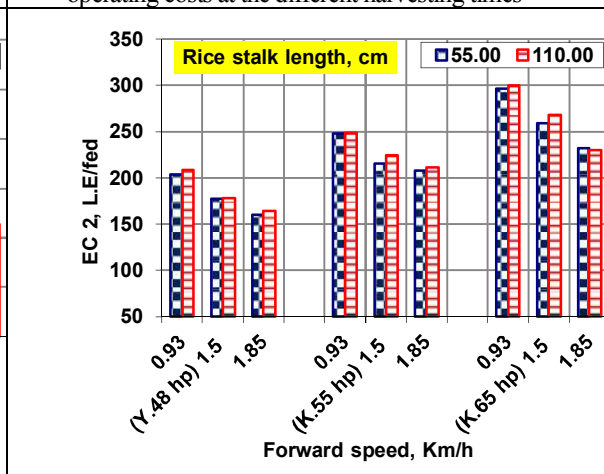


Fig. 37: Effect of the combine forward speeds on the operating costs at the different rice stalk lengths.

Economic data analysis for the three different combines under study: the total operating costs through two harvesting seasons: season 2016 with using the speaking wireless diagnosing device and season 2015 without using it. The rice harvesting seasons were calculated for two months approximately and summed at 8 hours/day and the total cost of replacing spare parts before and through the season and the operating costs of fuel, lubrication and operators wages were discounted to get the net profit as been cleared in the Table (7):

Table.7: Economic data analysis for the tested combine models.

Model		Total area fed.	Total operating costs, L.E	Spare parts costs, L.E	Fuel and lubrication costs, L.E	Operators wages, L.E	Net profit L.E
Y.48 hp	2015	217	57590	8200	5725	4340	39325
	2016	358	78740	7530	9300	7160	54750
K.55 hp	2015	333	73210	9550	8575	6660	48425
	2016	443	97500	8450	11375	8860	68815
K.65 hp	2015	375	82510	10100	9675	7500	55235
	2016	519	114185	9650	13375	10380	80780
Profit ratios according using device, %					Y.48 hp (28.17 %)	K.55 hp (29.63%)	K.65 hp (31.62%)

CONCLUSION

The main results are summarized as follow:

- 1- The results indicated that the maximum values of noise intensity (NI) were (98.97, 92.84 and 96.35 db), for the three different combine models of {(Y.48), (K.55) and (K.65)} respectively at FV of 1.85 km/h for Ht of 5.00 pm and 55 cm for RL.
- 2- The results showed that the three operators under study which wears the headphones their hearing levels were normal while the three others were moderated whose don't wear the headphones.
- 3- The results indicated that the operators response degree RD increasing ratios from RD2 than RD1 were (18.18, 28.57 and 40.0 %) for the maximum values for the three different combine models of {(Y.48), (K.55) and (K.65)} at 1.85 km/h of the FV for Ht of 5.00 pm and RL 110 cm.
- 4- The results indicated that the operators blood pressure decreased to the normal levels due to using the protective headphones to record the lowest values of the (OBP 2) as (112/63, 114/66 and 115/67 mm Hg), respectively for the combine operators at 0.93 km/h of FV for Ht of 9.00 am and 55 cm of RL.
- 5- The results indicated that the operators heart rate HR decreased to the normal levels due to using the protective headphones to record the lowest values of the (HR 2) as (76, 82 and 85 pulse/min), respectively for the combine operators at 0.93 km/h of FV for Ht of 9.00 am and 55 cm of RL.
- 6- The results indicated that the maintenance time M reduction ratios from M2 than M1 were (42.44, 52.19 and 92.80 %) for the maximum values {(29.50, 28.97 and 29.32) & (16.98, 13.85 and 16.69) min/fed} for the three different combine models of {(Y.48), (K.55) and (K.65)} at 1.85 km/h of the FV for Ht of 5.00 pm and RL 110 cm.
- 7- The results indicated that field efficiency Fe increasing ratios from M2 than M1 were (24.54, 17.44 and 22.28%) for the maximum values {(74.03, 77.92 and 76.85) & (98.10, 94.38 and 98.88) %} for the three different combine models of {(Y.48), (K.55) and (K.65)} at 1.85 km/h of the FV for Ht of 5.00 pm and RL 110 cm.
- 8- The results indicated that field capacity FC increasing ratios from FC2 than FC1 were (24.49, 16.81 and 21.74 %) for the maximum values {(0.74, 0.94 and 1.08) & (0.98, 1.13 and 1.38) fed/h} for the three different combine models of {(Y.48), (K.55) and (K.65)} at 1.85 km/h of the FV for Ht of 5.00 pm and RL 110 cm.
- 9- The results indicated that operating costs C increasing ratios from C2 than C1 were (24.53, 17.44 and 22.29 %) for the maximum values {(162.87, 205.70 and 236.68) & (215.82, 49.15 and 304.55) L.E/fed} for the three different combine models of {(Y.48), (K.55) and (K.65)} at 0.93 km/h of the FV for Ht of 5.00 pm and RL 110 cm.

REFERENCES

- 1) Arnaout, M. A. (1980). "A study of different rice harvesting methods in different field sizes with reference to grain losses". M. Sc. Thesis, Agric. Eng. Dept., Faculty of Agric., Zagazig University, Egypt.
- 2) Arndt, V.; D. Rothenbacher; H. Brenner; E. Fraisse; Z. Schender; B. Lien; U. Daniel and S. Schubert; Fliedner TM. (1996). Older workers in the construction industry: result of a routine health examination and a five -year follow up. *Occupational and Environmental Medicine* 53(10) : 686-691.
- 3) El-Haddad, Z. A; M. Y. El-Anssary and S. A. Aly (1995):Cost benefit study under integrated mechanization systems. *Misr J. Agr. Eng.*, 12 (1): 27-35.
- 4) Elise, .E.M.M; V. Kempen; H. Kruize; C. Hendrick.; H. Boshuizen and B. Caroline (2002). The association between noise exposure, blood pressure and Ischemic heart disease: *Environmental health prospect* 2002; 110:307-317.
- 5) El-Khateeb, H. A. (2005). "A study on performance of axial flow combine harvester in rice crop harvesting". The 13th Annual conference of the Misr society of Agr. Eng.,: 381-401.
- 6) El-Nakib, A.A; Z. Y. Abdel-Lateef, A. A. El-Messery and A. Khattab (2003). "Mechanical harvesting losses in rice crop using combine harvester". *Misr J. Agr. Eng.*, 20 (4): 889-907.
- 7) El-Sharabasy, M. M. A. (2007). "Total grain losses, energy and cost requirements for harvesting rice crops mechanically in delta Egypt". *Misr J. Ag. Eng.*, 24 (1):1-17.
- 8) Fouad, H. A; S. A. Tayel, Z. El-Hadad and H. Abdel-Mawla (1990). "Performance of two different types of combines in harvesting rice crop in Egypt". *AMA*. 21 (3): 17-22.
- 9) Gates, R. S. and D. G. Overhults (1992). "A survey of electronic environmental controllers". Published by the American Society of Agric. Eng. St. Joseph, Michigan [www. Asabe.org](http://www.asabe.org). 35(3): 993-998.
- 10) Ghonimey, M. I. and M. N. Rostom (2002)."Tech-Economical approach to combine harvesters evaluation". *Misr J. Agr. Eng.*,19 (1): 83-98.
- 11) Green M.S.; S. Melamed and J. Luz (1992). "Noise exposure, noise annoyance and their relation to psychological distress, accident and sickness absence among blue-collar workers". *The CORDIS Study J. Med. Sci* 28: 629-635.
- 12) Helmy, M. A; S. M. Gomaa, F. I.Hindy and R. R. Abu Shieshaa (1995). "Comparative study on two different rice combine harvester machines". *Misr J. Agr. Eng.*, 12 (2): 479-495.
- 13) Kepner, R. A.; R. Bainer and E.L. Barger (1982). "Principles of farm machinery". 3rd ed. avi pub Co. West part, Connecticut. USA. P. 464 – 468.
- 14) Lercher.P; J. Hortnagle and W.W. Koffer (1993). "Work noise annoyance and blood pressure ,combined effects with stressful working conditions". *International Archives on occupational and Environ Health* 65: 23-28.
- 15) Obelenis, V. and V. Malinauskiene (2007). "The influence of occupational environment and professional factors on the risk of cardiovascular disease". *Medicina (Kaunas)*; 43(2):96-102.
- 16) Oida , A. (1997). "Using personal computer for agricultural machinery management". Kyoto University. Japan. JICA publishing.
- 17) Rashid .M; J.K. Ghulam; A.J. Alam and A.-Ul-Haq. (2002). "Effect of 90 decibel noise of 4000 hertz on blood pressure in young adult". Retrieved Feb. 21, 2010, from <http://www.wayubmed.edu.pk/JAMC/PAST/16-2/Rashid.html>.

- 18) Reid, W. S. (2002). "An assessment of the control and safety needs of autonomous agricultural vehicles and implement systems on farm property". : 422-431 in automation technology for off-road equipment, Proceedings of the July 26-27, 2002 Conference (Chicago, Illinois, USA)., Australian Journal of Basic and Applied Sciences, 7(1): 494-497.
- 19) Ryan, R., D. Harry; P.Jim, and K. Wonmo (2011). "A dynamic grain flow model for a mass flow yield sensor on a combine" .PrecisionAgriculture, 12(5),: 732–749.
- 20) Sabitoni A.E. (2006). "Noise exposure associated with high blood pressure, stroke, and heart diseases". Archives of environmental health, Retrieved Feb.23, 2010. From <http://www.lhsfna.org/index.cfm/object>.
- 21) Singh, N. and S.C. Davar (2004). "Noise pollution–sources, effects and control". Journal of human ecology 16(3): 181-187.
- 22) Vermeer, W. F. Passchier and W. March (2000). "Noise exposure and public health. Environmental health perspectives". 108 (1) : : 123-131.
- 23) Wei, X.H., Li, Y.M. and J. Chen (2009). "System integration of working process intelligent monitoring and controlling devices for combine harvester". Transactions of the Chinese Society of Agricultural Engineering 25, :56–60.
- 24) Zareei, S., S. Abdollahpour, M. Moghaddam, and H. Sahrayan (2012). "Optimum setting of combine header for wheat harvesting using Taguchi method". Research on Crops, 13(3): 1142-1146.
- 25) Zhao, Y.; S. Zhang; S. Selins and R.Spear (1991). "A dose response relation for noise induced hypertension". Industrial medical journal 48:179-84.
- 26) Zhou, Y., Liu, M. S., Zhang, Z. D., and R. L. Huang (2008). "Research on application of fuzzy neural network in combine harvester". In Proceedings of the fifth international conference on fuzzy systems and knowledge discovery, IEEE Comp. Soc. :231–235.

تطوير جهاز إلكتروني ناطق لتشخيص الأعطال في آلات حصاد الأرز

* أحمد شوقي السيد السيد ، *محمود السيد العراقي و *وائل فتحي علي المتولي

* معهد بحوث الهندسة الزراعية – مركز البحوث الزراعية – مصر.

يهدف هذا البحث الي استحداث وتطوير جهاز إلكتروني لاسلكي لتحديد الأعطال سمعياً ملحق بكومباين حصاد الأرز الياباني لتشخيص الاعطال ليكون جزء من نظام تشغيله الكهربائي بسبب سوء رؤية لمبات الليد المتصلة بالحساسات والموجودة بتابلوه الكومباين بسبب حدة ضوء الشمس أو لتساعد الأتربة نتيجة عمليات الحصاد. تم تصميم الجهاز الإلكتروني لحماية كلا من الكومباين والمشغل من شدة الضوضاء المتولدة من الكومباين أثناء الحصاد والتي تتخطي الحدود المسموح بها لحماية حاسة السمع (٧٠ ديسيبل) وذلك باستخدام سماعة لاسلكية تمنع الضوضاء عن أذن المشغل وتخبره بعبارات منطوقة ومسجلة باللغة العربية عن مكان العطل ونوعه الاجراءات اللازمة لإصلاحه وذلك لتوفير وقت وتكاليف الصيانة لزيادة معدلات الاداء والتشغيل والكفاءة للكومباين. تتصل الدائرة الإلكترونية اللاسلكية الناطقة بحساسات الكومباين المتصلة بالميكروكومبيوتر الخاص بالكومباين لتتقل الإشارة الكهربائية للعطل الحادث الي وحدة ارسال متصلة بالجهاز الي السماعات اللاسلكية علي أذن المشغل والتي يتم توليفها مع التردد الخارج من وحدة الارسال لتشخيص الأعطال التالية: حرارة المحرك ، ضغط دورة تزييت المحرك، شحن البطارية، امتلاء خزان الحبوب، السرعة الدورانية لدرفيل الحصاد الرئيسي والدرفيل المعالج، سرعة بريمة الراجع وجنزير تصريف القش. حدود استقبال تردد الإشارة الخارجة من الجهاز الإلكتروني ١٥ متر حول مركز وجود الكومباين مما يسهل عملية مراقبة أداء الكومباين عن بعد.

تم إجراء التجارب الحقلية خلال موسمي حصاد أرز ٢٠١٥ و ٢٠١٦ علي ثلاثة موديلات مختلفة من الكومباينات وكذلك علي مشغليها وهم موديل يانمار ٢٠١٠ (٤٨ حصان) وكوبوتا ٢٠١١ (٥٥ حصان) وكوبوتا ٢٠١٢ (٦٥ حصان) علي الترتيب وذلك لمقارنة أدائهم تحت مستويات العوامل التالية: ١- ثلاثة سرعات للكومباين (٠,٩٣ ، ١,٥ ، ١,٨٥ كم/الساعة "بطئ" "قياسي" "سريع") ٢- وثلاثة أوقات مختلفة خلال اليوم (٩,٠ ص، ١٢,٠ ظ، ٥,٠ م) ٣- ومستويين من صنفين مختلفين في طول الساق (٥٥، ١٢٠ سم) وذلك عند مستوي رطوبة المحصول الموصي بها ٢٥%. تم إجراء القياسات لشقين رئيسيين أو لا علي المشغلين من قياس شدة الضوضاء و معدل الاستجابة للأعطال، ضغط الدم وعدد دقات القلب للمشغلين مع معامل كتلة الجسم ودرجة السمع لهم بعد الموسم. ثانيا علي الكومباين من قياس السعة والكفاءة الحقلية للكومباين وصافي الربح بعد خصم تكاليف الصيانة مقارنة بعدم تركيب الجهاز الإلكتروني السمعي الناطق.

واشتملت أهم النتائج علي التالي: أدي استخدام الجهاز الإلكتروني الي زيادة السعة والكفاءة الحقلية للكومباينات تحت الدراسة عن المواسم السابقة وذلك بنسب زيادة (٢٤,٤٩ ، ١٦,٨١ ، ٢١,٧٤%) للثلاثة موديلات علي الترتيب وذلك للسعة الحقلية باستخدام الجهاز. كذلك قلت تكاليف الصيانة الكلية لهذه الكومباينات مقارنة بنفس الموديلات في الموسم السابق وازداد العائد الاقتصادي لها بنسب زيادة (٢٨,١٧ ، ٢٩,٦٣ ، ٣١,٦٢%) علي الترتيب عن الموسم السابق. كذلك ازدادت معدل استجابة المشغلين للأعطال بنسبة ١٠٠%. كذلك أنه باستخدام سماعات الرأس قد قامت بحماية المشغلين تماما من الضوضاء المتولدة من الكومباين والتي وصلت أقصاها ل ٩٦ ديسيبل والتي تتجاوز الحدود المسموح بها ٧٠ ديسيبل وتحسنت حاسة السمع للمشغلين الذين استخدموا الجهاز مقارنة بزملائهم الذين قاموا بتشغيل نفس الموديل واستقرت لديهم معدلات ضغط الدم ونبض القلب مع معامل كتلة الجسم حول الحدود الطبيعية (٨٠/١٢٠، ١٠٠ نبضة/الدقيقة). لذلك نوصي باستخدام الجهاز الناطق لاسلكيا لتحديد الأعطال وتعميمها علي قطاع الزراعة الآلية وذلك لتحقيق زيادة معدلات التنمية الزراعية المصرية.

DRYING OF CHAMOMILE FLOWERS USING MICROWAVE OVEN

EL SAEIDY, E.A.¹, G.K.ARAFA² and FATMA A. NASR²

1: Department of Agricultural Engineering, Faculty of Agriculture, Menoufia University.

2: Agricultural Engineering Research Institute, Agriculture Research Center.

Abstract

A study was carried out to test and evaluate the use of microwave for drying chamomile flowers. The experiment was done at the Agriculture Engineering Department, faculty of Agriculture, Menoufia University. The experimental treatments include three different levels of power (450, 720, and 900 W) and three different loading treatments (1.5, 3, and 4.5 kg/m²). The drying behavior was simulated using two different models. The first model (Lewis) and the second (Henderson, and Pabis). The studied models were validated with the obtained drying data, and it was found that the most valid model to predict the moisture content changing during the drying process was Lewis model in terms of precision and application simplicity. Final quality of the dried chamomile was also determined. The quality tests of the dried chamomile showed that, using power of 900 W with load 3 kg/m² recorded the best dried chamomile quality in terms of essential oil yield and other components.

KEY WORDS: Microwave oven, Drying, Chamomile.

INTRODUCTION

The history of medicinal is associated with the development of civilizations. In all regions of the world, the history shows that these plants have always occupied an important place in medicine, the composition of perfumes, food and cooking. China is the birthplace of arable medicine. Some countries especially India, Egypt, Greece and Italy represent civilizations in which aromatic and medicinal plants had an important place.

Medicinal and aromatic plants cultivated area in the world has been increased, also the worldwide and local demand increasing for medicinal, aromatic plants and herbs. The total cultivated area of medicinal and aromatic plants recently increased in Egypt to about 42,000 feddan. Chamomile is one of major aromatic plants in Egypt. The total cultivated area of the chamomile was about 11000 feddan and the total production estimated was about 9000 ton, These records was illustrated according to the reports of the Agricultural economics and statistics, Ministry of Agricultural, Egypt (2014).

Chamomile is one of the most widely used medicinal plants in the world. It has been reported to be beneficial for relief of sleeping disorders, diarrhea, colic, wounds, mucositis, and eczema McKay and Blumberg (2006).

Microwave is a rapid dehydration technique that can be applied to dry, particularly to fruits and vegetables. The advantages of microwave are, short drying time, improved product quality and flexibility in producing a wide variety of dried produces El Saeidy and El Bltagy (2011).

During drying, food materials undergo physical, chemical, and biological changes, which can affect some natural attributes like texture, color, flavor and nutritional value. Therefore, a second objective of drying should be to produce dried food in good quality from nutritional and organoleptic standpoint Ghanem *et al.* (2013).

In Egypt, natural sun drying is one of the most common way to conserve agricultural products, considerable losses may occur during natural sun drying due to various influences, such as rodents, birds, insects, rain, storms and microorganisms. The quality of the dried products may also be lowered significantly Soliman (2016).

Offering advantages of energy-saving rapid drying rates, short processing times, deep penetration of the microwave energy, instantaneous and precise electronic control, and clean heating processes, microwave-assisted drying (MWD) has become a popular method that is currently used for many materials and processes Rattanadechoa and Makulb (2016).

The drying time can be reduced by using microwave energy, which is rapidly absorbed by the product water molecules and consequently results in rapid evaporation of water and thus higher drying rates. The interior temperature of dried microwave heated food is higher than the surface temperature and moisture is transferred to the surface more dynamically than during convective drying Torringa *et al.* (2001).

The most important aspect of drying technology is the Mathematical modeling of the drying process and equipment Its purpose is to allow design engineers to choose the most suitable operating conditions and then size the drying equipment and drying chamber accordingly to meet the desired operating conditions Darvishi^{et al} (2013).

MATERIALS AND METHODS

Materials:

Freshly-harvested chamomile plants (*Matricaria chamomilla*) were used for conducting the experimental work. The initial moisture content of the freshly harvested chamomile was about 354.54% (dry basis). Flowers of chamomile were loaded in the oven and the drying runs were stopped when the final moisture content reached about 12 % (dry basis) European Pharmacopoeia, 2005.

Laboratory microwave oven:

Specifications used during the experimental work. The microwave oven have 900W, the levels of output are (90,.....900W).

Measurements:

Moisture Content for chamomile flowers:

The initial moisture content of initial products was determined by drying the flowers in an electrical hot air oven at 70°C for 24 hours. The quantity of moisture presents in the material could be expressed according to either wet or dry basis, Al-Mashhoor (2015).

$$MC (%) = \frac{Wi - Wd}{Wi} \dots\dots\dots (1)$$

$$MCd(\%) = \frac{Wi - Wd}{Wd} \dots\dots\dots (2)$$

Where:

- MCw:** Moisture content on wet basis, %
- MCd:** Moisture content on dry basis, %
- Wd** : Weight of dry matter in product, Kg
- Wi** : Initial weight the fresh product, Kg

Drying rate:

$$DR (\%) = (Mt-dt- Mt)/dt\dots\dots\dots(3)$$

DR : Drying rate, %.

M_t : moisture content (Kgwater/Kg dry matter) at time t.

M_{t+dt} : moisture content (Kgwater/Kg dry matter) at time t+dt.

Microwave drying efficiency:

To calculate microwave drying efficiency the following equation was used (Al-Mashhoor 2015).

$$\eta_m = W_r * \frac{LHV}{P} * 100 \dots \dots \dots (4)$$

Where:-

- η_m : Microwave drying efficiency, %
- W_r : Water removal, (Kg/s)
- LHV : Latent heat of vaporization 2256.7*10³, (J/Kg)
- P : Power consumed, (1350), (W).

Examined drying models for simulating the drying data:

1- Lewis model:

$$MR = \exp (-K_L t) \dots \dots \dots (5)$$

$$MR = \frac{M - M_f}{M_o - M_f} \dots \dots \dots (6)$$

Where,

- MR = Moisture ratio, dimensionless
- M = Instantaneous moisture content during the drying process, %(d.b)
- M_o = Initial moisture content of chamomile samples, % (d.b).
- M_f = Final moisture content of chamomile samples, % (d.b).
- K_L = Drying constants, min⁻¹
- t = Drying time, min

2- Henderson and Pabis model

$$MR=A\exp(-K_h t)\dots \dots \dots (7)$$

Where,

- A : Drying constants, dimensionless
- K_h : Drying constants, min⁻¹

Lewis and Henderson and Pabis model has been applied to fit the drying data of chamomile. After converting it's for the exponentially form and calculating the constants (K_h and A) from relating the moisture ratio (MR) of the sample with the drying time (T).

RESULTS AND DISCUSSION

Influence of drying parameters on the change in chamomile moisture content:

Figs (1 a,b and c) illustrate the change in chamomile moisture content as related to drying time at different levels of loads and microwave power. As shown in the figure, the reduction in moisture content of chamomile with the experimental treatments and it increased with the increase of microwave power, and the load.

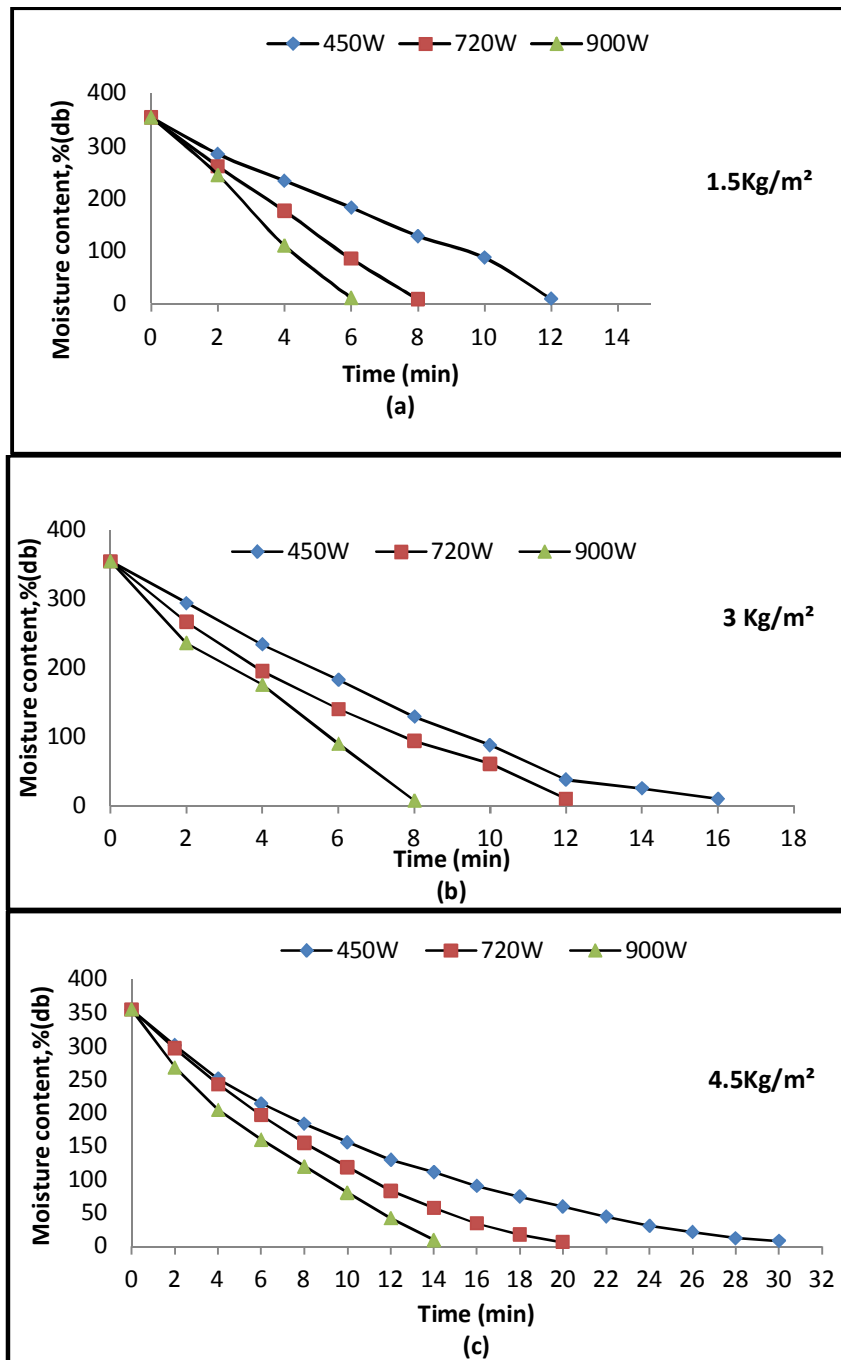


Fig. (1) Chamomile moisture content as related to drying time at different levels of microwave power and loads.

Effect of different parameters on drying rate:

Figs (2 a, b and c) describe the relation between the drying rates and moisture content for different microwave power 900, 720 and 450W and three loading levels 1.5, 3 and 4.5 kg/m². The drying rate decrease continuously with decreasing moisture content. This is due to that; the amount of free moisture was very high which was easily removed in the first stage of the drying process.

At the loading level 1.5 kg/m^2 the change of drying rate for chamomile flowers which dried in different microwave powers of 900, 720 and 450 W are shown in Figure. (2 a) Clear differences can be seen in drying rate at different powers and all the drying rates were apparently decreased. As can be seen depending on the drying conditions, the average drying rates at constant rate period were 0.59, 0.49 and 0.44 g.w/g.w.d.m.min. For different microwave powers of 900, 720 and 450 respectively.

At the loading level 3.0 kg/m^2 the change in drying rate for chamomile which dried at 900, 720 and 450 W is shown in Figure. (2 b). Clear differences can be seen in drying rate between different powers and all the drying rates were apparently decreased. Depending on the drying conditions, the average drying rates at similar period were 0.55, 0.44 and 0.30g.w/g.w.d.m.min. at microwave powers 900, 720 and 450 respectively.

At the loading level 4.5 kg/m^2 the change of drying rate for chamomile follows the same trends as shown in Figure. (2 c). The average drying rates at similar time were 0.43, 0.29 and 0.25g.w/g.w.d.m.min for different powers of 900, 720 and 450 respectively.

Increasing the microwave power from 180W to 900W tends to increase the drying rate. This result coincide with Al-Mashhoor (2015).

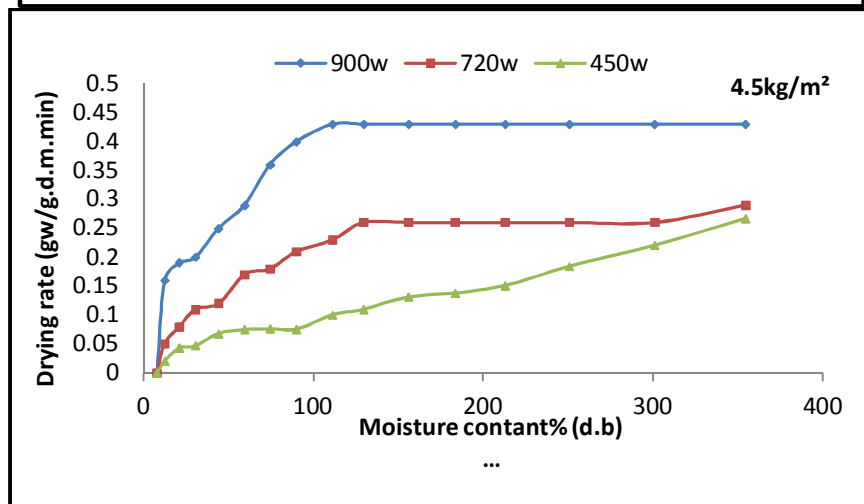
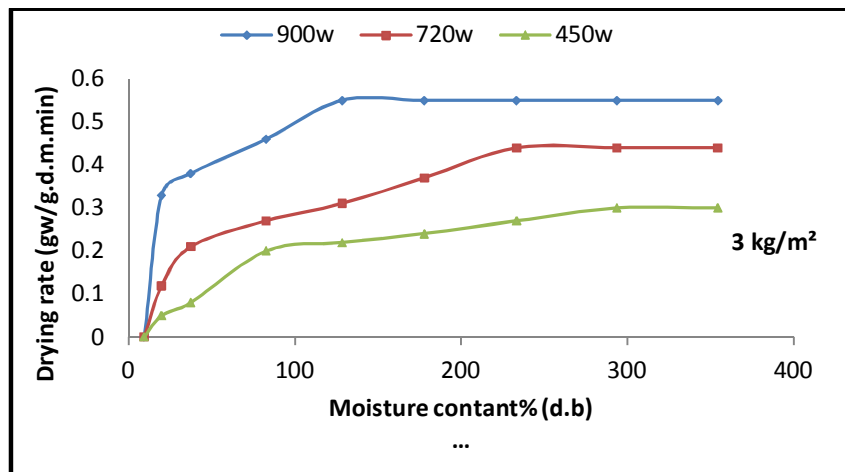
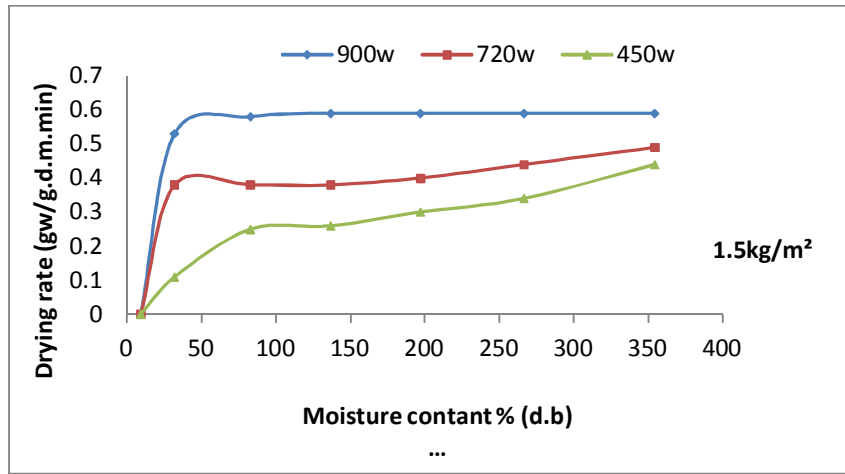


Fig. (2) Chamomile drying rate as related to moisture content at different levels of microwave power and loads.

Effect of the studied parameters on drying efficiency:

Figs (3 a, b and c) describe the relation between the drying efficiency and drying time at different microwave powers of 900, 720 and 450W, and three loading levels of 1.5, 3 and 4.5 kg/m². The drying efficiency was relatively high at the beginning of the drying time. Longer. The figures show that the efficiency increased with increasing loading level and it was decreased with decreasing the microwave power where the highest efficiency was 29.84% at loading level of 4.5 kg/m² and microwave power of 900W, while the lowest was 10.65% at loading level 1.5 kg/m² and 450W.

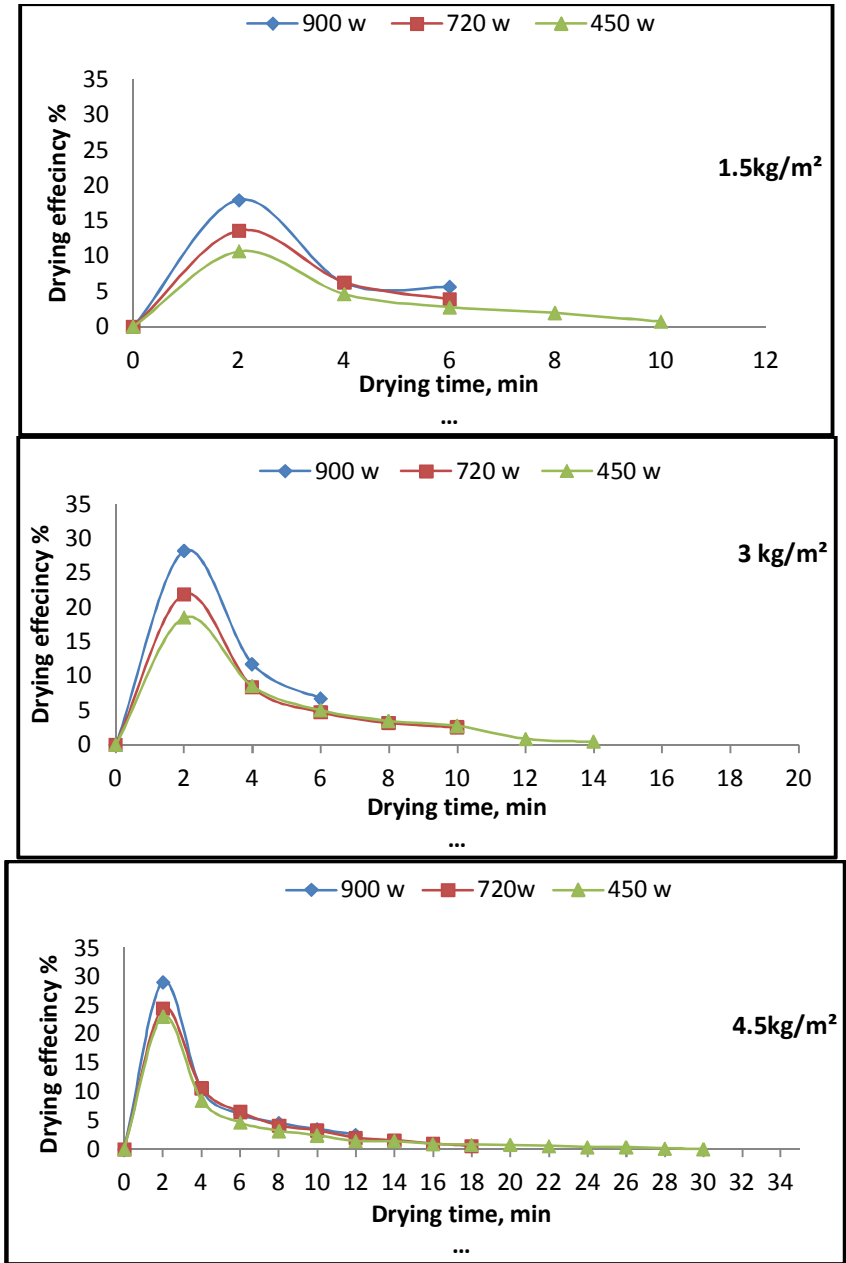


Fig. (3) Chamomile drying efficiency as related to drying time at different levels of microwave power and loads.

Analysis of thin layer drying using Lewis equation:

The values of drying constant (k_L) for the Lewis's model (1) could be obtained from the exponential relationship between the moisture ratio (MR) of the tested sample versus drying time for all studied drying parameter as shown in Figs (4 a, b and c). The computed values of the drying constant (k_L) are listed in Table (1).

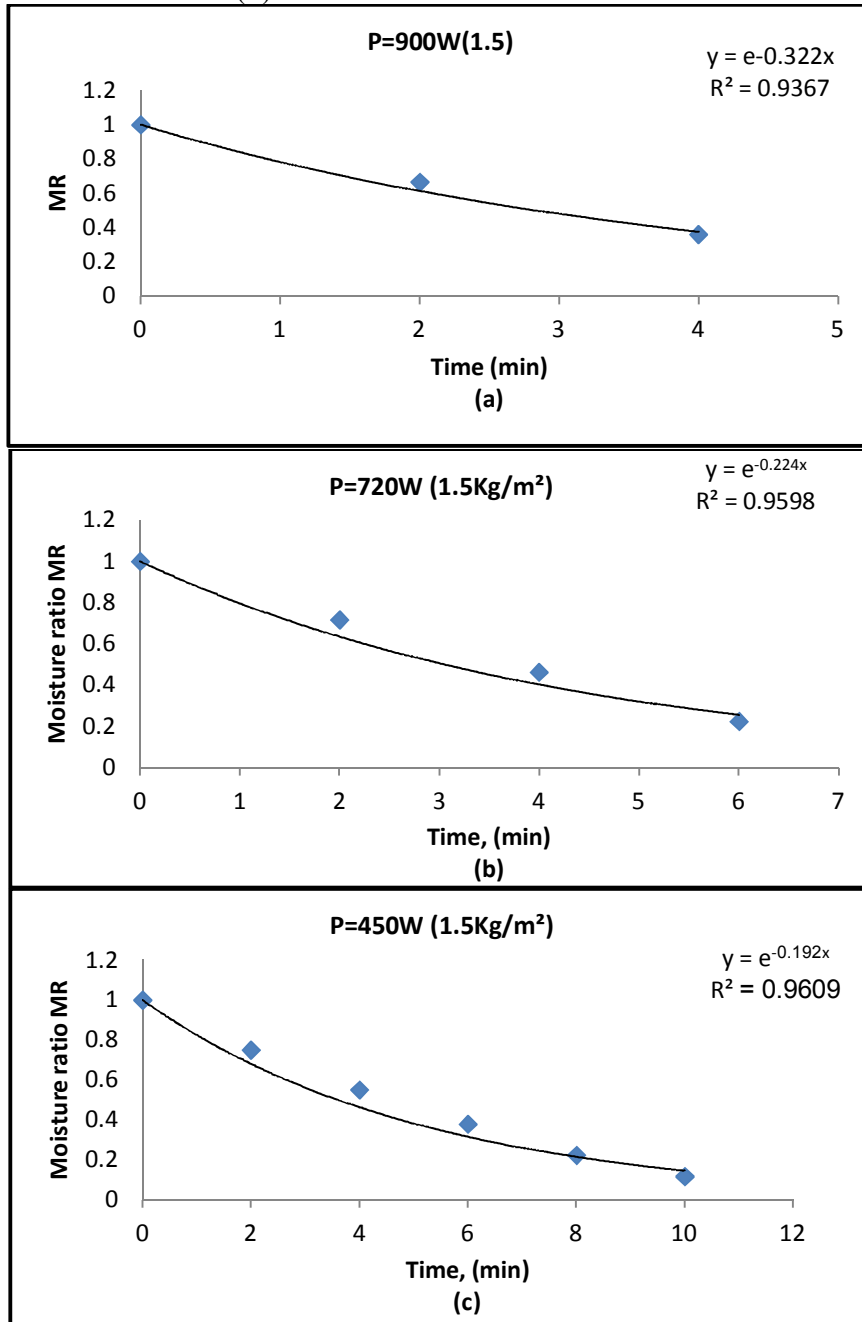


Fig. (4): Determination of the drying constant; (k_L) of Lewis's equation at different power and load 1.5 kg/m².

Table (1): Drying constant (k_L) for Lewis equation at different levels of microwave power and crop load.

Microwave power (W)	Drying Constant K_L		
	Crop load kg/m^2		
	1.5	3.0	4.5
450	0.192	0.126	0.113
720	0.224	0.184	0.15
900	0.322	0.253	0.168

As shown in Table (1) the drying constant (k_L) increased with the increase of microwave power and it was decreased with the increase of load. A multiple regression analysis was employed to relate the studied parameters (P and L) with the drying constant (k_L). The analysis showed that, the nature of dependence could be expressed by the following equation:

$$K_L = 0.00018(P) - 0.01777(L) + 0.09723 \quad (8)$$

[$R^2 = 0.9175$; SE = 0.0149]

Where:

- k_L = Drying constant 1/min
- P = Microwave power W
- L = load kg/m²

The above mentioned analysis revealed that the constant (k_L) was dependent on both load (L) and microwave power (P).

Analysis of microwave power drying of chamomile using Henderson and Pabis's equation:

The values of drying constant (k_h) and (A) for Henderson and Pabis model (1) could be obtained from the exponential relationship between (MR) drying time. The exponent of the drying curve represents the drying constant (k_h) while the intercept represents the constant (A) as shown in Figs (5 a, b and c). The computed values of the drying constants (k_h and A) are listed in Table (2).

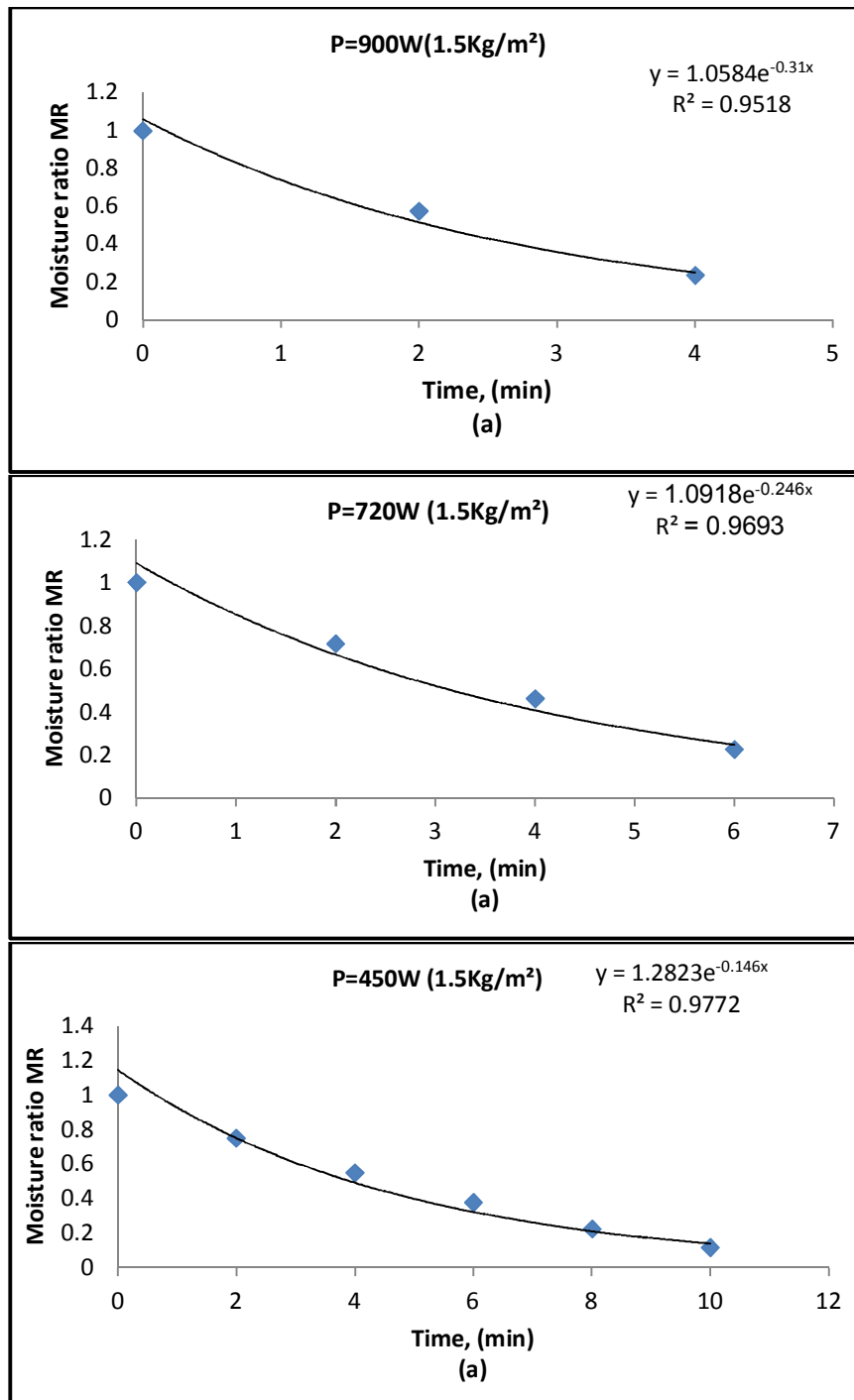


Fig. (5): Determination of the drying constant; (k_h, A) of Henderson and Pabis's equation at the different microwave power and load 1.5kg/m².

As shown in Table (2) the drying constant (k_h) increased with the increase of microwave power (P) and the drying constant (k_h) decreased with the increase of loads (L). The dependence of drying constant (k_h) of equation (7) on the experimental parameters was further studied using the multiple regression analysis. The obtained relationship could be presented as follows:

$$K_h = 0.00022(p) - 0.0236 (L) + 0.1119 \tag{9}$$

[R² = 0.8679; SE = 0.02426]

Where:

- k_h = Drying constant 1/min
- P = Microwave power W
- L = load kg/m²

The above mentioned analysis revealed that the constant (k_h) was dependent on both load (L) and microwave power (P).

Table (2): Drying constant (k_h) for Henderson and Pabis equation at different levels of microwave power and crop load.

Microwave power(W)	Drying Constant k _h		
	Load kg/m ²		
	1.5	3	4.5
450	0.146	0.145	0.131
720	0.246	0.196	0.175
900	0.31	0.232	0.182

Table (3): The calculated drying constant (A) of equation (7).

Microwave power(W)	Drying Constant A		
	Load kg/m ²		
	1.5	3	4.5
450	1.282	1.3924	1.4054
720	1.109	1.1906	1.2849
900	1.0315	1.0488	1.1353

As shown in the Table (3), the values of constant (A) increased with the increase of load and decreased with the increase microwave power. The dependence of drying constant (A) of equation (7) on the experimental parameters was further studied using the simple and multiple regression analysis. It was found that, the drying constant (A) was depending upon the load and microwave power. Moreover, Fig. (5) illustrate the best fit equation relation the drying consistent (A) with the drying load at different power.

$$A = -0.0059 (p) + 0.04361(L) + 1.4914 \tag{10}$$

[R² = 0.9614; SE = 0.0298]

Where:

- A = Drying constant 1/min
- P = Microwave power W
- L = load kg/m²

The above mentioned analysis revealed that the constant (A) was dependent on both load (L) and microwave power (P).

Applicability of the drying models:

Lewis model:

The results of simulation analysis indicated that, equation (5) described the drying behavior of chamomile flowers satisfactorily as indicated by the high values of coefficient of determination

and low values of standard error (SE). Figs (6 and 7) show the measured and predicted values of moisture content at the minimum and the maximum levels of microwave power and load.

Henderson and Pabis model:

The results of simulation analysis indicated that, Henderson and Pabis model also described the drying behavior and predicted the change in moisture content of chamomile flowers satisfactorily as indicated by the high values of coefficient of determination and low values of standard error as shown in Figs (8 & 9).

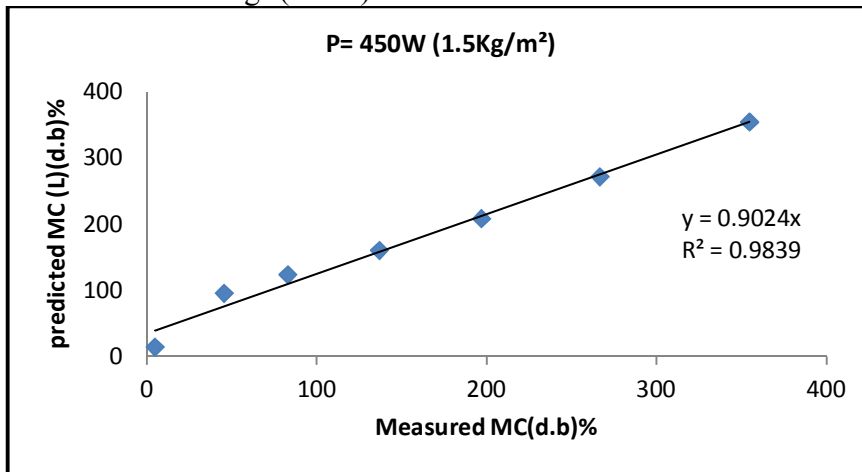


Fig. (6) Measured and predicted values of chamomile moisture content using Lewis model at load (1.5kg/m²) and power (450W).

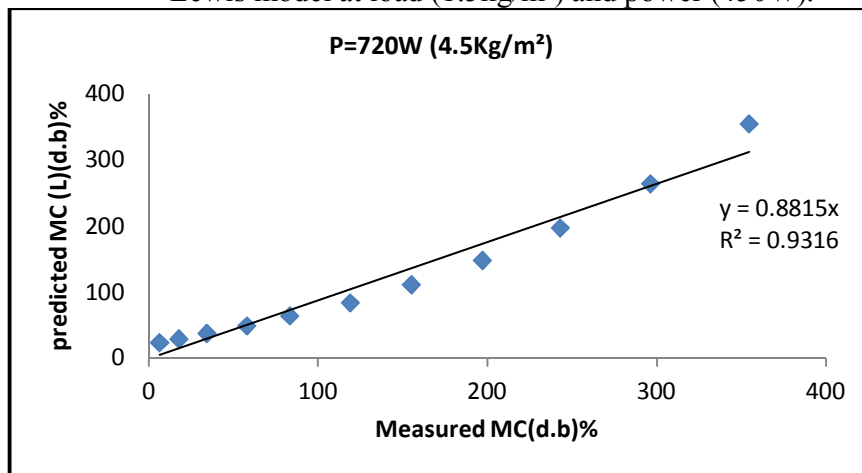


Fig. (7): Measured and predicted values of chamomile moisture content using Lewis model at load (4.5kg/m²) and power (720W).

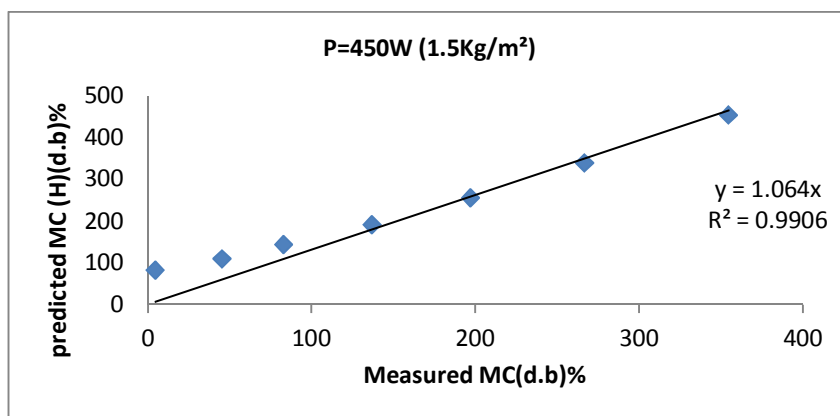


Fig. (8): Measured and predicted values of chamomile moisture content using Henderson and Pabis model at load (1.5kg/m²) and power (450W).

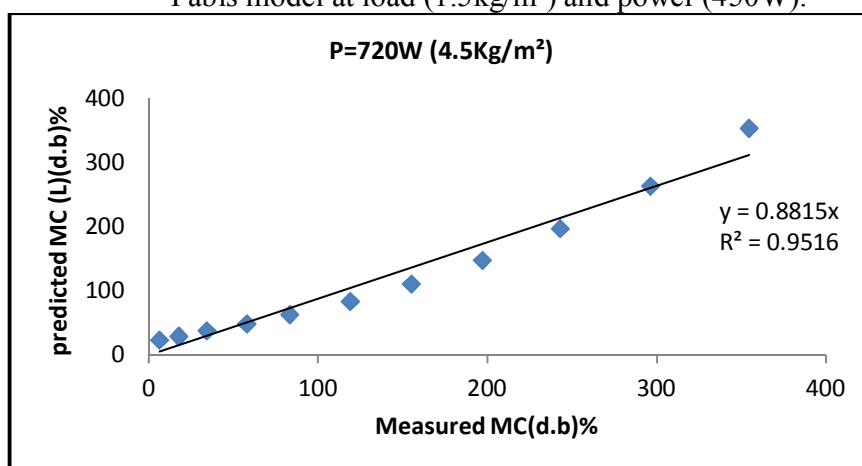


Fig. (9): Measured and predicted values of chamomile moisture content using Henderson and Pabis model at load (4.5 kg/m²) and power (720W).

Comparative evaluation of the studied drying models:

A comparison study for the two drying models (Lewis's and Henderson and Pabis's models) was conducted to assess the most proper drying model for simulating and describing the drying behavior of chamomile plant under the studied range of experimental parameters. In general, the overall average of the obtained coefficient of determination (R^2) and the standard error (SE) for the observed and predicted moisture content revealed that, both studied models could describe the drying behavior of chamomile satisfactory. On the other hand, Lewis's model could be considered more proper model in terms of precision and application simplicity for describing the drying behavior of chamomile plant and predicted the change in moisture content during the laboratory drying process.

Chamomile Samples Quality:

Effect of different parameters on the essential oil yield:

The effect of microwave drying on the essential oil yield of chamomile is illustrated in Fig. (10). The essential oil yield of chamomile remarkably affected by using the different microwave power (900, 720 and 450W) and crop loads (1.5, 3.0 and 4.5 Kg/m²). Generally, drying the plant material before distillation high is resulted in increasing or be creasing the essential oil yield depending on time of drying and load. The highest oil yield (.77ml / 100g. dry weight) was obtained from fresh sample plant. Drying the chamomile by microwave (900W and 3.0Kg/m² load)

reduced the oil yield to .50% ml/100g d.w., While increasing the load and decreasing the power (4.5 Kg/m² and 450W) decreases the oil yield to 0.08 ml/100g d.w. At all loading levels, the highest essential oil yields were obtained through microwave power of 900W.

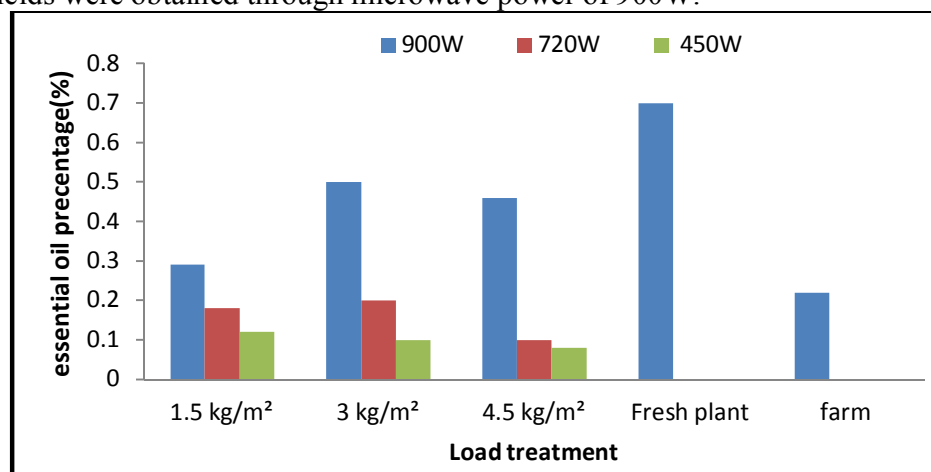


Fig. (10) Effect of microwave treatment on essential oil yield of chamomile flowers.

Effect of different parameters on the essential oil composition:

The analysis of oil samples showed that microwave treatment had significant effect on the chemical composition of chamomile flowers Fig. (11). The concentration of Farnesene was slightly higher in fresh flowers and 450Wdried flowers (1.2987 and 4.2869%). While it was found to be the lowest at 900W. The concentration of Bisabolo oxide B was slightly higher in 450W and 900W450Wdried flowers (16.0292 and 13.6317%) when compared with 450W while its concentration was only 2.4025% at 720W. The percentage of Bisabolon oxide B was found to be lowest at (720 and 450W) whereas in other power 900W of drying it was higher (8.9274%) than fresh flowers. The percentage of Bisabolo was found to be lowest in (720 and 450W) whereas in other power 900W of drying it was higher (5.1601%) than fresh flowers. The percentage of Chamazulene was found to be lowest in (720 and 450W) whereas in other power 900W of drying it was higher (3.3303%) than fresh flowers. However, the amount of Bisabolo oxide A Was observed to be higher in microwave power 900Wdried flowers(56.2554%)followed by fresh flowers (56.1599)while in 720 and 450W dried flowers it was 11.5589 and 37.8452% ,respectively. The result also shows that the microwave power 900W is more suitable and is recommended for obtaining higher oil yield.

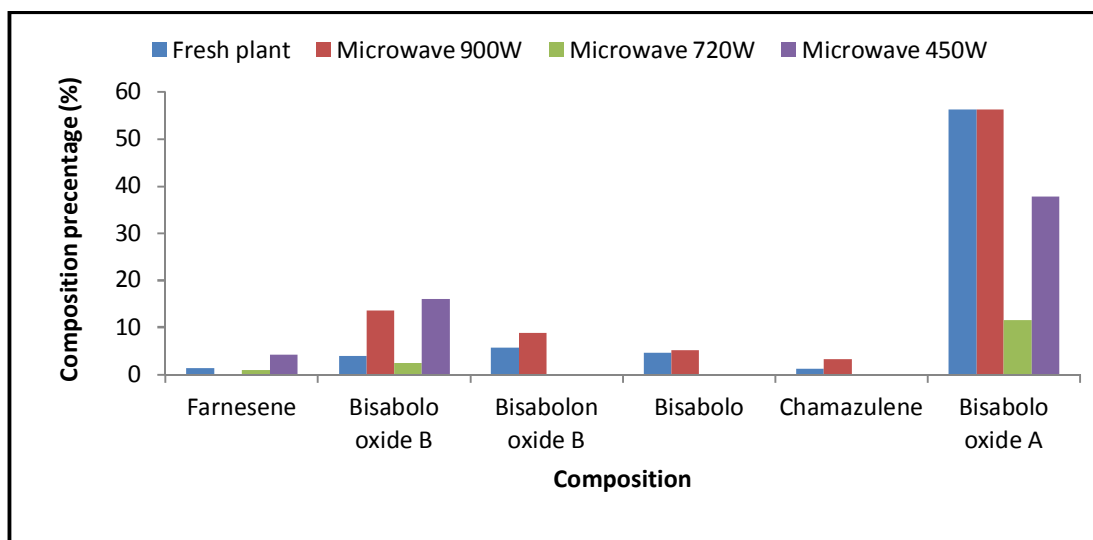


Fig. (11) Effect of microwave treatment on compounds of essential oil for chamomile flowers.

REFERENCES

- 1- Agricultural economics and statistics Research Institute, Ministry of Agricultural, Egypt (2014).
- 2- Al-Mashhoor.M. B. M.H. (2015). Effect of different drying methods on the properties of some medicinal and aromatic plants. PhD Thesis. Menoufiya University of Agricultural Engineering Department.
- 3- Darvishi. H.; M.H. Khoshtaghaza; G. Najafi and F.Nargesi (2013). Mathematical modeling of green pepper drying in microwave convective dryer.J.Agric.Sci.Technol.15, 457–465.
- 4- El Saeidy, E. and A. El Bltagy (2011). Microwave Drying and Its Effect on the Quality Aspects of Egyptian Jew’s Mallow (Corchorous Olitorious) leaves. J. 11 International Congress on Mechanization and Energy in Agriculture- Turkey Volume: Proceeding Pages: 463-468.
- 5- Eurpean Pharmacopoeia. (2005). Ph.Eur. 5.00. Deutscher Apotheker verlag, Stuttgart, P.4392.
- 6- Ghanem,T.H.; M.A. EL-Said Shetawy; N. El Badry and M.M. Badr (2013). A Comparative study between several drying techniques of dates. Egypt. J. Agriculture Research. 91(2B).
- 7- Mukay, D.L. AND J.B.Blumberd (2006). "A review of the bioactivity and potential beath benefits of chamomile tea (Matricaria recutita L.)" Phytotherapy research 20: 519-530.
- 8- Soliman, O. S.(2016). Some engineering factors affecting solar drying of date. Master thesis. Suez Canal University of Agricultural Engineering Department.
- 9- Rattanadecho P. and N. Makul (2016). Microwave-Assisted Drying: A Review of the State-of-the-Art. International Journal of Drying Technology, 34, (1),: 1–38.
URL: <http://dx.doi.org/10.1080/07373937.2014.957764>
- 10- Topping, E.; E. Esveld; I. Scheewe; R. B. Vanden and P. Bartels (2001). Osmotic dehydration as a pre-treatment before combined microwave-hot air drying of mushrooms. J. Food Eng., 49(2):185-191.

تجفيف أزهار البابونج باستخدام فرن الميكرويف

د. إيهاب عبدالعزيز الصعدي^١، جمال كمال عرفه^٢، فاطمة علي نصر^٢

- ١ - قسم الهندسة الزراعية - كلية الزراعة - جامعة المنوفية - مصر.
- ٢ - معهد بحوث الهندسة الزراعية - مركز البحوث الزراعية - مصر.

أجريت تلك الدراسة لاختبار وتقييم استخدام الميكرويف لتجفيف أزهار البابونج. وتم إجراء هذه التجربة بقسم الهندسة الزراعية - كلية الزراعة - جامعة المنوفية. وشملت المعاملات التجريبية ثلاث مستويات مختلفة من الطاقة (٩٠٠ - ٧٢٠ - ٤٥٠ وات) وثلاث احمال (١,٥ - ٣ - ٤,٥ كجم/م^٢). وقد تمت محاكاة السلوك التجفيفي باستخدام نموذج Lewis ونموذج Henderson and Pabis. وتم التأكد من مدي محاكاة النماذج مع بيانات التجفيف المتحصل عليها، ووجد أن نموذج Lewis هو الأكثر تمثيلاً للتنبؤ بالتغير في المحتوى الرطوبي أثناء عملية التجفيف بالنظر لدقته وسهولة تطبيقه. وتم كذلك متابعة الجودة النهائية للبابونج المجفف. وأظهرت النتائج أن كلا النموذجين المدروسين يمكن لهما وصف السلوك التجفيفي للبابونج. أظهرت إختبارات جودة البابونج المجفف أن استخدام الميكرويف عند ٩٠٠ وات مع حمل ٣ كجم/م^٢ هي الأفضل جودة للبابونج على أساس نسبة الزيت بالنبات المجفف وكذلك مكوناته.

EVALUATION OF USING CANOLA BIODIESEL AS A SUBSTITUTE FOR DIESEL FUEL

EL-WEHISHY, M. M.¹, M. M. MOSTAFA², A. I. MOUSSA¹ and M. A. EL-NONO²

¹ Agricultural Engineering Research Institute, ARC, Dokki, Giza, Egypt.

² Faculty of Agriculture, Ain Shams University, Cairo, Egypt.

Abstract

In order to solve the problem of using diesel because of many problems such as lack of continuity the diesel, Biodiesel is produced and tested as fuel for this purpose. A large amount of biodiesel was produced from canola oil as source of oil therefore methanol alcohol had been added with potassium hydroxide (KOH) as catalyst. After 8 hours, biodiesel was separated from glycerol where glycerol was under the biodiesel by gravity. Many ratios of blended canola biodiesel with petroleum diesel is performed and tested in Misr Petroleum Company labs to specify the mixtures properties. Results showed that with increasing ratio of biodiesel in mixture, increasing some properties of fuel such as density, viscosity, pour point and flash point. On the other hand, decreasing some properties of fuel such as calorific value and Cetane No.

Keywords: Canola Biodiesel; Biodiesel Physical Properties; Producing Biodiesel from Canola.

INTRODUCTION

As petroleum resources decline and as concern about global warming heightens, the quest for a renewable, sustainable and more environmentally friendly fuel source continues (O'Brien, 2004). Biodiesel is one such candidate that is proposed to replace a significant percentage of petroleum diesels in this century. Biodiesel is a common word for monoalkyl esters, a product formed from the catalyzed reaction of triglycerides (vegetable oil) and alcohol that meet ASTM standards. Biodiesel combusts similarly in diesel engines to petroleum-based diesel, while also having the added advantages of domestic origin, derivation from a renewable feedstock, biodegradability, non-toxicity, cleaner emissions, superior lubricating properties (Joshi, 2008). Biodiesel is less toxic than salt and biodegrades as fast as sugar. Regular diesel fuel particulates are carcinogenic. Using canola biodiesel as fuel, or mixing it with diesel fuel, can reduce the production of these cancer-causing emissions. Biodiesel can be used neat or blended in any proportion with petroleum diesel, the most common being B20 (20% biodiesel). Adding just 20% biodiesel to regular diesel improves the diesel's cetane rating by 3 points, which improves engine operation.

Biodiesel is a nonpetroleum-based fuel that generally consists of fatty acid methyl esters (FAME) or fatty acid ethyl esters (FAEE), derived from the transesterification of triglycerides (TAG) with methanol or ethanol, respectively. Biodiesel can be derived from a variety of feed stock oils, such as cottonseed, canola, and soybean oil. In transesterification, low molecular weight alcohol (e.g., ethanol, methanol, propanol and butanol) in the presence of a catalyst, such as sodium hydroxide or potassium hydroxide, chemically breaks the molecule of the triglyceride (oil) into methyl or ethyl esters of the oil with glycerol as a by-product (Schuchardt *et al.* 1998).

MATERIALS AND METHODS

The source of the biodiesel

The main source of the produced biodiesel is obtained from canola's oil. Oil was brought from The Standard Farm in El-Kilo 69, Alexandria-Cairo Desert Road, Production Sector,

Agricultural Research Center, Ministry of Agriculture, Egypt. Also, triolein, hexane, anhydrous methanol (99.9%) and KOH were purchased from Elictrosaint Chemical Co. in Kafr El-Sheikh.

Determining of fatty acid composition

The Gas Chromatography (GC) analysis standards and tests were in High Institute of public Health Alexandria University. The standards were solution of glycerol, 1- mono-olein, 1,3-di-olein (1% 1,2 isomer) and triolein. n-Hexane (HPLC grade) was used as a solvent to dilute the samples for GC analysis. GC has been used to determine the fatty acid composition percentage of canola oil and its physicochemical properties determined as per BIS method (Arun, *et al.*, 2013). Canola oil contains some different types of fatty acids. Different fractions of each type of fatty acids influence on the fuel properties.

Pilot Biodiesel Plant

Biodiesel was obtained from a pilot Biodiesel plant which is available at the Tractor Test Station in Sabahia, Alexandria, Egypt. Fig.1 shows the pilot biodiesel plant. The pilot plant consists of two processors with heater for each one, three pumps, a chemical mixing tank and a purification unit for dry washing.

Transesterification Process

Two major inappropriate properties that influence the production process are water content and FFA (free fatty acid) percentage in the oil. Vegetable oil is not suitable direct replacements for diesel fuel in engines; however, it is possible to reduce the viscosity of vegetable oil, improve the physical properties through transesterification process.



Fig. 1: Pilot biodiesel plant in Alexandria

The trans-esterification is an equilibrium reaction and the transformation occurs essentially by mixing the reactants. The presence of catalyst accelerates the reaction to the product side. In order to achieve high yield of esters the alcohol has to be used in excess. In coexist of an alcohol and a catalyst, the reaction converts triglyceride to fatty acid alkyl ester, and glycerol is secondary product.

More alcohol is used because of the reaction is reversible to push reaction to product side. The molar masses of the esters are approximately one sixth that of the triglycerides which in turn leads to significant reduction in the viscosity. Thus it is therefore a good process to make petro diesel substitutes from vegetable oils.

Calculation of molar ratio

-As it is known, according to the molecular mass of canola oil and applying molar ratio 6:1; the number of oil moles could be estimated as follows:

Mass of oil, g = Batch volume, ml × oil density, g/ml

Number of oil moles = Mass of oil, g / oil molecular weight, g/mole

The resulted number of oil moles represents the parts of oil (one) in the applied molar ratio 6:1.

-Number of methanol moles = number of oil moles × parts of methanol (6 in the applied molar ratio).

Mass of methanol = number of methanol moles × methanol molecular weight (32 g/mole).

Amount of methanol = mass of methanol / methanol density (0.79 g/ml)

-The required amount of catalyst KOH 1% by weight of the above specified batch of oil.

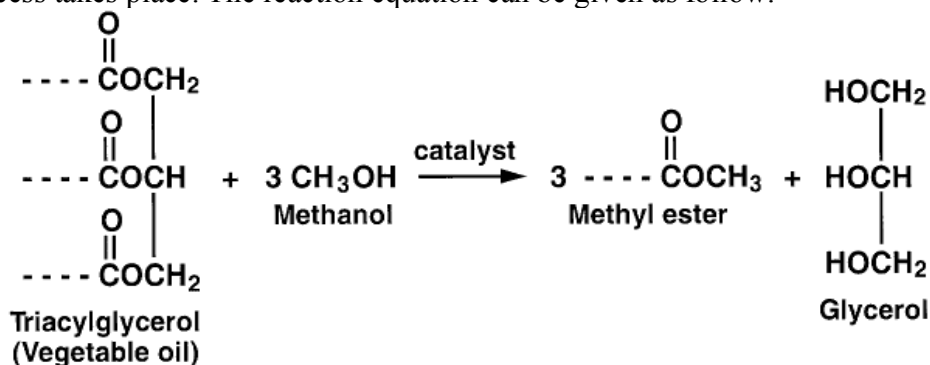
Procedures of transesterification

Berman *et al.* (2011) and Conceicao *et al.* (2007) reported that oil was heated up to 80 °C to evaporate water then was let to cool down to 50 °C. Caylr and Kusefoglu (2008) reported that oil was heated up to 80 °C to evaporate water and then was left to cool down to 55 °C. The biodiesel was produced from 150 liters of canola's oil where 5 batches have been made. The procedures of the trans-esterification include the following steps:

- The oil was pre-heated to 55 °C so as the needed temperature for the trans-esterification process.
- Titration process. No need to titrate canola oil as long as it is new. The amount of KOH needed per liter for fresh oil is 4.9 gm of KOH / liter of oil.
- In the premix tank, the potassium hydroxide (147 g) is added to methanol (6 liter) and then stirred well by the closed circulation pump for about 20 min. potassium methoxide is formed as shown in the following equation:



- Potassium methoxide were pumped to the heated canola oil (30 liter) in the processor tank then they were stirring during circulation for 2 h. During this time, trans-esterification process takes place. The reaction equation can be given as follow:



The theory of this operation is that the fatty acids of the oil exchange places with the OH group of the alcohol producing glycerol and the methyl ester (Moussa, 2003). The transesterification is three steps reaction as shown below in Fig. 2

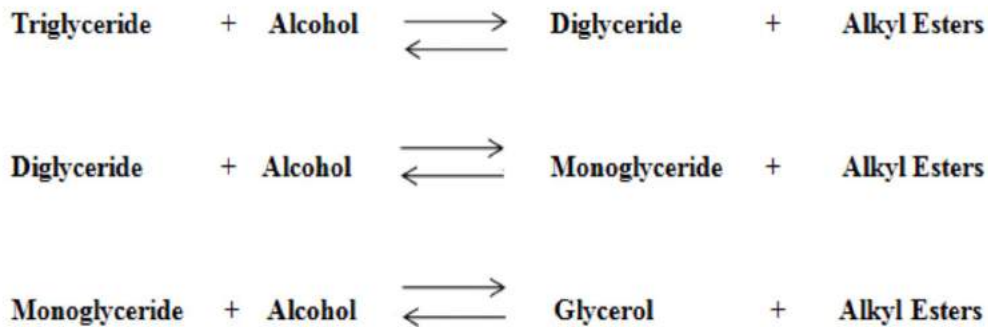


Fig. 2: Stepwise reaction of transesterification

The circulation is terminated and the mixture is allowed to make phase separation after eight hours. The glycerol is then decanted from the bottom while methyl ester is separated from ester phase.

Testing of biodiesel

In order to obtain biodiesel fuel with good quality, six mixtures were processed which ratios of biodiesel were 0, 10, 20, 30, 40 and 100% of the mixture. It is called for 0% of biodiesel percent in mixture B0 where it is tradition diesel and for 100% of biodiesel percent in mixture B100 where it is pure biodiesel. And so B10, B20, B30 and B40 were performed. Samples were sent to Misr petroleum company labs to measure some properties of fuel. Properties were density, viscosity, calorific value, Cetane No, pour point and flash point.

RESULTS AND DISCUSSION

Properties of biodiesel and diesel fuel

The physical and the thermal properties of the product. As commonly practiced, the biodiesel is usually blended with the diesel fuel, and the 20% mix (B20) is the most commonly used. The physical and thermal properties of the biodiesel B100 and the B20 mix were measured, determined and compared to the diesel fuel as well. These properties are shown in table (1).

Table (1) Comparison between water and dry washing

Properties	Diesel (B0)	Biodiesel (B100)	Standard of biodiesel	Standard method
Density, kg/L at 15 °C	0.846	0.882	0.86 – 0.9	D287
Calorific value, MJ/L	40	38.3	37.27	D240
Viscosity, mm ² /s at 40 °C	3.3	5.75	4 – 6	D445
Cetane number	47	54	48 – 65	D613
Pour Pint, °C	-3	3	-5 – 10	D97
Flash Point, °C	34	80	100 – 170	D93

From the previous table it showed that the properties of B100 and B0 were in the allowable limit as ASTM standard.

Density

It can be observed from the readings that canola oil has the highest density of 0.946 kg/l as compared to canola methyl ester of 0.882 kg/l. The diesel fuel sample was observed to have a density value of 0.846 kg/l which is lower than canola oil, methyl ester and its blends. The Density of biodiesel increased by increasing biodiesel percent as seen in Fig. (3).

Calorific value

Heating value of fuels is an important measure of its releasing energy for producing work. So the lower heating value of biodiesel is attributed to the decrease in engine power. The energy release of biodiesel is slightly lower than that of petroleum diesel since it contains lower calorific value. The heating value of canola oil is 37.7 MJ/Kg whereas that of canola oil methyl ester (B100) is 38.3 MJ/Kg. while it was 40 MJ/L for diesel fuel as in Fig. (4).

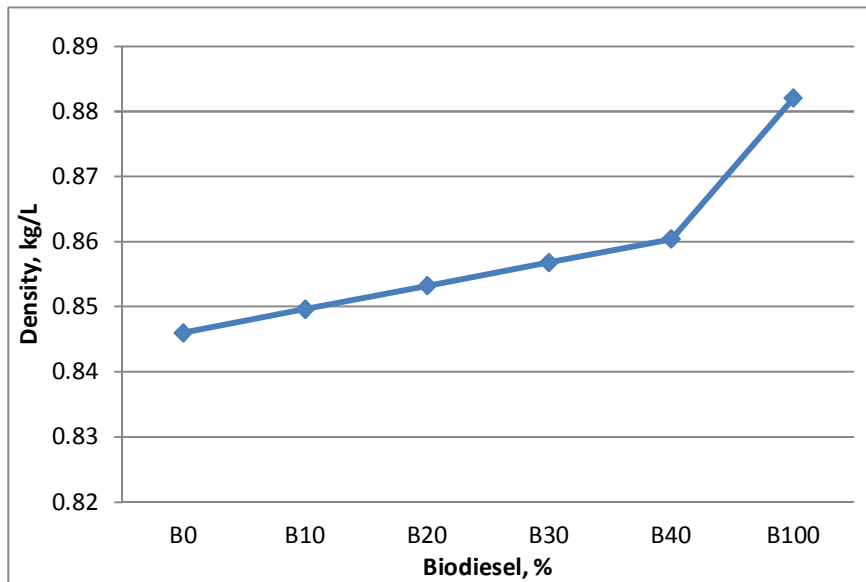


Fig. 3: Effect of biodiesel percent on density

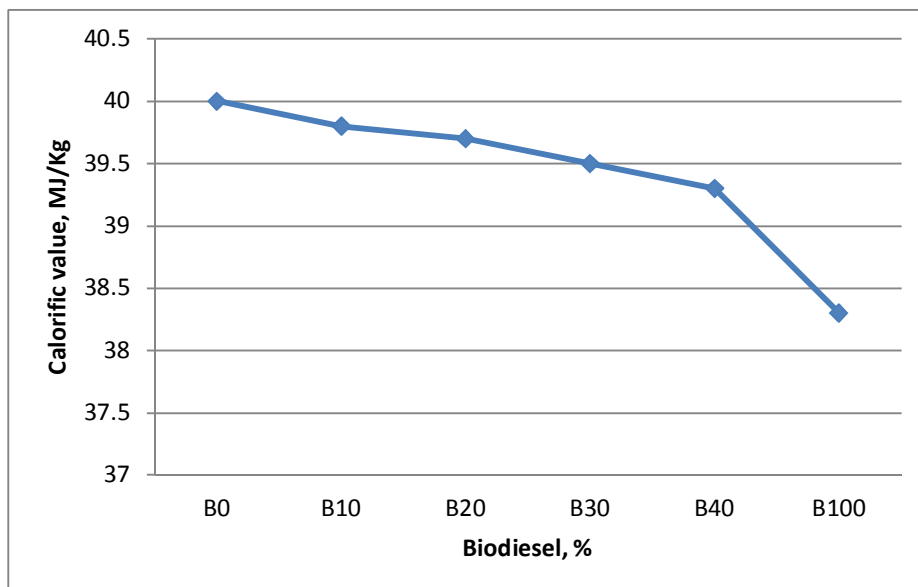
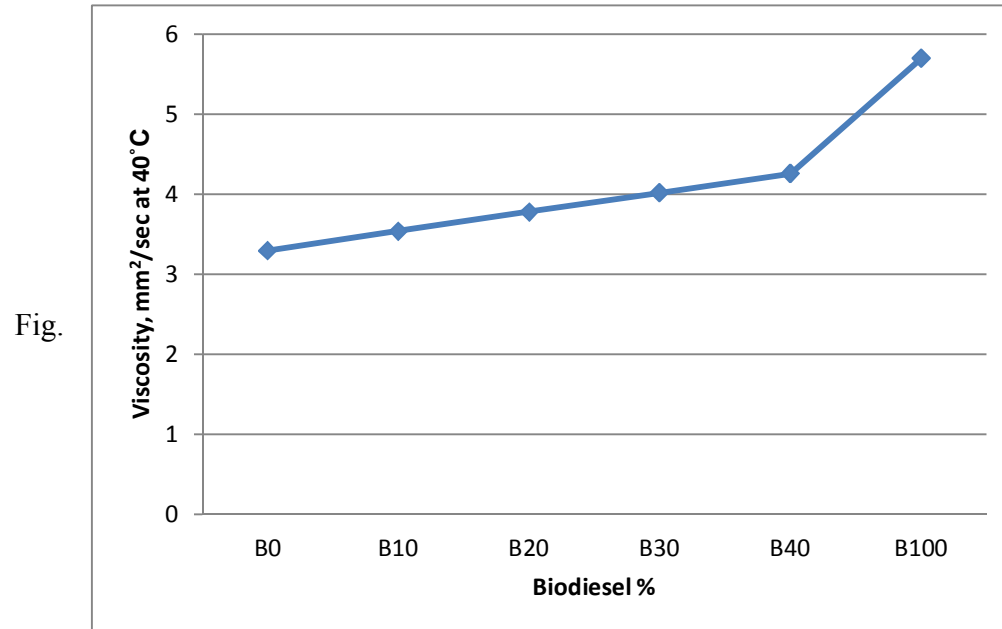


Fig. 4: Effect of biodiesel percent on calorific value

Viscosity

The viscosity value of canola oil is 37 mm²/sec at 40 °C where those of canola oil methyl esters (B100) is 5.75 mm²/sec compared to diesel fuel 3.3 mm²/sec at 40 °C. The high level in viscosity of biodiesel is lead to significant improvement in lubricity as in Fig. (5).



5: Effect of biodiesel percent on viscosity

Cetane No.

CN of biodiesel B100 was higher than petroleum diesel. CN was increased by increasing the percent of biodiesel. It was 47 for diesel and 54 for biodiesel B100 as shown in Fig. (6).

Pour Point

The pour point of biodiesel B100 was higher than diesel fuel. The problem of high pour point in biodiesel was appeared in cold weather, and its solution is to heat the fuel before using it. The pour point of diesel is -3 °C while canola biodiesel was 3 °C. See Fig. (7).

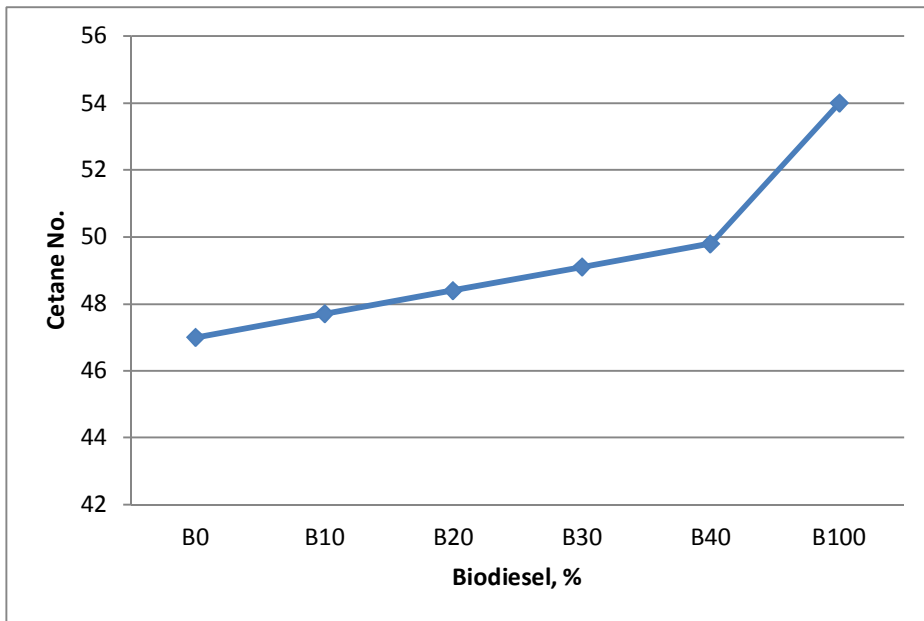


Fig. 6: Effect of biodiesel percent on Cetane No.

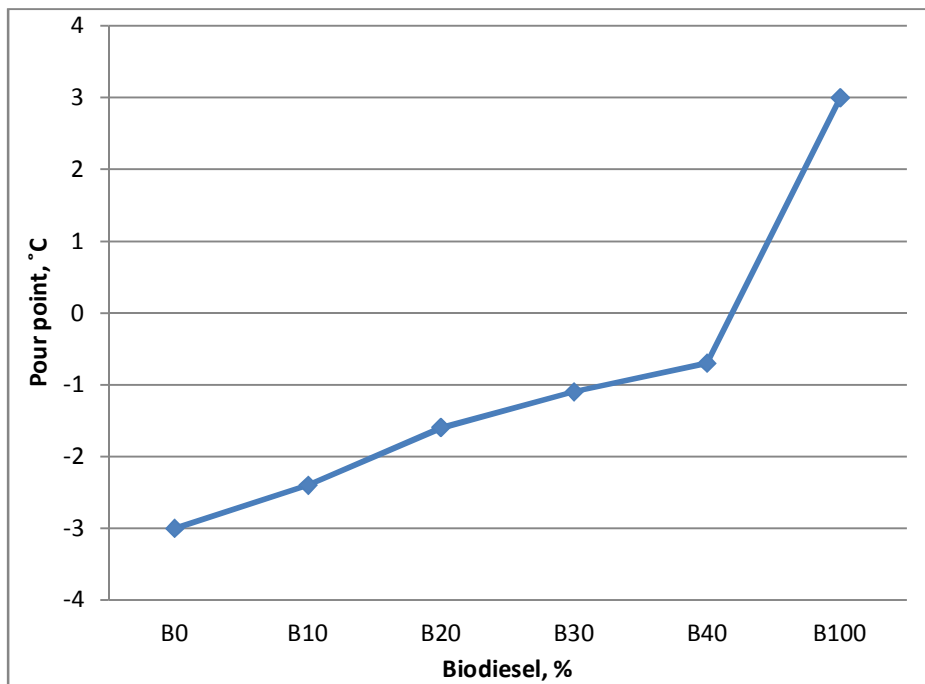


Fig.

7: Effect of biodiesel percent on Pour point

Flash Point

The flash point of canola oil methyl esters is much lower than those of canola oil. The flash point of canola oil is 246 °C while canola methyl ester was 80 °C. The flash point of B100 was 80 °C, while, it was 34 °C for diesel fuel, and it is showed that the biodiesel is safe in handling and storage than diesel as in Fig. (8).

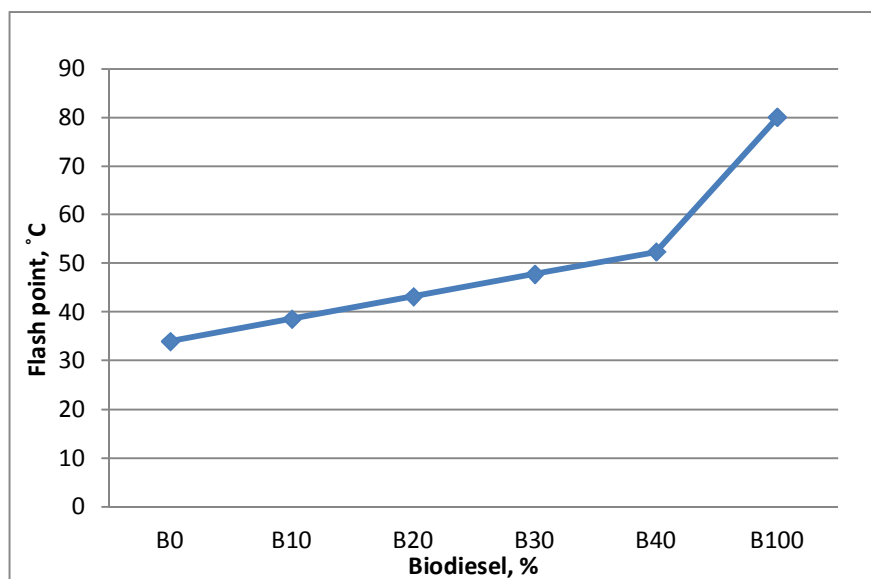


Fig. 8: Effect of biodiesel percent on flash point

REFERENCES

1. Arun, K.V., S. K. Chattopadhyay and S. R. Sen. (2013). Fuel properties, engine performance and environmental benefits of biodiesel produced by a green process. *Applied Energy*, 105: 319–326
2. Berman, G.Y., E. D. Conceicao and W. R. Gerpen. (2011). Biodiesel processing and production. *Fuel Processing Technology*, 86: 1097– 1107.
3. Caylr, L. P. and U. T. Kusefoglul. (2008). Environmentally friendly production technology of biodiesel. *Jelgava*, 28: 161-164.
4. Elshazly, S. Sahar. (2015). Manufacturing a new dry wash unit for biodiesel purification and comparing it with wet wash method. *Alexandria University*, 80.
5. Joshi, H. C. (2008). Optimization and characterization of biodiesel production from cottonseed and canola oil (Doctoral dissertation, Clemson University).
6. Moussa, A. I. (2003). Transestrification process to manufacture methyl ester of waste vegetable oil. *The 11th Annual Conference of the Misr Society of Ag. Eng.*: 851-866.
7. O'Brien, R.D. (2004). Assessment of a dry and a wet route for the production of biofuels from microalgae: energy balance analysis. *Bioresource Technology*, 102 (8): 5113–5122.
8. Saengprachum, S. J., B. S. Ogunsina, A. O. Adelaja and M. Ogbonnaya. (2013). Study of an Effective Technique for the Production of Biodiesel from Jatropha Oil. *Journal of Emerging Trends in Engineering and Applied Sciences (JETEAS)*, 2(1): 79-86.
9. Schuchardt, C. M., S. D. Rios, C. G. Torras, J. F. Salvado, J. M. Mateo-Sanz and L. Jiménez. (1998). Microalgae-based biodiesel: A multicriteria analysis of the production process using realistic scenarios. *Bioresource Technology*, 147: 7–16.
10. Sivaramakrishnan, K., and P. Ravikumar. (2012) Determination of cetane number of biodiesel and its influence on physical properties. *ARPN journal of engineering and applied sciences* 7.2: 205-211.

تقييم استخدام وقود الكانولا الحيوي كبديل لوقود الديزل

محمد محمود الوحيشي^١ ، مبارك محمد مصطفى^٢ ، علي ابراهيم موسى^١ ، محمود أحمد النونو^٢

^١ معهد بحوث الهندسة الزراعية - مركز البحوث الزراعية - الدقي - جيزة - مصر.
^٢ كلية الزراعة - جامعة عين شمس - القاهرة - مصر.

لحل مشاكل استخدام وقود الديزل في المجتمعات الريفية منها توفر و استمرارية وجود الوقود ، تم انتاج و اختبار الوقود الحيوي. تم انتاج كمية كبيرة من الوقود الحيوي و استخدم زيت الكانولا كمصدر للزيت ثم تمت اضافة كحول الميثانول مع هيدروكسيد البوتاسيوم كعامل حفاز. بعد مرور ٨ ساعات ، تم فصل الوقود الحيوي عن الجلسرين بواسطة الجاذبية الأرضية حيث كان الجلسرين مترسباً في الأسفل. تم عمل خلطات من الوقود الحيوي مع الديزل التجاري بنسب مختلفة و تم اختبار الخصائص في معامل شركة مصر للبتروول لتلك الخلطات. وجد أنه مع زيادة نسبة الوقود الحيوي في المخلوط تزداد بعض خصائص الوقود مثل الكثافة ، اللزوجة نقطة الانسكاب و نقطة الوميض. و على الجانب الآخر تتخفف بعض الخصائص مثل القيمة الحرارية و رقم السيتان.

EVALUATION OF DIFFERENT COOLING SYSTEMS TO INCREASING LED LIFE OPERATED BY PHOTOVOLTAIC CELL

BAHNASY , A. M.*; M. I. ELMEADAWY*; I. M. EL-SEBAEE *
AND M. A. ABDEL-MAKSOU**

* *Agric. Eng. Res. Inst. (AEnRI), Giza.*

** *Mariout Research Station D.R.C.*

Abstract

This paper provided many types of heat sink that found at the local shops in Egypt and its prices are low, which is applied to low and medium power LED light source to compare its performance. The theoretical calculation is done and the experiments are recognized in Tractor and Farm Machinery Test and Research Station –Alex. It's well known that LED is an excellent choice to replace the incandescent lamp for saving energy. The research problem when the high power LED is applied, there is only about 20% of the input power converts to light energy, the rest of power is converts to heat which should be carry out from the LED chips, otherwise, the high heat concentration results in a serious problem to decrease LED life. The most important issue of the LED research is to find many types of heat sink that found at the local shops in Egypt to solve the problem of LED over-heating and cooling the increasing of temperature of base and surface of the LED. There are many suitable types of heat sink that found at the local shops operated with the low power LED up to 10 watts. In the other side the LED with power up to 20 watts can operate with the heat sink with fan available in the local shops in Egypt. The best heat sink is number (2), the maximum temperature at the base of the LED (10 Watts) without fan is 49°C and the surface temperature is 80°C. The result indicated that the best heat sink is number (2), the maximum temperature at the base of the LEDs (20 Watts) with fan is 45°C and the surface temperature is 70°C. It was also found that the direct use of the LEDs 10 and 20 watt without a cooling unit leads to damage at 78 and 90 °C at the base of the LED respectively. We also found that the LEDs that are powered by direct current (without using inverter) provide 20% energy saving compared with the LEDs are power by alternating currents and the LEDs long life increased according to the technical recommendations in the catalog when the temperature below at the base of the LED not increase of 60 and 80 °C for each of the LEDs 10 and 20 watts respectively.

Keywords: heat sink; LEDs; cooling system; local heat sink.

INTRODUCTION

In recent years, LED devices were widely used in many areas like street lamps. LED light source has many advantages over traditional light sources, such as high lighting efficiency (lumens/Watt), low electricity consumption, quick response time, and long life time. However, the application of high brightness LEDs still faces severe thermal challenges in removing the unavoidable waste heat, which directly influences the lighting efficiency, light quality, and lifetime of LEDs [Michael *et al* 2007 and Fei Y. *et al* 2013]. Life time of LED depends on thermal management, construction or package, operating environment or ambient temperature and driving current from the power source. The efficiency of LED is around 20 to 25%, where only 20 to 25 % of energy supplied is used for illumination and the rest 75 to 80% of energy is dissipated as heat. If this heat is not dissipated appropriately, the life time of LED reduces drastically Fei Y. *et al* (2013)

Rammohanl A. and R. C. Kumar (2016) reported that the Junction temperature of the LED depends on the current supplied and type of cooling system used. Higher junction temperature with poor cooling leads to shift in the light colour and drastically reduces the LED life. Heat sink and heat pipes are best solution for heat dissipation and in some applications active cooling systems using electric fan provided best results for LED lamps.

Po-Jen Cheng *et al.* (2015) designed the LEDs combined with the cooling module of the aluminum-acetone flat plate heat pipe by the experimental and numerical simulation for obtaining high efficiency in heat removal. The high power LEDs with and without heat pipe cooling module is compared. The numerical simulation is built and agrees with the experiment. The heat removal efficiency of the cooling module reaches 92.09% and drops the junction temperature of LED about 36 °C. This cooling module has proven to be effective in solving the heat concentration problems associated with the LED chips. In short, the phase change cooling module will apply on the electronic component of high heat concentration for more effective cooling method.

Jeevaraj S (2014) mentioned that forced-air cooling technique, one of the effective methods for thermal management of electronic equipment cooling, is commonly used in a conventional-size heat sink. Conventional or mini sized heat sinks are commonly used in many industrial applications as cooling devices, because of their easy serviceability, high reliability, simplicity in the mechanism of heat transfer and ease of testing. heat sink is designed and investigated for different velocity variation at the inlet to select appropriate fan to cool the heat sink and also effect of ambient conditions on the heat sink are studied. In order to optimize the chip usage parametric study is carried out by varying the ambient temperature, keeping the inlet velocity constant. It is found that at 12 m/s inlet velocity, the maximum ambient temperature allowed to operate the chip is 45 °C.

Ramos-Alvarado B. *et al.* (2013) the entropy generation minimization process indicated that the mini channel cold plate had a lower flow resistance than the base design reported in previous investigations. Due to the different length scales presented in this problem, a small-scale model was developed using a simple thermal resistance formulation for the chips, in order to calculate the chip junction temperature at different operating conditions. Overall, it was found that the mini channel cold plate design is a better thermal management option than micro jets for the cooling of high-power LEDs.

Pawar *et al.*(2015) the increasing heat load of the device needs to be removed for maintaining the efficient performance of the device. The exponential increase in thermal load in air cooling devices requires the thermal management system (i.e. heat sink) to be optimized to attain the highest performance in the given space. Adding fins to the heat sink increases surface area but it increases the pressure drop. This reduces the volumetric airflow and the heat transfer coefficient.

The aim of this research to adopt different types of heat sink that found at the local shops to solve the problem of LED over-heating.

MATERIALS AND METHODS

Experimental tests were conducted on the 10 types of heat sink as shown in Fig. (1). The theoretical calculation is done and the experiments are recognized in Tractor and Farm Machinery Test and Research Station –Alex.



Fig (1): types of heat think with and without fan.
Local Heat sink to cooling the LEDs.

The heat sink is the last stack of the LED package. The heat sink that is attached to a LED should have

good thermal conductivity and good emissivity as both these properties help to conduct or move heat outside the package. The thermal conductivity and emissivity varies with heat sink material. The specification of the heat sinks without fan for LEDs 10 Watts and with fan for LEDs 20 Watts shown in Tables (1,2) respectively. Choosing the appropriate heat sink material based on conductivity and emissivity is important, at the same time designing the heat sink is complicated due to cost, weight, manufacturability and available space. The maximum temperature mostly occurs in the middle part of the heat sink. The heat sink should be designed based on the power rating of the LED.

LED is mounted at middle of the flat portion. The blades like portion around the LED mounting area are called as fins. In most of the LEDs Aluminum is used as heat sink because of its thermal conductivity and emissivity, cost, availability, light weight and manufacturing process is easier compared to other materials. Thermal conductivity is (204.3Watt/m° C) and emissivity (0.02-0.9) of Aluminum heat sink at 25°C [Li-Kai Wu and Bob Kao (2011)].

Table (1): specification of the heat sinks without fan for LEDs 10 Watts

Heat sink no	1	2	3	4	5
Height (H) [mm]	30.5	27.1	32	27.1	27.1
Length (L) [mm]	50	50	50	50	50
Width (W) [mm]	65	70	50	70	67
Base Thickness (b) [mm]	6	8	7	6	7
Fin Thickness (t) [mm]	1.2	1.2	1	1.2	1
Number of fins	22	22	17	22	17
Fin Spacing (s) [mm]	2	2	3	2	3
Material	Al (6063-T6)				
Heat Transfer Mode	Radiation/Natural Convection				
Emissivity	0.85	0.85	0.85	0.85	0.85
Heat Sink Orientation	Horizontal Base Fins Down				

A sample analysis of a LED attached to a heat sink that will be mounted in several orientations as shown in Fig. (1). The heat sink is cooled via natural convection and radiation or with fan. The LED is attached to the base of a heat sink with the dimensions in mm shown in the figure below. Thermal interface material is placed between the LED and heat sink to electrically isolate the two and reduce the thermal interface resistance. Not using a suitable thermal conductive material will lead to either an insufficient wetting area or a high thermal resistance between LED and heat sink base both immediately resulting in an extra temperature increase of the LED surface and base .

Table (2): specification of the heat sinks with fans for LEDs 20 Watts

Heat sink no	1	2	3	4	5
Height (H) [mm]	40.6	40.6	40.6	40.6	40.6
Length (L) [mm]	50	50	50	50	50
Width (W) [mm]	65	70	50	70	67
Base Thickness (b) [mm]	6	8	7	6	7
Fin Thickness (t) [mm]	1.2	1.2	1	1.2	1
Number of fins	22	22	17	22	17
Fin Spacing (s) [mm]	2	2	3	2	3
Material	Al (6063-T6)				
Heat Transfer Mode	Forced convection				

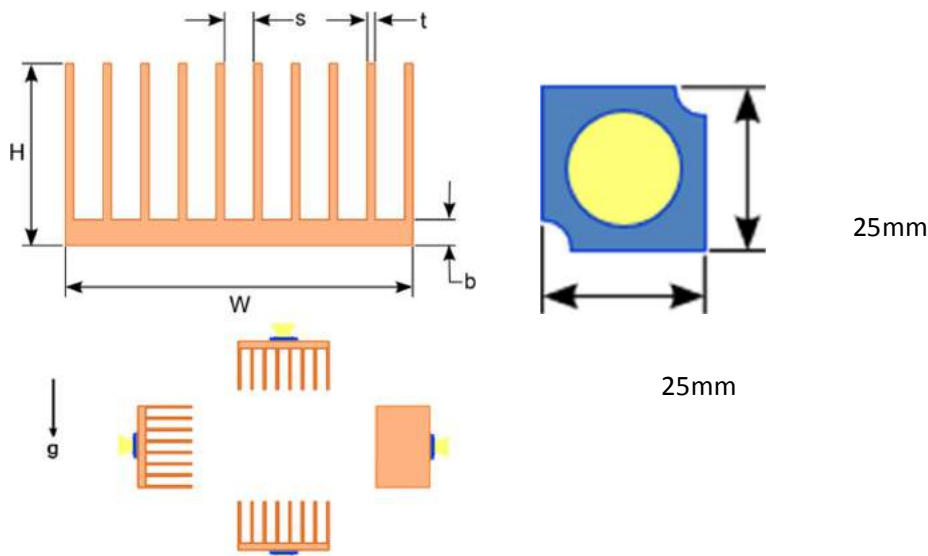


Fig (2): general heat sink dimensions.

Operating time

The light circuit designed to work the LEDs at night and shut down when the sun rises by using the light circuit control as shown in Fig. (3). It is designed to save the power at day and open the circuit automatically at night and shut down when the sun rises.

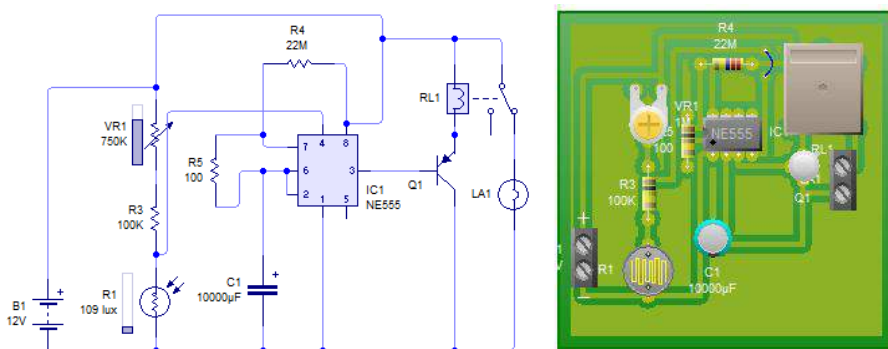


Fig (3): Light circuit control diagram

There are many instruments used to measure the variables as shown below.

DC power supply:

DC power supply (GPR-3510HD) as shown in Fig. (4) with a maximum voltage and amps of 35(V) and 10 (A), input rating 570 Watts at 220 volt, the weight is 18.5 Kg and its dimensions are (225 X145 X420 mm).The DC power supply is directly connected to LEDs and supplies the direct current (D.C.) for two kinds of input powers involving 10 and 20W.



Fig (4): DC power supply (GPR-3510HD).

Digital multimeter

The digital multimeter is used to measure the temperature by thermocouple type T the measure from -200°C to +350°C and an error range of ±0.5°C. Thermocouples are connected to the digital multimeter. All measured temperature points are 3 T-type thermocouples composed of the materials of copper and nickel. The first is attached on the surface of the LED chip to measure the maximum temperature (T_L). The second measured point on chip side as the base of the led (T_S), the third point is placed on back side to measure the ambient temperature (T_a). When the temperatures and illumination of LED riched to steady state and their recording curves appear as a horizontal line, one experimental team stops. Every team spends about one hour.

Thermal resistances

The thermal resistances, which are generally employed to assess the thermal performances of a thermal module and also an important parameter in thermal module, design (Jung C. W. 2014)

$$R_T = \frac{\Delta T}{Q_{in}} = \frac{T_L - T_A}{Q_{in}} \dots\dots\dots (1)$$

Where:

- R_T = the total thermal resistance (°C/W),
- ΔT = the temperature difference (°C),
- Q_{in} = the input power of LEDs (W),

The Electrical power of the LED is determined by multiply the forward voltage (volts) and input current (amps).The surface temperature should be maintained at or below 135°C to maximize the life of the LED.

RESULTS AND DISCUSSION

The temperatures at the surface and the base of the led were measured every 5 mints by using digital multimeter under 12 volts DC and 5 types of fin heat sink with LED 10 watt and 20 watts available in the local shops. The theoretical calculation of the heat sinks is calculated by using (heat sink calculation program at (<https://www.heatsinkcalculator.com/demo.html>)) and the theoretical calculation of the heat sinks were shown in Table (3, 4). The types of the heat sinks available in local shops are suitable for cooling the led (10 Watts) without fan.

Table (3): The theoretical calculation of the 5 types of heat sinks without fan for LEDs 10 Watts

Heat sink no	1	2	3	4	5
Convection Dissipation [Watts]	6.69	6.29	6.66	6.38	6.47
Radiation Dissipation [Watts]	3.31	3.71	3.34	3.62	3.53
Power Source					
Source Length [mm]	25	25	25	25	25
Source Width [mm]	25	25	25	25	25
Interface Conductivity [Watts/(m·°C)]	6.62	6.62	6.62	6.62	6.62
Thermal Parameters					
Ambient Temperature [°C]	21	21	21	21	21
Source Temperature [°C]	75	77.4	78	76.4	76.8
Temperature Difference [°C]	54	56.4	57	55.4	55.8
Heat Sink Thermal Resistance [°C/W]	5.40	5.64	5.70	5.54	5.58

Table (4): The theoretical calculation of the 5 types of heat sinks with fan for LEDs 20 Watts

Heat sink no	1	2	3	4	5
heattransfer mode	Forced convection				
Volumetric flow rate (m ³ /sec)	0.00296	0.0031	0.0034	0.00314	0.00344
Power Source					
Source Length [mm]	25	25	25	25	25
Source Width [mm]	25	25	25	25	25
Interface Conductivity[Watts/(m·°C)]	0.46	0.46	0.46	0.46	0.46
Thermal Parameters					
Ambient Temperature [°C]	21	21	21	21	21
Source Temperature [°C]	66.8	66.9	69.8	66.9	70
Temperature Difference [°C]	45.8	45.9	48.8	45.9	49
Heat Sink Thermal Resistance [°C /W]	0.529	0.538	0.683	0.539	0.692

Effect of cooling systems on LED (10 watts) temperature without fan:

Results in Figs (5, 6) show the effect of cooling systems without fan on the temperature for the base and the surface of the LED 10 Watts at different time for 5 types of heat sink at the local shops in Egypt. The results indicated the temperature for the base and surface of the LED increased by increasing period time, but the increasing of temperature from 0–10 minutes is too high compared to the time from 10–20 minutes for all types of heat sinks that used at the base of the LED and the increasing of temperature become slowly from 20–40 minutes and after this period time the temperature reach stability for all heat sink at the base of the LED.

Also, the result indicated that the best heat sink is number (2) because the maximum temperature of the LEDs (10 Watts) without fan is 49°C and 80°C at the base and surface respectively, and the worst heat sink is number (3) because the maximum temperature at the base of the LEDs (10 Watts) without fan is 66°C and the surface temperature is 92°C.

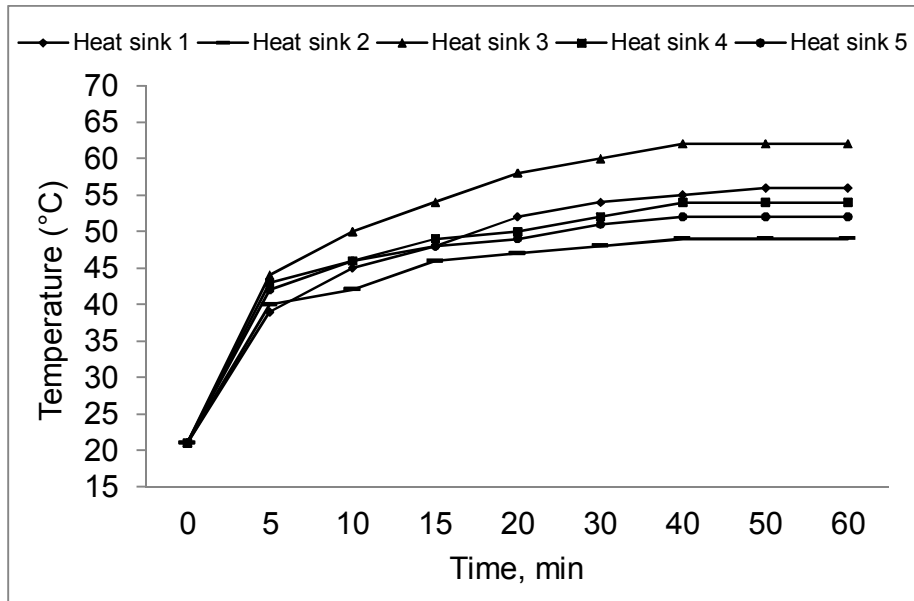


Fig (5): Effect of cooling systems without fan on the temperature at the base of the LED 10 Watts for different time.

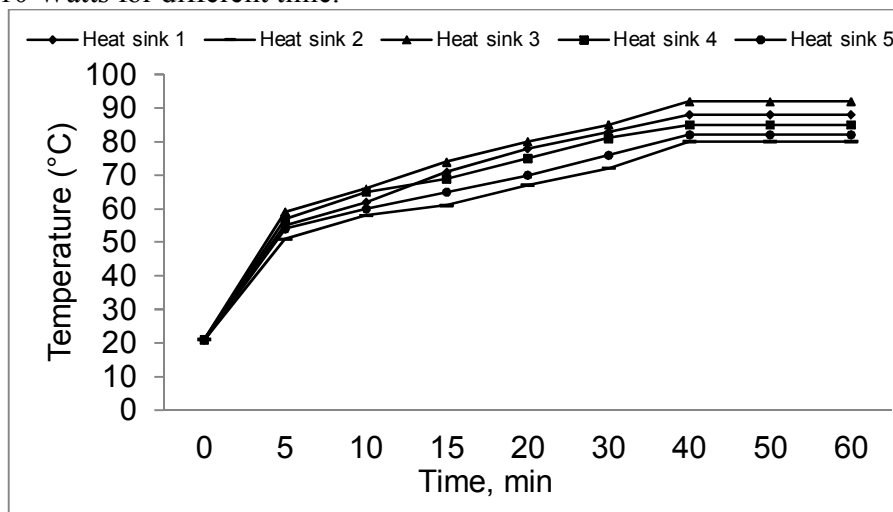


Fig (6): Effect of cooling systems without fan on the LED surface temperature (10 Watts) for different time.

Effect of cooling systems on led temperature 20 watts with fan:

Results in Figs (7, 8) show the effect of cooling systems with fan on the temperature for the base and the surface of the LED 20 Watts at different time for all heat sinks. The results indicated that the temperature for the base and surface of the LED increased by increasing period time, but the increasing of temperature from 0–10 minutes is too high compared to the time from 10–20 minutes for all types of heat sinks at the base of the LED and the increasing of temperature become slowly from 20–40 minutes and after this period time the temperature reach stability at the base of the LED for all heat sinks.

Also, the results indicated that the best heat sink is number (2) because the maximum temperature of the LEDs (20 Watts) with fan is 45°C and 70°C at the base and surface respectively,

and the worst heat sink is number (3) because the maximum temperature at the base of the LEDs (20 Watts) with fan is 55°C and the surface temperature is 79°C.

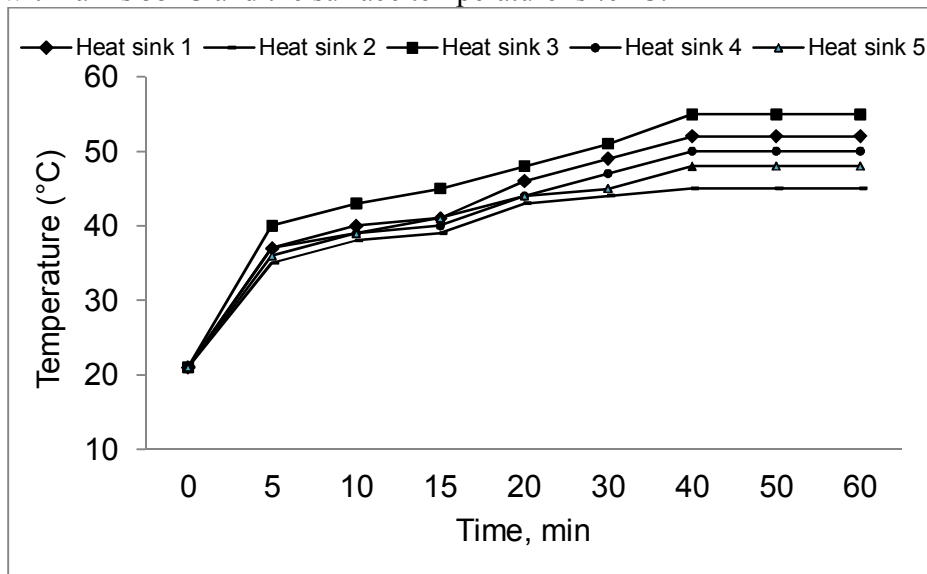


Fig (7): Effect of cooling systems with fan on the temperature at the base of the LED 20 Watts for different time.

The preliminary test was to determine the maximum temperature at the base of the LED without any heat sink. It was also found that the direct use of the LEDs 10 and 20 watts without a cooling unit leads to damage at 78 and 90 °C at the base of the LED respectively.

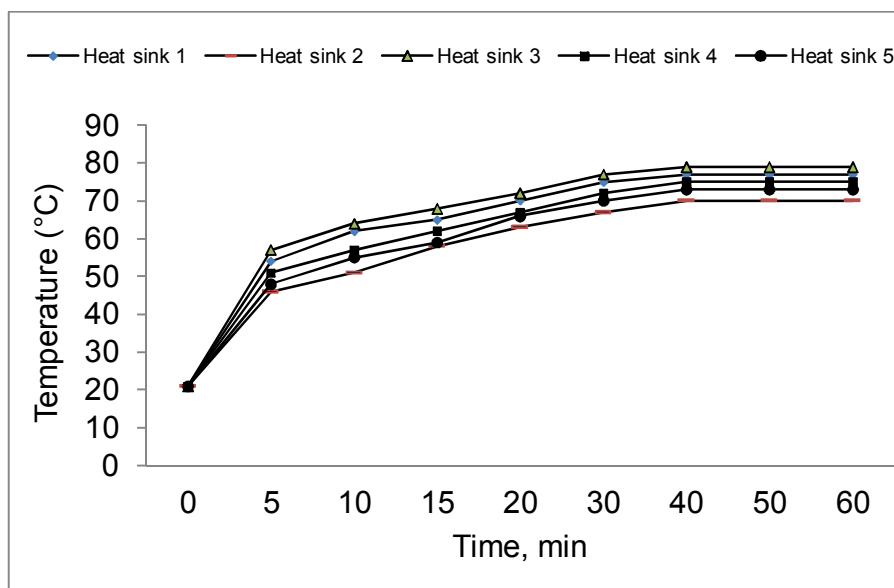


Fig (8): Effect of cooling systems with fan on the LED surface temperature (20 Watts) for different time.

CONCLUSION

The most important issue of the LED research is to find many types of heat sink that found at the local shops to solve the problem of LED over-heating and cooling the increasing of

temperature of base and surface of the LED. There are many suitable types of heat sink that found at the local shops operated with the low power LED up to 10 watts. In the other side the LEDs with power up to 20 watts can operate with the heat sink with fan available in the local shops in Egypt. The best heat sink is number (2), the maximum temperature at the base of the LEDs (10 Watts) without fan is 49°C and the surface temperature is 80°C. The result indicated that the best heat sink is number (2), the maximum temperature at the base of the LEDs (20 Watts) with fan is 45°C and the surface temperature is 70°C. It was also found that the direct use of the LEDs 10 and 20 watt without a cooling unit leads to damage at 78 and 90 °C at the base of the LED respectively. We also found that the LEDs that are powered by direct current (without using inverter) provide 20% energy saving compared with the LED are power by alternating currents. The LEDs long life increased according to the technical recommendations in the catalog when the temperature below at the base of the LED not increase of 60 and 80 °C for each of the LEDs 10 and 20 watts respectively.

REFERENCES

1. Fei Y., K. Pan, Yu Guo and S. Chen (2013). Study on Thermal Degradation of High Power LEDs during High Temperature and Electrical Aging - 978-1-4799-2250-5/13.
2. Jeevaraj S (2014). Numerical investigation on heat sink by computational fluid dynamics (cfd). IJRET: International Journal of Research in Engineering and Technology eISSN: (3) : (452-457).
3. Jung C. W. (2014). Analyzing Thermal Module Developments and Trends in High-Power LED. Vol. 2014, Article ID 120452, pp: 1-111, international Journal of Photo energy.
4. Li-Kai Wu and Bob Kao (2011). Experimental Research of Vapor Chamber in Active Cooling Mode. Cooler Master CO. Innovative technique center. 9F, No.786.
5. Michael R. Kramas, B. S. Oleg and M.M. Regina (2007). Status and Future of High-Power Light-Emitting Diodes for Solid- State Lighting. Journal of Display Technology, 3, Issue. (2) : (160-175).
6. Pawar S.P, N.C. Ghuge, and D.D. Palande. (2015) Review-Design and Analysis of Heat Sink Optimization and its Comparison with Commercially Available Heat Sink. International Journal of Application or Innovation in Engineering & Management., 4, (8), : 101-104.
7. Po-Jen Cheng, David T.W. Lin, Wu-Man Liu, Jui-Ching Hsieh and Chi-Chang Wang (2015) the study of an innovative heat removal model of the aluminum-acetone flat plate heat pipe on high power LEDSB. Transactions of the Canadian Society for Mechanical Engineering, 39, (3), : 739 – 748.
8. Rammohan1 A. and R. C. Kumar (2016) A Review on Effect of Thermal Factors on Performance of High Power Light Emitting Diode (HPLED). Journal of Engineering Science and Technology Review 9 (4) : 165 – 176.
9. Ramos-Alvarado B., Bo Feng and G.P. Peterson (2013) Comparison and optimization of single-phase liquid cooling devices for the heat dissipation of high-power LED arrays. Applied Thermal Engineering. 59, : 648 - 659.

تقييم أنواع مختلفة من أنظمة التبريد لإطالة عمر الليدات التي تعمل بالخلايا الفوتوفولتية

احمد محمد فوزى بهنسى* ، محمد ابراهيم سعد المعداوى*
اسلام محمد السيد السباعى* و محمود عبدالفتاح عبدالمقصود**

* معهد بحوث الهندسة الزراعية – مركز البحوث الزراعية - جيزة
** مركز بحوث الصحراء - جيزة

نظرا لان الطاقة الشمسية مصدر رئيسى وهام من مصادر انتاج الطاقة المتجددة خلال هذا القرن وتتجه جهود كثير من الدول لاستخدام الطاقة الشمسية بمختلف صورها وترصد لها المبالغ اللازمة لتطوير تكنولوجيا استغلال الطاقة الشمسية كاحدى أهم مصادر الطاقة المتجددة والبحوث الخاصة بها، ونظرا لتطور نظم الاضاءة باستخدام الليدات التي كان لها الاثر الكبير فى تخفيض استهلاك الطاقة سواء فى المزارع أو المنازل وكذلك المناطق الزراعية الموجودة فى مناطق بعيدة عن مصدر التيار الكهربى التقليدى والتي تحتاج الى مصادر للاضاءة تكون رخيصة وذات جودة عالية. ونجد أن كشافات الليدات المنتشرة حاليا نوعان الاول هي كشافات الليدات التي تعمل بالتيار المتردد مباشرة مع الكهرياء المنزلية أو تعمل باستخدام الطاقة الشمسية ولكن عن طريق انفرتر لتحويل التيار من مستمر الى متردد وهذا النوع اسعاره مرتفعة جدا والفاقد فى الطاقة يكون كبير حيث ان عملية التحويل من التيار المستمر الى التيار المتردد تستهلك نسبة مهدرة من الطاقة والنوع الثانى من كشافات الليدات التي تعمل باستخدام الطاقة الشمسية مباشرة والتي تعمل بالتيار المستمر.

والمشكلة الاساسية تتلخص فى ارتفاع درجة حرارة الليدات بسرعة مما يقلل من عمرها الافتراضى بالإضافة لعدم وجود منظومة تبريد محددة لكل نوع من الليدات التي تعمل مباشرة مع الطاقة الشمسية وعدم توفرها فى الاسواق المحلية ، وكان لابد من التفكير فى حلول عملية بسيطة لخفض درجات حرارة الليدات التي تعمل بالطاقة الشمسية مباشرة بوحدة تبريد متوفرة فى السوق المحلى المصرى حتى يكون امكانية تطبيقها متاحة وبأسعار منخفضة. لذا فان الهدف من هذا البحث هو تقييم أنظمة تبريد مختلفة تقلل من درجة حرارة الليدات وتزيد من عمرها وبأسعار منخفضة. حيث تم استخدام عدد ١٠ وحدات من أنظمة التبريد المختلفة المتاحة فى السوق المحلى مع مجموعة من الليدات ذات قدرات ١٠ و ٢٠ وات. ونجد من النتائج المتحصل عليها انه يمكن استخدام سطح التبريد (heat sink) فقط مع الليدات ذات القدرة ١٠ وات والاقبل من ذلك أما الليدات ذات القدرات من ٢٠ وات والاعلى من ذلك لابد من استخدام مروحة مع سطح التبريد (heat sink). نجد ان الاستخدام المباشر لليدات ال ١٠ و ٢٠ وات بدون وحدة تبريد يؤدي الى انهيارها عند ٧٨ و ٩٠ درجة على اسفل سطح الليد بالترتيب.

ووجد ايضا ان افضل نوع لتبريد الليدات هو استخدام سطح التبريد رقم ٢ مع الليد ذو القدرة ١٠ وات بدون مروحة حيث كانت درجة الحرارة على سطح الليد ٨٠ درجة مئوية وكانت درجة الحرارة على اسفل الليد ٤٩ درجة مئوية. اما بالنسبة لليد ذو القدرة ٢٠ وات بمروحة وجد ان افضل نوع هو استخدام سطح التبريد رقم ٢ حيث كانت درجة الحرارة على سطح الليد ٧٠ درجة مئوية وكانت درجة الحرارة على اسفل الليد ٤٥ درجة مئوية. ونجد ان الليدات التي يتم استخدامها بدون وجود انفرتر وتعمل بالتيار المستمر توفر فى الطاقة بمقدار ٢٠% عن التي تقوم باستخدام انفرتر وتعمل بالتيار المتردد. ونجد ان الليدات يطول عمرها الى فترة الصلاحية الخاصة بها عندما يكون درجة الحرارة على اسفل الليد ٦٠ و ٨٠ درجة كما هو موصى فى كتالوج الليدات ال ١٠ و ٢٠ وات بالترتيب.

BIOLOGICAL CONTROL OF INSECT PESTS USING A FIELD INSECT'S TRAP OPERATED BY PHOTOVOLTAIC CELLS

ELMEADAWY, M. I.*; I. M. EL-SEBAEE*;
A. A. EL-KEWAY * and M. A. ABDEL-MAKSOU**

* *Agric. Eng. Res. Inst. (AEnRI)ARC, Giza.*

** *Mariout Research Station D.R.C.*

Abstract

The aim of this research was to develop a new model of solar led light trap and sex attractive trap with vacuum fan, provide no harm to the nature and also have low cost involvement so that it can be operated by most of the farmers. The trap was conducted to develop a new model of solar light trap and attractive trap with vacuum fan and the solar light system including solar panel, charging unit, battery and LED bulb installed with the light trap so that this solar light trap can control the insect pests of different crops effectively. Farmers meet the problems of various types of insect pests that harm crops and result in loss of productivity each year. The most important results of the research are that the solar light trap works during the day and night, the general efficiency of the developed trap more than the efficiency of the JT trap (the control treatment) by about 68.8%. experiments was carried out was tested at the Research Center of Mariout in Amriya of the Center for Agricultural Research with the system of attractiveness of fruit flies from sunrise to sunset in the months of June and July, August, September and October in addition to the solar light trap could capture flies at nights with LEDs. From the data the general efficiency of the developed trap more than the efficiency of any trap because it works all day. In addition the develop trap can be used with many types of pheromones and any colors of LEDs with many wave length to attractive many types of insects that the farmer need to captured.

Keywords: solar light trap., Biological control, insect pests,

INTRODUCTION

Agriculturalists has tried to find other ways instead of chemical method such as using lights to tempt pests which is popular way for farmers. However, this way is still lack of electric energy for bulbs because the farm is far away, and trap is also expensive.

Nowadays there are many ways to destroy insect and reduce damages from pest. Farmers use many ways of conventional techniques with insects and pests such as, Biological Alternatives, Non Biological Alternatives, Plant Resistance, Cultural Methods, Mechanical and Physical Methods, Legal Control, Chemical Control, Integrated Pest Control, Natural or Organic Farming.

Draz *et al.*(2016) Obtained results declared that the pest had 7-8 annually generation. Jackson traps that placed in center of orchard and hanged at 2 m height more efficient than others for male catches. Highest numbers of PFF male attack orchards of Navel orange intercropping with Guava, while the lowest were with Navel orange and Guava. Each of season and kind of orchard or intercropping system had combined and significant effect on mass trapping.

Mabrouk, M. S.O. and M. Ab. - Moez Mahbob (2015) A trap with red and black light colour was the best attractive equipment for the wax moths. Where, the red colour traps caught the greatest number of moths, recording, 50.0% of the total moth captured, while the, white color traps caught the fewest number of moths recording only 23.27% with average 42.977% when the traps is far from the colonies by 6 meters only, while they were 50.94 and 3.7% with average 38.58 % when the distance between the colonies and light trap were 12 meters. Future research is

recommended for better understanding of the effect of trap color on the diversity and abundance of non-target insects captured.

Bera P. K. (2015) The development of this solar light trap and successful demonstration of this tool in different crop areas by the farmers in four districts of West Bengal including ZARS, Mohitnagar resulted that as an alternate of chemical pesticide, this tool may be considered as important for its ecofriendly nature and low cost involvement to both the farmers and agricultural experts. The solar light trap model will be very much effective for the control of different insect pests of all crops without any use of chemical pesticides in the agricultural fields in near future.

Sermisri N., and C. Torasa (2015) developed a solar energy-based insect pests trap by using ultraviolet light emitting diode tube to lure the insect pests and 12 volt battery as power supply to light emitting diode tube. The battery charging system derives electrical energy from 20 watts of solar cell for use at night. This proposed Solar Energy-Based Insect Pests Trap has an automatic control system to lure insect pests when there is no sunlight and the system will be stop when the sun shines. The results of the system installation test showed that this proposed Solar Energy-Based Insect Pests Trap could lure several types of insect pests in vegetable and coconut plantations including Brotispa, Elephus beetles, and Aphis, etc.

Hanson *et al.* (2012) There was no significant difference between traps connected to solar panels(solar traps) and traps not connected to solar panels (control traps) in the number of *Aedes vexans*, *Coquillettidia perturbans*, *Culiseta inornata*, and *Aedes dorsalis* that they collected. Batteries connected to solar panels operated traps significantly longer than batteries without solar panels. Making the operation of traps less labor-intensive would increase the number of traps that can be deployed and/or the number of sites sampled.

There for the aim of this research was to develop a new model of solar led light trap and sex attractive trap with vacuum fan, provide no harm to the nature and also have low cost involvement so that it can be operated by most of the farmers

MATERIALS AND METHODS

The advantage of solar LED light is easy to use and can be applied to various crops. The solar LED pest control light is mainly composed by solar panels, batteries, control circuit, LED lamps and fan and other components.

During the day, energy from the solar panels will be stored in the storage batteries at night, the electrical energy from the battery could drive circuit of LED light to control pest. The light-trap is the most commonly used sampling device to study the pests of flight characteristics. However, the effectiveness of light-trapping as an insect sampling method was influenced by many environmental variables from meteorological to cosmic factors.

Modified trap can help in reducing pest populations and maintain them below economic levels, thus reducing crop losses and the need for more costly control measures that may also have undesirable environmental side-effects.

The sex attractive trap design

There are many pests can be capture by the developed trap with sex attractive or bait attractive. The Mediterranean fruit fly, *Ceratitidis capitata* (Wiedemann), is one of the world's most destructive fruit pests. Because of its wide distribution over the world, its ability to tolerate colder climates better than most other species of fruit flies, and its wide range of hosts, it is ranked first among economically important fruit fly species. Its larvae develop and feed on most deciduous, subtropical, and tropical fruits and some vegetables. Although it may be a major pest of citrus, often it is a more serious pest of some deciduous fruits, such as peach, pear, fig, and apple.

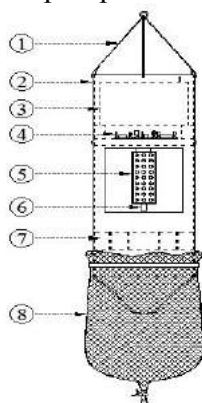
To determine the number of the Mediterranean Fruit Fly (MFF), *Ceratitis capitata*, the develop trap was baited with the sex attractants in capsule lure trimedlure (for MFF). The capsules were fixed on the top of the fan in the traps. The capsules were regularly exchanged every month.

Design of developed trap.

The developed trap consists of solar panels, charger control, vacuum fan, control circuits, LED, Trapping net and leg support base as shown in Fig.1 and the diagram of the developed trap is shown in Fig.2. The function of solar panels is to convert the solar radiant energy to the electrical energy by charger control which is then stored to the battery for the load to use, the control circuit is the core of the solar LED pest control system.



Fig. (1) The develop trap with solar panel energy



1	Trap sling
2	Main body
3	12-V DC Battery
4	DC Electric circuits control
5	12-V DC led
6	Sex attractants
7	12-V DC fan
8	Trapping net

Fig. (2)The schematize diagram of the develop trap

Design of solar panel

The solar radiation in Alexandria city is greater in summer and less in winter and the annual average sunshine hours are good. The LED pest control light is required to work at night (from sun rise to sun set), the solar energy components that used to operate the developed trap was

constructed to operate all parts of the developed trap .Most of the used materials used are already available in the local market in standard form. These include:

- 12V battery, 14 Amps,
- solar panel, 50 watts and 17 volts,
- Charge controller,

Design of LED light control

There are many types of colors LED used with the solar trap depends on the type of the pests. Based on the sensitive wavelength range of most of the pests with photo taxis, LED is selected as the light source. Carry out superimposing light distribution and utilize the photo taxis and chemo taxis of the target pests to attract and kill pests.at the developed trap the (white) LED are used to attract the pests. The light circuit consists to work at night and shut down when the sun rises by using the light circuit control as shown in fig (3).

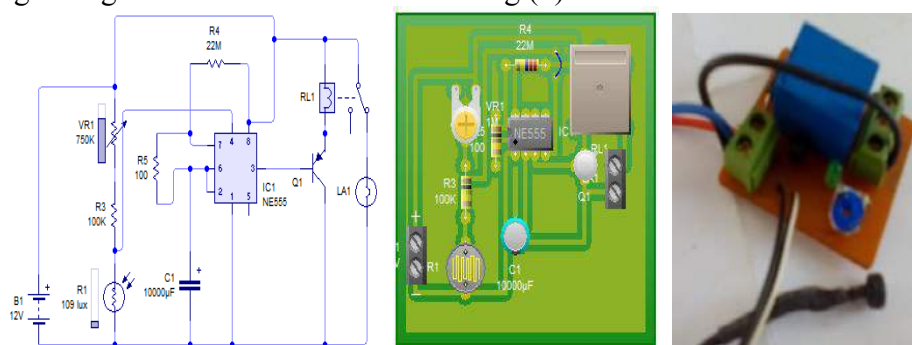


Fig (3): Light circuit control

Design of fan timing circuit control and Trapping net

The destroyer (vacuum) trap (fan) is shaped to fight insects in all directions, the fan is having powerful vacuum, with combined optimal airflow design to draw insects into mess (net) collection chambers where they die. It is designed on basis of design value of 2000~2,500rpm low speed to high-flow rate suction, designed for safety. It is run by the 12 V- DC power sources. The trap designed to work the fan for one minute every five minutes by using the timing circuit as shown in Fig (4).

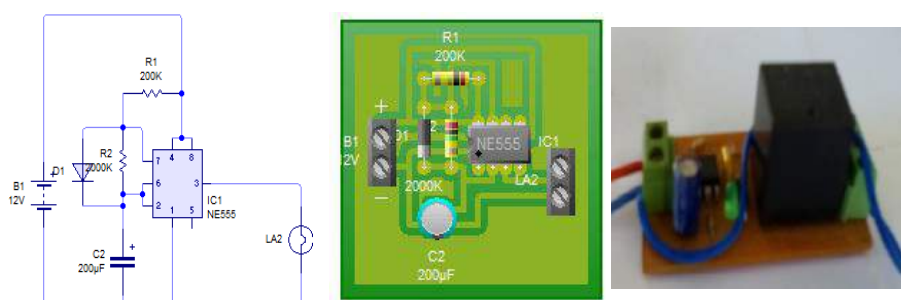


Fig (4): Timing circuits control

The net is made with small diameter of plastic net and it is having capability to store three months of pests. It is flexible to open and close and remove the pests.

The JT trap (control treatment)

The JT is older version of trap used to capture adults of the Mediterranean fruit fly, *Ceratitis capitata* (Wiedemann). Credits: USDA and one of the most economical traps commercially available in Egypt. It is used as a control treatment as shown in Fig (5). It is easy to carry, handle

and service, providing the opportunity of servicing a greater number of traps per man-hour than other commercial traps. Adults are collected primarily by use of sticky-board traps and baited traps (JT) (USDA 1997). This trap is mainly used with para pheromone lures to capture male fruit flies. The most common lures used with the JT are: trimedlure (TML). The body of a standard JT is a delta shaped object made of waxed cardboard material. The additional parts include: 1) a white or yellow rectangular insert of waxed cardboard. The insert is covered with a thin layer of sticky material known as “stickem” (Tangle foot) used to trap flies once they land inside the trap body, 2) a polymeric plug and a plastic basket that holds the lure plug and 3) a wire hanger placed at the top of the trap body.



Fig. (5) The JT trap

RESULTS AND DISCUSSION

The effect of period on attractiveness of insect pests for the white LED light

The flies were collected from a grower in Mariout region by solar light trap (white led) were placed in agricultural areas. This experiment was carried for a period of five months from June to October. So, results in Fig (6) show the effect of white led light with develop trap on attractiveness of insect pests compared of the dark trap (control). The results indicated that the number of attractiveness of insect pests for white led light trap were 195, 315, 407, 228 and 265 males/trap/month in June, July, August, September, October, respectively compared zero males in dark trap. Also the results indicated that the flies during July and August (from 5 to 13 weeks) were a high than any months at the period of five months, from this data in general, the total numbers of the flies captured from the white LED light with developed trap were 1410 males compared with zero for the dark trap (control).

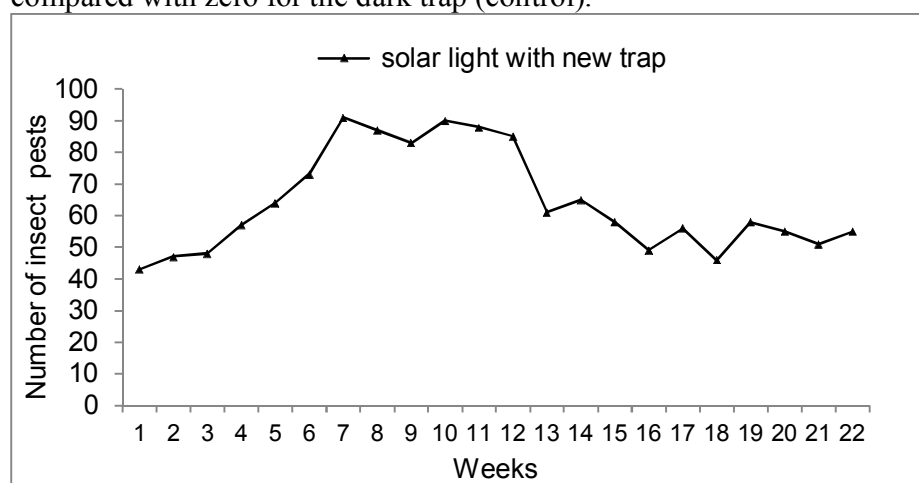


Fig (6): Effect of period on attractiveness of insect pests for the white LED light.

The effect of sex attractants on attractiveness of insect pests with developed trap and JT trap.

Results in Fig (7) show the effect of the sex attractants with developed trap on attractiveness of insect pests compared to JT trap (control). The results indicated that the number of attractiveness of insect pests for the sex attractants with developed trap are 407, 678, 894, 440 and 421 males/trap/month compared with JT trap are 229, 392, 542, 267 and 252 males/trap/month in June, July, August, September, October, respectively. Also the results indicated that the flies during July and August (from 5 to 13 weeks) are more than any months at the period of five months from June to October (22 weeks)

In general the total numbers of the flies captured from sex attractants with develop trap are 2840 males compared to the JT trap 1682 for a period of five months from June to October, from this data the efficiency of the sex attractants with develop trap is more than the efficiency of the JT trap with 68.84%.

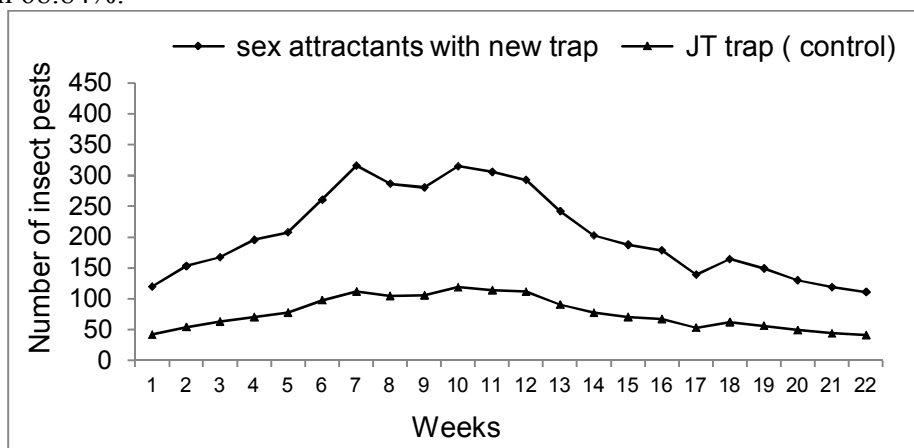


Fig (7): The effect of sex attractants on attractiveness of insect pests with developed trap and JT trap.

The effect of solar light and sex attractants with the develop trap on attractiveness of insect pests compared to JT trap.

In Fig (8) show the effect of solar light and sex attractants with the developed trap on attractiveness of insect pests compared to JT trap (control). The results indicate that the number of attractiveness of insect pests for develop trap are 602, 993, 1301, 668 and 686 males/trap/month in June, July, August, September, October, respectively compared with JT trap were 150.5, 248.25, 260.2, 167 and 137.2 males/trap/month in June, July, August, September, October, respectively. Also the results indicate that the flies during July and August (from 5 to 13 weeks) are more than any months at the period of five months from June to October (22 weeks).

In general the total numbers of the flies captured from develop trap were 4250 males compared to the JT trap 1682 for a period of five months from June to October; from this data the efficiency of develop trap more than the efficiency of the JT trap with 152.67%.

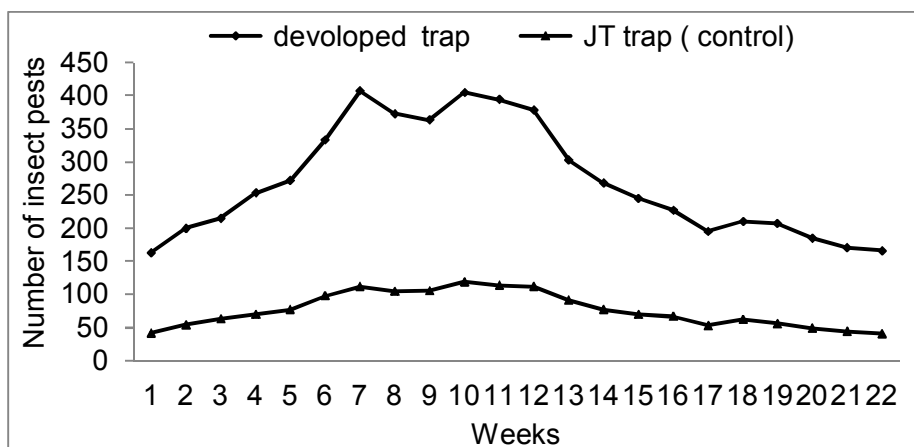


Fig (8): Effect of developed trap and JT trap from June to October on attractiveness of insect pests.

From the data the general efficiency of the developed trap is more than the efficiency of any trap because it works all day. The developed trap can use many types of pheromones and any colors of LEDs with many wave lengths to attract many types of insects that the farmer needs to capture.

The power requirement for the developed trap

The maximum power used to operate the developed trap was 20W for fan and 5 W for LED. The developed trap was designed to work the fan for one minute every 5 minutes, the light circuit consists to work at night and shut down when the sun rises. The solar components consist to provide the trap with power at this case. The fan operates for four hours every day and the lamp works for 13 hours maximum. The total power required for the trap at day was 40 watts for fan from sunrise to sunset and 105 watts for fan and LED at night.

CONCLUSION

The trap was developed to create a new model of solar light trap and attractive trap with vacuum fan, providing no harm to nature and also having low cost involvement so that it can be operated by most of the farmers. For that purpose firstly a model of light trap with plastic structure was developed, then a solar light system including solar panel, charging unit, battery and LED bulb installed with the light trap so that this solar light trap can control the insect pests of different crops effectively.

The results indicated that:

- The flies during July and August are more than any months at the period of five months from June to October.
- The total numbers of the flies captured from the white LED light with developed trap were 1410 males compared with zero for the dark trap (control).
- The total numbers of the flies captured from sex attractants with developed trap were 2840 males compared to the JT trap 1682 for a period of five months from June to October, from this data the efficiency of the sex attractants with developed trap more than the efficiency of the JT trap with 68.84%.
- The total numbers of the flies captured from developed trap were 4250 males compared to the JT trap 1682 for a period of five months from June to October; from this data the efficiency of developed trap more than the efficiency of the JT trap with 152.67%.

- In general the efficiency of the developed trap more than the efficiency of any trap because it works all day .the develop trap can use many types of pheromones and any colors of LEDs with many wave length to attractive many types of insects that the farmer need to captured.

RECOMMENDATION

Other types of baits should be used not only sex attractant for males but it also for both sexes for both species, as food attractant (Buminalor protein hydrolyzate). The buminal bait should be used with developed trap and record the captured flies males and females weekly. And many types of LED could use to attractants many types of flies as the farmer need in the seasons.

REFERENCES

1. Bera P. K. (2015) Development of a New Solar Light Trap Model and Its Utilization as IPM Tool in Agriculture. Volume 2, Issue 3: 549-554.
2. Draz K. A., R. M. Tabikha, M. A. El-Aw, I. R. El-Gendy and H F. Darwish (2016). Population activity of peach fruit fly *Bactrocera zonata* (Saunders) (Diptera: Tephritidae) at fruits orchards in Kafer El-Shikh Governorate, Egypt. *Arthropods*, 5(1): 28-43
3. Hanson S. M., A. L. Johnson., Y. Hou and M. D. Hellwig (2012) Recharging Centers for Disease Control Light Trap Batteries with Solar Panels. *International Journal of Applied Science and Technology* 2 (7): 76-80.
4. Mabrouk, M. S.O. and M. Ab. - Moez Mahbob (2015) Effect of Different Coloured Light Traps on Captures and Controlling Wax Moth (Lepidoptera: Pyralidae). *Egypt. Acad. J. Biolog. Sci.*, 8(2): 17-24.
5. Sermsri N., and C. Torasa (2015) Solar Energy-Based Insect Pest Trap. *Procedia - Social and Behavioral Sciences* (197):2548 – 2553.
6. USDA. (1997). New lure may help conserve helpful, sterile medflies, News& Events.<http://www.ars.usda.gov/is/pr/970731.htm>.

المكافحة الحيوية للآفات الحشرية باستخدام صاندة حشرات حقلية تعمل بالخلايا الفوتوفولتية

محمد ابراهيم سعد المعداوى * ، اسلام محمد السيد السباعي *
عبد الفتاح عبدالرؤف القويعى * و محمود عبد الفتاح عبدالمقصود **

* معهد بحوث الهندسة الزراعية – مركز البحوث الزراعية - جيزة
** مركز بحوث الصحراء – جيزة

الهدف من البحث هو تصنيع صاندة حشرات بخامات محلية بسيطة ومنخفضة التكاليف، وتم تعظيم عمل الصاندة بحيث تعمل على مدار الـ ٢٤ ساعة بالطاقة الشمسية المباشرة نهاراً ومن بطاريات تخزين الطاقة الشمسية ليلاً. يواجه المزارعون مشكلة الآفات الموسمية التي تدمر معظم المحاصيل الزراعية بشكل خطير، حيث يلجأ المزارع الى احدى طرق الوقاية أو المكافحة للتغلب على هذه المشكلة، ومن هذه الطرق الميكانيكية، البيولوجية، الكيمائية وغيرها من الطرق. ومن أكثر هذه الطرق استخداماً الطرق الكيماوية وذلك باستخدام محاليل المبيدات الكيماوية والتي تؤثر بدرجة كبيرة ومباشرة على المزارعين والمستهلك، هذا فضلاً عن التأثير الضار على الثروة الحيوانية والبيئة بالإضافة الى التأثير السلبي على الصادرات. ومن الطرق التي كثر في الأونة الأخيرة استخدام مصائد الحشرات، منها المصائد ذات الجاذبات الجنسية والضوئية. ومن هنا كان التفكير في صاندة حشرات مركبة تستخدم جاذبات جنسية نهاراً وجاذبات ضوئية ليلاً وإصطياد الحشرات بالشفط الجبرى بمروحة ١٢ فولت تعمل بالطاقة الشمسية المباشرة من الخلايا الفوتوفولتية أو المخزن منها بالبطارية، ومن هنا يتم تعظيم عمل صاندة الحشرات لتعمل على مدار الـ ٢٤ ساعة. وتم تطوير وتصنيع الصاندة من مواسير بلاستيكية قطر ٧ بوصة ومروحة ١٢ فولت ولمية ليد للجذب الضوئي ليلاً. وكل هذه المنظومة تعمل بالطاقة الشمسية من خلال خلايا شمسية ووحدة شحن وبطارية ودائرتي تحكم الأولى للتحكم في تشغيل اللبة ليلاً فقط والثانية للتحكم في تشغيل المروحة لمدة دقيقة واحدة بعد كل خمس دقائق توقف وذلك لشفط المتجمع من الحشرات في الخمس دقائق حول الجاذبات الجنسية نهاراً أو ضوء اللبة ليلاً ثم دفعها الى كيس تجمع الحشرات.

ومن أهم النتائج المتحصل عليها من البحث :

- اعلى تجمع للحشرات خلال الموسم كان خلال شهري يوليو وأغسطس .
- استخدام الليدات ذات اللون الابيض مع صاندة الحشرات المطورة ادى الى التقاط ١٤١٠ حشرة مقارنة بصفر مع الظلام (الكنترول) خلال الفترة من يونيو إلى أكتوبر .
- بلغ العدد الكلي للحشرات التي تم التقاطها بالجاذبات الجنسية مع صاندة الحشرات المطورة ٢٨٤٠ حشرة مقارنة مع صاندة الحشرات (JT) ١٦٨٢ حشرة خلال الفترة من يونيو إلى أكتوبر ، من هذه البيانات نجد ان كفاءة صاندة الحشرات المطورة مع الجاذبات الجنسية كانت أعلى من الكفاءة الصاندة الكنترول (JT) بمقدار ٦٨,٨٤٪.
- بلغ العدد الكلي للحشرات التي تم التقاطها بصاندة الحشرات المطورة ٤٢٥٠ حشرة مقارنة مع الصاندة الكنترول ١٦٨٢ حشرة خلال الفترة من يونيو إلى أكتوبر. من هذه البيانات كفاءة صاندة الحشرات المطورة كانت أعلى من الكفاءة الصاندة الكنترول بمقدار ١٥٢,٦٧٪.
- بشكل عام كفاءة صاندة الحشرات المطورة سوف تكون أعلى كفاءة من أى صاندة أخرى لأنها تعمل خلال ٢٤ ساعة ، بالإضافة الى امكانية استخدام ألوان متعددة من الليدات وبأطوال موجية مختلفة على حسب نوع كل حشرة مع الجاذبات الجنسية المناسبة معها بالإضافة لكونها تعمل وتفصل اوتوماتيكياً ودون تدخل اى فرد.

**INNOVATED FAST SYSTEM TO DETECT RESISTANCE
OF VERTIMEC (ABAMECTIN) IN THE TWO SPOTTED-SPIDER MITE,
TETRANYCHUS URTICAE KOCH**

RANIA AHMED ABD EL-WAHAB

Plant Protection Research Institute, Agricultural Research Institute, EGYPT
rania-proline@hotmail.com

Abstract

Incremented resistance of pesticides remains a fundamental problem for unacceptable effects on environment. So there is a need to detect it faster and then find effective tools to reduce it as soon as possible specially in mites such as *Tetranychus urticae*. Resistant mites were affected by climate change also in the same time, which contributed in the increase of pesticides' resistance. Essential problem is depending on the detection of resistance by simple innovated instrument powered by solar energy. It is depending on the determination of the changes of electromagnetic field forces affected by case of certain exposed mites as samples. Gained differences of electromagnetic forces were confirmed by assessment of resistance ratios (RRs) which recorded 8.52- and 4.53- folds for resistant Vertimec (Abamectin) strains on cotton and soybean, resp., upon Vertimec LC50s. Likewise, they were 5.97- and 4.29- folds for field Vertimec strains on cotton and soybean, resp. Hence, there was no significant differences between resistant and field strains while such occurred with high significance between them and susceptible strain. It could be concluded that, climate changes have a link with pesticides' resistance which increased expectations to use easy and fast system to detect it under field conditions.

Keywords: Climate Changes, Detector, Electromagnetic, *Tetranychus*, Resistance and Vertimec.

INTRODUCTION

Pesticide resistance is an essential subject particularly when it is related to the two spotted spider mite, *Tetranychus urticae*. So it's vital to take the most important component of climate changes as a top priority when the resistance is the issue which agriculturists should give a hand to it. Increased levels of both UV and CO₂ in Egypt amid the cotton and soybean development of this examination through 2016 interacted with sprayed miticide, Vertimec (Abamectin 18 g l⁻¹ EC).

Moreover, pests existed a noteworthy explanation behind crop production' calamity worldwide even with the broad utilization of chemical pesticides. Over half of all insecticides were organophosphates, pyrethroids, organochlorines, carbamates, and biopesticides, and they were proceeded at numerous ecological, agricultural, medical, and financial issues. Imperatively, as a result of overwhelming utilization of synthetic insecticides, a selection pressure was forced on insect populaces, bringing about the development of resistance against hopeful compound(s). Particular metabolic pathways utilized by insects to change over hindrances into less poisonous structures or their expulsion from the framework are featured. Utilizing the proteomics approach, responsible proteins affected by pesticides in insects and then alterations of them by pesticides' resistance could be distinguished, also (Dawkar *et al.*2013). The available tool to assay pesticides' resistance is depending on Immunochromatographic dip-stick-format kits. They were created to distinguish resistance to carbamates and organophosphates and others. Strips were upon polyclonal antisera versus resistance of pesticides which related to esterase isozymes isolated from

insects. They were simply used by farmers anywhere (Kranthi, 2005). But still the problem which is related to cost and accuracy. Using electromagnetic fields as traps or even to attract or eject pests, is an ordinary known. It was started by Gerharz (1991) who situated the electromagnetic field nearby or in a pest control. Gadget was chosen from the gathering comprising of insect traps, insect teasing stations containing a pest poison, and pointer stations also. For instance, a wide assortment of regular pest traps for slithering insects could be retrofitted with an electromagnetic field generator. Devices could have the generator to a focal area of a trap with an electromagnetic field generator, contained or not, a chemical or biological attractant.

So there is a need to get a priceless device that would be able to get fast and accurate results to help farmers to discover the problem in the beginning before its development. In the same time, there will be a new use of electromagnetic fields to detect pesticides' resistance in order to protect the environment of more quantities of acaricides.

Mites with certain changes in their bodies provided electric changes and then with the present magnetism in the instrument, electromagnetics field are available to react effectively with exposed mites. Nevertheless, resulted electromagnetic fields' forces were assessed and their Axis Graph Magnetic Meter also by the innovated instrument in order to detect pesticides' resistance easily and vastly as presented in this paper.

MATERIALS AND METHODS

-Innovated Instrument Components:

The prototype of the instrument was showed at Fig. (1) with all of its components. Solar panel with its attachments. DC-Motor, electromagnetic field resulted from two magnets and with the passage of electric current then the required field was gained. Whenever the current is gone through mites, the electrophysiological differences appeared in changes of voltages at LCD monitor. Microcontroller system (PIC16F627A) was used to detect the resistance through electrochemical changes in the resistant strain in comparable with the other sensitive one. The sensor, UGN3503U was used to determine the magnetic field strength and varying voltage provided at output proportional which picked up to the field strength. Also, Electromagnetic interference (EMI) detector was attached to the present circuit to provide and confirm accurate readings of the final electromagnetic field strength. Comparison was appeared in both of the magnetic field force and the current conductance with attention to any differences in food resource, weather conditions, etc.

Fig. (1) Instrument Prototype Parts:

- 1-Solar Panel
- 2-Container of battery, microcontroller system (PIC16F627A), UGN3503U, EMI and others
- 3-Power
- 4- Blue Light Emitting Diodes (LEDs)
- 5- Red Light Emitting Diodes (LEDs)



-Maintenance of *Tetranychus urticae* strains:**Susceptible strain**

Colonies of the spider mite, *T.urticae* were raised under lab conditions ($25\pm 2^{\circ}\text{C}$, and $60\pm 5\%\text{RH}$) at Plant Protection Research Institute for several years without exposure to any contaminations or pesticides.

Resistant strain

Original colony of the spider mite, *T.urticae* was set up from mites gathered from castor oil plants without exposing to pesticides. It was raised under laboratory conditions ($25\pm 2^{\circ}\text{C}$, and $60\pm 5\%\text{RH}$) to assess the action of Vertimec (Abamectin $18\text{ g l}^{-1}\text{ EC}$) against *T.urticae* grown-up females. The leaf-dip technique presented by Dittrich (1962) was utilized. All treatments were done under laboratory conditions and each was replicated three times. Likewise, control discs were dipped in water only. Mortality percentages were determined and corrected by using Abott's formula (1925). Pooled data were subjected to probit analysis (POLO PC) (LeOra software, 1994). The original strain females were selected for Vertimec for 20 generations according to Yang *et al.* (2002) with some modifications. 1000 adult females of this colony started this selection. Every two generations, the LC50 and LC90 were evaluated. New LC50 was applied as subsequent selection pressure. The next selection transferred to untreated leaves. LC50 estimations of the selected strain were compared to those of the susceptible strain. LC50 of Field colony was got after exposure to the recommended concentrations of Vertimec under certain values of UV and CO₂ which interacted with sprayed pesticide on infested cotton and soybean with *T.urticae*. Then, the resistance ratio (RR) was computed. Field colony was got after exposure to the recommended concentrations of Vertimec under certain values of UV and CO₂ which interacted with sprayed pesticide on infested cotton and soybean with *T.urticae*.

-Determination of electromagnetic fields:

Samples of *T.urticae*, about 100 adult females, were placed inside the instrument. Resistant and field strains were compared with the control which were reared on cotton and soybean leaves. Differences of electromagnetic fields' forces and Axis Graphs were appeared and recorded by the microcontroller system.

-Data Analysis

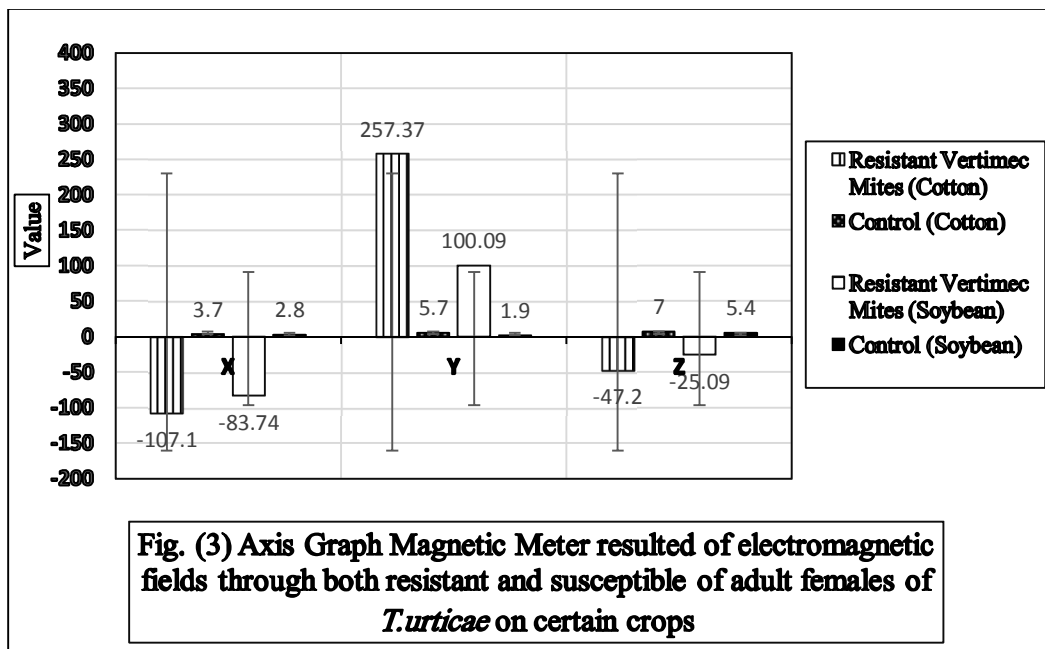
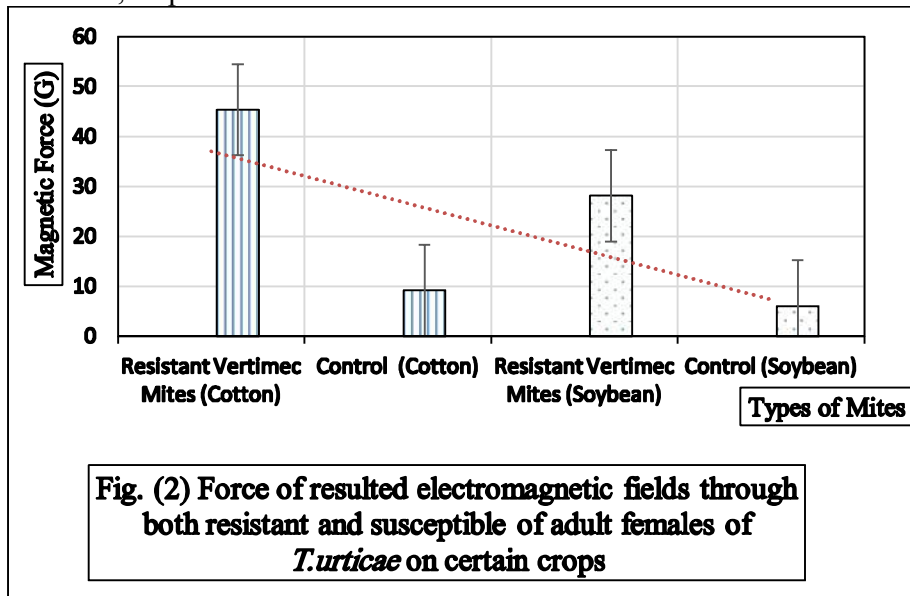
SPSS (V.16) was used to show differences among resistant, field and susceptible strains under electromagnetic' forces instrument. Jonckheere-Terpstra Test, Friedman Test, Kendall's W and others were used to test significance between resistance and susceptible cases at probability with 5% and 1%.

RESULTS AND DISCUSSION

Data revealed that strength of electromagnetic fields was changed particularly with significant differences between resistant and susceptible mites as appeared at Fig. (2). Direct determination recorded high strength of electromagnetic fields in case of resistant = mites to Vertimec on cotton followed by resistant strain on soybean with 45.37 and 28.14 G, respectively. Therefore, there were specific differences in Axis Graph Magnetic Meter resulted of electromagnetic fields through both resistant and susceptible of adult females of *T.urticae* on certain crops as appeared at Fig. (3).

Jonckheere-Terpstra Test showed that Std. Deviation of J-T Statistic = .957* among grouping variables of mites. Therefore, both Chi-Square and Median were = 3.000^a and 28.140^a. While, Kruskal-Wallis Test showed that Chi-Square = 2.000^b at 5%. Proximity Matrix proved that a dissimilarity matrix with 51.587 as euclidean distance among variables while a similarity matrix was determined by the correlation between vectors of values was -.997-.

Subsequently, toxicity of Vertimec was compared both of field and resistant strains with the susceptible strain of *T.urticae* on cotton. Whereas, LC₅₀ values were 1542.91, 1915.47 and 258.45 μLL⁻¹, resp., which showed that LC₅₀ of cotton field strain exposed to moderately levels of CO₂ and UV recorded so close value to that of 20th generation of the laboratory resistant strain. The same situation was in the case of LC₉₀s which recorded 14207.39, 16328.37 and 1420.74 μLL⁻¹, resp. Relative to the laboratory strain (S), the resistant ratios (RR) to Vertimec for *T.urticae* laboratory resistant strain and field strain, showed at Table (1). RR's at Vertimec LC₅₀s were 5.97-folds and 8.52-folds, resp. The



same trend was occurred in case of assessment of Vertimec resistance in *T.urticae* strain on soybean. Data showed that LC₅₀ values were 4013.25, 4220.17 and 198.82 μLL⁻¹, resp., which

showed that LC₅₀ of cotton field strain exposed to moderately levels of CO₂ and UV recorded so close value to that of 20th generation of the laboratory resistant strain. The same situation was in the case of LC₉₀s which recorded 17210.74, 19102.35 and 780.34 μLL^{-1} , resp. Relative to the laboratory strain (S), the resistant ratios (RR) to Vertimec for *T.urticae* laboratory resistant strain and field strain, showed at Table (1).

Table (1) Assessment of Vertimec toxicity against certain strains of adult females of *T.urticae*

G.	Crops	Vertimec Lethal Concentrations				LC ₉₀ /LC ₅₀ Ratio
		LC ₅₀		LC ₉₀		
		Main μLL^{-1}	*RR ₅₀	Main μLL^{-1}	*RR ₉₀	
Field	Cotton	1542.9 ^a	5.97	14207.3 ^a	9.99	9.21
Resistant		1915.4 ^a	8.52	16328.3 ^a	11.49	8.52
Susceptible		258.45 ^b		1420.74 ^b		5.50
Field	Soybean	4013.25 ^a	4.29	17210.74 ^a	22.10	4.29
Resistant		4220.17 ^a	4.53	19102.35 ^a	24.48	4.53
Susceptible		198.82 ^b		780.34 ^b		3.92

*Resistance ratio (RR) = LC₅₀ or LC₉₀ of Resistant Strain/ LC₅₀ or LC₉₀ of Susceptible Strain

RR's at Vertimec LC₅₀s were 5.97- folds and 8.52- folds, resp. The same trend was occurred in case of assessment of Vertimec resistance in *T.urticae* strain on soybean. Data showed that LC₅₀ values were 4013.25, 4220.17 and 198.82 μLL^{-1} , resp., which showed that LC₅₀ of cotton field strain exposed to moderately levels of CO₂ and UV recorded so close value to that of 20th generation of the laboratory resistant strain. The same situation was in the case of LC₉₀s which recorded 17210.74, 19102.35 and 780.34 μLL^{-1} , resp. Relative to the laboratory strain (S), the resistant ratios (RR) to Vertimec for *T.urticae* laboratory resistant strain and field strain, showed at Table (2). RR's at Vertimec LC₅₀s were 4.29- folds and 4.53- folds, resp. According to Hayashi scale (1983), RRs of both strains resistant to Vertimec LC₅₀, infested cotton and soybean, could be ranked as low resistance. Friedman Test proved the highest significant effect of certain crops on LC₅₀s values at 1% (Chi-Square = 12.684**). Kendall's Coefficient of Concordance (Kendall's W^a) = .705** with highly significant Chi-Square = 12.684 at 1%.

Pesticides resistance in *Tetranychus urticae* is a portent which caused by many reasons. One of their causes is the introduction of exceeding levels of UV and CO₂, which could assume a critical part to get a resistant field strain. Vertimec, an articulated miticide, LC₅₀ of the research center safe strain which kept up under selection pressure till F40 and the resistant field strain in comparison with susceptible strain were 2099.38, 200.01 and 50.822 μLL^{-1} , resp. Additionally, the raised esterases and mixed function oxidases (MFO) in both the laboratory and the field resistant strains had basically characterized the impact of extensive radiation of UV on the surpassed resistance levels recorded for the two strains (Abd El-Wahab and Taha, 2014). Consequently, expanded CO₂ and global warming can be relied upon to positively influence the concoction barrier flagging framework in plants. Those factors will render them more vulnerable pest assault. The expanded number of produced generations every year and incessant populace flare-ups of potential pests require ceaseless uses of high measure of pesticides. It will boost exposed mites and insects to create pesticides' resistance vastly (Petzoldt and Seaman,

2007). Further, prolongation of insects' lifespan is prolonged under high CO₂ and temperature. Besides, such climate variations will stabilize such insecticide resistant in assortments of pests in their populations. Therefore, all mentioned will make more prominent harm plants even under broad pesticides measures. Also, a few classes of pesticides have been appeared to be less powerful in controlling pests at higher temperatures (Musser and Shelton, 2005).

Vertimec (Abamectin) resistance in *T. urticae* was also reported by several authors (Beers *et al.* 1998). Stumpf and Nauen (2002), investigating enzymes involved in abamectin resistance in the two-spotted spider mite, observed that resistant strains (NL-00 and COL-00) presented several fold higher of MFO (cytochrome P450-dependent monooxygenase) activity than the susceptible strain. Abamectin resistance in strain NL-00 was strongly synergized by PBO (piperonyl butoxide) and DEM (diethyl maleate), suggesting that MFO and GST (glutathione S-transferases) might be involved in abamectin resistance. Astonishingly, levels of cytochrome P450 monooxygenases, specifically, CYP6CM1 in mix with a simple to utilize counter acting agent identification framework permit a quick, dependable, and extremely touchy detection of pesticides' resistance to insects, and certainly to *Bemisia tabaci*, to Neonicotinoid and Pymetrozine (Nauen *et al.* 2013). Nevertheless, Li *et al.* (2016) demonstrated that *Myzus persicae* (Sulzer), from tobacco field in Chongqing, China, and their sensitivities to 4 insecticides. Results demonstrated that resistance ratios were RR = 6.51 and 6.03 which meant populaces have created minor imperviousness to Imidacloprid. One populace (NC) has achieved a high resistance level to Cyhalothrin (RR = 41.28), five populaces indicated medium level ($10.36 \leq RR \leq 20.45$), and the other six stayed powerless ($0.39 \leq RR \leq 3.53$). As respects Carbosulfan, three populaces have created medium resistance, four populaces indicated just minor resistance, and the other five ($0.81 \leq RR \leq 3.97$) were as yet vulnerable. Populace SZ built up a medium level (RR = 14.83) to Phoxim, the other 11 were vulnerable ($0.29 \leq RR \leq 2.41$). To examination the potential resistance system, restraint impacts of synergists and detoxifying compound exercises were identified. The outcomes showed that the MFO was the most vital detoxifying catalyst presenting Imidacloprid resistance, and CarE was most imperative to Cyhalothrin, Carbosulfan and Phoxim. The examination gave an exhaustive overview of insecticide resistance of *M. persicae* in Chongqing, and proposed that distinctive districts should take comparing administration to postpone the insecticide resistance advancement and draw out the convenience of insecticides. Furthermore, magnetic fields were tested on mites, *Tetranychus urticae* and *Polyphagotarsonemus latus* which infested tomato leaves (Al-Ani, 2010). Some leaves were passed through 500 Gauss magnetic field and others were sprayed with magnetic water. Results showed the significant decrease of mites' individuals and raised numbers of mites' eggs. That was explained upon hyperactivation of some enzymes in exposed mites to lay down more eggs. Even though, magnetic water showed its effect on the preparation of spray liquids against on the viability of plant protection agents as showed by Wachowiak and Kierzek (2002). They reported raised effectiveness in the control of *Phytophthora sp.* infested potato, after the use of these fungicides diluted in magnetic water. Likewise, magnetic water incremented the efficacy of acaricides against *Tetranychus urticae*. They were Talstar, Omite, Magus and Omite by the use of one and three magnetizers, one magnetizer and two semi-rings (Górski *et al.*, 2009).

In addition, development of exposure methods to certain magnetic field is developed at this paper. Electromagnetic field as shown could play an important role to detect resistance of pesticides in mites through an electromagnetic interference (EMI) detector by translating electrophysiological changes occurred mainly at glutamate-gated chloride channels (GluCl_s) and γ -aminobutyric acid-gated rdl and glutamate-gated GluCl _{α} chloride channels (GABACl) and resulted to Vertimec'

resistance in mites (Riga *et al.*,2017). Then all recorded readings would be collected and stored at the cloud to be available whenever needed through Internet of Things system (IOT). Besides, data base was connected and joined with resistance ratios (RRs) which were gained from both fields and laboratory' data. Such system will be easier to be used by farmers wherever they are being. But utilizing the electromagnetic fields depending on physiological differences in resistant mites is appeared to be newly emergence trial through this paper. Besides, the solution of metabolic resistance in mites is already done by exposure to specific colors of light emitting diodes (LEDs).Each color could be linked to reduce metabolic pesticides resistance in specific pest on certain plant (Abd El-Wahab,2015; Abd El-Wahab and Abouhatab,2014; Abd El-Wahab and Bursic,2014; Abd El-Wahab *et al.*2014). Hence, LEDs with different colors are able to be connected with the full innovated system to do the two required steps: firstly to detect the pesticides' resistance and secondly to stop or reduce it effectively.

CONCLUSION

To conclude, as the pesticides' resistance is a big problem that leads to disasters affect the environment, there is a new innovated instrument to detect and then reduce it. The solution is depending on differences in electromagnetic forces in resistant strains of *T.urticae* in comparable with susceptible strain. Then, resistance ratios have confirmed the presence of formed resistance. As a consequence, such device is capable to detect resistance to pesticides and farmers can count on it efficiently.

REFERENCES

1. Abd El-Wahab, R.A.2015.Direct Effects of Light Emitting Diodes (LEDs) on The Two-Spotted Spider Mite, *Tetranychus urticae*. Int J Sci Res Agricul Sci, 2(Proceedings),pp.79-85.
2. Abd El-Wahab R A and Abouhatab, E. E. 2014. Effects of Light Emitting Diodes (LEDs) On the Insect Predators Behavior against the Two Forms of *Tetranychus urticae*. Int. J. Chem. Biol. Sci. (IJCBS) 1 (4): 36-45.
3. Abd El-Wahab R A and Bursic V .2014. Light Emitting Diodes (LEDs) Reduce Vertimec, Resistance in *Tetranychus urticae* (Koch).Int. J. Chem. Biol. Sci. (IJCBS) 1(3):28-40.
4. Abd El-Wahab, R.A. and Taha, T. M. 2014. The Relation Between Vertimec Resistance in The Two-Spotted Spider Mite, *Tetarnychus urticae* and Climate Changes in Egypt. Int.J. Chem. Biol. Sci. 1(3): 1-10.
5. Abd El-Wahab, R.A. and Lazic, S. and Bursic, V.2014. Compatibility among Insect Predators and Light Emitting Diodes (LEDs) against the two forms of *Tetranychus urticae* in Greenhouses. Int. J. Chem. Biol. Sci. (IJCBS) 1 (5): 20-27.
6. Abott, W.S. 1925. A method of computing effectiveness of an insecticides. J. Econ. Entomol. 18:265-267.
7. Al-Ani, N. 2010. Effect of magnetic field on mites. J Al-Nahrain Univ.13 (3):104-109.
8. Beers, E.H., Riedl, H. and Dunley, J.E. 1998. Resistance to abamectin and reversion to susceptibility to fenbutatin oxide in spider mite (Acari: Tetranychidae) populations in the Pacific Northwest. J. Econ. Entomol. 91: 352-360.
9. Dawkar, V.V., Chikate, Y.R., Lomate, P.R., Dholakia, B.B., Gupta, V.S. and Giri, A.P. 2013. Molecular insights into resistance mechanisms of Lepidoptera insect pests against toxins. J. Proteome Res.12 (11):4727-4737.
10. Dittrich, V.1962. A comparative study of toxicological test methods on a population of the two-spotted spider mite, *T.urticae*. J. Econ. Entomol. 55: 633-648.

11. Gerharz, R.1991. Pest dislodgement by electromagnetic fields. <http://www.freepatentsonline.com/H000998.pdf>
12. Górski,R., Wachowiak M., and Tomczak, M.2009. The effect of water magnetized with negative magnetic field on effectiveness of selected zoocides in the control of two-spotted spider mite (*Tetranychus urticae* Koch). J. Plant Prot. Res. 49(1):87-91.
13. Hayashi, A.1983.History, present status and management of insecticide resistance. Pest Resistance to Pesticides Soft Sciences, Tokyo, pp.31-53.
14. Kranthi, K. R. 2005. 'Insecticide Resistance -Monitoring, Mechanisms and Management Manual'. Published by CICR, Nagpur, India and ICAC, Washington.pp153.
15. LeOra Software.1994. POLO-PC.A User's Guide to Probit or Logit Analysis LeOra Software, 28 p., Berkeley, CA.
16. Li,Y., Xu,Z., Shi,L., He,L., and Shen,G.2016.Insecticide resistance monitoring and metabolic mechanism study of the green peach aphid, *Myzus persicae* (Sulzer) (Hemiptera: Aphididae),in Chongqing, China. Pesticide Biochem.Physiol.132:21-28.
17. Musser, F. P and Shelton A. M. 2005. The influence of post-exposure temperature on the toxicity of insecticides to *Ostrinia nubilalis* (Lepidoptera:Crambidae). Pest Manag Sci. 61:508- 510.
18. Nauen, R., Raming, K., and Wölfel, K. 2013. <http://www.google.com/patents/WO2013182613A1?cl=en>
19. Petzoldt, C. and Seaman, A. 2007. Climate Change Effects on Insects and Pathogens. Fact Sheet. <http://www.climateandfarming.org/clr-cc.php>.
20. Riga,M., Bajda,S., Themistokleous,C., PapaDaki,S.,Palzewicz,M.,Dermauw,W., Vontas,J. and Van Leeuwen,T.2017. The relative contribution of target-site mutations in complex acaricide resistant phenotypes as assessed by marker assisted backcrossing in *Tetranychus urticae*. Scientific RePoRTs, 7:9202-9214, DOI:10.1038/s41598-017-09054-y
21. Stumpf, N. and Nauen R. 2002. Biochemical markers linked to abamectin resistance in *Tetranychus urticae* (Acari-Tetranychidae). Pestic. Biochem. Physiol., 72: 111-121.
22. Wachowiak M., Kierzek R. 2002. Wpływ dawki środka ochrony roślin, dodatku adiuwanta i wielkości kropel na efektywność zwalczania agrofagów. Prog. Plant Protection/Post. Ochr.Roślin 43 (2): 994–997.
23. Yang,X.,L.L. Buschmann,K.Y. Zhu and D.C. Margolies.2002.Susceptibility and detoxifying enzyme activity in two spider mite species (Acari : Tetranychidae) after selection with three secticides.J.Econ.Entomol.95:399-406.

نظام مبتكر سريع لاكتشاف المقاومة للفيرتيميك (أبامكتين) فى العنكبوت ذو البقعين
Tetranychus urticae Koch

راتيا أحمد عبد الوهاب

معهد بحوث وقاية النباتات، مركز البحوث الزراعية، مصر
rania-proline@hotmail.com

لا تزال مقاومة مبيدات الآفات المتزايدة مشكلة أساسية لآثارها الغير مقبولة على البيئة ومن ثم وجب اكتشافها أسرع وإيجاد *Tetranychus urticae* Koch وسائل فعالة لخفضها بأسرع مما يمكن وخاصة فى الأكاروسات مثل: وقد تأثرت الأكاروسات المقاومة للمبيدات بتغير المناخ أيضا فى نفس الوقت مما ساهم فى زيادة المقاومة للمبيدات حيث تكمن المشكلة الأساسية التى تعتمد على اكتشاف المقاومة بجهاز مبتكر بسيط يعمل بالطاقة الشمسية ويعتمد على تحديد التغيرات فى قوى المجال الكهرومغناطيسي الذى يتأثر بالأكاروسات التى تتعرض له كعينات التغيرات فى قوى المجال الكهرومغناطيسي تم تأكيدها بقياس نسب المقاومة التى تم تسجيلها كالتالى: ٨,٥٢- و ٤,٥٣- مثل، لكلامن السلالات المقاومة للفيرتيميك (أبامكتين) على القطن وفول الصويا على التوالي. وبالمثل تم تسجيل نسب مقاومة ٥,٩٧- و ٤,٢٩- مثل لسلالات الفيرتيميك الحقلية على القطن وفول الصويا على التوالي. وبالتالي، لم تكن هناك فروق ذات دلالة احصائية بين السلالات المقاومة للفيرتيميك و السلالات الحقلية بينما وجدت الفروق بمعنوية عالية بين هاتين السلالتين و السلالة الحساسة. ويمكن التلخيص بأن التغيرات المناخية لها علاقة بمقاومة المبيدات التى عملت على زيادة التوقعات باستخدام نظام بسيط وسريع لكشف المقاومة تحت الظروف الحقلية.

POTENTIAL OF ECOLOGY SUBSTRATE CULTURE FOR PRODUCING CELERY IN URBAN

ABUL-SOUD, M. and M. S. A. EMAM

Central Laboratory for Agricultural Climate, Agricultural Research Centre, Giza, Egypt

Abstract

One of the major current development problems facing Egypt and the world is growing phenomenon of poverty that led to hungry and malnutrition. Ecology urban agriculture via substrate culture and vermicomposting process could play a vital role in fighting poverty; hungry and increase food security beside mitigate climate change impacts. The current study was carried out during two winter seasons of 2015/ 2016 and 2016/2017 under green roof system condition at the Central Laboratory for Agricultural Climate, Agricultural Research Center, Egypt. The study investigated different vermicompost rates (Ver.) (5, 10 and 15 %) as a substrate amendment mixed with two natural substrates (sand and sand: rice husk (1:1 v/v)) combined with three different volume of pots (5, 7.5, and 10 L) on vegetative growth, yield and quality of Celery (*Apium gravealens* var. *dulace* cv. Royal crown). The statistical design of the study was split split plot. The revealed results indicated that the physical and chemical properties were affected by vermicompost implement. Sand + rice husk remarked by lightest weight and the highest physical properties and lowest chemical properties values. Increasing vermicompost rate combined with both substrates from 5 to 15 % reduced the bulk density while increased the total pore space, Air porosity, and water hold capacity (%) beside increase the vegetative, yield and nutrients contents of celery. Also, increasing the pot volume from 5 to 10 L had a positive effect on vegetative, yield, quality characteristics and N, P and K content of celery. The highest yield of celery was recorded by pot 7.5 L + sand + rice husk + Ver. 15 % and pot 10 L + sand + rice husk + Ver. 15 % in first and second season respectively. Pot 10 L + sand + rice husk + Ver. 15 % had the highest quality characteristics and N, P and K (%) contents of celery. The obtained economical results promoted the implement of pot 7.5 L + (sand or sand: rice husk) + (Ver. Rate 10 or 15 %) in ecology urban substrate culture to presented the high economic benefits.

Keywords: Urban, ecology, soilless culture, vermicomposting, organic wastes, substrate culture, sand, rice husk, food security, vegetative growth and yield of celery.

INTRODUCTION

The real challenges that face the urbanization under the climate change impacts, water shortage and high population are pollution, food security, poverty and hungry. The need to convert city from consumption state to productivity state with pay more attention to the environmental become more necessary. Ecology culture take in concern the food security needs with friendly environmental (Abul-Soud 2015 and Abul-Soud and Mancey 2015).

The role of urban agriculture in sustainable production and food security in urban and peri-urban areas mainly were investigated in soil (Mawoisa *et al.*, 2011, Grewal and Grewal 2012, Probst *et al.*, 2012, Hara *et al.*, 2013, Rego 2014, Wertheim-Heck *et al.*, 2014 and Bvenura and Afolayan 2015) and the importance of leafy vegetables on human health in poor urban and peri-urban (Uusiku *et al.*, 2010, Nicklett and Kadall 2013, Wertheim-Heck *et al.*, 2014 and Bvenura and Afolayan 2015).

Under Egyptian conditions, the implement of green roof in producing vegetables was under the spot in the recent decade. The urban agriculture research take a little attention especially in the

last few years and most investigations were on leafy vegetables (Abul-Soud *et al.*, 2014, Abul-Soud 2015, Abul-Soud and Mancey 2015, Abul-Soud *et al.*, 2015a, Ahmed *et al.*, 2017). Abul-Soud 2015 mentioned that the use of substrate culture techniques in producing vegetables under urban agricultural led to avoid the problems of urban soil contamination, shortage of soil, water and natural resources beside maximizing the production. Alternating peat moss and perlite substrate by local substrate such as sand, rice husk and vermicompost contribute in reducing the cost and increase the sustainability of the city by producing food create not just positive environmental impact but also on economic scale.

The substrate type had significant effect on the vegetative, yield characteristics and N, P and K contents of celery, lettuce, salad and red cabbage. Sand + vermicompost substrate had a superior impact compared to peat + perlite.

Regarding to pot volume effect, the pot volume had a significant positive effect on the growth and yield of the leafy vegetables under the study while this effect was not significant on N, P and k contents of celery, lettuce, salad and red cabbage plants. The positive effect resulting from improve the root system that increase the water and nutrients uptake by increasing the pot volume (Abul-Soud 2015).

Vermicomposting is double process which earthworms play a major role in digesting the organic wastes to worm manure (vermicompost) and microbes play a secondary process (humification) in decrease C: N ratio and enhanced the decomposition (worm cast) into more stabilized dark, earth-smelling soil conditioner and nutrient-rich compost that is rich in major and micronutrients (Abul-Soud *et al.*, 2009). Different urban organic wastes can be vermicomposting by special species of earthworms include urban solid waste (Alves and Passoni, 1997), food wastes (Singh and Sharma, 2002), paper waste (Gajalakshmi *et al.*, 2002), kitchen wastes, paper and fruit and vegetable wastes (Abul-Soud *et al.*, 2009), among others. It is also a sustainable solution for management of organic wastes which are major source of environmental pollution (Lazcano *et al.*, 2009). The final product, named vermicompost, is very different from the original waste material, mainly because of the increased decomposition and humification. Possibly due to less soluble salts, greater cation exchange capacity, better physical properties, higher microbial and enzymatic activity, and higher content of available nutrients producer acceptance of vermicompost is greater than that of compost (Atiyeh *et al.*, 2002, Edwards, *et al.*, 2004, Tognetti, *et al.*, 2005, Abul-Soud *et al.*, 2009). Needless to say that the most important point of utilizing vermicomposting was mitigating the CO₂ emission from the different organic wastes through sequestration of the organic carbon into substrate and organic nutrient solution forms that could be utilize in ecology soilless culture of different vegetables led to more mitigation of CO₂ emission (Abul-Soud *et al.*, 2009, 2014 a and 2015 a,b).

The aim of this work was to study the ability of producing celery environmentally friendly and investigate the use of local substrate in sustainable production for enhancing food security in urban under Egyptian condition. More or less, offering different options for use the vermicomposting technology in recycling the urban organic wastes, the sustainable use of agricultural residues and green roof.

MATERIALS AND METHODS

This study was carried out in the experimental unit of the green roof at the Central Laboratory for Agricultural Climate (CLAC), Agriculture Research Center (ARC), Egypt, during winter seasons of 2015/2016 and 2016/2017.

Plant material:

Celery (*Agium gravealens var. dulace* cv. Royal crown) seeds were sown on the first week of October of both two seasons 2015 and 2016 respectively, in polystyrene trays. After 5 - 6 weeks, the celery seedlings were transplanted into different substrate mixtures and volumes of black plastic pots. Each pot contained one plant. The final plants spacing was 25 cm in the row and 30 cm in between.

The vermicomposting process:

The Epigieic earthworms *Lumbriscus Rubellus* (Red Worm), *Eisenia Fetida* (Tiger Worm), *Perionyx Excavatus* (Indian Blue) and *Eudrilus Eugeniae* (African Night Crawler) were used. Indoor system of vermicomposting was used in this investigation for producing the vermicompost. The vermicomposting process and vermicompost production were done according to Abul-Soud *et al.*, 2009, 2014, 2015 (a and b). Kitchen wastes (vegetables, fruits, foods, breads, tea, eggshells wastes and etc.) + shredded newspaper and paper (Sh. P) in proportions (80: 20 %) were vermicomposting as an urban organic wastes Table (1). Chemical composition of vermicompost after 3 months of vermicomposting process were estimated and presented in Table (2).

Table (1): Chemical composition of different agricultural wastes.

Raw material	C/N ratio	Macro elements %				
		N	P	k	Ca	Mg
<i>Kitchen wastes</i>	4.2	0.59	0.44	0.56	0.98	0.62
<i>shredded newspaper</i>	169.0	0.017	0.01	0.00	0.19	0.01
<i>The mix</i>	76.5	0.54	0.38	0.49	0.73	0.55

Table (2): The chemical composition of macro nutrients (%) and heavy elements of vermicompost.

<i>Vermicompost</i>	C/N	N (%)	P (%)	K (%)	Ca (%)	Mg (%)
		1:13.4	1.45	1.04	1.24	1.08
		Pb	Ni	Cd	Co	
		8.25	4.07	0.27	1.83	

System materials

Different growing volume pots (the size of pots were 6, 8 and 12 L/pot were filled with 5, 7.5 and 10 L of different substrates and vermicompost proportions). Sand and rice husk were washed by water and nitric acid (in concentration 0.15%) multi times to get ride from undesirable salts or weeds. Different proportions of vermicompost were mixed with sand and sand: rice husk (1:1 v/v). The pots were arranged in 3 rows over aluminum tables (1 x 2 x 0.6 m); every table was contained 24 pots. Each three tables were represented as one experimental plot.

Nutrient solution (Abul-Soud 2015) was pumped via submersible pump (110 watt). Water tanks 120 L were used in close system of substrate culture. Plants were irrigated by using drippers of 2 l/hr capacity. The fertigation was programmed to work 6 times / day and the duration of irrigation time depended upon the season. The irrigation scheduled was programmed by using digital timer (one minute). The EC of nutrient solutions were adjusted by using EC meter to the required level (2.5 dsm⁻¹).

The investigated treatments

Three factors were investigated under the study to perform 18 treatments as follows:

- 1 - Two different substrate mixtures sand (S.) (100 %) and sand: rice husk (S. + R.H) (1: 1 v/v).
- 2 - Different pot (substrates) volumes 5, 7.5 and 10 L/ pot/ plant as small (S), medium (M) and large (L) pot volume respectively.

3 – Three different rates of vermicompost 5 (Ver. 5%), 10 (Ver. 10%) and 15 % (Ver. 15%) mixed with substrates (v/v).

The experimental design was split split plot with 3 replicates where substrate mixtures were assigned as main plots and pot volumes allocated as subplots while vermicompost rate take a place as sub-subplots.

All the other agriculture practices of celery cultivation were in accordance with the standard recommendations for commercial growers by Agriculture Research Center (ARC), Ministry of Agriculture, Egypt.

The measurements

Physical and chemical properties of different substrates and vermicompost rates mixtures illustrated in **Table (3)**. Bulk density (*B.D*), total pore space (T.P.S), water hold capacity % (W.H.C) and air porosity % (A.P) were estimated according to Wilson (1983) and Raul (1996). The pH of the potting mixtures were determined using a double distilled water suspension of each potting mixture in the ratio of 1:10 (w: v) (Inbar *et al.*, 1993) that had been agitated mechanically for 2 h and filtered through Whatman no.1 filter paper. The same solution was measured for electrical conductivity (EC mmhos⁻¹) with a conductance meter that had been standardized with 0.01 and 0.1M KCl.

The vegetative and yield characteristics (plant height (cm), no. of leaves, head fresh weight (g), average leaf weight (g) and dry matter content (%)) were measured at harvesting (after 70 – 75 days from transplanting).

Random three heads of celery / treatment were used to estimate the quality properties according to A.O.A.C (1990) as follows: vitamin C (mg/100g), and total soluble solids (TSS %) using hand refract meter.

For mineral analysis of leaves (N, P and K were estimated, Three celery samples of each plot were dried at 70 °C in an air forced oven for 48 h. Dried leaves were digested in H₂SO₄ according to the method described by Allen (1974) and N, P and K contents were estimated in the acid digested solution. Total nitrogen was determined by Kjeldahl method according to the procedure described by FAO (1980). Phosphorus content was determined using spectrophotometer according to Watanabe and Olsen (1965). Potassium content was determined photo-metrically using Flame photometer as described by Chapman and Pratt (1961).

The environmental and economic study:

1. Nutrient save /ton = Nutrient % (after composting) x 10 (Abul-Soud *et al.*, 2015)
2. Substrate cost = 0.05 LE / L for both substrates * pot volume + (1.0 L vermicompost * Ver. Rate * pot volume).
3. Other cost calculated on based of seedlings, fertigation cost, plastic pots and etc..
4. The price of celery in the range (3 – 5 LE per unit (plant)) depending on the head weight (g).

The statistical analysis:

Data were statistically analyzed by computer using SAS program for statistical analysis. The differences among means for all traits were tested for significance at 5 % level according to the procedure described by Snedecor and Cochran (1981).

RESULTS AND DISCUSSION

The effect of vermicomposting process on the urban organic wastes

The use of vermicomposting process in recycling the organic urban wastes such as kitchen wastes (vegetables, fruits, foods, breads, tea, eggshells wastes and etc..) + shredded newspaper and paper led to save the organic matter and essential nutrients for plants while increased the total N, P, K, Ca and Mg % of the vermicompost as compared to the raw materials while C/N ratio

decreased as a result of N fixation, concentrated the nutrients and bulk reduction as Table (2) showed. The heavy metals contents of vermicompost were in the friendly range lower than the commercial composts in the Egyptian market. Vermicomposting is defined as a low cost technology system for processing organic wastes (Hand *et al.*, 1988). Different organic wastes can be used in vermicompost production by different species of earthworms which include urban solid waste); city leaf litter and food wastes, paper waste and residues of plant decomposition. (Alves and Passoni, 1997, Singh and Sharma, 2002 and Abul-Soud 2015).

The nutrients contents of urban organic wastes were saved via vermicomposting. The revealed results presented in Fig. (1) Show that, vermicomposting had a vital role in saving the organic carbon and essential nutrients instead of losing them by an ordinary treatments (incineration or burial) of urban organic wastes. The nutrient save (Kg / ton) via using vermicomposting process gave good evidences for recycling the urban organic wastes in save significant amounts of nutrients and at the same time the various application of vermicomposting output (Abul-Soud *et al.*, 2014 and Abul-Soud 2015). Mitigating the CO₂ emission from urban organic wastes through sequestration of the organic carbon into vermicompost that could be utilize in ecology soilless culture of different vegetables led to more mitigation of CO₂ emission via plants.

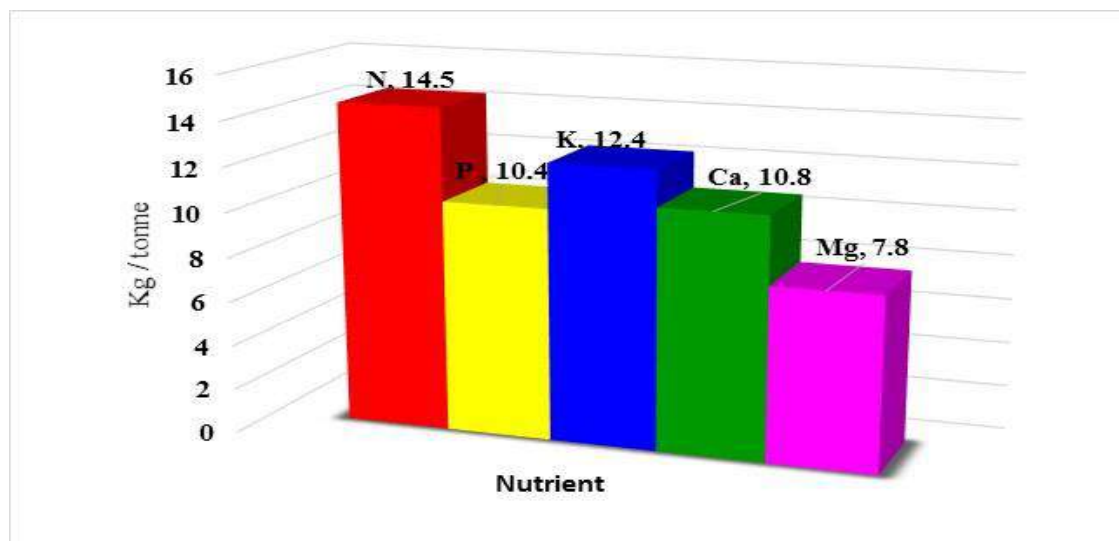


Fig. (1): The nutrient saved (Kg/ton) via vermicomposting of urban organic wastes

The physical and chemical properties of different substrate mixtures

The results of physical and chemical properties of different vermicompost mixtures are presented in Table (3). Increasing the pot volume from 5 L up to 10 L led to increase the weight of substrate/pot (Kg/pot). The heavy weight of substrate/pot may cause risk in urban agriculture concerning kids. Also the use of rice husk mixed with sand (1:1 v/v) led to reduce the weight of substrate. In green roof systems as an urban agriculture method, the weight of substrate/pot should take in concern especially with children and elders. The substrate treatment S. + R.H was lighter than sand as a substrate.

The obtained results demonstrated that increasing the vermicompost rate from 5 to 15 % led to increase the total pore space (T.P.S), water holding capacity % (W.H.C), air porosity % (A.P) and E.C while decrease the bulk density (kg/L) of different substrates. The vermicompost rate 15 %

mixed with both substrates recorded the highest values T.P.S, W.H.C, A.P (%), E.C (dS⁻¹) and the lowest results of B.D and pH.

The obvious results could be explained by referring to the high potential of vermicompost in improving the physical and chemical properties of sand and sand +rice husk Abul-Soud *et al.*, 2014, 2015 (a and b), Abul-Soud 2015).

Regarding the chemical properties (E.C and pH), the obtained data indicated that increasing the rate of vermicompost led to increase E.C and decrease pH of different mixtures as a result of high contents of nutrients of vermicompost (Tognetti, *et al.*, 2005 and Venugopal, *et al.*, 2010, Abul-Soud *et al.*, 2014, 2015 (a and b), Abul-Soud 2015).

Table (3): The effect of vermicompost rates on physical and chemical properties of different mixtures and control.

Pot Vol.	Substrate mixtures	Wt. Kg/pot	B.D Kg/l	T.P.S %	Physical		Chemical	
					W.H.C %	A.P %	E.C dS ⁻¹	pH
Small 5 L	S. + 5 %	7.78	1.56	27.3	23.0	4.3	1.18	7.4
	S. + 10 %	7.56	1.51	31.7	27.1	4.6	1.70	7.5
	S. +15 %	7.33	1.47	36.5	33.0	3.5	2.42	7.7
	S.+ R.H.+5%	5.31	1.06	39.8	32.8	6.9	0.86	7.3
	S.+ R.H.+10%	5.22	1.04	55.0	46.5	8.5	1.38	7.4
	S.+ R.H.+15%	5.12	1.02	60.5	49.0	11.5	1.92	7.4
Medium 7.5 L	S. + 5 %	11.67	1.56	27.3	23.0	4.3	1.18	7.4
	S. + 10 %	11.33	1.51	31.7	27.1	4.6	1.70	7.5
	S. +15 %	11.00	1.47	36.5	33.0	3.5	2.42	7.7
	S.+ R.H.+5%	7.96	1.06	39.8	32.8	6.9	0.86	7.3
	S.+ R.H.+10%	7.82	1.04	55.0	46.5	8.5	1.38	7.4
	S.+ R.H.+15%	7.68	1.02	60.5	49.0	11.5	1.92	7.4
Large 10 L	S. + 5 %	15.56	1.56	27.3	23.0	4.3	1.18	7.4
	S. + 10 %	15.11	1.51	31.7	27.1	4.6	1.70	7.5
	S. +15 %	14.67	1.47	36.5	33.0	3.5	2.42	7.7
	S.+ R.H.+5%	10.62	1.06	39.8	32.8	6.9	0.86	7.3
	S.+ R.H.+10%	10.43	1.04	55.0	46.5	8.5	1.38	7.4
	S.+ R.H.+15%	10.25	1.02	60.5	49.0	11.5	1.92	7.4

The effect of pot volume, substrate type and vermicompost rate on vegetative growth and yield of celery.

The effect of pot volume, substrate type and vermicompost rate and their interactions on vegetative growth and yield of celery are presented in **Table (4)**. Increasing the pot volume from 5 to 7.5 L led to increase the vegetative and yield characteristics while increasing up to 10 L didn't presented the same effect. The highest plant height, No. of leaves and head fresh weight of celery were recorded by pot volume 7.5 L.

The substrate sand + rice husk gave the highest No. of leaves and head fresh weight of celery compared to substrate sand that recorded the highest plant height.

The obtained results in Table (4) showed that increasing the vermicompost rate from 5 to 15 % led to increase the vegetative and yield records. The highest results were recorded by vermicompost rate 15 % while the lowest values gave by 5%.

Regarding the interaction effect between pot volume and substrate type, both pot volume 7.5 and 10 L combined with substrate sand + rice husk recorded the highest vegetative and yield characteristics while pot 5 L gave the lowest plant height.

The interaction between pot volume and vermicompost rate as presented in Table (4) showed in general the highest vegetative and yield results presented by pot 7.5 L + Ver. 15 % while pot 5 and 7.5 L + Ver. 5 % showed the lowest records of vegetative and yield.

The results of substrate type combined with vermicompost rate presented that S. + R.H. combined with Ver. 15 % had the highest vegetative and yield characteristics while the lowest varied between S. + Ver. 5 % and S. + R.H. + Ver. 5 %.

Regarding the interaction effect among pot volume, substrate type and vermicompost rate, data illustrated that the highest plant height, No. of leaves and head fresh weight of celery were obtained by pot 7.5 L + S. + R.H. + Ver. 15 % followed by pot 7.5 L + S. + Ver. 15 %. The lowest values gave by pot 5 L + S. + Ver. 5 %.

Abul-Soud 2015 and Ahmed *et al.*, 2017 mentioned that the pot volume and substrate type had a significant positive effect on the vegetative and yield characteristics of celery, lettuce, salad and red cabbage. These results agreed with Abul-Soud *et al.*, 2014, Abul-Soud 2015 and Abul-Soud *et al.*, 2015 a and b, the use of vermicompost as a substrate amendments had a significant encouragement impacts on the growth and yield of sweet paper, snap bean, lettuce and strawberry. The vermicompost contained an essential nutrients for supporting the plant nutrient requirements beside the high organic matter and assist in improve the physical and chemical properties of substrates. Bachman and Metzger (2008) studied the addition of vermicompost in media mixes of 10% VC and 20% VC had positive effects on plant growth of marigold, tomato, green pepper, and cornflower. A consistent trend obtained also indicated that the best plant growth responses, with all needed nutrients supplied, occurred when vermicompost constituted a relatively small proportion (10% to 20 %) of the total volume of the container medium mixture, with greater proportions of vermicompost in the plant growth medium not always improving plant growth (Subler *et al.*, 1998 and Atiyeh *et al.*, 2002). In addition, Abul-Soud *et al.*, 2014, Abul-Soud 2015 and Abul-Soud *et al.*, 2015 (a and b) found that using vermicompost in soilless culture improve plant growth and yield under Egyptian conditions. Replacement of peat with moderate amounts of vermicompost produces beneficial effects on plant growth due to the increase on the bulk density of the growing , and to the decrease on total porosity and amount of readily available water in the pots (Litterick *et al.*, 2004, Bachman and Metzger, 2007; Grigatti *et al.*, 2007). Evidences caught up from the literature focusing on vermicompost application support our previous results on different crop such as tomato (Patil *et al.*, (1998) and Arancon *et al.*, (2003) and strawberry (Arancon *et al.*, 2004) which showed that the application of vermicompost enhanced soil fertility and improved soil properties.

Table (4): The effect of pot volume, substrate type and vermicompost rate and their interactions on vegetative growth and yield of celery.

Treatments		First season 2015/2016			Second Season 2016/2017			
Pot Vol.		Plant height (cm)	No. of leaves	Head fresh wt. (g)	Plant height (cm)	No. of leaves	Head fresh wt. (g)	
Pot 5 L		48.9 B	23.3 C	486.6 B	47.8 C	27.6 A	505.8 B	
Pot 7.5 L		50.5 A	28.4 A	601.0 A	52.2 A	26.9 A	611.9 A	
Pot 10 L		50.3 A	25.8 B	586.7 A	50.7 B	26.7 A	609.3 A	
Substrate type								
Sand (S)		51.4 A	23.3 B	542.2 B	51.3 A	24.9 B	559.8 B	
Sand + Rice husk (R.H)		48.3 B	28.3 A	574.0 A	49.1 B	29.1 A	591.5 A	
Vermicompost rate								
Ver. 5 %		47.7 C	21.9 C	517.9 C	46.8 B	22.4 C	516.9 C	
Ver. 10 %		50.2 B	25.8 B	557.5 B	51.8 A	27.2 B	582.5 B	
Ver. 15 %		51.8 A	29.6 A	598.8 A	52.0 A	31.6 A	627.6 A	
Pot Vol. * Substrate type								
Pot 5 L	S.	50.8 b	24.7 c	463.5 d	50.00 b	25.8 c	494.0 e	
	S. + R. H.	47.0 c	23.4 cd	509.6 c	45.67 c	29.3 ab	517.5 d	
Pot 7.5 L	S.	53.2 a	23.1 cd	585.9 ab	53.50 a	25.7 c	597.2 b	
	S. + R. H.	47.8 c	32.0 a	616.2 a	50.83 b	28.2 b	626.7 a	
Pot 10 L	S.	50.3 b	22.2 d	577.1 b	50.50 b	23.4 d	588.2 c	
	S. + R. H.	50.2 b	29.3 b	596.3 ab	50.83 b	29.9 a	630.4 a	
Pot Vol. * vermicompost rate								
Pot 5 L	Ver. 5 %	46.5 d	23.0 d	455.7 e	43.25 d	22.3 e	456.5 f	
	Ver. 10 %	49.7 bc	29.0 b	498.8 de	50.25 bc	27.8 bc	518.5 e	
	Ver. 15 %	50.5 b	33.1 a	505.3 d	50.00 bc	32.7 a	542.3 d	
Pot 7.5 L	Ver. 5 %	48.0 cd	19.8 e	543.8 cd	49.00 c	20.5 f	553.8 c	
	Ver. 10 %	49.7 bc	22.8 d	585.7 bc	52.00 b	27.5 c	614.0 b	
	Ver. 15 %	53.7 a	27.3 bc	673.7 a	55.50 a	32.8 a	668.0 a	
Pot 10 L	Ver. 5 %	48.5 c	23.1 d	554.3 c	48.25 c	24.3 d	540.3 d	
	Ver. 10 %	51.2 b	25.6 c	588.2 bc	53.25 ab	26.4 c	615.0 b	
	Ver. 15 %	51.1 b	28.6 b	617.6 b	50.50 bc	29.3 b	672.5 a	
Substrate type * vermicompost rate								
S.	Ver. 5 %	49.9 c	20.1 d	517.3 c	49.33 b	20.9 d	497.0 f	
	Ver. 10 %	53.1 a	22.9 c	533.2 c	53.33 a	24.2 c	559.5 d	
	Ver. 15 %	51.3 bc	27.0 b	576.0 b	51.33 ab	29.8 b	622.8 b	
S. + R. H.	Ver. 5 %	45.4 e	23.8 c	518.6 c	44.33 c	23.8 c	536.7 e	
	Ver. 10 %	47.4 d	28.7 b	581.9 b	50.33 b	30.3 b	605.5 c	
	Ver. 15 %	52.2 ab	32.3 a	621.7 a	52.67 a	33.3 a	632.3 a	
Pot Vol. * Substrate type * vermicompost rate								
Pot 5 L	S.	Ver. 5 %	49 def	19.0 j	446.2 h	45.50 e	19.5 i	441.5 j
		Ver. 10 %	52.5 abc	25.2 def	468.0 fgi	52.50 b	26.5 de	503.0 h
		Ver. 15 %	51 bcd	30.0 bc	476.3 fgi	52.00 b	31.3 b	537.5 fg
	S.+R. H.	Ver. 5 %	44 h	27.0 cde	465.2 gi	41.00 f	25.0 ef	471.5 i
		Ver. 10 %	47 f	32.8 b	529.5 efg	48.00 cde	29.0 c	534.0 g
		Ver. 15 %	50 cde	36.2 a	534.2 ef	48.00 cde	34.0 a	547.0 f
Pot 7.5 L	S.	Ver. 5 %	52 abc	20.2 hij	542.3 e	53.00 ab	22.5 gh	540.0 fg
		Ver. 10 %	53.5 ab	22.3 fghi	579.2 bcde	53.00 ab	23.0 fg	584.0 d
		Ver. 15 %	54 a	26.8 de	636.2 b	54.50 ab	31.5 b	667.5 b
	S.+R. H.	Ver. 5 %	44 i	19.5 ij	545.2 e	45.00 e	18.5 i	567.5 e
		Ver. 10 %	46 ghi	23.2 fgh	592.2 bcde	51.00 bc	32.0 ab	644.0 c
		Ver. 15 %	53.3 ab	27.7 cd	711.2 a	56.50 a	34.0 a	668.5 b
Pot 10 L	S.	Ver. 5 %	48.8 def	21.2 ghij	563.3 cde	49.50 bcd	20.7 hi	509.5 h
		Ver. 10 %	53.2 ab	21.2 hij	552.3 de	54.50 ab	23.0 fg	591.5 d
		Ver. 15 %	49 def	24.2 efg	615.5 bcd	47.50 cde	26.5 de	663.5 b
	S.+R. H.	Ver. 5 %	48.2 efg	25.0 def	545.3 e	47.00 de	28.0 cd	571.2 e
		Ver. 10 %	49.2 def	30.0 bc	624.0 bc	52.00 b	29.8 bc	638.5 c
		Ver. 15 %	53.2 ab	33.0 b	619.7 bc	53.50 ab	32.0 ab	681.5 a

The effect of pot volume, substrate type and vermicompost rate on quality characteristics of celery.

The effect of different treatments on quality characteristics of celery are presented in **Table (5)**. Referring the effect of different pot volume, data showed that using pot vol. 10 L gave the highest dry matter, TSS (%) and Vit.C (mg/100g) in reverse of using pot vol. 5 L. increasing the pot vol. had a significant effect on the quality characteristics of celery.

Substrate S. + R.H. recorded higher results of quality characteristics of celery compared to substrate sand.

Increase the rate of vermicompost resulted in significant increase of TSS and Vit. C. while decreased the dry matter (%).

Table (5) illustrated the interaction in between and among the different factors (pot Vol., Substrate type and vermicompost rate) on the quality characteristics of celery as follows:

1. Pot Vol. * substrate type: pot 10 L combined with S. +R.H. recorded the highest results of TSS and Vit. C in both seasons, the highest values of dry matter were given by pot 7.5 L + S. + R.H. and pot 10 L + S. in first and second season respectively.
2. Pot Vol. * vermicompost rate: The highest values of TSS and Vit. C. were given by pot 10 L +Ver. 15 %. Pot 10 L +Ver. 5 % presented the highest values of dry matter. The lowest quality characteristics of celery were illustrated by Pot 5 L +Ver. 5 %.
3. Substrate type * vermicompost rate: sub. S. + Ver. 5 % and S. + Ver. 10 % demonstrated the highest results of dry matter (%) in the first and second season respectively. In general, the highest records of TSS and Vit. C. presented by S. +R.H. combined with Ver.15 %.
4. The revealed results of interaction effect among pot Vol., Substrate type and vermicompost rate on the quality characteristics of celery (Table 5) indicated that pot 10 L + S. + Ver. 5 % had the highest dry matter (%) while the highest TSS and Vit. C. recorded by pot 10 L + S. + Ver. 15 % and pot 10 L + S. + R.H. + Ver. 15 % in first and second season respectively. On the other hand, the lowest quality characteristics of celery were presented by pot 5 L + S. + Ver. 15 % and pot 5 L + S.+R.H. + Ver. 15 %.

These results could be explained as a result of enhancing the physical and chemical properties of substrate by increasing the vermicompost rate as a substrate amendment especially with S. + R. H. that led to enhance the vegetative growth, yield and quality characteristics of celery Abul-Soud *et al.*, 2014, Abul-Soud 2015 and Abul-Soud *et al.*, 2015 (a and b) . Vermicomposts are comprised of large amounts of humic substances which release nutrients relatively slowly in the soil that improve its physical and biological properties of soil and in turn rise to much better plant quality (Muscolo *et al.*, 1999). Also increase the pot / substrate offer more comfortable condition for root growth and allows the plants to have better nutrient uptake, sufficient growth and development to optimize water and oxygen holding (Verdonck *et al.*, 1982; Albaho *et al.*, 2009 and Abul-Soud 2015). These results coincided with that recommended for vermicompost application for encouraging plant growth and quality through increasing the available forms of nutrients (nitrates, exchangeable P, K, Ca and Mg) for plant uptake of strawberry (Arancon *et al.*, 2004).

Table (5): The effect of pot volume, substrate type and vermicompost rate and their interactions on quality of celery.

Treatments		First season 2015/2016			Second Season 2016/2017			
Pot Vol.		Dry matter (%)	TSS (%)	Vit. C (mg/100g)	Dry matter (%)	TSS (%)	Vit. C (mg/100g)	
Pot 5 L		8.5 C	5.02 C	27.21 C	8.39 C	5.89 B	30.4 B	
Pot 7.5 L		9.4 A	5.27 B	30.48 B	8.77 B	6.09 AB	31.7 B	
Pot 10 L		9.2 B	5.71 A	34.64 A	8.92 A	6.19 A	35.4 A	
Substrate type								
Sand (S)		8.9 B	5.35 A	31.40 A	8.49 A	5.44 B	31.2 B	
Sand + Rice husk (R.H)		9.2 A	5.32 A	30.16 B	8.69 A	6.68 A	33.7 A	
Vermicompost rate								
Ver. 5 %		9.3 A	5.07 C	27.66 C	8.82 A	5.72 C	27.8 C	
Ver. 10 %		8.9 B	5.21 B	30.42 B	8.71 B	6.03 B	32.3 B	
Ver. 15 %		8.8 B	5.74 A	34.26 A	8.55 C	6.42 A	37.3 A	
Pot Vol. * Substrate type								
Pot 5 L	S.	8.1 d	5.01 d	26.23 d	8.02 e	5.47 c	28.8 d	
	S. + R. H.	8.9 c	5.05 d	28.20 c	8.75 bc	6.33 b	31.9 bc	
Pot 7.5 L	S.	8.9 c	5.22 c	33.04 b	8.69 c	5.43 c	31.2 c	
	S. + R. H.	9.9 a	5.33 c	27.93 c	8.86 b	6.74 a	32.2 bc	
Pot 10 L	S.	9.5 b	5.83 a	34.94 a	9.37 a	5.41 c	33.7 b	
	S. + R. H.	8.8 c	5.60 b	34.34 a	8.46 d	6.96 a	37.2 a	
Pot Vol. * vermicompost rate								
Pot 5 L	Ver. 5 %	8.3 e	4.87 e	24.77 f	7.55 e	5.60 d	26.7 d	
	Ver. 10 %	8.2 ef	4.91 e	27.18 e	8.31 d	5.86 c	29.6 c	
	Ver. 15 %	9.0 d	5.31 c	29.70 d	9.30 b	6.25 abc	34.8 b	
Pot 7.5 L	Ver. 5 %	9.6 b	5.07 de	26.77 e	9.19 b	5.78 d	26.0 d	
	Ver. 10 %	9.3 c	5.16 cd	30.19 cd	8.49 c	5.97 bed	32.0 bc	
	Ver. 15 %	9.4 bc	5.61 b	34.50 b	8.65 c	6.51 a	37.0 b	
Pot 10 L	Ver. 5 %	10.1 a	5.28 c	31.45 c	9.73 a	5.79 d	30.8 c	
	Ver. 10 %	9.3 c	5.55 b	33.91 b	9.34 b	6.26 ab	35.4 b	
	Ver. 15 %	8.1 f	6.32 a	38.57 a	7.70 e	6.52 a	40.1 a	
Substrate type * vermicompost rate								
S.	Ver. 5 %	9.5 a	5.11 bc	27.84 d	8.80 ab	5.15 d	27.0 d	
	Ver. 10 %	8.8 d	5.22 b	30.77 c	8.91 a	5.45 cd	30.7 c	
	Ver. 15 %	8.4 e	5.73 a	35.59 a	8.37 d	5.70 c	36.0 b	
S. + R. H.	Ver. 5 %	9.2 bc	5.04 c	27.48 d	8.84 ab	6.29 b	28.7 cd	
	Ver. 10 %	9.1 c	5.19 b	30.07 c	8.51 c	6.60 b	33.9 b	
	Ver. 15 %	9.3 ab	5.76 a	32.92 b	8.72 b	7.14 a	38.6 a	
Pot Vol. * Substrate type * vermicompost rate								
Pot 5 L	S.	Ver. 5 %	8.0 f	4.98 efg	25.33 gh	6.98 j	5.13 k	24.9 h
		Ver. 10 %	7.9 f	4.84 fg	26.45 fg	8.12 h	5.56 hijk	27.1 fgh
		Ver. 15 %	8.6 e	5.20 de	26.90 fg	8.96 ef	5.71 ghij	34.5 bcde
	S.+R.H	Ver. 5 %	8.7 e	4.77 g	24.20 h	8.11 h	6.06 efgh	28.6 fgh
		Ver. 10 %	8.5 e	4.98 efg	27.90 f	8.50 g	6.15 efg	32.1 def
		Ver. 15 %	9.5 cd	5.41 de	32.50 d	9.64 c	6.78 bcd	35.0 bcd
Pot 7.5 L	S.	Ver. 5 %	9.9 bc	5.04 ef	27.90 f	9.12 def	5.11 k	26.2 gh
		Ver. 10 %	8.5 e	5.17 e	32.56 d	8.56 g	5.34 ijk	30.8 ef
		Ver. 15 %	8.5 e	5.46 d	38.65 b	8.39 g	5.84 fgghi	36.5 bc
	S.+R.H	Ver. 5 %	9.3 d	5.10 ef	25.63 gh	9.25 d	6.45 de	25.8 h
		Ver. 10 %	10.1 b	5.15 e	27.81 f	8.42 g	6.59 cde	33.1 cdef
		Ver. 15 %	10.3 ab	5.75 c	30.35 e	8.90 f	7.18 ab	37.6 b
Pot 10 L	S.	Ver. 5 %	10.5 a	5.31 de	30.29 e	10.30 a	5.22 jk	29.8 fg
		Ver. 10 %	10.0 b	5.65 cd	33.31 d	10.06 b	5.46 ijk	34.2 bcde
		Ver. 15 %	8.1 f	6.52 a	41.23 a	7.76 i	5.56 hijk	37.1 b
	S.+R.H	Ver. 5 %	9.6 c	5.24 de	32.60 d	9.15 de	6.36 def	31.8 def
		Ver. 10 %	8.7 e	5.45 d	34.50 cd	8.61 g	7.05 abc	36.6 bc
		Ver. 15 %	8.0 f	6.12 b	35.91 c	7.63 i	7.47 a	43.09 a

The effect of pot volume, substrate type and vermicompost rate on N, P and K contents of celery.

Increase the pot vol. from 5 up to 10 L led to increase significantly the N, P and K contents of celery head as Table (6) illustrated.

Sand substrate recorded the highest values of N, P and K contents of celery head in the first season while S. + R.H. gave the highest results in the second season.

Also, increase the vermicompost rate from 5 to 15 % as a substrate amendment led to increase N, P and K contents of celery.

On the other hand, the interaction between pot Vol. and substrate type showed that the highest records of N, P and K contents of celery were given by pot 10 L + S. and pot 10 L+. in first and second season respectively. Pot 5 L + S. had the lowest results.

Regarding to Table (6), the interaction between pot vol. and vermicompost rate indicated that pot 10 L + Ver 15 % gave the highest values of N, P and K contents of celery in contrast of pot 5 L + Ver. 5 % that recorded the lowest results.

Substrate S. + Ver. 15 % presented the highest results of N, P and K contents of celery in the first season while in the second season the highest N, P and K contents of celery recorded by S.+R.H + Ver. 15 %. The lowest contents were given by S. + Ver. 5 %.

Table (6) illustrated the interaction effect among pot volume, substrate type and vermicompost rate on N, P and K contents of celery. The revealed results demonstrated that pot 10 L + S. + Ver. 15 % had the highest records in the first season while pot 10 L + S. + R.H. + Ver. 15 % presented the highest of N, P and K contents of celery in the second season. On the other hand, the lowest celery contents of N, P and K were showed by pot 5 L + S. + Ver. 5 % and pot 5 L + S. +R.H. + Ver. 5 %.

These results agreed with many investigation that mentioned the increase in vermicompost rate and pot volume led to increase the nutrient uptake that resulted increase N, P and K contents of strawberry, sweet pepper, eggplant, lettuce, celery, white cabbage, red cabbage, spinach and mallow (Abul-Soud *et al.*, 2014, Abul-Soud 2015, Abul-Soud and Mancey 2015, Abul-Soud *et al.*, 2015 (a and b) and Ahmed *et al.*, 2017). The use of different organic and inorganic substrates allows the plants to have better nutrient uptake (Verdonck *et al.*, 1982; Albaho *et al.*, 2009).

Table (6): The effect of pot volume, substrate type and vermicompost rate and their interactions on N, P and K contents of celery.

Treatments		First season 2015/2016			Second Season 2016/2017			
Pot Vol.		N (%)	P (%)	K (%)	N (%)	P (%)	K (%)	
Pot 5 L		3.08 B	0.74 B	2.95 C	3.15 B	0.75 B	3.29 B	
Pot 7.5 L		3.46 A	0.75 B	3.20 B	3.58 A	0.82 A	3.45 B	
Pot 10 L		3.52 A	0.82 A	3.42 A	3.56 A	0.85 A	3.69 A	
Substrate type								
Sand (S)		3.52 A	0.82 A	2.21 A	3.34 B	0.80 A	3.29 B	
Sand + Rice husk (R.H)		3.19 B	0.71 B	3.18 A	3.52 A	0.82 A	3.66 A	
Vermicompost rate								
Ver. 5 %		3.00 C	0.67 C	2.96 B	3.00 C	0.70 C	3.21 C	
Ver. 10 %		3.31 B	0.74 B	3.12 B	3.49 B	0.81 B	3.45 B	
Ver. 15 %		3.74 A	0.89 A	3.50 A	3.79 A	0.91 A	3.76 A	
Pot Vol. * Substrate type								
Pot 5 L	S.	3.21 bc	0.77 bc	2.97 b	3.03 c	0.75 b	3.20 c	
	S. + R. H.	2.95 c	0.71 cd	2.95 b	3.26 bc	0.75 b	3.38 c	
Pot 7.5 L	S.	3.65 a	0.83 ab	3.21ab	3.47 ab	0.81 ab	3.20 c	
	S. + R. H.	3.27 b	0.66 d	3.20 ab	3.69 a	0.84 a	3.69 ab	
Pot 10 L	S.	3.70 a	0.87 a	3.46 a	3.51 ab	0.84 a	3.48 bc	
	S. + R. H.	3.33 b	0.77 bc	3.38 a	3.62 a	0.86 a	3.91 a	
Pot Vol. * vermicompost rate								
Pot 5 L	Ver. 5 %	2.86 d	0.63 d	2.74 e	2.91 c	0.65 d	3.05 c	
	Ver. 10 %	3.04 cd	0.71 d	2.89 de	3.07 c	0.77 c	3.26 c	
	Ver. 15 %	3.36 bc	0.88 ab	3.25 bc	3.47 b	0.84 bc	3.56 bc	
Pot 7.5 L	Ver. 5 %	3.10 cd	0.66 d	3.03 ce	3.08 c	0.67 d	3.23 c	
	Ver. 10 %	3.39 bc	0.72 cd	3.17 bcd	3.76 ab	0.85 b	3.42 bc	
	Ver. 15 %	3.91 a	0.86 ab	3.41 b	3.91 a	0.94 a	3.69 ab	
Pot 10 L	Ver. 5 %	3.07 cd	0.72 d	3.11 bc	3.04 c	0.78 bc	3.36 bc	
	Ver. 10 %	3.52 b	0.80 bc	3.30 bc	3.67 ab	0.82 bc	3.67 b	
	Ver. 15 %	3.97 a	0.95 a	3.86 a	3.99 a	0.95 a	4.06 a	
Substrate type * vermicompost rate								
S.	Ver. 5 %	3.11 c	0.71 c	3.03 bc	2.97 d	0.71 c	3.07 c	
	Ver. 10 %	3.47 b	0.80 b	3.16 b	3.34 c	0.81 b	3.25 c	
	Ver. 15 %	3.99 a	0.95 a	3.45 a	3.70 b	0.89 a	3.57 b	
R. H.	Ver. 5 %	2.90 c	0.63 d	2.89 c	3.04 d	0.70 c	3.36 bc	
	Ver. 10 %	3.16 c	0.68 cd	3.08 bc	3.65 b	0.82 b	3.65 ab	
	Ver. 15 %	3.50 b	0.84 b	3.56 a	3.88 a	0.94 a	3.97 a	
Pot Vol. * Substrate type * vermicompost rate								
Pot 5 L	S.	Ver. 5 %	2.97 fg	0.65 ghi	2.84 bc	2.84 c	0.64 d	3.00 c
		Ver. 10 %	3.11 efg	0.74 efgh	2.91 bc	2.95 c	0.75 cd	3.21 bc
		Ver. 15 %	3.56 cde	0.92 abc	3.15 b	3.31 bc	0.86 bc	3.39 bc
	S.+R.H	Ver. 5 %	2.74 bc	0.61 hi	2.63 c	2.98 c	0.66 cd	3.10 c
		Ver. 10 %	2.96 fg	0.68 fghi	2.87 bc	3.18 bc	0.78 bc	3.31 bc
		Ver. 15 %	3.15 defg	0.84 bc	3.35 ab	3.63 ab	0.81 bc	3.72 ab
Pot 7.5 L	S.	Ver. 5 %	3.20 cdefg	0.74 efgh	3.06 bc	3.00 c	0.69 cd	3.00 c
		Ver. 10 %	3.59 cde	0.81 bcf	3.25 b	3.60 ab	0.83 bc	3.19 bc
		Ver. 15 %	4.17 ab	0.93 ab	3.31 b	3.82 ab	0.90 ab	3.40 bc
	S.+R.H	Ver. 5 %	3.00 fg	0.58 i	3.00 bc	3.15 bc	0.65 d	3.45 bc
		Ver. 10 %	3.18 defg	0.63 hi	3.09 bc	3.91 ab	0.87 bc	3.65 b
		Ver. 15 %	3.64 cd	0.78 cfg	3.50 ab	4.00 a	0.98 ab	3.98 ab
Pot 10 L	S.	Ver. 5 %	3.17 defg	0.75 dfgh	3.18 b	3.07 bc	0.78 bc	3.20 bc
		Ver. 10 %	3.71 bc	0.86 abce	3.31 b	3.48 b	0.84 bc	3.34 bc
		Ver. 15 %	4.23 a	1.00 a	3.89 a	3.97 a	0.89 b	3.91 ab
	S.+R.H	Ver. 5 %	2.97 fg	0.69 fghi	3.03 bc	3.00 c	0.77 c	3.52 bc
		Ver. 10 %	3.33 cdef	0.73 efgh	3.29 b	3.86 c	0.79 bc	4.00 ab
		Ver. 15 %	3.70 cde	0.89 abcd	3.82 a	4.00 a	1.01 a	4.20 a

The economic impact assessment of urban horticulture

The economic and environmental factors of urban agriculture should take in concern, for that the study estimated the economic impact. The use of local non-expensive substrates and agriculture residues (rice husk) in urban substrate culture for producing leafy vegetables (celery) besides the recycling of urban organic wastes via vermicomposting technique could contribute strongly in mitigate the climate change impacts while convert consumed cities to resilience cities. Integrating ecology soilless culture and vermicomposting in urban agriculture located on (rooftop) and in (kitchen) buildings will share in improve the food safety and security enrich the lives of city dwellers and conserve building energy.

The study canceled the direct and indirect impacts of urban cultivation on rooftop through water, soil and energy save, reducing the warm urban island, sequestrate air CO₂ by the cultivation vegetable crops, enhance the nutritional values of fresh vegetables, generate O₂, reduce, recycle and reuse the urban wastes and etc...

Table (7) presents the economic impact of pot volume, substrate type and vermicompost rate interactions in urban agriculture of celery. The use of sand and sand + rice husk were much cheaper compared to the reference substrate (Abul-Soud 2015) peat + perlite (1:1 v/v). The highest economical results presented by the treatment pot vol. 7.5 L + S. R.H. + Ver. 15 % regarding to the average cost and the highest price of yield.

Table (7): The economic impact of pot volume, substrate type and vermicompost rate interactions in urban agriculture of celery.

Pot vol.	Sub.	Ver. rate	No. of plants / table	Ave. head wt. (g)	Cost (LE)			Return (LE)	Benefit (LE)
					Subst.	Others	Total		
Pot 5 L	S.	Ver. 5 %	24	443.9	7.2	36.6	43.8	72	28.2
		Ver. 10%	24	485.5	8.4		45.0	72	27.0
		Ver. 15%	24	506.9	9.6		46.2	96	49.8
	S.+R.H.	Ver. 5 %	24	468.4	7.2		43.8	72	28.2
		Ver. 10%	24	531.8	8.4		45.0	96	51.0
		Ver. 15%	24	540.6	9.6		46.2	96	49.8
Pot 7.5 L	S.	Ver. 5 %	24	541.2	10.2	37.8	48.0	96	48.0
		Ver. 10%	24	581.6	11.4		49.2	96	46.8
		Ver. 15%	24	651.9	12.6		50.4	120	69.6
	S.+R.H.	Ver. 5 %	24	556.4	10.2		48.0	96	48.0
		Ver. 10%	24	618.1	11.4		49.2	120	70.8
		Ver. 15%	24	689.9	12.6		50.4	120	69.6
Pot 10 L	S.	Ver. 5 %	24	536.4	13.2	40.2	53.4	96	42.6
		Ver. 10%	24	571.9	14.4		54.6	96	41.4
		Ver. 15%	24	639.5	15.6		55.8	120	64.2
	S.+R.H.	Ver. 5 %	24	558.3	13.2		53.4	96	42.6
		Ver. 10%	24	631.3	14.4		54.6	120	65.4
		Ver. 15%	24	650.6	15.6		55.8	120	64.2
* Pot 8 L	Peat : perlite		24	5.4.0	96.0	54.0	140.0	96	- 44.0

*Reference data (Abul-Soud 2015)

Average prices were calculated depending on Obor market prices (Main wholesale market) regarding (400 – 500 g = 3 LE, 500 – 600 = 4 LE and 600 – 700 g = 5 LE). http://www.oboormarket.org.eg/prices_today.aspx

The total cost was affected partly by the cost of pot volume and vermicompost rate as presented in Table (6). Increasing the pot volume from 5 to 10 L as well as increasing the vermicompost rate

from 5 to 15 % led to increase the substrate cost from 7.2 to 15.6 LE / 24 celery plant / table (1 x 2 m). The main cost was fertigation that drive the force to use vermi-liquid or vermicompost-tea to reduce the cost.

The economic benefits and net return of cultivating the rooftop by celery were not estimated according to the target in reducing the cost and improve the food security in urban area under climate change impacts. The average price/ yield / season changed strongly depending on the head weight, season and the market. The average price of celery was in the range of 3 to 5 LE regarding to the head weight (400 – 500 g = 3 LE, 500 – 600 = 4 LE and 600 – 700 g = 5 LE). The average price calculated on the commercial price not on the client price.

CONCLUSION

The implement of local substrate such as sand and/or rice husk with vermicompost as substrate amendment performed ecology vegetable production via simple substrate culture in urban. Urban and rural areas could contribute strongly in food security and mitigate climate change impacts. Also, producing celery plants in urban via roof garden system and vermicomposting for satisfying the food security needs, reduce the urban horticulture costs and urban pollution, conserve the environmental and natural resources. The study recommended the using of substrate sand + rice husk combined with vermicompost rate 10 and 15% in pot volume 7.5 and 10 L for producing celery on agronomy and economic scales.

ACKNOWLEDGMENT

This study was promoting by the activities of " Integrated environmental management of urban organic wastes using vermicomposting and green roof (VCGR) project" funded by Science and Technology Development Fund (STDF), Egypt by providing the vermicompost.

REFERENCES

1. A.O.A.C. (1990). Association of Official Analytical Chemists, official methods of analysis 15th Ed., Arlington, index of method number 920. 181.
2. Abul-Soud M., Emam M.S.A. and Abd El-Rahman N.G. 2015a. The potential use of vermicompost in soilless culture for producing strawberry. *Int. J. Pl. and Soil Sci.*, 8 (5): 1 – 15.
3. Abul-Soud, M 2015. Achieve food security of some leafy vegetables in urban (How to create resilience cities?). *Global J. Adv. Res.*, 2 (10):1705 – 1722.
4. Abul-Soud, M. and Mancy A.G.A. 2015. Urban horticulture of molokhia and spinach environmentally via green roof system and vermicomposting outputs. *Global J. Adv. Res.*, 2 (12):1832 – 1847.
5. Abul-Soud, M., Emam M.S.A., Abdrabbo M.A.A. and Hashem F.A. 2014. Sustainable urban horticulture of sweet pepper via vermicomposting in summer Season. *J. Adv. in Agric.*, 3 (1): 110-122.
6. Abul-Soud, M., Emam M.S.A., Hawash A.H., Hassan M. and Yahia Z. 2015b. The utilize of vermicomposting outputs in ecology soilless culture of lettuce. *J. Agric. and Ecol. Res.*, 5 (1): 1-15.
7. Abul-Soud, M., Medany M., Hassanein M.K., Abul-Matty S.H. and Abu-Hadid A.F. 2009. Case study: Vermiculture and vermicomposting technologies use in sustainable agriculture in Egypt. 7 th Int. Conf. Organic Agric., Cairo, Egypt. *J. Agric.*, 87 (1): 389 - 403.
8. Ahmed S.H., Emam M.S.A. and Abul-Soud M. 2017. Effect of different vermicompost rates and pot volume on producing celery and red cabbage under urban horticulture condition. *Zagazig J. Agric. Res.*, Vol. 44 (4):1245-1258.

9. Albaho M., Bhat N., Abo-Rezq H. and Thomas B. 2009. Effect of Three Different Substrates on Growth and Yield of Two Cultivars. *Eur. J. Sci. Res.* 28(2): 227-233.
10. Allen, S.E. 1974. *Chemical Analysis of Ecological Materials*. Black-Well, Oxford, 565.
11. Alves, W.L. and Passoni, A.A. 1997. Compost and vermicompost of urban solid waste in *Licania tomentosa* (Benth) seedlings production to arborization. *Pesqui. Agropecu. Bras.* 32 (10), 1053–1058.
12. Arancon N.Q., Edwards C.A., Bierman P., Welch C. and Metzger J.D., 2003. Effects of vermicomposts on growth and marketable fruits of field-grown tomatoes, peppers, and strawberries. *Pedobiologia* 47,: 731–735.
13. Arancon, N.Q., Edwards C.A., Atiyeh R. and Metzger J.D. 2004. Effects of vermicomposts produced from food waste on the growth and yield of greenhouse peppers. *Bioresource Technol.*, 93: 139-144.
14. Atiyeh, R. M., Edwards, C. A., Metzger, J. D., Lee, S. and Arancon, N. Q. 2002. The influence of humic acids derived from earthworm-processed organic wastes on plant growth. *Bioresource Technology* 84,: 7–14.
15. Bachman G.R. and Metzger J.D. 2007. Physical and chemical characteristics of a commercial potting substrate amended with vermicompost produced from two different manure sources. *HortTechnology* 17,: 336-340.
16. Bachman, G.R. and Metzger J.D. 2008. Growth of bedding plants in commercial potting substrate amended with vermicompost. *Biores. Tech.*, 99: 3155-3161.
17. Bvenura C. and Afolayan A.J. 2015. The role of wild vegetables in household food security in South Africa: A review. / *Food Research International* 76: 1001–1011.
18. Chapman, H.D. and Pratt P.F. 1961. *Methods of analysis for soil, plant and water*. Calif. Univ., USA.
19. Edwards C.A., Dominguez J. and Arancon N.Q. 2004. The influence of vermicompost on plant growth and pest incidence. In: *Soil Zoology for Sustainable Development in the 21st Century* (Shakir S.H., Mikhail W.Z.A., eds). Cairo. 396-419.
20. FAO, 1980. *Soil and Plant Analysis*. Soils Bulletin 38/2,250.
21. Gajalakshmi S., Ramasamy E.V. and Abbasi S.A. 2002. High-rate composting-vermicomposting of water hyacinth [*Eichhornia crassipes* (Mart.) Solms]. *Bioresour. Technol.*, 83,: 235-239
22. Grewal S.S. and Grewal P.S. 2012. Can cities become self-reliant in food? *Cities* 29: 1–11
23. Grigatti M., Giorgonni M.E. and Ciavatta C. 2007. Compost-based growing: influence on growth and nutrient use of bedding plants. *Bioresource Technol* 98,: 3526-3534.
24. Hand P., Hayes W.A., Frankland J.C. and Satchell J.E. 1988. The vermicomposting of cow slurry. *Pedobiologia.*; 31: 199–209.
25. Hara Y., Murakami A., Tsuchiya K., Palijon A.M. and Yokoharid M.A. 2013. Quantitative assessment of vegetable farming on vacant lots in an urban fringe area in Metro Manila: Can it sustain long-term local vegetable demand? *Applied Geography*, 41,: 195-206.
26. Inbar Y., Hadar Y. and Chen Y. 1993. Recycling of cattle manure: the composting process and characterization of maturity. *Journal of Environmental Quality* 22,: 857-863.
27. Lazcano C., Arnold J., Tato A., Zaller J. G. and Domínguez, J. 2009. Compost and vermicompost as nursery pot components: effects on tomato plant growth and morphology. *Spanish Journal of Agricultural Research*, 7(4),: 994-951.
28. Litterick A.M., Harrier L., Wallace P., Watson C.A. and Wood M. 2004. The role of uncomposted materials, composts, manures, and compost extracts in reducing pest and disease

- incidence and severity in sustainable temperate agricultural and horticultural crop production – A review. *Critical Reviews in Plant Sciences*. 23:453-479.
29. Mawoisa M., Aubry C. and M. Le Bail. 2011. Can farmers extend their cultivation areas in urban agriculture? A contribution from agronomic analysis of market gardening systems around Mahajanga (Madagascar). *Land Use Policy* 28: 434–445.
 30. Muscolo A., Bovalo F., Gionfriddo F. and Nardi F. 1999. Earthworm humic matter produces auxin-like effects on *Daucus carota* cell growth and nitrate metabolism. *Soil Biol. Biochem.*, 31:1303-1311.
 31. Nicklett EJ and Kadell A.R. 2013. Fruit and vegetable intake among older adults: A scoping review. *Maturitas* 75: 305–312.
 32. Patil M.P., Humani N.C., Athani S.I. and Patil M.G. 1998. Response of new tomato genotype Megha to integrated nutrient management. *Advances in Agricultural Research in India* 9: 39-42.
 33. Probst L., Houedjofonon E., Ayerakwa H. M. and Haas R. 2012. Will they buy it? The potential for marketing organic vegetables in the food vending sector to strengthen vegetable safety: A choice experiment study in three West African cities. *Food Policy* 37: 296–308.
 34. Raul, I.C. 1996. Measuring physical properties. Rutgers Cooperative Extension. New Jersey Agriculture Experiment Station. New Jersey University.
 35. Rego L.F.G. 2014. Urban vegetable production for sustainability: The Riortas Project in the city of Rio de Janeiro, Brazil. *Habitat International* 44: 510-516.
 36. Singh, A. and Sharma, S. 2002. Composting of a crop residue through treatment with microorganisms and subsequent vermicomposting. *Biores. Technol.* 85, 107–111.
 37. Snedecor, G.W. and Cochran W.G., 1981. "Statistical Methods" 7th ed., Iowa State Univ., Press, Ames, Iowa, USA, 225-330.
 38. Subler S., Edwards C.A. and Metzger J.D. 1998. Comparing composts and vermicomposts. *Biocycle* 39,: 63–66.
 39. Tognetti C., Laos F., Mazzarino M.J. and Hernandez, M.T. 2005. Composting vs. vermicomposting: A comparison of end product quality. *Compost Science & Utilization*, 13,: 6-13.
 40. Uusiku N.P., Oelofse A., Duodu K.G., Bester Megan J. and Faber M. 2010. Nutritional value of leafy vegetables of sub-Saharan Africa and their potential contribution to human health: A review. *Journal of Food Composition and Analysis* 23: 499–509.
 41. Venugopal A., Chandrasekhar M., Naidu B.V. and Raju, S. 2010. Vermicomposting in sericulture using mixed culture of earthworms (*Eudrillus eugineae*, *Eisenia foetida* and *Perionyx excavates*) - A review. *Agricultural Reviews*, 31(2),: 150-154.
 42. Verdonck O., De Vleeschauwer D. and De Boodt M. 1982. The influence of the substrate to plant growth. *Acta. Hortic.* 126: 251-258.
 43. Watanabe, F.S., and Olsen S.R. 1965. Test of an ascorbic acid method for determining phosphorus in water and NaHCO₃ extracts from soils. *Soil Sci. Soc. Am. Proc.* 29:677-678.
 44. Wertheim-Heck S.C.O., Spaargaren G. and Vellema S. 2014. Food safety in everyday life: Shopping for vegetables in a rural city in Vietnam. *Journal of Rural Studies* 35: 37-48.
 45. Wilson, G.C.S. 1983. The physico- chemical and physical properties of horticultural substrate. *Acta Hort* 150: 19-32

استخدام البيئات الزراعية لإنتاج الكرفس في المناطق الحضرية

محمد أبو السعود ومحمد سعد على امام

المعمل المركزي للمناخ الزراعي، مركز البحوث الزراعية، الجيزة، مصر

أحد أهم المشاكل الرئيسية للتنمية التي تواجه مصر والعالم هي ظاهرة تزايد الفقر التي أدت إلى الجوع وسوء التغذية. ويمكن أن تلعب الزراعة البيئية الحضرية عن طريق الزراعة بالبيئات وتقنية الكمر بدودة الأرض دورا في مكافحة الفقر والجوع وزيادة الأمن الغذائي إلى جانب التخفيف من آثار تغير المناخ.

أجريت هذه الدراسة خلال فصلى شتاء ٢٠١٥/٢٠١٦ و ٢٠١٦/٢٠١٧ تحت ظروف نظام زراعة الأسطح بالمعمل المركزي للمناخ الزراعي، مركز البحوث الزراعية، مصر. اوضحت الدراسة ان اضافة مستويات مختلفة من مكورة دودة الأرض (٥، ١٠، ١٥%) كمحسنات لخلطات التربة مع بيئتين طبيعيتين الرمل والرمل: سرسة الأرز بنسبة ١:١ حجما مع ثلاثة أحجام مختلفة من الأخص (٥، ٧، ١٠ لتر) على النمو الخضري، المحصول وجودة الكرفس. التصميم الأحصائي لهذه الدراسة هي قطع منشقة مرتين.

أظهرت النتائج أن الصفات الفيزيائية والكيميائية للبيئات تأثرت باضافات مكورة دودة الأرض. لوحظ ان رمل + سرسة الأرز كانت أخف وزنا وأعلى في الصفات الفيزيائية وأقل القيم في الصفات الكيميائية. زيادة معدل اضافة مكورة دودة الأرض للبيئات من ٥ إلى ١٥% جنبا إلى جنب خفضت الكثافة الظاهرية في حين زادت مساحة المسام الكلي، مسامية الهواء، والقدرة على الاحتفاظ بالماء بجانب زيادة النمو الخضري، والمحصول ومحتوى الكرفس من العناصر. أيضا، زيادة حجم الأخص من ٥ إلى ١٠ لتر كان له تأثير إيجابي على النمو الخضري، والمحصول، وصفات الجودة ومحتوى الكرفس من النيتروجين والفسفور والبوتاسيوم.

تم تسجيل أعلى محصول للكرفس بالأخص حجم ٧،٥ لتر + رمل + سرسة الأرز + مكورة دودة الأرض بنسبة ١٥% و الأخص حجم ١٠ لتر + الرمل + سرسة الأرز + مكورة دودة الأرض بنسبة ١٥% في الموسم الأول والثاني على التوالي. الأخص بحجم ١٠ لتر + الرمل + سرسة الأرز + مكورة دودة الأرض بنسبة ١٥% كانت أعلى في صفات الجودة ومحتوى الكرفس من النيتروجين والفسفور والبوتاسيوم وقد عززت النتائج الاقتصادية التي تم الحصول عليها حصول الأخص ٧،٥ لتر مع (الرمل أو الرمل: سرسة الأرز) + (معدل ١٠ أو ١٥%) في الزراعة بالبيئات البيئية في الحضر الحصول على أعلى عائد اقتصادي.

PRODUCE TOMATO USING WATER OF SHRIMP FARM IN AQUAPONIC SYSTEM

MOHAMED, H. M.¹, M. A. AMER ², C. LEONARDO ³,
U.A. EL-BHAIRY ⁴AND M .F. OSMAN ⁵

1. Central Laboratory for Agriculture Climate, Agricultural Research Center, Giza, Egypt.
 2. Department of Animal Production, Fac. of Agric., Ain Shams University, Cairo, Egypt.
 3. Department of Horticulture, Fac. of Agric., Ain Shams University, Cairo, Egypt.
 4. Department of Horticulture, Fac. of Agric., University of Catania, Italy.
 5. General Authority for Fish Resources Development, Ministry of Agriculture and land reclamation Cairo, Egypt.
-

Abstract

This study was conducted at the Central Laboratory for Agricultural Climate (CLAC), Agricultural Research Center (ARC), Ministry of Agriculture and land reclamation, Egypt, to investigate the effect of using different shrimp stocking densities (*Macrobrachium rosenbergii*) on production and quality of tomato *Lycopersicon esculantum* L. cv. Castle rock grown in nutrient film technique (NFT) during seasons of 2007 and 2008. Three stocking densities of shrimp (50, 100 and 150 unit/m³) were tested in this experiment. The shrimp water of the different stocking densities was used as nutrient solution compared with chemical nutrient solution (control) in closed NFT system. Different measurements were recorded throughout the experimental period such as: number of leaves, total leaf area, early and total yield, total soluble solids (TSS), ascorbic acid (V.C) for tomato plants, for shrimp, total yield, average weight of shrimp and (NH₄, NO₃, P, K, Ca, Mg) concentration in shrimp rearing water. The experiment was arranged in a complete randomized block design with 3 replicates. The collected data indicated that all shrimp densities reduced tomato production both early and total yields compared to control. Increasing shrimp density from 50 to 100 shrimp/m³ resulted in increasing early and total yield of tomato, but less than that obtained from control. On the other hand, increasing shrimp density to 150 unit/m³ reduced most of all measurements for plant. Shrimp yield varies with different densities, the highest yield was obtained with 100 shrimp/m³ and the lowest with 50 shrimp/m³. Concerning the average weight for shrimp, 50 shrimp/m³ gave the best result and the lowest was obtained with 150 unit/m³. Finally this study indicated that growing tomato in integrated aquaculture system with density of 100 unit/m³ and NFT has potential for improving yield and quality of tomato and nutrient use efficiency but still less than the control.

Key words: Soilless culture, Nutrient film technique (NFT), Nutrient Solution.

INTRODUCTION

Sustainable agriculture combines plant and animal production, integrates natural biological cycles, and makes the most use of non-renewable resources (Gold, 1999). Aquaponics is an integrated system that links hydroponic plant production with recirculating aquaculture (Tyson *et al.*, 2004). The major system advantages are removing fish waste by plants and reduced water usage and nutrient discharge to the environment for both systems (Rakocy *et al.*, 1997). In aquaponic system, biofiltration by nitrifying bacteria maintains water quality for the fish, converting waste ammonia to nitrate nitrogen for plants (Timmons *et al.*, 2002). The potential of plants and fish for production in aquaponic has been investigated (Adler *et al.*, 1996, McMurtry *et al.*, 1997, Rakocy, 1992; Watten and Busch, 1984). Recirculating aquaculture-hydroponic systems

are designed to provide an artificial, controlled environment that optimizes the growth of fish (or other aquatic species) and soil-less plants, while conserving water resources (Rakocy and Hargreaves, 1993). One of the most complex and important subsystem of re-circulating aquaculture is the bio-filtration and removal of fish waste. Recirculating system must incorporate both solid removal and biological filtration and the water reconditioning process to achieve proper water quality for fish and plants (Harmon, 2001). Rakocy *et al.*, (2000) stated that the hydroponic component in the Aquaponic system serves as a biofilter, and therefore a separate biofilter is not needed as in other recirculating systems. Aquaponic system have the only biofilter that generates income, which is obtained from the sale of hydroponic produce such as vegetables, herbs and flowers (Rakocy *et al.*, 2004). In the integrated aquaponic system, nutrients, which are excreted directly by the fish or generated by the microbial breakdown of organic wastes, are absorbed by plants cultured hydroponically (without soil). Fish feed provides most of the nutrients required for plant growth. As the aquaculture effluent flows through the hydroponic component of the recirculating system, fish waste metabolites are removed by nitrification and direct uptake by the plants, thereby treating the water, which flows back to the fish-rearing component for reuse (Rakocy *et al.* 2000). Plants, such as tomatoes, are an ideal complementary crop in an integrated system because they grow rapidly in response to the high levels of dissolved nutrients that are generated from the microbial breakdown of fish wastes (Rakocy, 1992).

Armstrong submerged aquatic plants, *Elodea densa*, were included in recirculating *Macrobrachium rosenbergii* culture systems to examine their ability to remove nitrogenous metabolites excreted by the shrimp. Ammonia and nitrite concentrations were typically an order of magnitude less in systems with *Elodea* than without when shrimp were stocked at equal densities. Peak ammonia and nitrite concentrations reached 4.0 mg NH₄-N/l and 5.7 mg NO₂-N/l in systems without plants, but were only 0.2 and 0.4 mg/l, respectively, in systems with plant (Kenneth and David, 1983). Nutrient concentrations were lower than the levels normally found in hydroponic system with inorganic nutrient solution, but they were generally acceptable for aquaponic system because nutrients were produced daily (Rakocy *et al.* 2004). Nutrient film technique (NFT) has been successfully incorporated into a number of aquaponic systems (Rakocy *et al.*, 2006). The waste from intensive aquaculture facilities is predominantly from feed and includes uneaten feed (feed waste), undigested feed residues and excretion of nitrogen compounds (Chaves *et al.*, 1999). Nitrates (NO₃-N) and orthophosphates (PO₄-P) are major pollutants for receiving water bodies. On the other hand the same nutrients are essential elements for good plant growth (Clarkson and Lane, 1991). The fish and plants are grown in a mutually beneficial, symbiotic relationship. Un-ionized ammonia-nitrogen is produced as an intermediate by-product of protein metabolism by the fish and high concentrations of this nitrogen can cause mortality. However, some forms of nitrogen can be used as a plant nutrient, and are removed from the water by the plant roots as the water circulates through the hydroponic unit. Thus, a harmful by-product of fish production becomes a beneficial input for plant production (Rakocy *et al.*, 1993).

According to that, the aim of this study was to investigate the effect of using different shrimp densities on production and quality of tomato grown in aquaponic system with shrimp.

MATERIALS AND METHODS

The experiment was conducted at The Central Laboratory for Agriculture Climate (CLAC), Agriculture Research Center, Egypt. During two summer seasons of 2007 and 2008.

The system used in this experiment was consisted of shrimp rearing tanks, filtering unit and hydroponic system for growing tomato plants. For rearing shrimp fiberglass tanks (1 x 1 x 0.8 m) were established under ground surface, the tanks were isolated with 1000 micron black

polyethylene sheet, the total water volume was 800 liter for each tank. Each shrimp rearing unit was connected with NFT system with submersible pump lifting 300L of water per hour directly to the filtration unit (two 20-L buckets). The bottom bucket filled with gravel 0.5 - 5 ml while the top bucket filled with perlite in order to remove the solid wastes. The clear water (after filtration) was directed to the NFT gullies. NFT gullies were made from 250 micron poly-ethylene sheets. Gully width was 30 cm and 2 meter length, the gully was leaned sloped beds with 1% slop towards the shrimp tanks. The NFT unit designed to allow shrimp effluent to flow over the plant roots, so essential nutrients can be extracted by the plant.

Tomato (*Lycopersicon esculantum L.*), cv. Castle rock was used in this experiment. Seedlings were cultivated in netted pots and placed in a trough filled with thin layer of diluted nutrient solution in nursery till roots started to emerge, then small plants were transplanted in the NFT system. The planting was ten days after shrimp introducing to the tanks. The planting density was four plants per unit. the management of the plants was only spraying with micronutrient solution for overcoming the deficiency symptoms, no pesticide or fungicide were used during the whole period of the experiment.

Shrimp (*Macrobrachium rosenbergii*) post larvae was used in the experiment, were ranged between in initial weight 0.3- 0.4 g. The shrimp were fed pelleted feed containing 40% protein, at 2-20% of biomass during different periods of rearing (Table1). Feeding rate for shrimp was based upon the mean weight of the population. A feeding schedule can be developed based upon:

Mean individual weight determined from samples obtained every 3 weeks. As described by D'Abramo and Brunson, (1996), and Mohanta, (2000). Three densities of shrimp 50, 100 and 150 shrimp per m³ were used in this study compared with chemical nutrient solution in regards to the productivity and quality of tomato grown in integrated system with Shrimp. The composition of the chemical nutrient solution described by El-Behairy, (1994) is illustrated in Table (2). The electrical conductivity was adjusted at 2.5 mmhos-1.

Tomato growth parameters and production:

Several different parameters were recorded on tomato plants including: number of leaves, surface leaf area (cm²), early and total yield (g/plant), total soluble solids (TSS) (%) and Vit. C content (mg/100g).

Shrimp production:

Some parameters were recorded on Shrimp including: total yield (g) and mean shrimp weight (g).

Water parameters:

NH₄, NO₃, P, K, Ca and Mg concentration were determined monthly in water of the shrimp rearing tanks. The experiments were lasts for five months and repeated for two seasons (A.O.A.C., 1990).

Data analysis:

The experiment was arranged as a complete randomized block design with three replicates. The collected data were analyzed using ANOVA statistical analysis as described by (Snedicor and Cochran, 1980) and the least significant difference (LSD) was used in comparison among means.

RESULTS AND DISCUSSION

Tomato growth parameters and production:

Number of leaves/plant:

Table (3) presented the effect of using different shrimp densities on number of leaves / tomato plant. Data recorded after 30, 60, 90, 120, 150 days from transplanting showed that increasing shrimp density/m³ from 50 toward 150 shrimp/m³ significantly decreased number of leaves per plant. However, the control treatment recorded the highest number of leaves /plant. Similar trend was observed in the second season.

The effects of using different stoking densities of shrimp on total leaf area, early and total yield of tomato fruits, TSS% and vitamin C are illustrated in Table (4).

Total leaf area:

Data collected from both seasons illustrated that increasing shrimp density from 50 towards 150 shrimp/m³ significantly decreased leaf area. On the other hand, the control treatment gave the highest leaf area followed by 50 shrimp/m³ on ($P \geq 0.05$) significant difference was observed between both the control and 50 unit/m³ treatments.

Early and total yield:

However, data collected throughout the both seasons illustrated that increasing shrimp density from 50 to 100 shrimp/m³ significantly increased the early and yield of tomato fruits. On the contrary, increasing shrimp density up to 150 shrimp/m³ significantly decreased the early and total yield. Nevertheless, control treatment recorded the highest values.

Total soluble solids (TSS %):

Data collected from the first and second season showed that the lowest TSS % recorded by both control treatment and 50 shrimp/m³. On the other hand, increasing shrimp density up to 100 significantly led to increase TSS % in tomato fruits, while increasing shrimp density up to 150 shrimp/m³ significantly decreased TSS %.

Vitamin C:

Data collected from the first season indicated that Vit. C content of tomato fruits had affected by shrimp density where the highest Vit. C content recorded by control treatment followed by 50 shrimp/ m³ with significant difference with all other shrimp density. Otherwise, increasing shrimp density from 50 towards to 150 shrimp /m³ decreased Vit. C content in tomato fruit. Similar trend was recorded in the second season.

Shrimp production:

Concerning shrimp yield of different densities, data in Table (5) showed that the lowest shrimp density 50 shrimp/m³ gave the highest mean weight of shrimp (27.72 g). Although the average weight /shrimp in 50 shrimp/m³ treatment was higher than the others, the total shrimp produced/m³ of water was higher in the 100 shrimp/m³ comparing with the other treatments. The significant differences among the treatments were true during the both tested seasons in mean weight of shrimp and total shrimp yield .

Mineral composition of shrimp water:

Figs (1 through 6) illustrated the mineral composition of shrimp water during the whole experimental period. In genral, data showed that the minieral composition of the shrimp water was influenced by shrimp density. Regarding the NH₄ content (ppm) in shrimp water compared with control nutrient solution. Data collected from the first season after 30, 60, 90, 120, 150 days of the experiment illustrated that increasing shrimp density significantly increased NH₄ content in shrimp water; where, the highest NH₄ content (ppm) was recorded in 150 followed by 100 then

50 unit/m³, while control treatment recorded the lowest concentration. Similar trend was observed in the second season.

Regarding the NO₃ content (ppm) in shrimp water compared with control nutrient solution. Data collected from both seasons indicated that increasing shrimp density decreased NO₃ content (ppm) in shrimp water throughout the experimental time. Control treatment recorded the highest values of NO₃ content (ppm) of rearing water, data collected in both seasons illustrated that the highest values of NO₃ content (ppm) of rearing water was recorded by 50 shrimp/m³, While, the lowest values of NO₃ content (ppm) of rearing water was recorded by 150 shrimp/m³. There was a significant difference between all treatments.

On the other hand, P content (ppm) of rearing water for different shrimp densities was increased by decreasing the shrimp density. The highest values of P content of rearing water was observed by control treatment followed by 50 shrimp/m³ treatment while the 150 shrimp/m³ treatment presented the lowest value of P (ppm) content of rearing water as showed in Fig (3). The differences among the treatments were significant.

Concerning the effect of different shrimp densities on the K content (ppm) of rearing water compared to control treatment, data in Fig (4) indicated that control treatment recorded the highest values of K content (ppm) along the study period followed by 100 shrimp/m³ treatment. The lowest K content (ppm) of rearing water was observed in 150 shrimp/m³ treatment.

Figs, (5, 6) represented the effect of different shrimp densities on the Ca and Mg contents (ppm) of rearing water compared to control treatment. Data showed that increasing shrimp density from 50 to 150 shrimp/m³ significantly reduced the content of Ca and Mg ppm in rearing water. The highest values of Ca and Mg contents in rearing water were observed by control treatment followed by 50 shrimp/m³ treatment, while the 150 shrimp/m³ treatment recorded the lowest value of Ca and Mg (ppm) contents of rearing water. The differences among the treatments were significant ($p \leq 0.05$).

From the all over results, it was clear that using 50 shrimp /m³ did not affect number of leaves and total leaf area comparing with control while using 100 shrimp /m³ increased both characters. On the contrary, using 150 shrimp /m³ reduced both of them significantly. Increasing shrimp density led to decrease number of leaves and total leaves area as result of oxygen deficit and nitrification reduction, which reduced nitrate concentration in shrimp rearing water. Adams *et al.* (1978) reported that reduction of nitrate concentration in the 150 shrimp/m³ might be the season for reducing the number of leaves and leaf area. The lower concentration of nitrate produced from the higher number of fish could be a result of oxygen deficit resulted from the higher number of fish which reduced the consumption (Cuenco *et al.*, 1985).

On the other hand, all treatments reduced early and total yield comparing with control. This reduction could be a result of lower concentration of K released into the shrimp water. Increasing shrimp density up to 100 shrimp/m³ resulted in the highest early and total yield compared to 50 and 150 shrimp /m³. The reduction of yield in 50 shrimp/m³ could be a result of increasing nitrate and lower concentration of K. On the contrary, using 150 shrimp/m³ reduced early and total yield as a result of very low concentration of nitrate producing small vegetative growth and reduced yield as obtained in this study (Adams *et al.*, 1978). As a same result, Lopez-galarza *et al.*, (2001) found that K/N ratio less than 1.9 reduced early and total yield of strawberry plant significantly. The reduced yield obtained in all shrimp densities could be also due to the lower P and the higher NH₄ compared to the control treatment.

Regarding shrimp yield, data showed that increasing shrimp densities reduced mean weight of shrimp. The reduction in mean weight of shrimp when densities increasing from 50 shrimp/m³

to 100 and 150 shrimp/m³ was significant, while increasing shrimp densities from 100 to 150 shrimp/m³ was not significant. This could be the result of using lower shrimp densities allow more growth due to consume more food than that high densities. Feeding rate for shrimp based on shrimp size where small shrimp consume a high percent (D'Abramo and Brunson, 1996; Mohanta, 2000). Although the 50 shrimp/m³ produced higher mean weight of shrimp, 100 shrimp /m³ produced more shrimp yield, because the increase number of shrimp retrieve the reduction of mean weight of obtained shrimp.

Table 1: Feeding schedule for *M. rosenbergii* broodstock:

Month	Estimated (biomass g)	Feed (%of body weight)	Feed (g /day)
January	180	20	36
February	500	15	75
March	1.300	10	135
April	4.000	6	240
May	4.000	5	400
June	8.750	4	350
July	12.250	3	367.5
August	14.000	3	420
September	15.300	3	459
October	16.500	2	330
November	19.500	2	390
December	18.000	2	360

Table 2: Macro and micro nutrient concentrations in the used chemical nutrient solution for control treatment

Element	Concentration (ppm)
N	250
P	35
K	350
Ca	180
Mg	50
Fe	3.0
Mn	1.0
Cu	0.1
Zn	0.06
Mo	0.01
B	0.1

Table 3: Effect of shrimp densities on aquaponic on number of tomato leaves.

Treatments	Days after transplanting					
	0	30	60	90	120	150
First season						
50 shrimp/m ³	6.58	30.67	75.00	133.83	161.92	173.67
100 shrimp/m ³	6.42	29.00	66.00	121.25	152.08	166.58
150 shrimp/m ³	6.50	23.25	61.08	114.00	143.08	155.42
Control	6.50	35.33	77.33	143.33	168.92	190.83
LSD	N.S	1.134	2.08	1.26	1.29	1.65
Second season						
50 shrimp/m ³	6.50	32.12	68.50	139.50	168.42	180.83
100 shrimp/m ³	6.58	30.08	68.50	126.58	158.17	169.67
150 shrimp/m ³	6.67	24.00	63.67	118.67	149.08	160.75
Control	6.67	36.67	80.83	148.92	175.25	198.50
LSD	N.S	0.99	0.81	0.85	1.18	2.12

Table 4: Effect of shrimp densities on aquaponic on total leave area, early and total yield and some fruit quality of tomato.

Treatments	Total leaf area (cm ²)	Early yield (g/plant)	Total yield (g/plant)	TSS (%)	V.C (mg/100g)
First season					
50 shrimp/m³	7493.43	276.92	1213.92	4.30	21.36
100 shrimp/m³	6394.84	424.75	1750.60	4.55	18.19
150 shrimp/m³	5717.88	204.50	1131.25	4.38	17.44
Control	7650.21	709.17	2395.83	4.46	24.11
LSD	374.88	13.55	59.35	N.S	2.213
Second season					
50 shrimp/m³	7587.45	299.83	1259.79	4.40	22.36
100 shrimp/m³	6500.02	470.92	1786.58	4.67	18.99
150 shrimp/m³	5828.31	221.75	1159.17	4.48	18.12
Control	7703.38	722.00	2420.00	4.52	24.47
LSD	321.31	7.91	52.23	N.S	2.780

Table 5: Effect of shrimp densities in aquaponic on average weight of shrimp (g/shrimp) and total shrimp weight (g/shrimp).

Treatment	Mean weight (g/shrimp)	Total yield (g/m ³ water)
First season		
50 shrimp/m³	27.72	1027.71
100 shrimp/m³	18.20	1190.83
150 shrimp/m³	16.40	1107.08
LSD	0.39	10.94
Second season		
50 shrimp/m³	27.36	1037.08
100 shrimp/m³	19.92	1285.42
150 shrimp/m³	15.90	1120.50
LSD	0.73	18.34

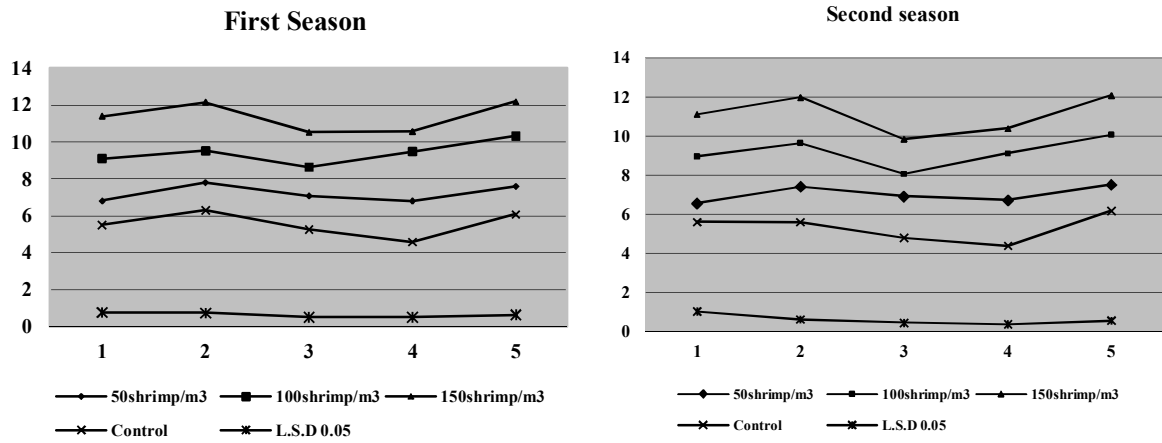


Fig 1: Effect of shrimp densities in aquaponic on NH₄ concentration in the shrimp water

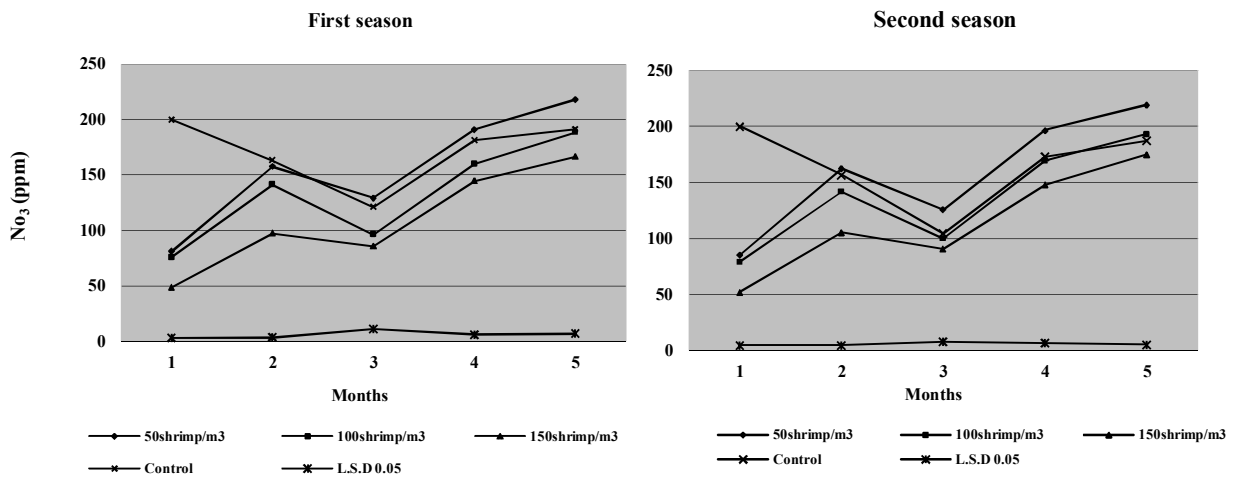


Fig 2: Effect of shrimp densities in aquaponic on NO₃ concentration in the shrimp water

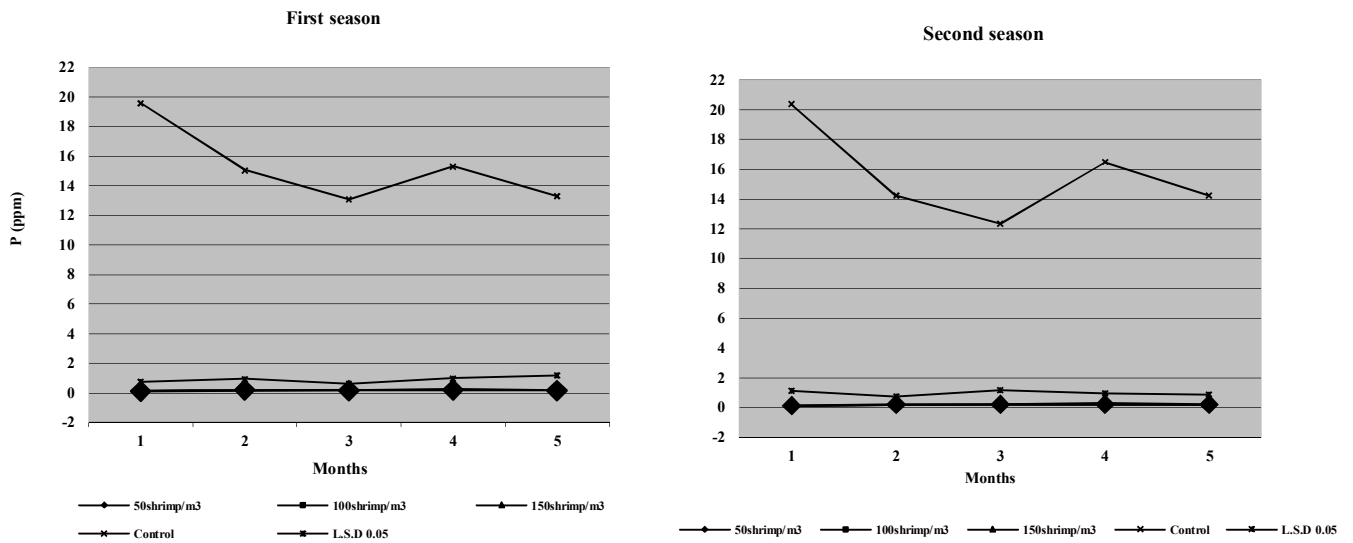


Fig 3: Effect of shrimp densities in aquaponic on P concentration in the Shrimp water

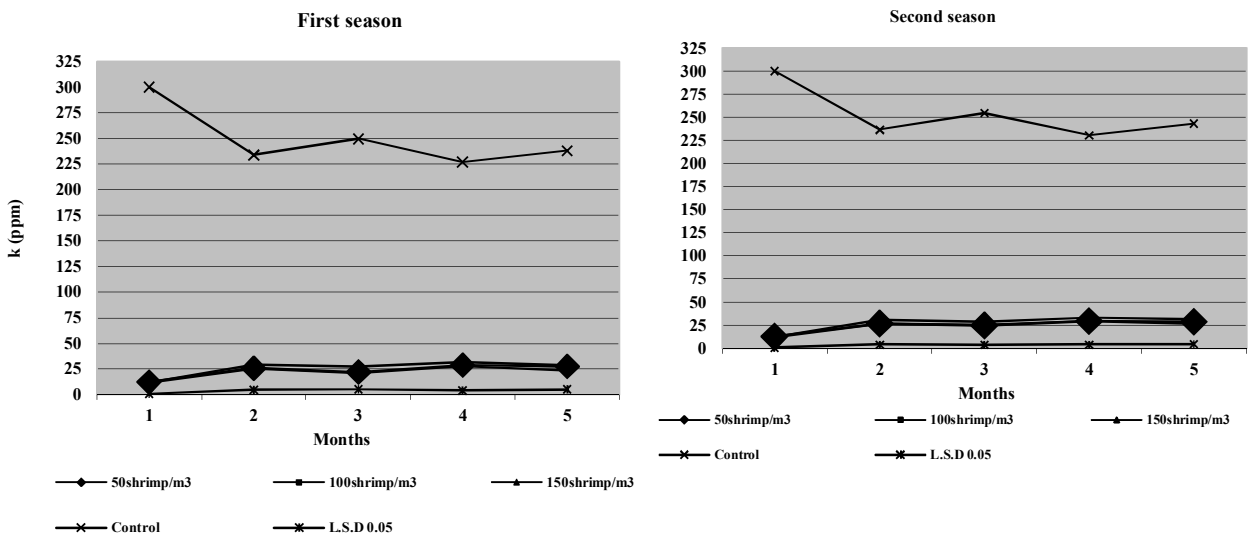


Fig 4: Effect of shrimp densities in aquaponic on K concentration in the Shrimp water

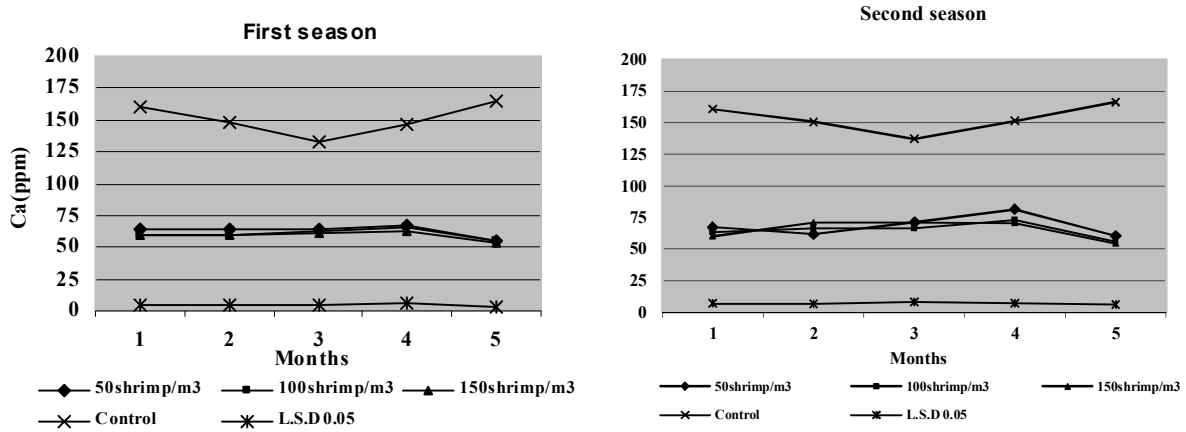


Fig 5: Effect of shrimp densities in aquaponic on Ca concentration in the shrimp water

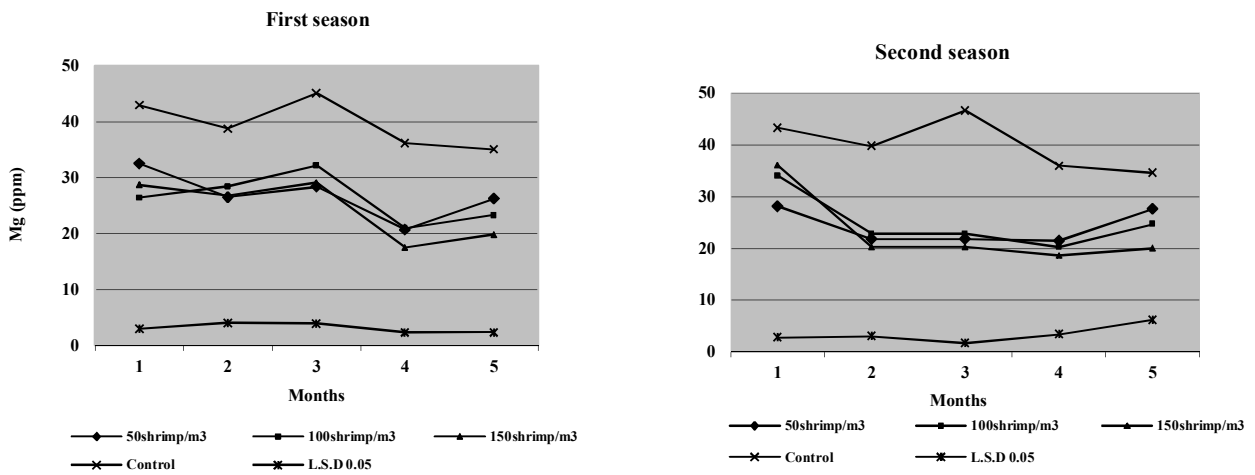


Fig 6: Effect of shrimp densities in aquaponic on Mg concentration in the shrimp water

CONCLUSION

It could be concluded that the best number of shrimp/m³ in aquaponics system for tomato is 100 to produce higher shrimp and tomato yield with good average weight of shrimp.

More research is needed with increase oxygen to test the possibility of using higher number of shrimp /m³, as well as increasing the tomato yield.

REFERENCES

- 1- A.O.A.C. (1990). *Official Methods of Analysis* of the Association of Official Analytical Chemists. 15 th ed. published by the association of Official analytical chemists, Inc. Anlington, Virginia 22201, U.S.A.
- 2- Adams, P., J.N Davides and G.W. Winsor (1978). Effect of nitrogen, potassium and magnesium on the quality and chemical composition of tomato grown in peat. *J Hort.*, 53:115-112.
- 3- Adler, P.R., F. Takeda; D.M. Glenn and S.T. Summerfelt (1996). Utilizing byproducts to enhance aquaculture sustainability. *World Aquaculture* 27 (2): 24-26.
- 4- Chaves, P.A.; R.M. Sutherland and L.M. Laird (1999). An economic and technical evaluation of integrating hydroponics in a recirculation fish production system. *Aquaculture Economics & management*. 3 (1):83-91.
- 5- Clarkson R. and S. D. Lane (1991). Use of a small-scale nutrient film hydroponic technique to reduce mineral accumulation in aquarium water. *Aquaculture and fisheries management*. 22.: 37 - 45.
- 6- Cuenco, M.L.; R.R. Stickney and W.E. Granti (1985). Fish bioenergetics and growth in aquaculture pods: I. Individual fish model development. *Ecological Modeling*. 27: 169-190.
- 7- D'Abramo L.R. and M.W. Brunson (1996). Production of Freshwater Prawns in Ponds. Southern Regional Aquaculture Center Publication No 484.
- 8- El-Behairy, U.A. (1994). The effect of levels of phosphorus and zinc in the nutrient solution on macro and micronutrients uptake and translocation in cucumber (*Cucumis sativus L.*) grown by the Nutrient Film Technique. Ph.D.Thesis London University, Wye College Engld.299 PP.
- 9- Gold, M.V. (1999). Sustainable Agriculture: Definitions and Terms. Alternative Farming Systems Information Center, National Agricultural Library, Beltsville, MD.
- 10- Harmon, T. (2001). A look at filtration in aquaponic system: bead filters. *Aquaponics j.* 5 (3): 16 -19.
- 11- Kenneth E. C. and A. David. (1983). Removal of nitrogen by an aquatic plant, Elodea deans, in recirculating Macrobrachium culture systems. *Aquaculture*, 32, (3-4): 347-360.
- 12- Lopez-Galarza, s.; Maroto A. San Bautista; B. Pascual; J. Alagarda and M.S. Bono (2001). Productive behaviour of strawberry waiting bed plants in hydroponic cultivation under greenhouse. *Acta Hort.* 559:67-72.
- 13- McMurty, M.R.; D. C. Sanders; J.D. Cure and R. G. Hodson (1997). Effect of biofilter/ culture tank volume ratio on productivity of a recirculating fish/ vegetables co-culture system. *J Appl. Aquaculture* 7 (4):33-51.
- 14- Mohanta K.N. (2000). Development of Giant Freshwater Prawn Broodstock, Naga, The ICLARM Quarterly 23, (3),: 18-20.
- 15- Rakocy, J.E. (1992). Recirculating Aquaculture Tank Production Systems: Integrating Fish and Plant Culture. So. Regional Aquaculture Center Publ.No. 454.

- 16- Rakocy, J.E., D.S. Bailey; J.M. Martin and R. C. Shultz (2000). Tilapia production system for the Lesser Antilles and other resource-limited, tropical areas. : 651 – 662. Tilapia Aquaculture in the 21st century: Proc. from 5th Inter Symposium on Tilapia in Aquaculture, Rio de Janeiro, Brazil.
- 17- Rakocy, J.E.; D.S. Bailey; K.A. Shultz and W.M. Cole (1997). Evaluation of a commercial-scale aquaponic unit for the production of tilapia and lettuce. : 357–372. Fourth International Symposium on Tilapia in Aquaculture, Orlando, Florida.
- 18- Rakocy, J.E. and J.A. Hargreaves (1993). Integration of vegetable hydroponics with fish culture: A review. In J. Wang (Ed.), Techniques for Modern Aquaculture. St. Joseph, MI: American Society of Agricultural Engineers. : 112-136.
- 19- Rakocy, J.E.; J.A. Hargreaves and D.S. Bailey (1993). Nutrient accumulation in a recirculating aquaculture system integrated with hydroponic vegetable production. In J. Wang (Ed.), Techniques for Modern Aquaculture St. Joseph, MI: American Society of Agricultural Engineers. : 148-158.
- 20- Rakocy, J.E.; R.C Shultz; D.S Bailey And E.S Thoman (2004). Aquaponic production of tilapia and basil: comparing a batch and staggered cropping system. Acta Hort. 648:63-69.
- 21- Rakocy, J.E.; T.M. Losordo and M.P. Masser (2006). Recirculating aquaculture tank production systems: Aquaponics - integrating fish and plant culture. So. Region Aquaculture Center Publ No. 454:16 .
- 22- Snedecor, R. and W. Cochran (1980). Statistical methods. Sixth edition, Iowa State Univ. Press, Amer. Iowa, UAS.
- 23- Timmons, M.B.; J.M. Ebeling; F.W. Wheaton; S.T. Summerfelt and B.J. Vinci (2002). Recirculating aquaculture systems, 2nd Edition. N.E. Regional Aquaculture Center Publ. No. 01–002:769 .
- 24- Tyson, R.V.; E.H. Simonne; J.M. White and E.M. Lamb (2004). Reconciling water quality parameters impacting nitrification in aquaponics: the pH level. Proc. Fla. State Hort. Soc. 1177: 79-83.
- 25- Watten, B.J. and R.L. Busch (1984). Tropical production of tilapia (*Sarotherodon aurea*) and tomatoes (*lycopersicon esculantum*) in a small-scale recirculation water system. Aquaculture 41: 271 – 283.

إنتاج الطماطم باستخدام مياة مزارع الجمبرى فى نظام الاكوابونك التكاملى

محمد حسن محمد^١ ، محمد عبد الباقي عامر^٢ ،
شربينو ليوناردى^٣ ، أسامه احمد البحيرى^٤ ، محمد فتحى عثمان^٥

^١ المعمل المركزى للمناخ الزراعى ، مركز البحوث الزراعية، مصر

^٢ قسم الانتاج الحيوانى ، كلية الزراعة ، جامعة عين شمس ، مصر

^٣ قسم البساتين ، كلية الزراعة ، جامعة كاتانيا ، ايطاليا

^٤ قسم البساتين ، كلية الزراعة ، جامعة عين شمس ، مصر

^٥ رئيس الهيئة العامة لتنمية الثروة السمكية، وزارة الزراعة واستصلاح الأراضى ، مصر

تم اجراء الدراسة فى المحطة البحثية للمعمل المركزى للمناخ الزراعى ، مركز البحوث الزراعية ، وزارة الزراعة واستصلاح الأراضى ، الدقى ، مصر ، بهدف إستخدام نظام تكاملى لإنتاج الطماطم (*Lycopersicon esculantum L.*) صنف كاسل روك فى نظام الفيلم المغذى خلال موسمى ٢٠٠٧ ، ٢٠٠٨ تم اختبار ثلاث كثافات مختلفة للجمبرى (١٠٠، ٥٠، ١٥٠ جمبرى /م^٢) . وقد تم استخدام مياة الجمبرى كمحلول مغذى لتغذية نباتات الطماطم النامية (٤ نباتات) فى نظام الفيلم المغذى تحت نظام مغلق مع خزان تربية الجمبرى . وقد اوضحت النتائج ان كل معاملات الجمبرى قد أدت الى نقص المحصول المبكر والكلى للطماطم مقارنة باستخدام المحلول المغذى (المقارنة) . كما ان زيادة كثافة الجمبرى من ٥٠ الى ١٠٠ جمبرى /م^٢ تؤدي الى زيادة نسبة المحصول المبكر والكلى و محتوى الثمار من الاملاح الذائبة الكلية بينما يقل محتوى فيتامين ج . من ناحية اخرى ، فإن زيادة كثافات الجمبرى حتى ١٥٠ جمبرى /م^٢ أدى إلى خفض المحصول المبكر والكلى و محتوى الثمار من الاملاح الذائبة الكلية و فيتامين ج . ويمكن ان نستخلص من النتائج المتحصل عليها ان كثافة ١٠٠ جمبرى /م^٢ هي افضل كثافة للجمبرى لإنتاج الطماطم باستخدام نظام الفيلم المغذى فى نظام تكاملى مع الجمبرى وذلك من حيث الإنتاجية والجودة وكفاءة استخدام نباتات الطماطم للمياه.

